

THE SEISMIC RESPONSE OF INELASTIC STRUCTURES

A thesis  
submitted in partial fulfilment of the requirements  
for the Degree of  
Doctor of Philosophy in Civil Engineering  
at the University of Canterbury  
by  
Richard Deane Sharpe

University of Canterbury,  
Christchurch, New Zealand

1974

## ABSTRACT

Because of the importance being placed by modern building codes of practice on the need for the deterministic analysis of ductile frames as a means of assessing their ability to withstand severe seismic ground motions, an investigation of the more important factors affecting such analyses has been made. The problems encountered in writing a comprehensive computer program, with which the sensitivity of a two-dimensional inelastic frame can be measured, are dealt with in depth. These extend from that arising from the obvious need to simplify the input data and printed results, to that of the selection of an economic (and sufficiently accurate) numerical integration technique which can be shown to remain stable over a realistic frequency range. The difficulties met in designing a beam-model which will exhibit a moment-curvature relationship that can be satisfactorily tracked, are described and a recommendation made as to which method should be used. The sensitivity of a selection of frames to different aspects of their modelling is investigated in order to provide guidance as to the complexity of modelling that is required for dynamic analyses. In an attempt to correlate the damaging potential of various earthquake accelerograms, so that they may be related to the requirements of modern building codes of practice, a variety of possible scaling criteria were tested. Although no firm conclusions are reached as to which criteria is to be preferred, a series of inelastic analyses are reported, in which the varying effect of different earthquakes can be seen. Finally, two examples of structures whose design benefitted by their having deterministic dynamic inelastic analyses performed, are described, together with the computer program used.

## ACKNOWLEDGEMENTS

The research for this report was carried out in the Department of Civil Engineering, University of Canterbury, under the overall guidance of its Head, Professor H.J. Hopkins.

Grateful acknowledgement is made of the support and guidance given to the candidate by the supervisors of his studies, Dr. Athol J. Carr and Dr. Robin Shepherd, by members of the Department's staff, fellow students and by Mr. R.J.P. Garden, consulting engineer of Dunedin.

The entire staff of the University's Computer Centre facilitated this project by providing a friendly service.

The co-operation and interest shown by both the City of Christchurch's Engineer's Department and Beca, Carter, Hollings and Ferner, consulting engineers of Auckland, in the analyses of bridges designed by them, was greatly appreciated.

This study was financially supported, in part, by a generous grant from the New Zealand National Roads Board.

## CONTENTS

	Page
ABSTRACT . . . . .	i
ACKNOWLEDGEMENTS . . . . .	ii
LIST OF FIGURES . . . . .	vi
LIST OF TABLES . . . . .	ix
LIST OF SYMBOLS . . . . .	x
 CHAPTER ONE - INTRODUCTION AND SCOPE OF RESEARCH	 1
1.1 Introduction . . . . .	1
1.2 The art of idealization . . . . .	2
1.3 Choosing an earthquake . . . . .	3
1.4 Scope of the research . . . . .	4
 CHAPTER TWO - THE MOMENT-CURVATURE RELATIONSHIP . . . . .	 6
2.1 Introduction . . . . .	6
2.2 The shape of the moment-curvature relationship . . . . .	6
2.3 Conclusions as to the accuracy required . . . . .	12
2.4 Members with rising spring-rates . . . . .	14
 CHAPTER THREE - NUMERICAL INTEGRATION TECHNIQUES . . . . .	 18
3.1 Introduction . . . . .	18
3.2 Requirements of a satisfactory technique . . . . .	19
3.3 Natural modes . . . . .	19
3.4 Slaving of similar degrees of freedom . . . . .	21
3.5 Phantom frequencies . . . . .	21
3.6 Non-oscillatory modes of vibration . . . . .	25
3.7 Consideration of approximation operators . . . . .	30
 CHAPTER FOUR - THE COMPUTER PROGRAM . . . . .	 40
4.1 Introduction . . . . .	40
4.2 Coupling of degrees of freedom . . . . .	40
4.3 Partitioning stiffness matrices . . . . .	41
4.4 The damping model . . . . .	45
4.5 A non-linear beam model . . . . .	46
4.6 Member ductility - a definition . . . . .	51
4.7 Column moment - axial load interaction . . . . .	52
4.8 Tracking a moment-curvature relationship . . . . .	53
4.9 The Ramberg-Osgood hysteresis . . . . .	64



4.10	Vertical components of earthquakes . . . . .	65
4.11	Inertial loads from joint rotations . . . . .	66
4.12	Visual output . . . . .	66
4.13	Comparisons of results with other known results . . . . .	66
CHAPTER FIVE	- SENSITIVITY OF MODELLING . . . . .	67
5.1	Introduction . . . . .	67
5.2	Axial and shear deformation . . . . .	67
5.3	Allowances for joint size . . . . .	72
5.4	The shape of the moment-curvature hysteresis . . . . .	72
5.5	The representation of mass . . . . .	80
CHAPTER SIX	- CHOOSING AN EARTHQUAKE . . . . .	82
6.1	Introduction . . . . .	82
6.2	The frame . . . . .	82
6.3	Earthquake scaling . . . . .	83
6.4	Measuring an earthquake's damage potential . . . . .	84
6.5	Using maximum member ductilities to compare responses . . . . .	86
6.6	Conclusions . . . . .	90
CHAPTER SEVEN	- THE ANALYSIS OF TWO BRIDGE STRUCTURES . . . . .	99
7.1	Introduction . . . . .	99
7.2	The Durham Street railway overbridge . . . . .	99
7.3	The Auckland upper harbour crossing . . . . .	107
7.4	Conclusions . . . . .	117
CHAPTER EIGHT	- A SUMMARY WITH SUGGESTIONS FOR FURTHER STUDY . . . . .	119
REFERENCES	. . . . .	124
APPENDIX A	- ANALYSIS MODELS . . . . .	A-1
A.1	Structure I . . . . .	A-1
A.2	Structure II . . . . .	A-3
APPENDIX B	- DERIVATIONS . . . . .	B-1
B.1	The convergence criteria for a damped single-degree of freedom system (equation 3-x) . . . . .	B-1
B.2	The difference equation for a damped single-degree of freedom system (equation 3-xi) . . . . .	B-3

APPENDIX C	-	NOTES ON THE USE OF THE INELASTIC FRAME	
		DYNAMIC ANALYSIS COMPUTER PROGRAM . . . . .	C-1
C.1		Introduction . . . . .	C-1
C.2		The programming language . . . . .	C-1
C.3		Hardware requirements . . . . .	C-1
C.4		General procedures . . . . .	C-2
C.5		The form of the results . . . . .	C-3
C.6		Sign conventions . . . . .	C-4
C.7		The data deck . . . . .	C-6
C.8		The program structure . . . . .	C-14
APPENDIX D	-	COMPUTER PROGRAM LISTING . . . . .	D-1

## LIST OF FIGURES

	Page
2-1 Two simple oscillating systems . . . . .	7
2-2 Three alternative theoretical moment-curvature relationships . . . . .	7
2-3 Moment-time variations for one cycle of three different moment-curvature systems subjected to identical forced displacements . . . . .	9
2-4 The moment-curvature relationship for the steady-state oscillation of an elasto-plastic system . . . . .	11
2-5 The moment-curvature characteristic for one cycle of an idealized weakening elasto-plastic system . . . . .	11
2-6 The proportionate amplitude increase per cycle for a softening elasto-plastic single-mass system of ductility 'a' and plastic moment of resistance reduction factor 'b' . . . . .	13
2-7 A steel joint with a rising spring-rate . . . . .	15
2-8 A prestressed concrete joint with a rising spring-rate. . . . .	15
2-9 The moment - equivalent curvature relationship for the end of the steel beam shown in figure 2-7 . . . . .	17
3-1 Newmark's 'constant average' and 'linear' acceleration approximations for numerical integration . . . . .	26
3-2 Stability criteria for the numerical integration of a damped single degree of freedom system with Newmark's $\beta=1/6$ . . . . .	29
3-3 Verification of the numerical integration stability criteria using the response of a two-mass system . . . . .	31
3-4 Wilson's operator's time-step . . . . .	32
3-5 Comparative elastic responses using different numerical integration methods. . . . .	35
3-6 The algebraic differences between the responses shown in figure 3-5 . . . . .	36
3-7 Variation in response period-error with respect to the integration time-step . . . . .	38
4-1 Numbering patterns for degrees of freedom showing the effect of coupling or slaving . . . . .	42
4-2 The partitioning of the dynamic stiffness matrix . . . . .	42

		Page
4-3	Typical Caughey relationship between damping and natural frequency arising from the specification of the damping at two particular frequencies . . . . .	47
4-4	The beam model . . . . .	48
4-5	Beam plastic hinge model (small deflection theory) . . . . .	50
4-6	Column yield moment-axial load interaction model . . . . .	50
4-7	An example of moment-overshoot in the tracking of a bi-linear moment-curvature hysteresis . . . . .	54
4-8	Typical iterative relaxation at a time-step showing the erroneous disappearance of plastic hinges . . . . .	54
4-9	The effect of a revised iterative method in countering moment-overshoot . . . . .	58
4-10	The effect on a response of different methods for countering moment-overshoot . . . . .	59
4-11	Number of plastic hinges present during a typical inelastic analysis . . . . .	60
4-12	Using a variable time-step in order to avoid moment-overshoot . . . . .	63
5-1	The effect of shear deformation on the elastic line of a beam . . . . .	71
5-2	The effect of shear deformation on a plastic hinge pattern . . . . .	71
5-3	The effect of shear deformation on beam ductilities . . . . .	73
5-4	Matching a Ramberg-Osgood function with a bi-linear hysteresis . . . . .	76
5-5	Comparative displacement responses arising from the use of different beam moment-curvature relationships . . . . .	77
5-6	Comparative moment histories arising from the use of different beam moment-curvature relationships . . . . .	77
5-7	Typical moment-curvature tracks for different hysteretic functions . . . . .	79

6-1	Positions at which plastic hinges formed during the comparative analyses . . . . .	89
6-2	An example of the migration of plastic hinges up a frame during an earthquake (El Centro, May 18, 1940, N-S)	91
6-3	Maximum ductilities of outer beam sections - benchmarks	92
6-4	Maximum ductilities of outer beam sections - scaling by maximum ground accelerations . . . . .	93
6-5	Maximum ductilities of outer beam sections - scaling by a spectral velocity integral . . . . .	94
6-6	Maximum horizontal displacements - benchmark responses . . . . .	95
6-7	Maximum horizontal displacements - scaling by maximum ground accelerations . . . . .	96
6-8	Maximum horizontal displacements - scaling by a spectral velocity integral . . . . .	97
7-1	Durham Street railway overbridge, Christchurch . . . . .	101
7-2	Horizontal displacement responses of railway overbridge decks . . . . .	103
7-3	Relative horizontal displacement responses of railway overbridge decks . . . . .	105
7-4	Auckland upper harbour crossing - pier 5 . . . . .	109
7-5	Horizontal displacement responses of harbour-crossing deck . . . . .	111
7-6	Moment - axial load histories at top of left-hand pile	112
7-7	Moment - axial load histories at base of pier . . . . .	115
A-1	Structure I . . . . .	A-2
A-2	Structure II . . . . .	A-4
C-1	Subroutine structure of program . . . . .	C-16

## LIST OF TABLES

		Page
3-I	The typical natural frequencies of a 'shear' frame .	20
3-II	Basic parameters for analyses investigating integration schemes . . . . .	34
4-I	Solution times for partitioned equations . . . .	45
4-II	Comparison of response peak values (metres) . . .	61
5-I	Sensitivity of natural frequencies to axial and shear deformation . . . . .	69
6-I	Scaling factors for accelerograms . . . . .	85
6-II	Ductility ratios - earthquake scalings by maximum ground accelerations . . . . .	88
6-III	Ductility ratios - earthquake scalings by spectral velocity integral . . . . .	88
6-IV	Ductility ratios - benchmarks . . . . .	88
7-I	Summary of results for Durham Street railway overbridge	107
7-II	Summary of results of analyses of pier 5, transverse direction, Auckland upper harbour crossing . . . .	117

## LIST OF SYMBOLS

Subscripts have been left off those symbols with which their use follows accepted patterns in signifying the members of a series, the members of a vector or the elements of a matrix.

Symbol	
a	Ratio of maximum displacement to that necessary to cause initial yield
b	Factor denoting degradation of a yield plateau
d	Maximum displacement of a steady-state oscillation
f	Spring-hinge stiffness factor
h	Length of piece-wise integration time-step
k	Initial elastic stiffness
n	Number of nodes or joints Number of storeys
r	Radius of curvature of the member next to the plastic hinge Ramberg-Osgood function family indicator
t	Time
x	Displacement General solution
$\hat{x}$	Derived displacement at end of time-step
$\bar{x}$	Assumed displacement at end of time-step
$\ddot{x}_g$	Ground acceleration which is exciting a frame
y	Displacement
A	Arbitrary constant
C	Damping coefficient
D <sub>2</sub>	Diagonal elements of transformed dynamic stiffness
E	Young's modulus of elasticity
F	Denotes a general function
F'	Denotes the first differential of a general function
H	Plastic hinge length
I	Moment of inertia
K	Generalized stiffness
K*	Generalized dynamic stiffness
$\bar{K}$	Modified stiffness
L	Overall length of member
L <sub>22</sub>	Lower triangular section of transformed stiffness matrix

## Symbol

$M$	Mass lumped at a node or joint (i.e. discrete)
	Bending moment
$M_b$	Balanced load bending moment
$M_y$	Yield moment
$P$	Generalized forcing function
$P_b$	Balanced load axial load
$P_{y_c}$	Ultimate axial load (compression)
$P_{y_t}$	Ultimate axial load (tension)
$R$	Force
$\bar{R}$	Transformed force
$S_{12}$	Part of transformed stiffness matrix
$T$	Period of oscillation
$U_{dim}$	Energy tending to diminish a steady-state oscillatory motion
$\alpha$	Mass damping participation factor
	Substituted constant
$\beta$	Stiffness damping participation factor
	Newmark's piece-wise integration constant
$\gamma$	Modified eigenvalue
$\delta$	Denotes a relatively small part of the quantity it precedes
$\epsilon$	Angle of rotation of model plastic hinge
$\theta$	Constant
	Angle
$\lambda$	Fraction of critical damping
$\mu$	Eigenvalue or latent root of equations of motion
$\xi$	Solution to differenced equations of motion
$\pi$	Ratio of a circle's circumference to its diameter
$\rho$	Radius of curvature of equivalent plastic hinge
$\tau$	Wilson's operator's time-step length
$\phi$	Curvature of equivalent plastic hinge
$\phi_y$	Curvature at first yield
$\omega$	Frequency of oscillation
$\Delta$	Denotes an incremental part of the quantity it precedes
$f$	Denotes an unknown function
$\dot{\phantom{x}}, \ddot{\phantom{x}}$	Denote the first and second differentials with respect to time
$\{ \}$	Normally denotes a vector
$[ \ ]$	Normally denotes a matrix



## CHAPTER ONE

INTRODUCTION AND SCOPE OF RESEARCH1.1 INTRODUCTION

The need to allow the elements of a structural frame to plastically deform (both because of the energy absorption capacity thus available and because of the impracticability of constructing frames which will remain linearly elastic under the extremes of the likely ground motion) has led to an appreciation of the need for incorporating detailing for ductility in the final design of the frame.

Although the techniques required for carrying out the rudimentary dynamic analyses of inelastic space frames have been known for some time, it is only recently that codes of practice have acknowledged their existence and, in some cases, gone as far as to require at least an elastic response analysis to be carried out for frames which exceed a certain size. However, because the properties of the materials used in modern construction methods are not precisely known it has been possible for the designer to contend that not only are such analyses likely to be invalid, but also that the resulting design may be the product of the mathematical model chosen, rather than of the conditions which it will, in reality, have to withstand.

Given that a particular frame will have a certain response to a selected excitation, the designer is not very much better off unless he can interpret from this the sensitivity of his structure with regard to the mathematical model he is using, the accuracy of the information he has based it on and the relationship of the excitation both to the type of structure and the site on which it is to be built. Faced with an ever increasing accumulation of variables, it is no wonder that the designer may soon question the validity of any numerical dynamic analysis which may be proposed. Even if he proceeds with the analysis he is still required to interpret meaningfully the results. Most likely he would use a standard computer package program presented to him in the form of a 'black box' and so he would be forced to accept its techniques and restrictions in total without the opportunity to conduct his own series of sensitivity analyses each time.

Because inelastic frame analyses are computationally expensive, it is desirable that the final results be obtained in as few attempts at the analysis as possible.

The prevailing insecurity in inelastic analyses is mirrored in the way in which some modern codes of practice vary in their proposals

as to how to specify standard conditions or determine satisfactory performance. The New Zealand draft loading code [1], for instance, incorporates non-specific ductility requirements into general load factors. The prepared amendments to the City of Los Angeles Code of Building Practice [2] laid down much more specific criteria to be met for both the overall structure and individual members. This bold approach more realistically emphasizes the pertinent areas for careful attention. Because he is entering a new field in which he is rarely able to observe the effect of his judgements on the motion of his structure, the designer needs to be led in his choice of both the analysis procedures and modelling parameters.

## 1.2 THE ART OF IDEALIZATION

The art of mathematical modelling depends very much on the assumption that as the elements of the structure are more precisely represented, so is the validity of the total structural response increased. The sensitivity of the structure to changes or improvements in the structural element is not, however, immediately obvious or simple to predict. In this way, the use of single degree of freedom analytical models in such studies as the effect of stiffness degradation on earthquake ductility requirements by Clough [3] provide an admirable insight into the general significance of the shape of a structural member's moment-curvature hysteresis, but give the designer little reassurance in his decision as to how much significance he should place on this factor when he is confronted with the task of producing a response of a real multi-storey frame. As Liu [4] has pointed out, Clough's results were obtained by deterministic means and are highly dependent on the specific input excitation - thus implying that a non-deterministic or probabilistic method of analysis is necessary for a full study. In a similar fashion, Nickell [5, 6], Weeks [7], Çakiroğlu [38] and others, in evaluating the numerical integration techniques currently available, compare them as they relate to very simple systems. Because of the computational economics involved in applying these techniques to multi-degree of freedom models, it is necessary to evaluate possible refinements in techniques with respect to the overall accuracy being simultaneously obtained in other sections of the modelling.

In the studies of multi-degree of freedom systems that do take place it is obviously necessary to limit the number of variables which are to be evaluated for sensitivity. A major variable in any analysis is, of course, the structure to be used as the vehicle for such sensitivity studies. Hence, many concurrent conclusions are reached by independent

researchers concentrating on different aspects of their models. Cheng [8], for example, showed that axial deformations can significantly affect the eigenvalues of a mathematical model's stiffness matrix, but in doing so he took no account of the similar effect due to shear deformation of elements. On the other hand, Goel [9] found that whereas the P- $\Delta$  effect could influence an elastic response by as much as ten per cent, the corresponding inelastic response is unlikely to be changed by more than one per cent, regardless of the earthquake or building used for the comparison. He then points out that this is about the same change as would be produced by an equivalent modification to the elastic stiffness. It is this type of conclusion that the analyst will wish to remember.

### 1.3 CHOOSING AN EARTHQUAKE

The choice of an earthquake record for use in a deterministic analysis is, because of the seemingly infinite variations possible in its characteristics, the source of most concern once an acceptable analytical model has been decided upon. Many generalities can be stated about different families of earthquakes. An earthquake which produces a response spectrum with its major peaks in the short-period range, can be expected to cause larger deformations in the stiffer and lower structures than in those with longer natural periods. Built into an earthquake record are factors which are dependent upon the intrinsic properties of the recording site. Only by the use of micro-zoning techniques is it possible to consider the matching of a particular recorded excitation with that to be used in the analysis of a proposed structure on a specific site. Microzoning will not, however, be of much use in predicting the magnitude of the expected shock and so a statistical approach is needed. By translating the statistics of earthquake occurrence into energy-of-excitation terms Shinozuka [10] has, for example, presented a method by which a least favourable seismic structural response could be found. Even if this sort of information was freely available, an engineer trying to produce an economic design is likely to be hesitant in using and quoting a probabilistic approach which gives a least favourable response - unless he is sure that his structure is capable of withstanding it.

In using any idealized stiffness relationship for a deterministic analysis of a multi-degree of freedom frame, the existence of a threshold in the response is encountered if the frame is allowed to become partly inelastic. Unlike that of an elastic seismic analysis, the response is not proportional to the earthquake intensity. This effect is most clearly defined in the more simple structures, rather than in those which require

many plastic hinges to be developed before a collapse mechanism can be approached. This threshold between linear and non-linear behaviour manifests itself most markedly if comparisons are made between responses of a frame to one excitation scaled to a number of different intensities. Clough and Benuska [11] have shown analytical examples of this using a short section of the comparatively well-known El Centro, May 18, 1940 (North-South component) earthquake record. The complexity of the problem is apparent when it is realized that the significance of the use of a short record (thereby allowing comparatively few members to make excursions into their plastic ranges) is unknown. In the same study it was noticed that the 'whip-lash' effect in the upper storeys of a frame varied little with increasing earthquake intensity, although some proportionality in deflections was maintained at lower levels. These apparent incongruities are typical of the many which will inevitably surround such sensitivity analyses.

#### 1.4 SCOPE OF THE RESEARCH

In order to carry out the appropriate sensitivity analyses a computer program capable of considerable flexibility and generality was needed. The only inelastic frame analysis program readily available to the author was that developed by Walpole [12], but this contained many restrictive features and was generally unamenable (because of its structural idealizations) to those modifications which would be required. The computing capability available to a programmer is a real restriction on him and so the program that was subsequently produced was written to fit an IBM 360/44 computer with 128k bytes of core storage. Just as development was completed a Burroughs B6718 with virtual memory became available and the program, because of the limited time available, was adapted to the new system without any concerted effort to take every advantage of its special features. A fundamental aim during the design of the program was to introduce as much flexibility as possible (in terms of the geometric complexity of the frame to be input) while retaining the ability to check for, and edit out where possible, incompatible data. It was recognized that, because the program was to be used by researchers and engineers other than the programmer, as much use as possible should be made of the computer's ability to condense results into a partly pictorial form - as was achieved in describing the positions of the frame's plastic hinges. Although an essentially practical analysis method was being sought, it was necessary to evaluate, constantly, the accuracy and economy of each feature of generality introduced with respect to other features upon which

it depended. The result is a program which could certainly be made computationally just a little more economic (if stringent restrictions were to be placed on the modelling of the structure to be analysed) while remaining sufficiently flexible for possible use as the basis of future sensitivity studies.

It was originally hoped that the development of the program would merely provide a research tool which would then be used for sensitivity studies on the accepted variables encountered in any seismic inelastic dynamic analysis, but it was discovered that there was inconclusive evidence as to which were the most suitable mathematical modelling techniques for even the most fundamental parts of any practical dynamic analysis. Such basic items as the choice of a suitable numerical integration method should not concern the user of this type of program - yet it was to become increasingly obvious that these questions had to be resolved before the sensitivity of the modelling of a structure could be assessed.

The study of the sensitivity of simple inelastic framed structures to variations in the representation of their geometric and materials is therefore, of necessity, introductory by nature. Emphasis has been placed on producing economical solutions to highly complex processes. To have extended the scope of the study to other than two-dimensional frames would have been premature, in view of the lack of a satisfactory comprehension of the behaviour of the more simple cases. By choosing actual designs as illustrative examples in the section on special structures, the benefit of a reliable analysis method is shown in situations where there may have been no alternative solutions available to the designer.

It is intended to clarify, using a practical approach, the state of the art of deterministic inelastic analyses, in order that a more confident use can be made of them as they are progressively introduced by way of building-code requirements.

## CHAPTER TWO

THE MOMENT-CURVATURE RELATIONSHIP2.1 INTRODUCTION

In this chapter the importance of the moment-curvature relationship in determining the response of an inelastic member to a dynamic excitation is shown. Although it is difficult to include accurately even a simple hysteretic relationship in a deterministic dynamic analysis, it is of interest to see which aspects of its shape are the more important in achieving the maximum fidelity in the response. Because the relationship between the overall response of a multi-degree of freedom model and that of each of its constituent members is a complex one, a single degree of freedom system is chosen to exhibit the characteristics of various force-deflection hystereses. It is, nevertheless, possible to gauge qualitatively the general effect, in terms of energy storage and dissipation, that similar individual members will have on the whole structure's response.

After showing the detrimental effect of weakening sections on the response of most of those structural members which may become inelastic in resisting seismic forces, the possibility of special members with increasing spring-rates is introduced.

2.2 THE SHAPE OF THE MOMENT-CURVATURE RELATIONSHIP

Two possible trends which may exist in the behaviour of a structural member which contains a section with variable stiffness, can be clearly demonstrated by the two schematic models of figure 2-1. The inverted pendulum (figure 2-1a) which is supported by two compressible rollers will, when set in motion, continue to oscillate freely as the rollers alternatively slip down the narrowing slots with each cycle. In doing this, the oscillator's natural frequency will decrease, whilst the amplitude of motion increases as the rollers settle progressively into a limiting position of equilibrium. The second model (figure 2-1b) has, on the other hand, its spring member confined to the environs of a trumpet-shaped buffer so that its effective length is shortened and spring-rate increased with increasing deflection. Obviously, this oscillator cannot be resonated by a harmonic excitation to its base (even in the absence of damping) and its motion will, under normal damping conditions, decay very quickly. The behaviour characteristic of the first model would be detrimental to the stability of a structure if it were to occur in its members. Once excited, it would shake itself down until it was a

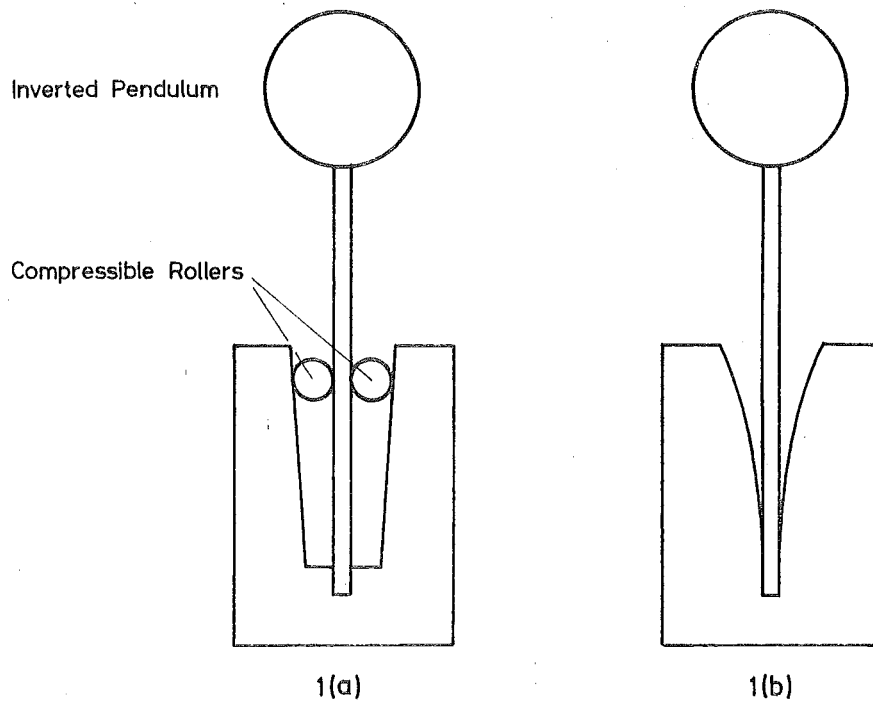


FIGURE 2-1 : TWO SIMPLE OSCILLATING SYSTEMS.

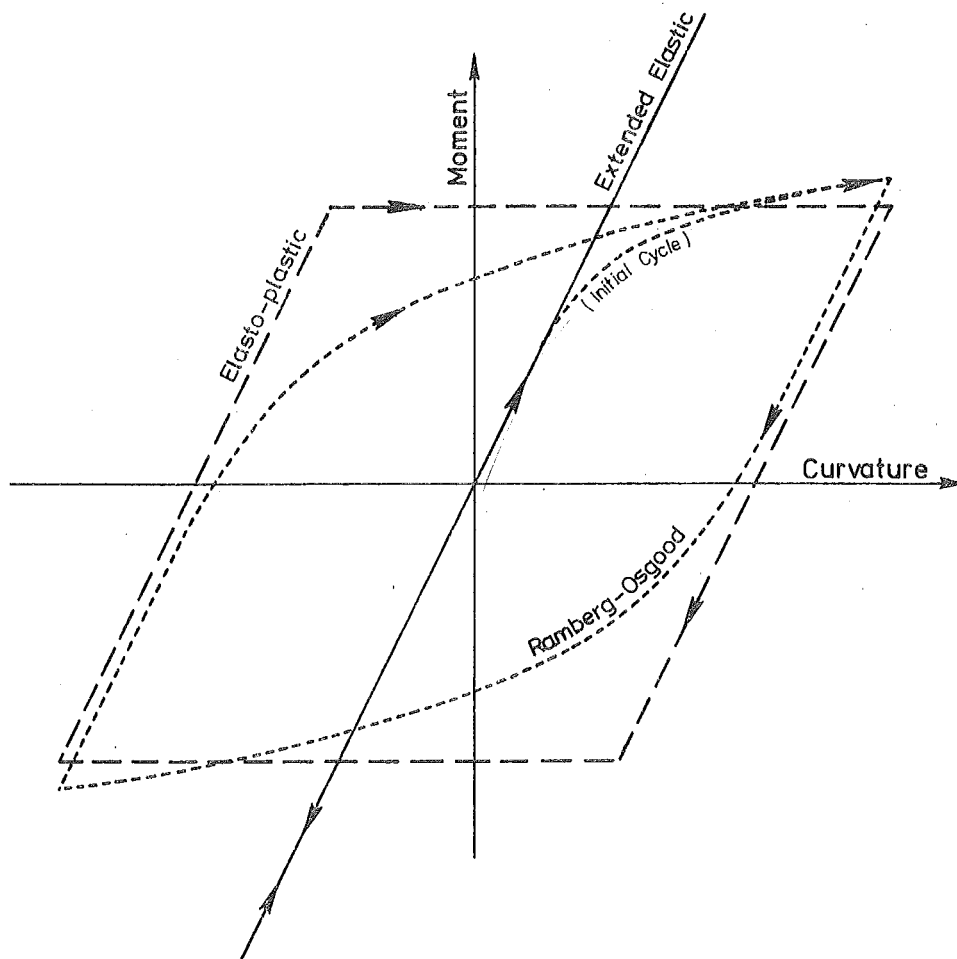


FIGURE 2-2 : THREE ALTERNATIVE THEORETICAL MOMENT-CURVATURE RELATIONSHIPS.

more flexible structure. Both systems, however, have no energy absorption capability, even though they are non-linear by nature.

If, on the other hand, the force-displacement relationship for a simple system is such that its loading path is different to that of its unloading path, then some expenditure or a release of energy will take place during its motion. For ordinary structural members this hysteretic relationship will result in some energy of motion being expended. It can easily be shown that the area enclosed by a force-displacement (c.f. moment-curvature) hysteresis is related to the amount of energy being stored and released by the system. As a development of this concept it is helpful to consider the time over which this energy is being transferred - as can be detailed in a plot of the applied force against time.

In figure 2-2 three alternative moment-curvature relationships are illustrated. These are

- a) a linear relationship,
- b) an elasto-plastic relationship - this being the particular case of a bi-linear function where the system has only a finite limited resistance which, on being reached, allows unbounded deflection to take place,
- c) one which follows a Ramberg-Osgood function (see chapter four).

It is helpful to consider a non-linear system as being primarily an (extended) elastic one, with additional external forces being applied to force it to conform to its non-linear response. In this case, the difference in ordinates of the elastic and one of the non-linear curves of figure 2-3 represents the instantaneous value of the necessary external force during the steady-state excitation of a system with the alternative moment-curvature variations of figure 2-2. The shaded areas, which represent the corrective force-time quantity, show the extent of the duration of the equivalent external loadings. Horizontal shading indicates that the external loadings are trying to increase the amplitude of motion, whereas the vertical shading indicates a diminishing amplitude being effected.

It is emphasized that the consideration of corrective external forces is conceptual only and does not directly relate to the physical resistance of the section being considered. It does, however, provide a vehicle for establishing the importance of the form of the force-displacement relationship. A comparison of the size of the two types of shaded areas over one cycle of the motion shows that, although the magnitude of the equivalent external forces may be large, their effective-



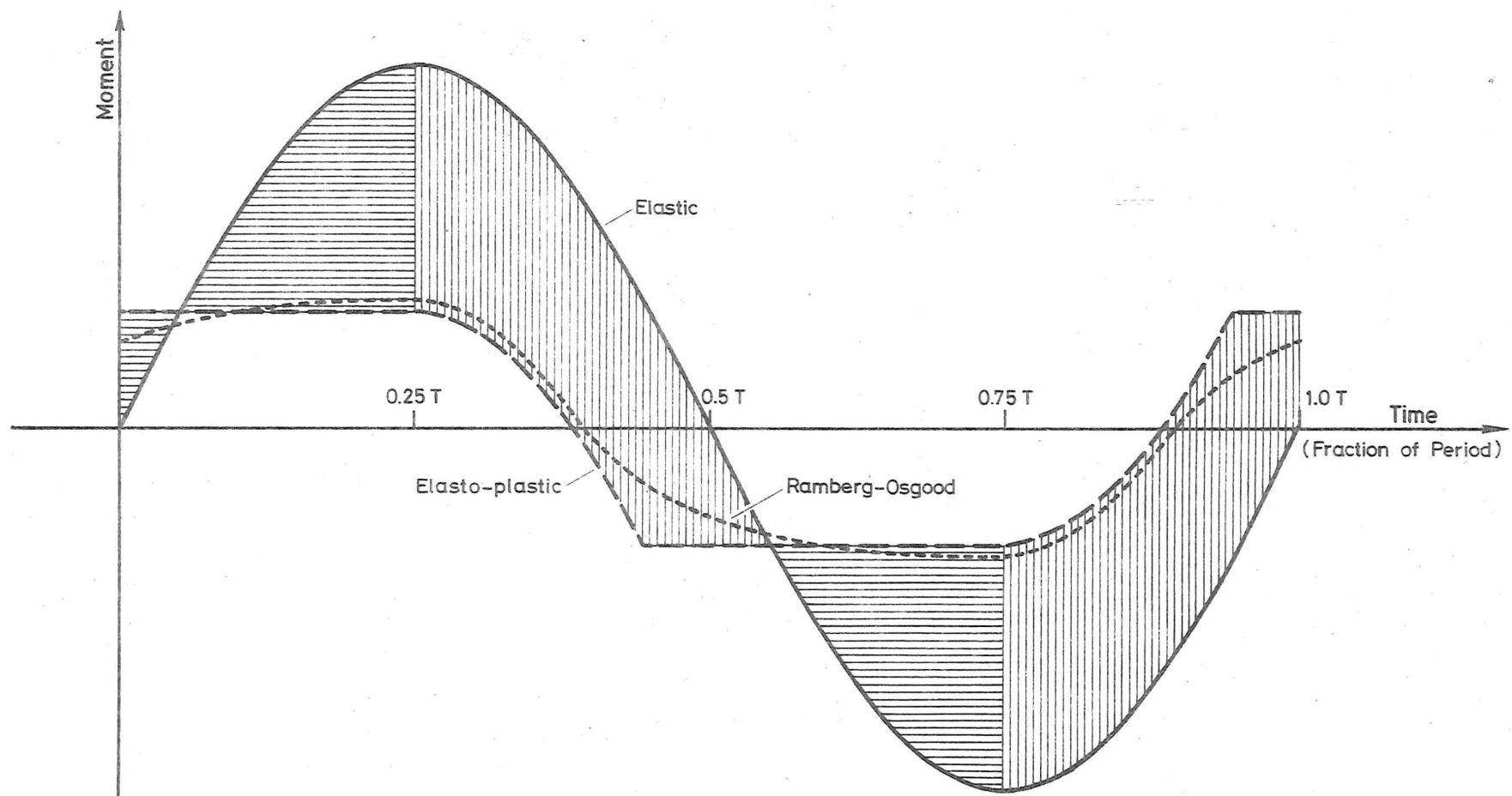


FIGURE 2-3 : MOMENT-TIME VARIATIONS FOR ONE CYCLE OF THREE DIFFERENT MOMENT-CURVATURE SYSTEMS SUBJECTED TO IDENTICAL FORCED DISPLACEMENTS.

ness will be related to their net effect, which may be the widely fluctuating difference between two large quantities. The selection of the force-displacement function is therefore paramount in determining this overall effect.

In order to measure further the significance of the shape of the force-displacement relationship, it is convenient to calculate, for a single-degree of freedom oscillator with elasto-plastic stiffness characteristics, the net amount of energy per cycle which is tending to reduce the amplitude of motion. Using the principle that the work done by a system is the product of the force and the displacement through which it moves, it can be shown that the energy tending to diminish a steady-state motion is the area of the hysteretic loop (figure 2-4) which is...

$$U_{\text{dim}} = \frac{4kd^2}{a} \left(1 - \frac{1}{a}\right)$$

where k = the (initial) elastic stiffness  
 d = the maximum displacement  
 a = the ratio of maximum displacement  
 to that necessary to cause initial  
 yield.

It follows that the more narrow the hysteresis, the less is the ability of the oscillator to absorb the energy being fed into it. A structural member, therefore, whose section hysteresees exhibit similar narrow characteristics, can only play an insignificant role in absorbing the energy of motion present in the dynamically excited frame.

The difficulty that a weakening member has in maintaining its energy-absorption can be demonstrated by a similar theoretical study of a simple elasto-plastic system, subjected to a steady-state oscillation but with a yield plateau which diminishes with each reversal of the load. One loading cycle for such a system is illustrated by figure 2-5. If the system is to be capable of absorbing the same amount of energy per cycle, regardless of the diminishing yield level, then the amplitude of the motion must increase in compensation. While assuming that the frequency of oscillation remains constant, the yield plateau level is allowed to decrease by a fraction 'b' of its previous value at each reversal of the direction of loading. Hence, two such reductions occur during each cycle. If the initially measured excursion into the plastic range produces a ductility of 'a' (where ductility is defined as the ratio of the maximum displacement to that required to cause first yield), then the equating

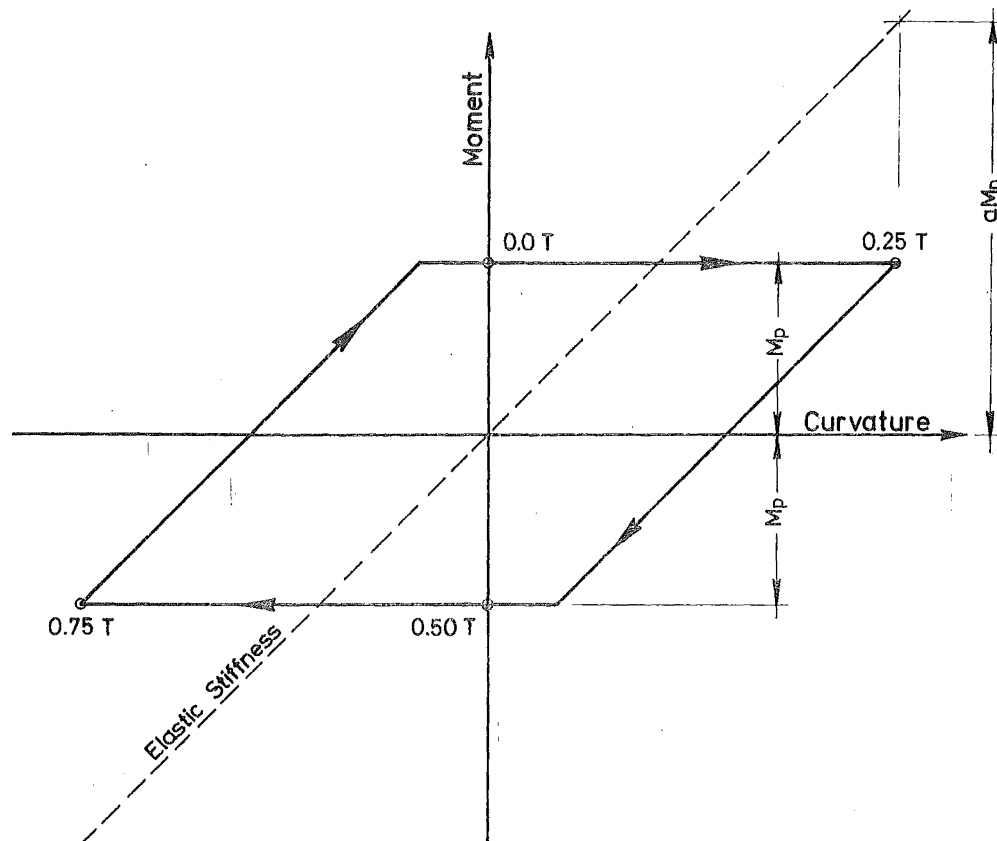


FIGURE 2-4: THE MOMENT-CURVATURE RELATIONSHIP FOR THE STEADY-STATE OSCILLATION OF AN ELASTO-PLASTIC SYSTEM.

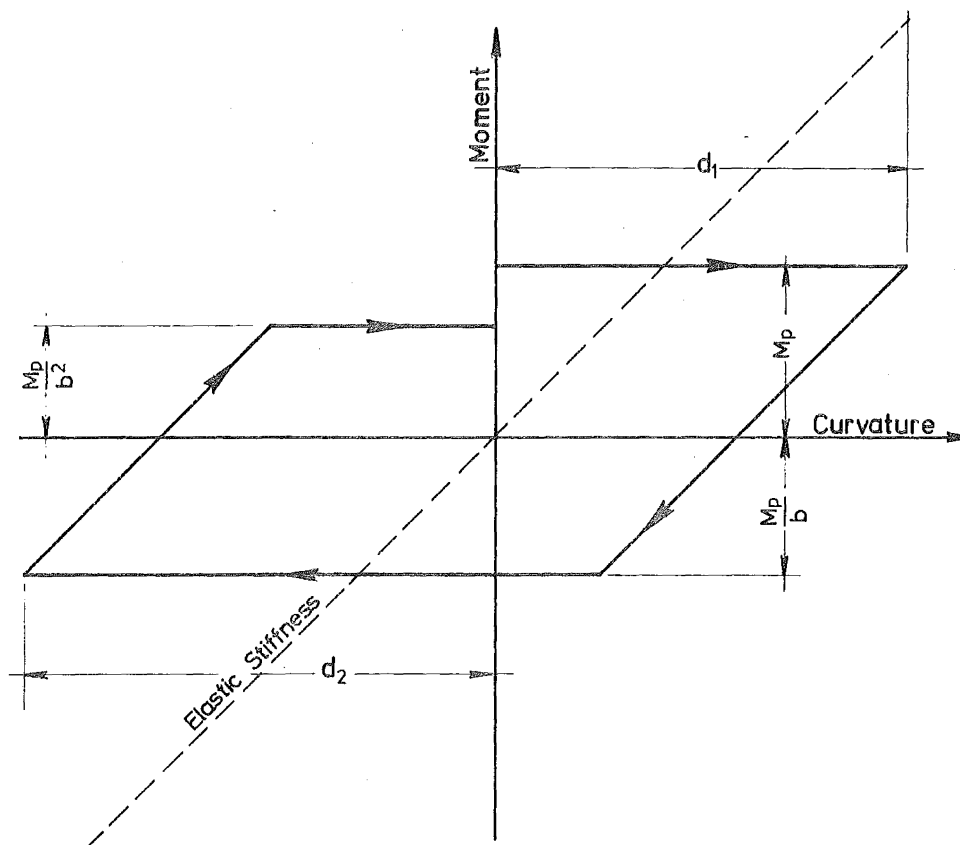


FIGURE 2-5: THE MOMENT-CURVATURE CHARACTERISTIC FOR ONE CYCLE OF AN IDEALIZED WEAKENING ELASTO-PLASTIC SYSTEM.

of the relationships giving the energy absorbed in each half-cycle gives...

$$\frac{d_2}{d_1} = \left[ 3 - \frac{7b^4 - 2b^3 - 2b^2 - 2b - 1 + 2ab^3}{2ab^4} \right] \frac{b^2}{1+b}$$

where  $d_1$ ,  $d_2$  are the respective maximum displacements (amplitudes) occurring in successive half-cycles. In a typical case where a member section's plastic moment of resistance is reduced by a factor of 9.89% (i.e.  $b=1.10$ ) and a section ductility of four is reached in the first half-cycle, an increase in maximum curvature of 10.8% is required if the same rate of energy absorption is to remain constant through the second half-cycle.

Further values of proportionate amplitude increases are shown (for a range of typical values) in figure 2-6. The results presented so far express the weakening effect of one cycle only. Providing that the same rate of weakening exists over the duration of several cycles, then the maximum deflection required to maintain a constant rate of energy absorption will increase according to a geometric progression. The corollary of this effect is just as important to a designer. The contribution which a member can make to the structure's resistance to dynamic excitation will fall off rapidly with the number of load reversals that the critical section experiences.

The complete reaction of a structural frame, composed of members which conform to one or more types of load-deflection functions, depends on a wider set of variables than those pertaining to the functions alone. In particular, the equivalent viscous damping inherent in the frame and the susceptibility of the particular frame to the particular excitation will both play significant roles in the production of the overall response.

### 2.3 CONCLUSIONS AS TO THE ACCURACY REQUIRED

Without attempting to relate quantitatively the effect of each attribute of a possible member load-deflection relationship on the final structural response, it can still be stated that its shape will be of sufficient significance so as to require as much care as possible in the attempt to model the behaviour of the member as built. The energy dissipation capabilities of a member which will progressively weaken with repeated loading, are seen to fall off drastically, even if the weakening per loading reversal is small. The importance of representing the load-deflection relationship as some sort of hysteretic (or looping) function

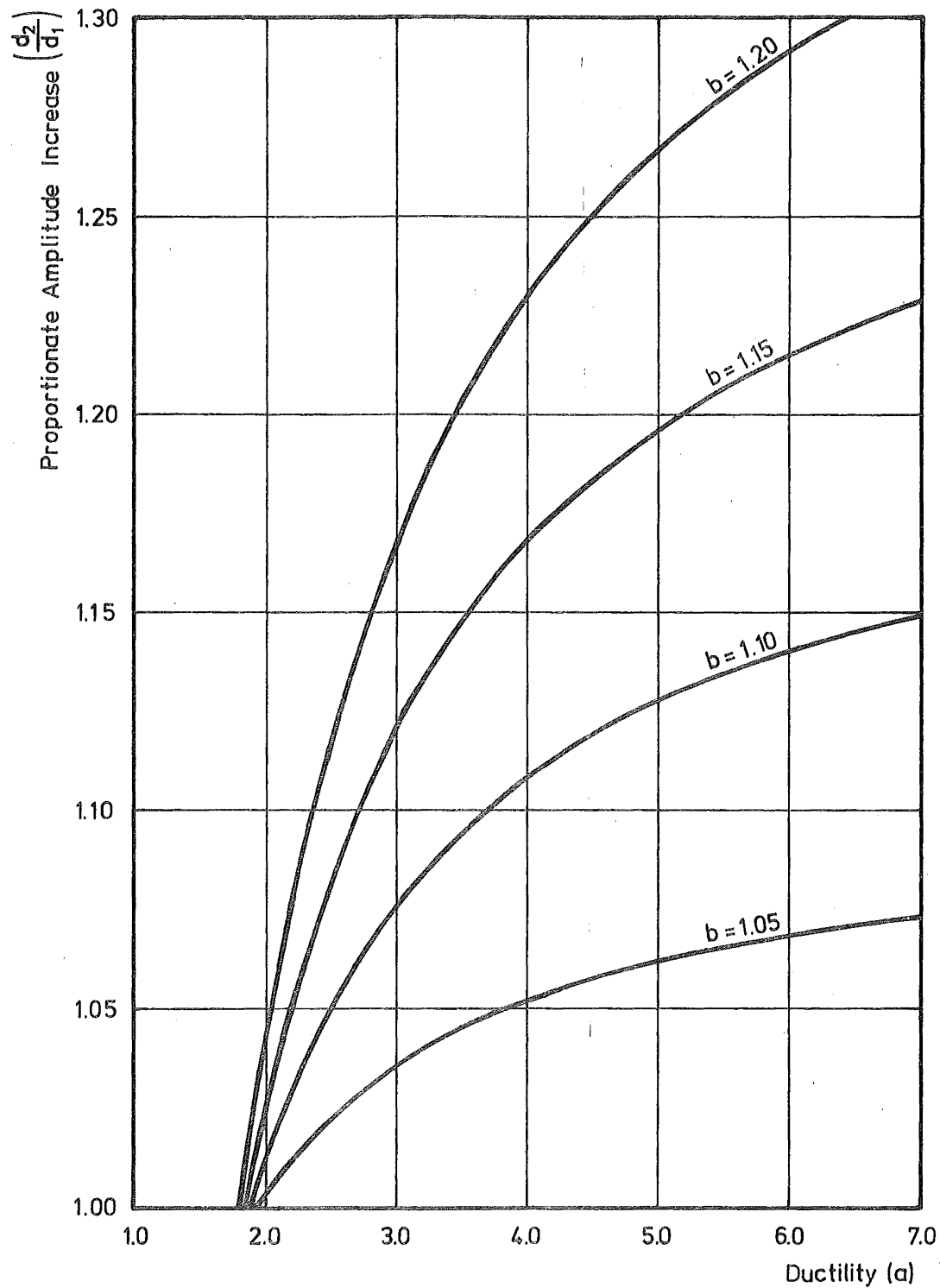


FIGURE 2-6 : THE PROPORTIONATE AMPLITUDE INCREASE PER CYCLE FOR A SOFTENING ELASTO-PLASTIC SINGLE-MASS SYSTEM OF DUCTILITY 'α' AND PLASTIC MOMENT OF RESISTANCE REDUCTION FACTOR 'b'.

is evident in the bearing that the width of such an hysteresis also has on the contribution the member can make to inelastic damping through energy absorption. In a wider sense, it can be seen that apparently small variations in the general shape of the chosen function may disclose an unexpectedly large sensitivity in the response.

At the level of this study, any attempt to try and quantify more explicitly the sensitivity of a structure to changes in its elemental force-displacement characteristics is not justified - on the grounds that the effect of other influences in the analysis have not been sufficiently isolated.

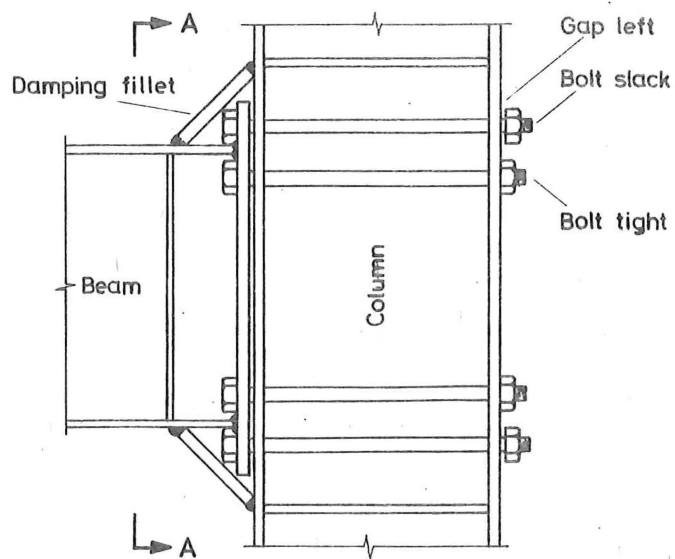
## 2.4 MEMBERS WITH RISING SPRING-RATES

### 2.4.1 Principle

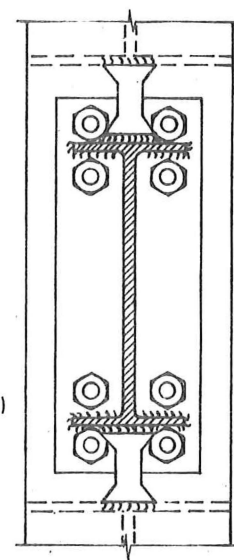
The deterioration of both the stiffness and strength of conventional structural members under cycling into the post-elastic range immediately raises the question of how the characteristics of the member can be altered to avoid one or both of these detrimental features. The most obvious answer is to design members which exhibit more favourable characteristics. As for the single-degree of freedom oscillator of figure 2-1b, it is possible to theorize as to a joint detail which will effectively result in the critical member section becoming progressively stiffer as the section moment is increased. If this effect can be combined with the ability to absorb reasonable amounts of energy, then it would be possible to design a frame which, like the oscillator in the trumpet-shaped cone, would not be susceptible to resonance - even in the absence of conventional damping. Garden and the author [13] have hypothesized as to what such joint details may look like. Their examples (figures 2-7, 2-8) have the advantage of being simple in concept and design.

### 2.4.2 A steel joint with rising spring-rate

The steel design (figure 2-7) offered for consideration has angled mild-steel fillets welded between the beam and column on both beam flanges. These are required to provide initial damping, through energy absorption, by yielding before the ultimate strength of the joint itself is reached. By leaving a number of the connecting bolts slack at erection time, an increased stiffness is achieved when the rotation of the beam relative to the column brings these into tension. Although difficulties will arise if the joint is cycled post-elastically so that the bolts yield, it is submitted that, in concept, superior characteristics are produced in the lower load range.

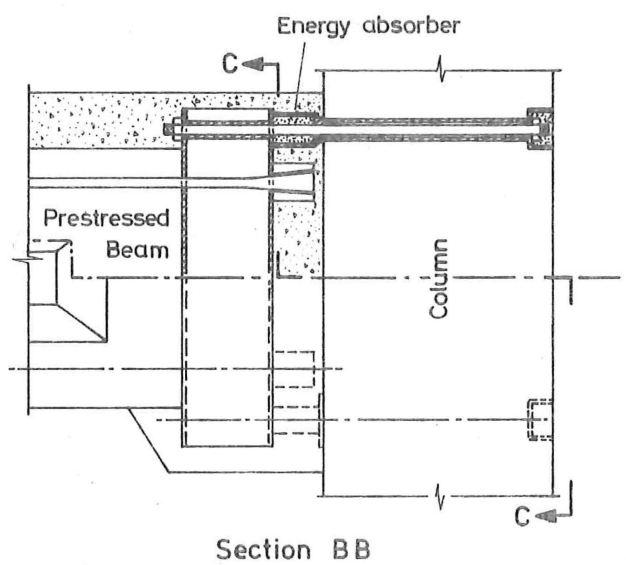


(Stiffener omitted for clarity)

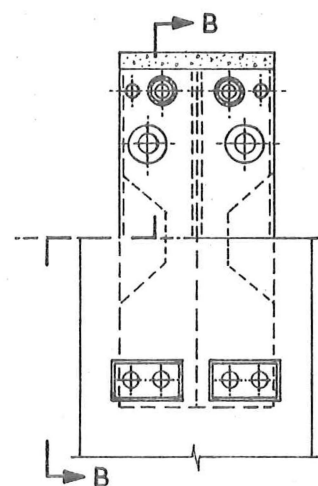


Section AA

FIGURE 2-7 : A STEEL JOINT WITH A RISING SPRING-RATE.



Section BB



Section CC

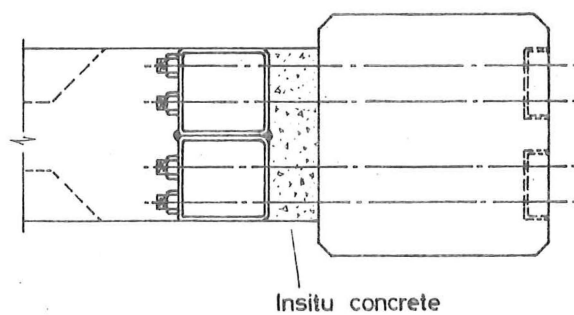


FIGURE 2-8 : A PRESTRESSED CONCRETE JOINT WITH A RISING SPRING-RATE.

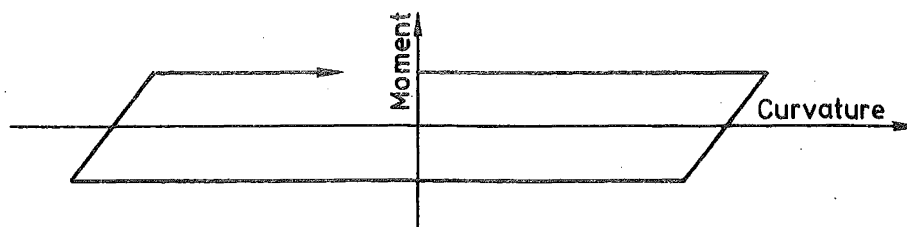
#### 2.4.3 A prestressed concrete joint with rising spring-rate

The undoubted extra cost that would be involved in producing the prestressed concrete beam-column joint (figure 2-8) could possibly be offset by the corresponding reduction in assembly cost, through less skill being required for this operation. Use is made of the high energy-absorption, available when concrete is forced to crush within a confining steel cylinder, in order to produce a fatter moment-curvature hysteresis. As with the steel joint, initially slack high-tensile bolts could be used to provide an increase in stiffness after a predetermined level of strain had been reached.

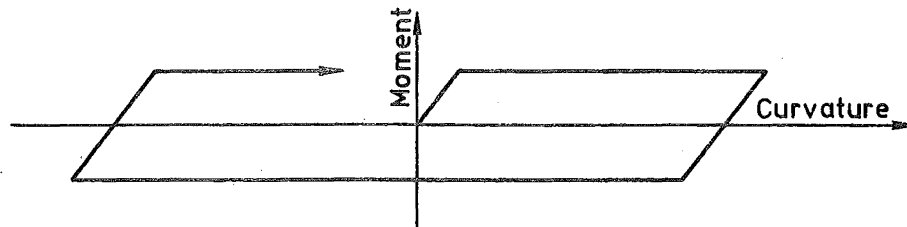
#### 2.4.4 Possibilities for further research

By showing that it is feasible to consider incorporating particularly desirable features into otherwise conventional member joints, the way is open for a separate research project to proceed in order to confirm the physical practicability of such ideas. The development of a cheap system which would allow the early development of a significant amount of damping at the critical joints or member sections would assist greatly in reducing the likely response of the frame. If moment-curvature relationships, such as that in figure 2-9d (which is a compound of those of the joint's elements), can be forced to occur, then the deleterious effect of long or repeated earthquakes causing 'shake-down' of a structure could be reduced. Such sacrificial components as may be necessary to achieve such behaviour, should be kept as simple and as accessible as possible to allow economic repairs to be made.

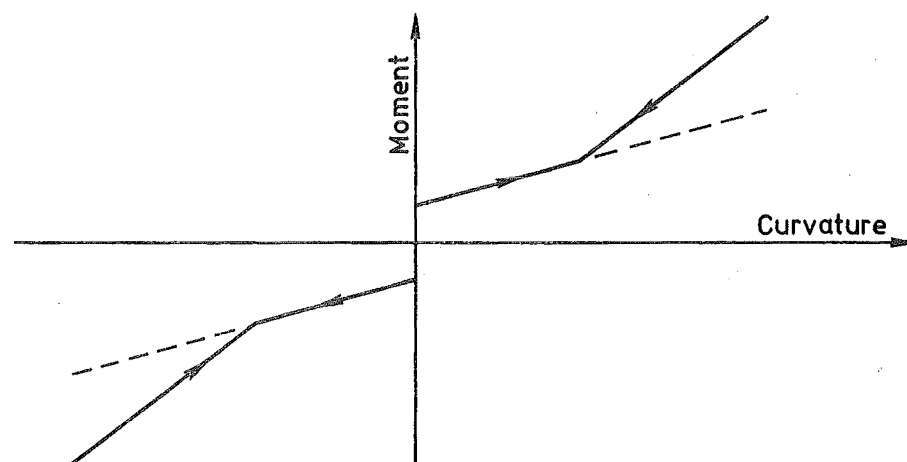




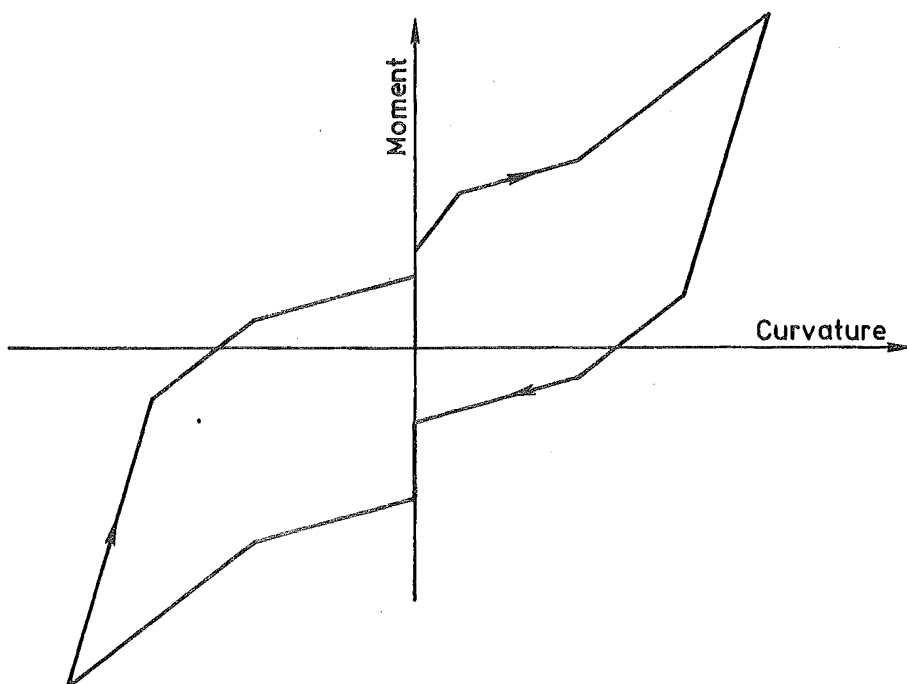
a). Contribution of plastic fillets in compression.



b). Contribution of plastic fillets in tension.



c). Contribution of both tight and initially slack bolts.



d). Combined characteristics of joint components.

FIGURE 2-9 : THE MOMENT - EQUIVALENT CURVATURE RELATIONSHIP FOR THE END OF THE STEEL BEAM SHOWN IN FIGURE 2-7.

## CHAPTER THREE

NUMERICAL INTEGRATION TECHNIQUES3.1 INTRODUCTION

An analysis to obtain the forced response of an elastic structure is commonly achieved by the step-by-step forward integration of the equations of motion for selected normal modes of vibration of the structure. In such a case it is usual for the major part of the final response to be dependent on those of the first few (i.e. those with the lowest frequencies of free vibration) modes. Hence, for most civil engineering structures likely to be so analysed, there has been little problem with the integration time-step being of the same order as that of the natural periods of the system being considered. Requirements for the stability of the integration technique have not been as severe a criteria as those for the accurate representation of the forcing function - this being, in a seismic analysis, the digitised accelerogram of an earthquake.

As the elastic superposition of modal responses does not apply in an inelastic dynamic analysis, the overall response is necessarily obtained implicitly, or explicitly, by the direct integration, in a piece-wise manner, of all the equations of motion of the structure. In this case, every one of the natural modes latently affects the mathematical integration procedure, and so there is a much greater chance of the higher modes of typical structures having periods of free vibration of the same order of magnitude as that time-step which would be considered otherwise adequate for an elastic analysis.

Some techniques, such as that involving the assumption of a constant average acceleration over the duration of a time-step, have the advantage of being unconditionally stable, but all of them involve, for realistic time-step sizes, varying degrees of error propagation due to phase shift, implicit equivalent damping and/or amplitude modification.

The use of explicit procedures for earthquake analyses is, at the moment, precluded by the brevity of the time-step required for the analysis of typical (framed) structures. Where the time-history is short, as in impulse- or shock-loading, this brevity is not such a practical limitation.

Previous studies by Nickell and others [5, 14, 15, 16] have tended to concentrate on the suitability of integration approximation operators in handling a sinusoidal forcing function. This allows an analytical solution to be used as a benchmark for the appraisal of the different

schemes. As, in general, a forcing function and the response of the structure to it can both be expressed as some combination of sinusoidal motions, this is a valid approach. However, such studies reveal little about the relative magnitude of error in the significant modes of the structure when the total response is produced.

### 3.2 REQUIREMENTS OF A SATISFACTORY TECHNIQUE

The foremost requirement is that the solution remains stable for a time-step which is large enough to make computational times an economic proposition for a forcing function of realistic length. If this can be achieved, then the next most important consideration is that errors in the response be kept to a minimum. If the artificial damping induced by a particular integration technique can be approximately assessed, then this can be allowed for when estimates of the inherent equivalent viscous damping in the real structure being modelled are sought. Phase shifts in the response, if small in relation to the fundamental periods of the structure, will normally be of little significance.

### 3.3 NATURAL MODES

The number of natural modes of undamped free vibration present in a system is equal to the number of uncoupled degrees of freedom which have associated masses. It is then up to the modeller to choose judiciously which (and how many) will be included. Walpole [12] chose to consider only the lateral mass at each floor. Thus, for a regular two-dimensional frame, there would be as many modes as there were storeys. In the particular case of a tall and regular 'shear' frame the highest natural frequency is approximately...

$$(2n-1)\omega_1$$

where  $\omega_1$  is the fundamental frequency

and  $n$  is the number of storeys.

Table 3-I illustrates the range of frequencies exhibited by such a thirteen-storey shear frame (adapted from structure II - appendix A). For such a frame, the range of frequencies does not approach a value which would give a natural period comparable to that used in digitising the earthquake accelerogram (i.e. approximately 1/80 sec.) or to that commonly used in a numerical integration scheme. The variation in column stiffness over the height of the frame has caused the frequencies predicted by the approximation formula to be less applicable.

Mode n	Frequency (Hz)	$(2n-1)\omega_1$
1	4.17	4.17
2	12.2	12.5
3	20.1	20.8
4	27.8	29.2
5	35.1	37.5
6	41.9	45.9
7	48.0	54.2
8	53.8	62.6
9	58.5	70.9
10	62.6	79.3
11	65.5	87.5
12	68.2	96.0
13	71.0	104.

TABLE 3-I : THE TYPICAL NATURAL FREQUENCIES OF A 'SHEAR' FRAME.

If instead of the lateral mass being lumped at each floor it is considered to be lumped at each joint or node (as is necessary with any non-rectangular frame), the resulting natural modes include some which are associated with the dilatory movement of masses at opposite ends of a floor beam or slab connecting member. Their natural frequencies are related to the axial compression-wave velocity of the connecting members and can, therefore, be several orders of magnitude larger than those of the simple translational modes of the frame. For example, the frequency of axial vibration of a selected reinforced concrete spandrel beam with a cross-section 1.10 by 0.40 metres, length of 3 metres and cantilevered with a mass of 50 000 kilograms at one end, is approximately 45 Hz. The fundamental frequency of this same frame from which this member was selected is of the order of 2 Hz.

In a likewise manner, if masses are associated with the vertical degrees of freedom of the nodes, then the integration procedure must also cope with modes of vibration arising from the axial elongation of columns. Even if a vertical ground acceleration is not applied to the frame, vertical accelerations will still occur in flexible frames as a result of the column extensions which arise from the horizontal response. The consideration of rotational degrees of freedom creates similar problems.

### 3.4 SLAVING OF SIMILAR DEGREES OF FREEDOM

In certain situations, such as in the analysis of rectangular frames, the effect of the inter-nodal internal vibration of beams can be realistically eliminated by the judicial coupling (or slaving of one to the other) of similar degrees of freedom. In particular, the horizontal degrees of freedom associated with each of the floor joints of one storey can be often coupled, without introducing any significant error, as the inter-joint deflection in such a system is rarely significant. In this way the flexibility of approach to the modelling of the frame is not lost.

The major disadvantage of slaving is in the extending of the bandwidth of non-zero coefficients in the stiffness matrix.

### 3.5 PHANTOM FREQUENCIES

#### 3.5.1 The phenomenon

If a degree of freedom is set up without an associated mass coefficient, but is allowed to attract damping forces in proportion to its velocity, some of the implicit integration schemes are found to be unconditionally unstable for a time-step satisfying the criteria for the stability (see section 3.6.2) of the piece-wise numerical integration of the undamped system. Although a degree of freedom which has no mass and attracts no damping is not an independent variable, this would not, at first, appear to preclude it from attracting forces other than from its stiffness (to linear displacement). By the preclusion of such damping forces a sensible and stable solution is obtained.

On first examination it would seem that, by allowing the formerly dependent degree of freedom to attract velocity-related forces, it is being forced to become independently variable. Thus, it is effectively bringing into play another natural mode of vibration whose frequency is high enough to transgress the previous stability criteria as it applies to the selection of a reasonable time-step. If this is so, it would then be appropriate to calculate the natural frequencies of these 'phantom' modes. Newmark [15] offered the following method of taking into account damping where the associated mass is zero.

" a) Assume a value of acceleration of the mass point even though the mass is zero.

b) Compute the velocity and displacement of the point and determine the damping force.

c) Now apply the net resistance, corresponding to the difference between the applied force and the damping force, to the structure and determine the displacements of the structure at all points when the prescribed displacements are put in at the points where masses exist.

d) Compute the acceleration at the end of the interval that is required to give the displacement determined in the preceding step.

e) Compare the acceleration so computed with the one initially assumed and repeat if necessary."

As Newmark pointed out, this procedure is considerably more complex than that for a massed degree of freedom. The introduction of an iteration into each step of the piece-wise integration is computationally uneconomic if the problem could possibly be handled explicitly.

### 3.5.2 An analysis of the effect of non-massed degrees of freedom

The effect of having non-massed degrees of freedom can be investigated analytically. The basic equations of free vibration of a viscously damped linear system can be represented, using d'Alembert's principle and matrix notation, by...

$$[M]\{\ddot{x}\} + [C]\{\dot{x}\} + [K]\{x\} = \{0\} \quad (3-i)$$

a solution of which, has the form  $\{x\} = A\{e^{\mu t}\}$

It follows that...  $\{\dot{x}\} = \mu\{x\}$

and...  $\{\ddot{x}\} = \mu\{\dot{x}\}$

Hence...  $\mu[M]\{\dot{x}\} + [C]\{\dot{x}\} + [K]\{x\} = \{0\}$

$$\text{i.e.} \quad \begin{bmatrix} \cdot & I \\ -K & -C \end{bmatrix} \begin{Bmatrix} x \\ \dot{x} \end{Bmatrix} = \mu \begin{bmatrix} I & \cdot \\ \cdot & M \end{bmatrix} \begin{Bmatrix} x \\ \dot{x} \end{Bmatrix} \quad (3-ii)$$

where  $\mu$  is an eigenvalue, or latent root, of the equation (the number of roots being twice the number of independent variables in the system). If the system is undamped, an eigenvalue is equivalent to minus the square of the angular frequency of a natural mode. If  $\{x\}$  is expanded to  $\begin{Bmatrix} x_1 \\ x_2 \end{Bmatrix}$  then (3-ii) becomes...

$$\left[ \begin{array}{cc|cc} \cdot & \cdot & I & \cdot \\ \cdot & \cdot & \cdot & I \\ \hline -K_{11} & -K_{12} & -C_{11} & -C_{12} \\ -K_{21} & -K_{22} & -C_{21} & -C_{22} \end{array} \right] \begin{Bmatrix} x_1 \\ x_2 \\ \dot{x}_1 \\ \dot{x}_2 \end{Bmatrix} = \mu \left[ \begin{array}{cc|cc} I & \cdot & \cdot & \cdot \\ \cdot & I & \cdot & \cdot \\ \hline \cdot & \cdot & M_1 & \cdot \\ \cdot & \cdot & \cdot & M_2 \end{array} \right] \begin{Bmatrix} x_1 \\ x_2 \\ \dot{x}_1 \\ \dot{x}_2 \end{Bmatrix} \quad (3-iii)$$

Walpole [12] assumes that  $C_{12} = C_{21} = C_{22} = M_2 = 0$ , where the subscript 2 refers to the unmassed degrees of freedom.

$$\text{i.e.} \quad \left[ \begin{array}{cc|cc} \cdot & \cdot & I & \cdot \\ \cdot & \cdot & \cdot & I \\ \hline -K_{11} & -K_{12} & -C_{11} & \cdot \\ -K_{21} & -K_{22} & \cdot & \cdot \end{array} \right] \begin{Bmatrix} x_1 \\ x_2 \\ \dot{x}_1 \\ \dot{x}_2 \end{Bmatrix} = \mu \left[ \begin{array}{cc|cc} I & \cdot & \cdot & \cdot \\ \cdot & I & \cdot & \cdot \\ \hline \cdot & \cdot & M_1 & \cdot \\ \cdot & \cdot & \cdot & M_2 \end{array} \right] \begin{Bmatrix} x_1 \\ x_2 \\ \dot{x}_1 \\ \dot{x}_2 \end{Bmatrix}$$

which condenses to...

$$\left[ \begin{array}{c|c} \cdot & I \\ \hline -\bar{K}_{11} & -C_{11} \end{array} \right] \begin{Bmatrix} x_1 \\ \dot{x}_1 \end{Bmatrix} = \mu \left[ \begin{array}{c|c} I & \cdot \\ \hline \cdot & M_1 \end{array} \right] \begin{Bmatrix} x_1 \\ \dot{x}_1 \end{Bmatrix}$$

where

$$[\bar{K}_{11}] = [K_{11}] - [K_{12}][K_{22}]^{-1}[K_{21}]$$

However, if degrees of freedom without associated masses are allowed to attract damping, then...

$$\left[ \begin{array}{cc|cc} \cdot & \cdot & I & \cdot \\ \cdot & \cdot & \cdot & I \\ \hline -K_{11} & -K_{12} & -C_{11} & -C_{12} \\ -K_{21} & -K_{22} & -C_{21} & -C_{12} \end{array} \right] \begin{Bmatrix} x_1 \\ x_2 \\ \dot{x}_1 \\ \dot{x}_2 \end{Bmatrix} = \mu \left[ \begin{array}{cc|cc} I & \cdot & \cdot & \cdot \\ \cdot & I & \cdot & \cdot \\ \hline \cdot & \cdot & M_1 & \cdot \\ \cdot & \cdot & \cdot & \cdot \end{array} \right] \begin{Bmatrix} x_1 \\ x_2 \\ \dot{x}_1 \\ \dot{x}_2 \end{Bmatrix}$$

As the full number of eigenvalues are still present, it is necessary to find the value of those associated with the 'massless' modes. This is best achieved by considering the solution for the eigenvalues in the limit as the mass  $M_2$  tends to zero.

The full equation (3-iii) can be rewritten as...

$$\left[ \begin{array}{cc|cc} -\mu I & \cdot & I & \cdot \\ \cdot & -\mu I & \cdot & I \\ \hline -K_{11} & -K_{12} & -C_{11} - \mu M_1 & -C_{12} \\ -K_{21} & -K_{22} & -C_{21} & -C_{22} - \mu M_2 \end{array} \right] \begin{Bmatrix} x_1 \\ x_2 \\ \dot{x}_1 \\ \dot{x}_2 \end{Bmatrix} = \begin{Bmatrix} 0 \\ 0 \\ 0 \\ 0 \end{Bmatrix}$$

By carrying out operations to the matrix rows and making the substitutions...

$$[C] = \alpha[M] + \beta[K] \text{ and } [\bar{K}_{11}] = [K_{11}] - [K_{12}][K_{22}]^{-1}[K_{21}]$$

it can be shown that...

$$\left[ \begin{array}{cc|cc} \bar{K}_{11} + (\alpha+\mu)\mu M_1 + \beta\mu\bar{K}_{11} & & -(\alpha+\mu)\mu K_{12}K_{22}^{-1}M_2 & \\ & & & \\ \hline -K_{21} - \beta\mu K_{21} & & -K_{22} - (\alpha+\mu)\mu M_2 - \beta\mu K_{22} & \end{array} \right] \begin{Bmatrix} x_1 \\ x_2 \end{Bmatrix} = \begin{Bmatrix} 0 \\ 0 \end{Bmatrix} \quad (3-iv)$$

For a non-trivial solution the determinant of the above equation (3-iv) is zero,

$$\text{i.e., } |M_1^{-1}\bar{K}_{11} + \gamma^2 I| | -K_{22} - \gamma^2 M_2 | - |K_{21} - \gamma^2 M_1^{-1} K_{12} K_{22}^{-1} M_2| = 0$$

$$\text{where } \gamma^2 = \frac{\mu(\alpha + \mu)}{1 + \beta\mu} \quad (3-v)$$

For simplicity, if a two-degree of freedom system with masses  $M_1$  and  $M_2$ , respectively, is now considered, then it can be shown, where the natural frequency associated with the mass 'M', is  $\omega_1^2 = -\frac{\bar{K}_{11}}{M_1}$ , that...

$$\gamma^4 M_2 + \gamma^2 \left[ K_{22} - \omega_1^2 M_2 + \frac{K_{21} K_{12}}{K_{22}} \times \frac{M_2}{M_1} \right] - \omega_1^2 K_{22} = 0$$

$$\text{i.e. } \gamma^2 = \frac{1}{2} \left[ -\frac{K_{22}}{M_2} + \omega_1^2 - \frac{K_{21} K_{12}}{K_{22} M_1} \right] \pm \frac{1}{2} \sqrt{\left[ -\frac{K_{22}}{M_2} + \omega_1^2 - \frac{K_{21} K_{12}}{K_{22} M_1} \right]^2 + \frac{4\omega_1^2}{K_{22} M_2}}$$

By inspection, at least one solution of  $\gamma^2$  is infinite in the limit as  $M_2$  tends to zero. Hence, from (3-v), one value of the eigenvalue  $\mu$  is also infinite. The system, therefore, has at least one natural mode with zero period.

In extending this concept back to a multi-degree of freedom system, it can be seen that the integration procedure is required to handle a system which, in its unreduced form, will have modes with zero period if some of the degrees of freedom have no mass associated with them, but are still allowed to attract velocity damping. A procedure which is unconditionally stable with respect to integration time-step length is therefore the only type which would be satisfactory. The constant average acceleration method (see chapter 3.7) fulfills this condition and its performance was verified in practice.



### 3.6 NON-OSCILLATORY MODES OF VIBRATION

#### 3.6.1 Supercritically damped modes

As the refinement of the modelling of structures for dynamic analyses continues more degrees of freedom need to be recognised in the model. These extra degrees of freedom have associated natural modes of vibration. In a framed structure, such as those being considered in this study, most of these extra modes correspond to the relative axial motions of the ends of members. The natural frequencies of these modes, when compared to those of the lateral modes of vibration, are high because they depend on the axial dilation-wave velocity of the member material.

Proponents of Newmark's [15] linear ( $\beta=1/6$ ) acceleration method (figure 3-1) for numerical integration, who prefer it to other methods because of its seemingly realistic physical representation of the motion of the structure, find that they are forced by the criteria for a stable solution (which is a function of the ratio of the integration time-step to the smallest natural period present) to specify a computationally uneconomic time-step.

It would seem reasonable to assume that, if, owing to the type of algorithm chosen to represent the system's viscous damping, some of the modes having the higher natural frequencies were supercritically damped, then these might be ignored in satisfying a solution's stability criteria. Critical damping is, by definition, that amount of damping required to enable the freely vibrating system to return to rest in the fastest possible time. Modes with greater than critical damping are, therefore, non-oscillatory and have a motion of the form  $f(\sinh \omega t)$ . Trial analyses, with a time-step based on the stability criteria corresponding to the highest sub-critically damped mode, have shown, however, that instability still occurs.

#### 3.6.2 The stability criteria for a damped system

Newmark's classical work [15] on the stability and convergence criteria to be satisfied in the numerical integration procedure deals only with the undamped single-degree of freedom system. A parallel derivation can be made for a damped single-degree of freedom system. The general equation of motion for a forced system is...

$$M\ddot{x} + C\dot{x} + Kx = P$$

which, for the case of free vibration, reduces to...

$$M\ddot{x} + C\dot{x} + Kx = 0 \quad (3-vi)$$

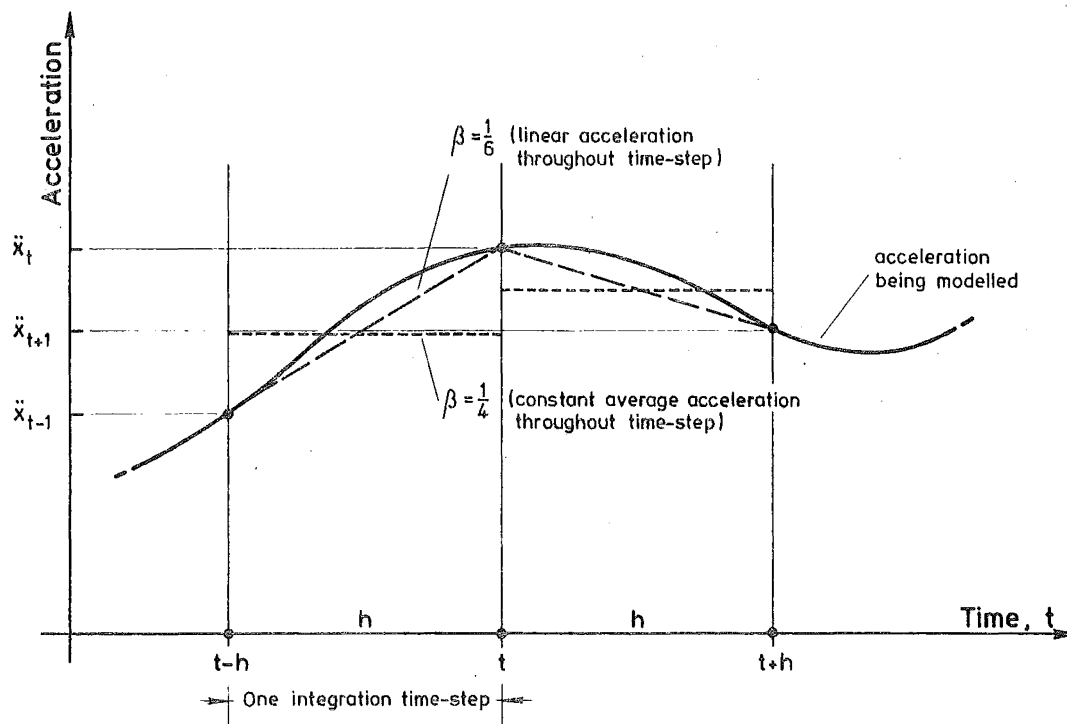


FIGURE 3-1 : NEWMARK'S 'CONSTANT AVERAGE' AND 'LINEAR' ACCELERATION APPROXIMATIONS FOR NUMERICAL INTEGRATION.

The stability of the solution to this depends on the complementary function, as the particular integral is related to the forcing function and, hence, will be stable. Only the more simple homogeneous case need, therefore, be considered. The fraction of critical damping,  $\lambda$ , is introduced as...

$$C = 2\omega\lambda M \quad (3-vii)$$

where  $\omega$  = the angular undamped frequency.

Newmark's two difference equations, (3-viii) and (3-ix), in which the

$$\dot{x}_{t+1} = \dot{x}_t + \ddot{x}_t \frac{h}{2} + \ddot{x}_{t+1} \frac{h}{2} \quad (3-viii)$$

$$x_{t+1} = x_t + \dot{x}_t h + \left(\frac{1}{2} - \beta\right) \ddot{x}_t h^2 + \beta \ddot{x}_{t+1} h^2 \quad (3-ix)$$

(  $x_t$  is the displacement at time 't', etc.,  
and 'h' is the time-step length).

parameter  $\beta$  is introduced to indicate how much of the acceleration at the end of the time-step will be taken into account in the velocity and displacement relations, can then be used with (3-vii) to produce a criteria for convergence of an iterative process which solves for the conditions at the end of the interval. For convergence...

$$\frac{\text{error in derived acceleration}}{\text{error in assumed acceleration}} \leq 1$$

$$\text{i.e.} \quad \frac{\text{derived acceleration} - \text{true acceleration}}{\text{assumed acceleration} - \text{true acceleration}} \leq 1 \quad \text{where the}$$

accelerations are those at the end of the time-step. The derived acceleration is calculated (equation 3-vi) from the derived velocity and displacement, which are the result of the assumed acceleration (equations 3-viii, 3-ix). This leads (appendix B) to...

$$\frac{h}{T} \leq \frac{1}{2\pi} \sqrt{\frac{1}{\beta}} \cdot \left[ \frac{1}{2\sqrt{\beta}} \cdot (-\lambda + \sqrt{\lambda^2 + 4\beta}) \right] \quad (3-x)$$

where 'T' is the period of the system. For the undamped ( $\lambda = 0$ ) case, this reduces to the criteria shown by Newmark...

$$\frac{h}{T} \leq \frac{1}{2\pi} \sqrt{\frac{1}{\beta}}$$

By extending Newmark's derivation for the undamped system, a parallel stability criteria can be found for the damped situation. The recursive equation representing the motion of the undamped system is...

$$x_{t+1} - (2-\alpha^2)x_t + x_{t-1} = 0$$

where  $\alpha^2 = \frac{\theta^2}{1+\beta\theta^2}$ ,  $\theta = \omega h$  and  $t-1$ ,  $t$ ,  $t+1$  are the ends of successive time-steps. A similar equation can be derived (appendix B) for the damped system...

$$\left(1 + \frac{\alpha^2\lambda}{\theta}\right)x_{t+1} - (2 - \alpha^2)x_t + \left(1 - \frac{\alpha^2\lambda}{\theta}\right)x_{t-1} = 0 \quad (3-xi)$$

It can be shown (Brand [17] and Fox [18]) that, where 'A' is a constant,

$$x = f(t) = A\xi^t$$

is a solution for this second-order difference equation. Hence, it is true that...

$$\left(1 + \frac{\alpha^2\lambda}{\theta}\right)\xi^{t+1} - (2 - \alpha^2)\xi^t + \left(1 - \frac{\alpha^2\lambda}{\theta}\right)\xi^{t-1} = 0$$

i.e.

$$\xi_{1,2} = \frac{(2-\alpha^2) \pm \sqrt{(2-\alpha^2)^2 - 4\left(1 - \frac{\alpha^2\lambda}{\theta}\right)}}{2\left(1 + \frac{\alpha^2\lambda}{\theta}\right)} \quad (3-xii)$$

There being two simultaneous solutions for  $\xi$ , it follows that, for the non-trivial case ( $\xi_1 \neq \xi_2$ ), the stability of the solution for 'x' is dependent on either both  $\xi_1$  and  $\xi_2$  being complex, or their respective moduli each being less than unity. For a complex solution to equation (3-xi) it follows from (3-xii) that...

$$(2-\alpha^2)^2 - 4\left(1 - \frac{\alpha^2\lambda}{\theta}\right) < 0$$

i.e.

$$\frac{h}{T} < \frac{1/\pi}{\sqrt{1-4\beta}} \cdot \sqrt{1-\lambda^2} \quad (3-xiii)$$

For the undamped ( $\lambda = 0$ ) system, this reduces to Newmark's relationship...

$$\frac{h}{T} < \frac{1/\pi}{\sqrt{1-4\beta}} \quad (3-xiv)$$

The overall stability criteria for the linear acceleration ( $\beta = 1/6$ ) method can be represented best by a plot (figure 3-2) of the fraction of critical damping,  $\lambda$ , against the ratio of time-step to natural period,  $\frac{h}{T}$ . Critical stability is unaffected by the amount of damping of the system and remains at  $\frac{h}{T} = \frac{\sqrt{3}}{\pi}$  because it can be shown that for

$$\lambda^2 > 1 - \frac{\pi^2 h^2}{3T^2}$$

where

$$0 < \frac{h}{T} < \frac{\sqrt{3}}{\pi}$$

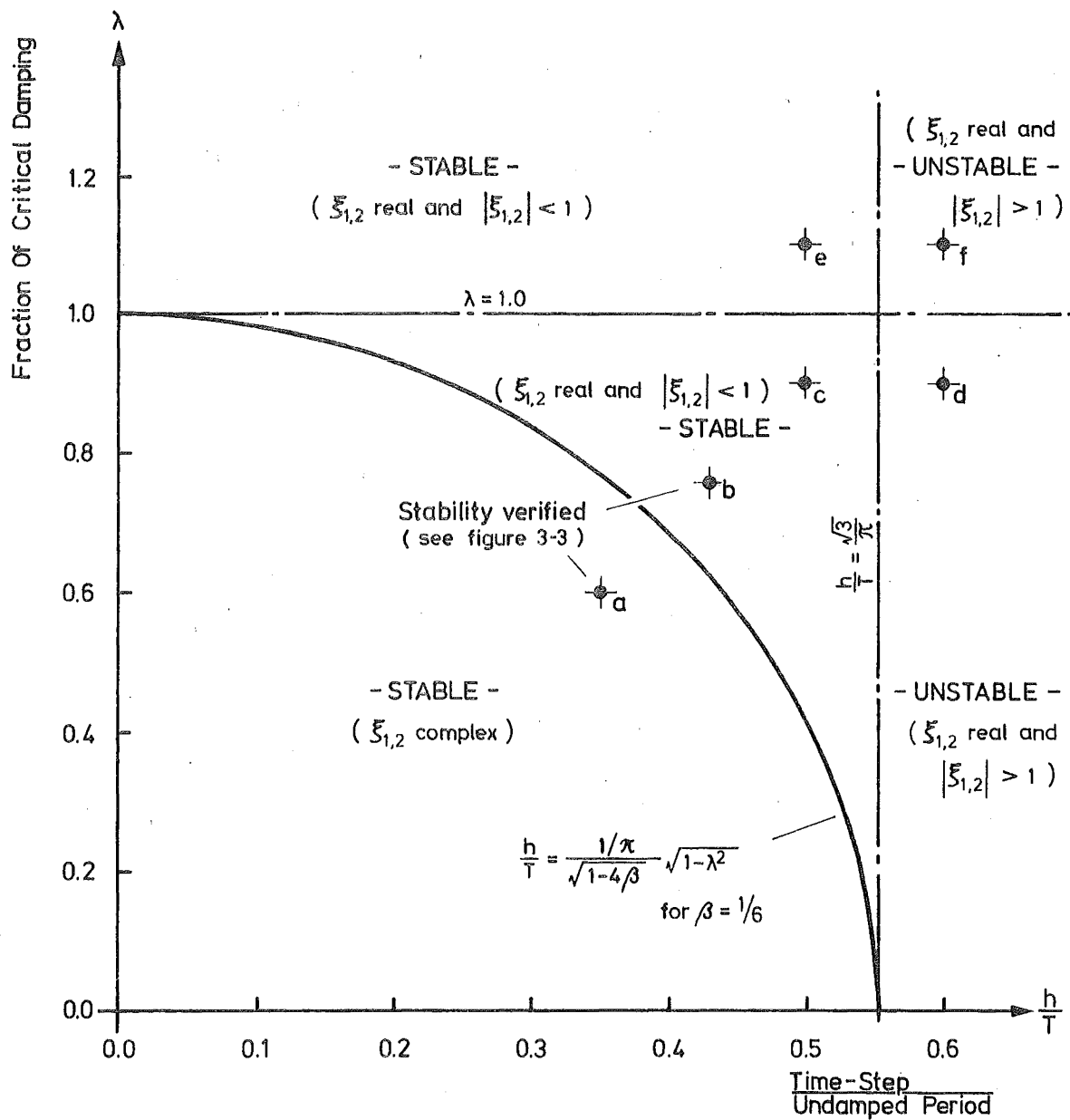


FIGURE 3-2: STABILITY CRITERIA FOR THE NUMERICAL INTEGRATION OF A DAMPED SINGLE DEGREE OF FREEDOM SYSTEM WITH NEWMARK'S  $\beta = 1/6$ .

$|\xi_1|, |\xi_2|$  are each less than unity - this also being sufficient for equation (3-xi) to have a stable solution, although with real roots. Verification of this stability criteria is shown in the six responses (figure 3-3) of a two-mass system (with undamped natural frequencies of 1.56 and 8.43 Hz), each response being derived using a different value of damping and integration time-step. Each of these responses, as shown in figure 3-2, corresponds to a different area of this stability criteria.

Unfortunately, this results in the linear acceleration approach being much less economic for use with those systems where member material dilation-wave velocities produce high natural frequencies - even though they may be highly damped. On the other hand, the constant average acceleration method (figure 3-1), for which  $\beta = 1/4$ , is seen from equation (3-xiii) to be still unconditionally stable for the damped system and so, despite its inherent velocity errors and its lack of an attractive physical representation of the acceleration response, it is the more economic model for such analyses.

### 3.7 CONSIDERATION OF APPROXIMATION OPERATORS

#### 3.7.1 Introduction

The step-by-step forward integration of the equations of motion involves the assumption of a relationship defining the motion at the end of the time-step with respect to that at its beginning. Unless a costly iterative procedure is used at each time-step, instead of a single cycle, then some error will inevitably be attracted, which may, in some cases, accumulate sufficiently to swamp the analysis. Nickell [5, 6] has shown the relative accuracy of the different schemes, developed by Newmark and Wilson, when they are applied to a steady-state sinusoidal forcing function. Such comparisons show clearly the period and amplitude errors likely, as well as any phase-shift that may occur.

If, however, a multi-degree of freedom system is being integrated, it is obviously important to know what the combined effect of each of the modes' amplitude-errors, period-errors and phase-shifts is likely to be. A technique, which may have certain dominant tendencies when used for integrating a system comprised of only one undamped degree of freedom, may be found to emphasize one particular feature when the combined response of a more complex system is calculated.

The integration relationships for three different values of Newmark's [15] and two types of Wilson's averaging operators [19] were compared for a medium-size system.

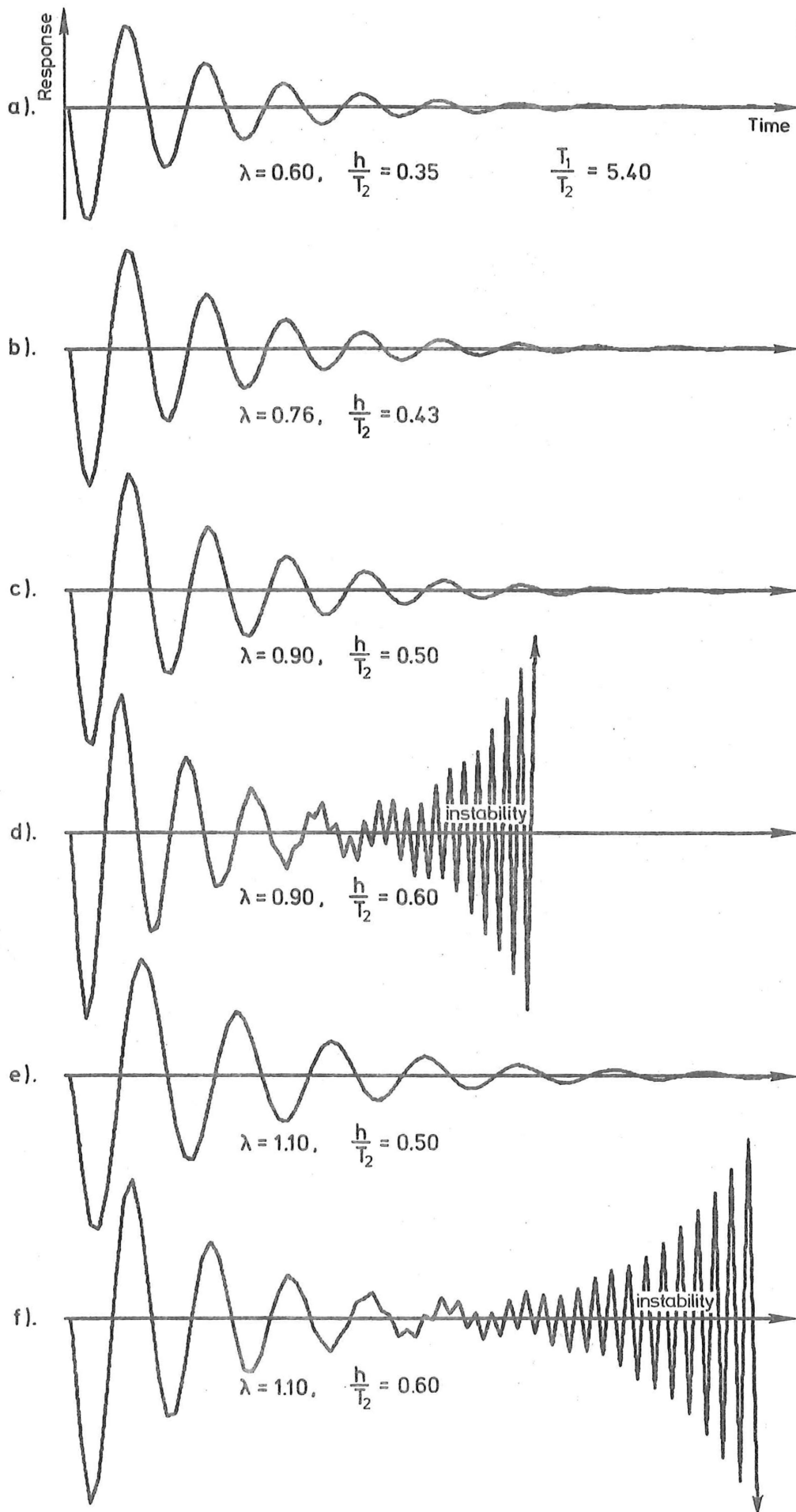


FIGURE 3-3 : VERIFICATION OF THE NUMERICAL INTEGRATION STABILITY CRITERIA USING THE RESPONSE OF A TWO-MASS SYSTEM.

### 3.7.2 The algorithms

A set of algorithms which embraces all the relevant variations of these relationships can be constructed. D'Alembert's principle for the forced motion of a multi-degree of freedom system gives (in matrix notation)...

$$[M]\{\ddot{x}\} + [C]\{\dot{x}\} + [K]\{x\} = -[M]\{\ddot{x}_g\}$$

The corresponding incremental system is given by...

$$[M]\{\Delta\ddot{x}\} + [C]\{\Delta\dot{x}\} + [K]\{\Delta x\} = -[M]\{\Delta\ddot{x}_g\} \quad (3-xv)$$

A scalar,  $\tau$ , is defined (figure 3-4) as being the time-step for Wilson's averaging operator technique. Hence, when Newmark's methods are being used,  $\tau$  equals 'h', the standard time-step length. Wilson's averaging operator assumes linear acceleration during the time-step  $\tau$ .

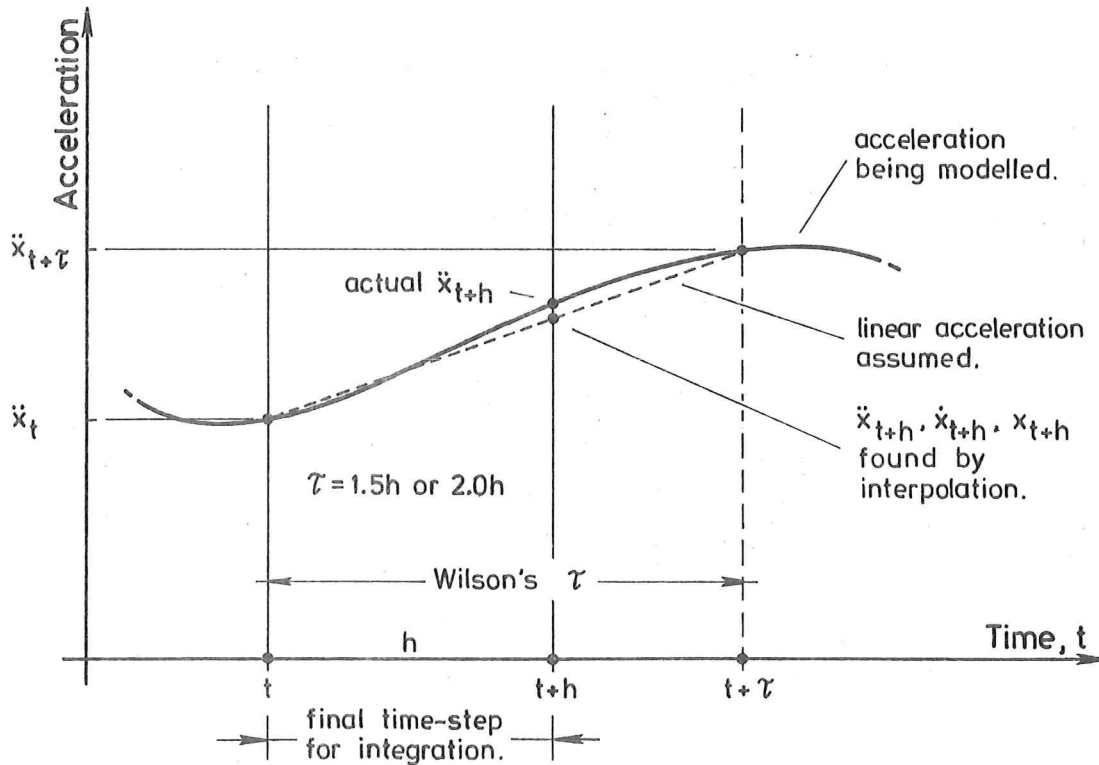


FIGURE 3-4 : WILSON'S OPERATOR'S TIME-STEP.

The algorithms are a series of difference equations which depend on the assumption as to the variation in the acceleration of the masses of the system over any time-step. The form of the variation is controlled by the parameter  $\beta$ .

In the general case, (3-xv) becomes...

$$[M]\{\Delta\ddot{x}\}_\tau + [C]\{\Delta\dot{x}\}_\tau + [K]\{\Delta x\}_\tau = -[M]\{\Delta\ddot{x}_g\}_\tau \quad (3-xvi)$$



where the notation  $\{ \}_\tau$  indicates that the increment is over a time-step of length  $\tau$ , starting at time 't'.

The following incremental equations can be derived from (3-viii) and (3-ix)...

$$\{\Delta \ddot{x}\}_\tau = \frac{1}{\beta \tau^2} \{\Delta x\}_\tau - \frac{1}{\beta \tau} \{\dot{x}_t\} - \frac{1}{2\beta} \{\ddot{x}_t\}$$

$$\{\Delta \dot{x}\}_\tau = \frac{1}{2\beta \tau} \{\Delta x\}_\tau - \frac{1}{2\beta} \{\dot{x}_t\} + \frac{\tau}{2\beta} (2\beta - \frac{1}{2}) \{\ddot{x}_t\}$$

The incremental displacement that would have occurred over time  $\tau$  is then found from (3-xvi), which gives directly...

$$\{\Delta x\}_\tau = [K^*]^{-1} \{\Delta R\}$$

$$\text{where } [K^*] = \frac{1}{\beta \tau^2} [M] + \frac{1}{2\beta \tau} [C] + [K]$$

$$\begin{aligned} \text{and } \{\Delta R\} &= -[M] \left\{ \{\Delta \ddot{x}_g\}_\tau - \frac{1}{\beta \tau} \{\dot{x}_t\} - \frac{1}{2\beta} \{\ddot{x}_t\} \right\} \\ &\quad - [C] \left\{ -\frac{1}{2\beta} \{\dot{x}_t\} + \frac{\tau}{2\beta} (2\beta - \frac{1}{2}) \{\ddot{x}_t\} \right\} \end{aligned}$$

$$(3-ix) \text{ gives } \{\Delta x\}_h = \beta h^2 \left\{ \{\Delta \ddot{x}\}_h + \frac{1}{\beta h} \{\dot{x}_t\} + \frac{1}{2\beta} \{\ddot{x}_t\} \right\}$$

$$\text{and } \{\Delta x\}_\tau = \beta \tau^2 \left\{ \{\Delta \ddot{x}\}_\tau + \frac{1}{\beta \tau} \{\dot{x}_t\} + \frac{1}{2\beta} \{\ddot{x}_t\} \right\}$$

$$\begin{aligned} \text{hence } \{\Delta x\}_h &= \beta h^2 \left\{ \frac{h}{\tau} \left[ \frac{1}{\beta \tau^2} \{\Delta x\}_\tau - \frac{1}{\beta \tau} \{\dot{x}_t\} - \frac{1}{2\beta} \{\ddot{x}_t\} \right] \right. \\ &\quad \left. + \frac{1}{\beta h} \{\dot{x}_t\} + \frac{1}{2\beta} \{\ddot{x}_t\} \right\} \end{aligned}$$

The velocities and accelerations at time 't+1' (i.e. at the end of the normal time-step of length 'h') then follow from (3-viii) and (3-ix), namely...

$$\{\dot{x}_{t+1}\} = \{\dot{x}_t\} + \frac{1}{2\beta h} \{\Delta x\}_h - \frac{1}{2\beta} \{\dot{x}_t\} + \frac{h}{2\beta} (2\beta - \frac{1}{2}) \{\ddot{x}_t\}$$

$$\{\ddot{x}_{t+1}\} = \{\ddot{x}_t\} + \frac{1}{\beta h^2} \{\Delta x\}_h - \frac{1}{\beta h} \{\dot{x}_t\} - \frac{1}{2\beta} \{\ddot{x}_t\}$$

### 3.7.3 Comparative analyses

To investigate the various schemes, Row's [20] six-storey, two-bay frame (described in appendix A) was chosen. Vertical and horizontal masses were considered at each node. The stability criterion (equation 3-xiv) for an analysis using Newmark's linear acceleration ( $\beta = 1/6$ ) technique requires a time-step of approximately 1/400 of a second.

The following elastic analyses were run using the first ten seconds of the El Centro, May 18, 1940 (North-South component) earthquake record.

Analysis	Newmark's $\beta$	Time-step $h$	$T/h$
a	1/4	1/400	(1)
b*	1/6	1/400	(1)
c	1/12	1/400	(1)
d	1/4	1/100	(1)
e	(1/6)	1/100	1.5
f	(1/6)	1/100	2.0

\* benchmark

( ) indicate that this value is standard for the method

TABLE 3-II : BASIC PARAMETERS FOR ANALYSES INVESTIGATING INTEGRATION SCHEMES.

The maximum top-storey displacement was recorded and used as a measure of the variation in response. As the constant average acceleration method ( $\beta = 1/4$ ) is free of amplitude-error and as the responses from analyses (a) and (b) were almost identical, analysis (b) was used as a benchmark. Figure 3-5 shows the top-storey responses superimposed on each other. Differences between all, except those using Wilson's operator, are hard to discern. To clarify these, figure 3-6 displays the algebraic differences between each of the responses and the benchmark ( $\beta = 1/6$ ,  $h = 1/400$  sec), plotted to an increased scale.

It is apparent from the amplitude-errors that both the system using Wilson's operator result in artificial damping being introduced. The magnitude of this introduced damping is seen to be a function of the ratio of Wilson's time-step  $\tau$  to the final time-step 'h' but would require a study of the decay response to an impulse to quantify its size. The difference between the response of analysis (c) ( $\beta = 1/12$ ) and the benchmark is very small compared to those of the Wilson's operator responses. Even at the increased scale, the constant average acceleration system with the coarse time-step of 1/100 sec. (analysis d) is still almost indiscernible from the benchmark. This implies that a saving of almost three-quarters of the time needed to run the benchmark analysis can be made, if the constant average acceleration approach is used,

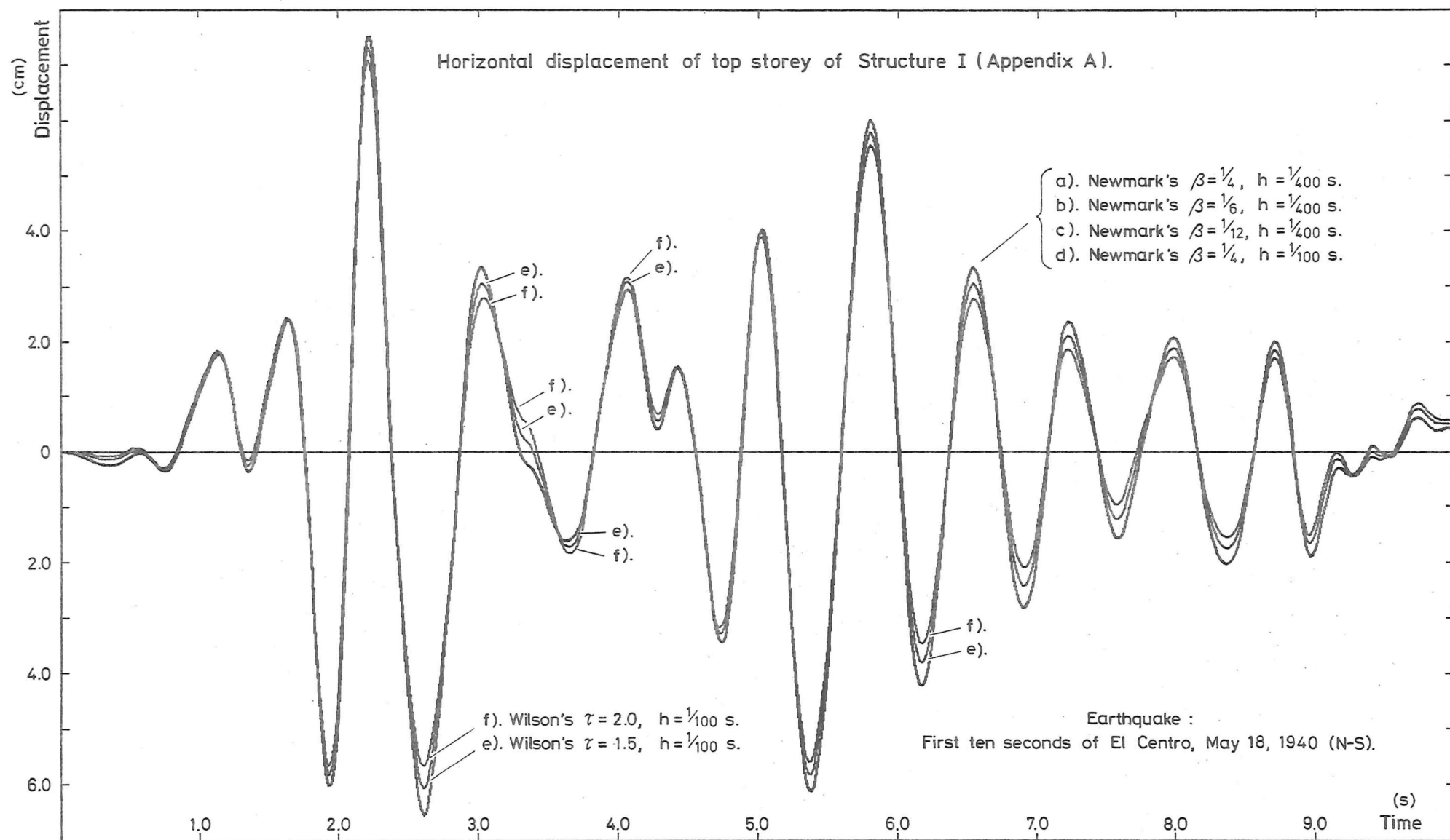


FIGURE 3-5 : COMPARATIVE ELASTIC RESPONSES USING DIFFERENT NUMERICAL INTEGRATION METHODS.

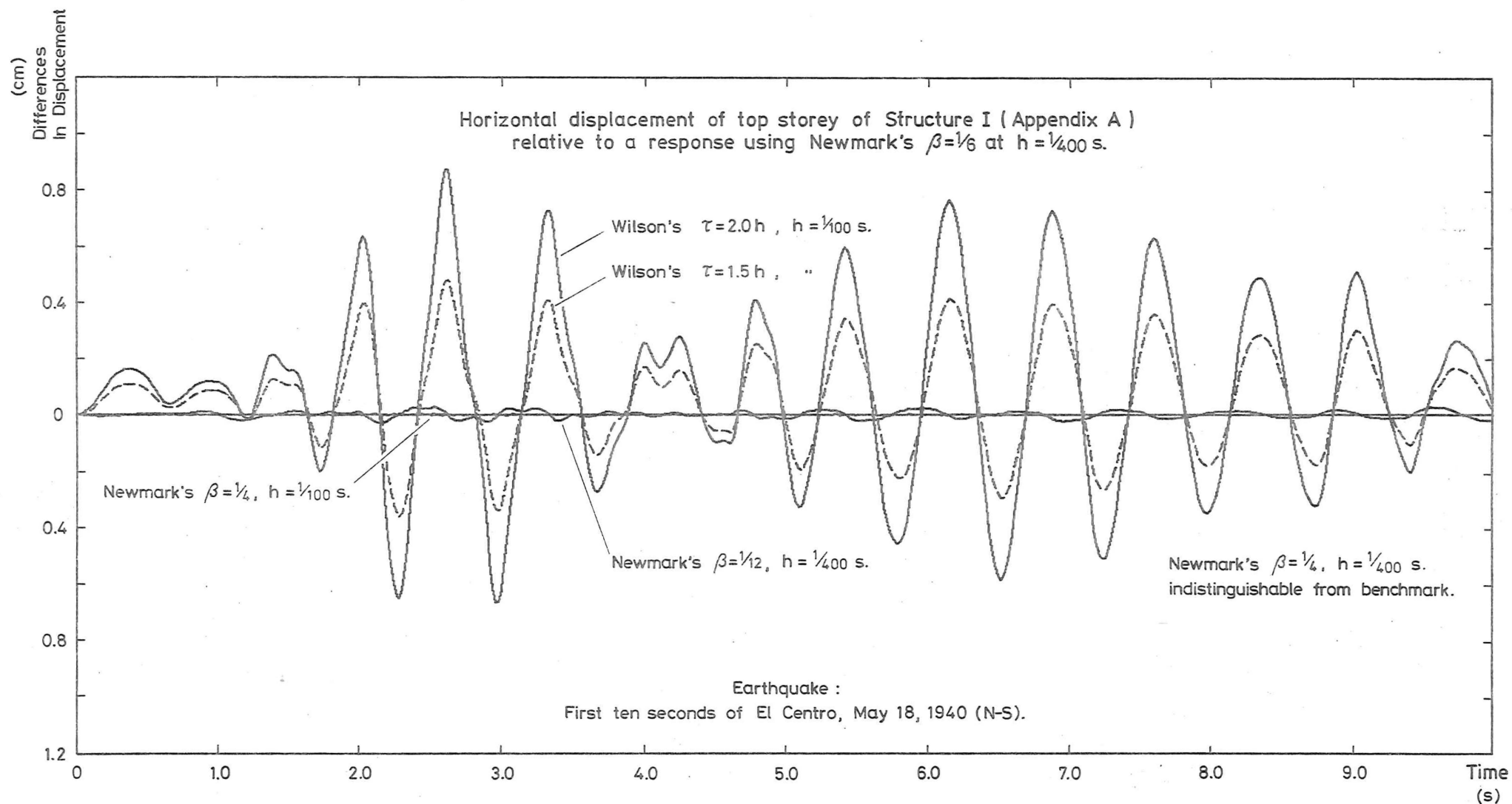


FIGURE 3-6 : THE ALGEBRAIC DIFFERENCES BETWEEN THE RESPONSES SHOWN IN FIGURE 3-5.

instead of the linear acceleration model for this frame. The limit on the length of the time-step then becomes, for this frame, that size which could still reasonably be expected to be compatible with an earthquake accelerogram whose peaks are digitised to an accuracy of at least 1/40 of a second. A time-step of 1/100 of a second is adequate for this purpose.

#### 3.7.4 The practical analysis

As far as the structural engineer is concerned, the most satisfactory scheme for an elastic response, when the economics are considered, is that using the constant average acceleration ( $\beta = 1/4$ ) technique with as big a time-step as he can justify. With typical structural frames and available excitation records this will be of the order of 1/100 of a second. Although he is assured stability of integration-procedure, he must still exercise his judgement to ensure that this time-step does not approach the natural periods of any of those modes making significant contributions to the response.

#### 3.7.5 Period-error

The inherent vibratory period-error in this numerical solution method would seem to be insignificant in an analysis which is generally looking for maximum values. Its lack of any artificial attenuation in response is an added advantage.

Nickell [5] gives comparisons between the exact solution and that using the constant average acceleration operator for a single-degree of freedom problem. The alarming vibratory period-error, which can be seen in his comparative response diagrams, is due to the large time-step being chosen with respect to the period of the oscillator. For a real structure, it is likely that there would be an order, or two, of magnitude between the natural periods of the most significant modes and a satisfactory time-step. The period-error for a simple harmonic vibration can be calculated from the relationship derived by Newmark, namely...

$$\frac{\text{Pseudo Period}}{\text{Exact Period}} = \frac{\pi h/T}{\sin^{-1} \left[ \frac{\pi h/T}{\sqrt{1+4\beta\pi^2 h^2/T^2}} \right]}$$

where 'T' is the natural period of vibration. The period-errors observed by Nickell appear to conform to this relationship. Figure 3-7, which shows the relationship as a function of the ratio,  $\frac{h}{T}$ , clearly indicates the general insignificance of the period-error over the most

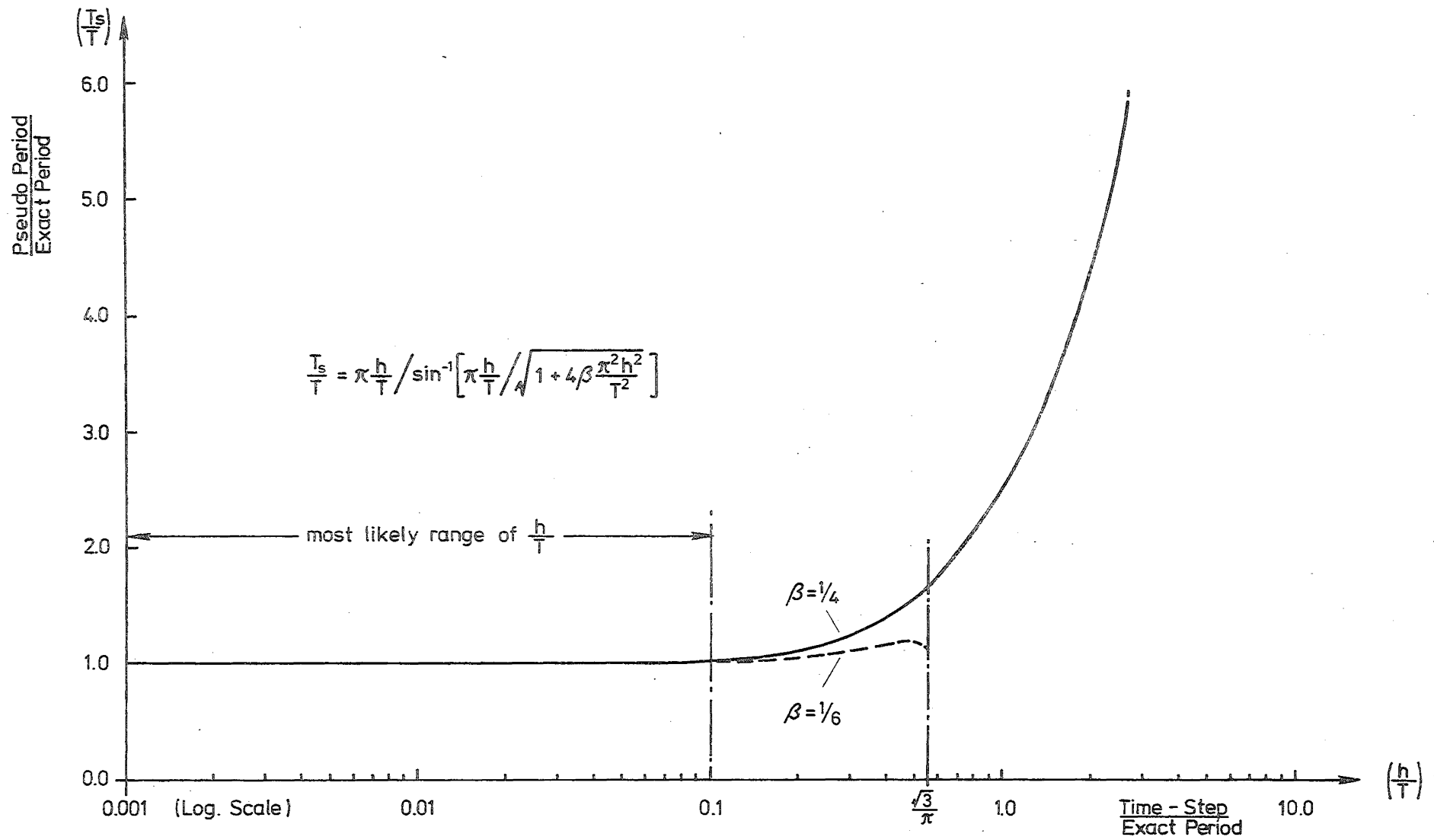


FIGURE 3-7: VARIATION IN RESPONSE PERIOD-ERROR WITH RESPECT TO THE INTEGRATION TIME-STEP.

likely range of the step-size/period ratio. The higher modes, for which the period-error may be relatively large, generally make an insignificant contribution to the total response.

### 3.7.6 Wilson's operators

When examining Wilson's [19] averaging operator (with  $\frac{T}{T} = 1.5$ ) for a single-degree of freedom system, Nickell also found that there was a significant amount of artificial damping inherent in the scheme. Weeks [7] has shown similar results. The multi-degree of freedom case shows similar appreciable amounts of damping.

It, therefore, follows that Wilson's averaging operator, although not subject to the severe stability criteria of the linear acceleration technique it employs, is considerably less attractive than the constant average acceleration method. Not only is it less accurate, but it also requires slightly more complex programming.

### 3.7.7 An advantage of numerical stability

The catastrophic instability exhibited by the linear acceleration ( $\beta = 1/6$ ) integration scheme can be used to an advantage. Should the time-step chosen be large enough to cause significant error, then this instability is usually also evident and the engineer is protected from obtaining misleading results. This safeguard is not present with the ' $\beta = 1/4$ ' or Wilson's schemes and so extra care must be taken when using them. Wilson's schemes have the added disadvantage of having amplitude-errors in such situations. The conclusion may be reached that computer analyses should have, as a default option, the ' $\beta = 1/6$ ' method to protect the inexperienced user against an incorrect choice for  $\beta$ .

## CHAPTER FOUR

THE COMPUTER PROGRAM4.1 INTRODUCTION

For some time there has been an increasing demand in New Zealand for a versatile computer program capable of simulating the response of inelastic framed structures to a digitised earthquake accelerogram. The only program readily available [12] was restricted to frames of regular geometry with mass being apportioned on a storey basis. As it was not written to conform with the individual-member finite-element concept, this program has become out-moded and would not have been amenable to the modifications necessary for the purposes of this study.

Many engineers appear to have become wary (and sometimes confused) by the complicated input required for many of the general-purpose computer programs. In the same way, potentially powerful programs are often handicapped by output which is tedious and unintelligible to anyone not intimately familiar with the actual programming. By introducing the free-formatting of input data (thereby removing the restriction that the input numbers must be punched in certain specified columns of the card) and producing output in a pictorial form where possible, an attempt has been made to improve the communication between the program and its user.

This chapter explains some of the more important considerations made during the development of a program to simulate the motion of a two-dimensional plane frame which may become inelastic when it is subjected to a ground excitation. The problems encountered in making a non-linear beam-model track satisfactorily a general moment-curvature relationship are discussed in depth. Descriptions are given of the damping model, the setting up of the numerical stiffness and the method employed in measuring the ductility requirements of members. Also mentioned are a few of the steps taken to refine the overall mathematical representation of the frame and improve the way in which the level of plasticity present can be communicated to the designer.

4.2 COUPLING OF DEGREES OF FREEDOM

In order to limit the effect of the frequency-proportional errors which are inherent in some piece-wise integration methods, it is desirable to try to keep the magnitude of the higher natural frequencies as small as possible. The stability criteria (see chapter three) for those integration methods which are not unconditionally stable, is also



frequency-dependent and could, where high natural frequencies are present, dictate the use of an integration time-step which would be too small to make the dynamic analysis economically viable.

A simple addition to the input data describing the position and restraints on a frame's kinematic degrees of freedom enables the program to slave automatically a degree of freedom at one node (or joint) to the corresponding degree of freedom of any other node. The ability to be able to do this is found to be of particular use in the elimination of those very high natural frequencies which arise from the relative movement in an axial direction of the nodes at either end of a beam member. By coupling the degrees of freedom describing the axial displacement of the member ends, the member becomes effectively inextensible. Because the masses associated with each of the coupled degrees of freedom are consequently lumped together, the system has one less dynamic degree of freedom.

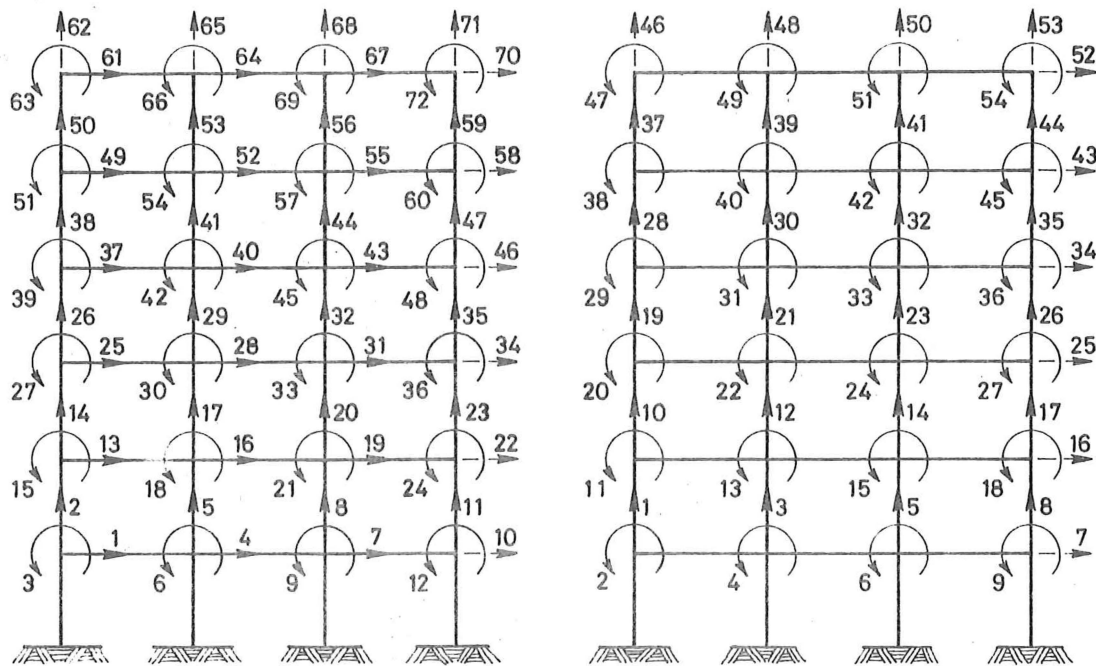
The cost of such coupling is, in general, a large increase in the bandwidth of the non-zero terms in the stiffness matrix and (where applicable) in that of the consistent mass matrix. This cost may be either partially or totally offset by a saving derived from a decrease in the number of dynamic degrees of freedom, for...

$$(\text{Equation solving effort}) \propto (\text{Number of dynamic equations}) \times (\text{bandwidth})^2$$

For example, a regular plane frame, six storeys high and three bays wide, would normally have 72 simultaneous equations of motion (i.e. three per joint for 24 joints) to solve - represented by a stiffness matrix with a bandwidth of 29. If the horizontal degrees of freedom of the joints at each floor-level were coupled so as to give only one lateral degree of freedom per floor, there would be 54 simultaneous equations and a bandwidth of 31 (see figure 4-1 for the numbering patterns). The solving effort, therefore, decreases in the ratio of 51 894 to 60 552 (i.e. 0.86:1). In this particular example, the number of storage positions required for the upper-triangularized and banded form of the stiffness matrix would drop from 975 to 744 - a saving of 24 per cent.

#### 4.3 PARTITIONING STIFFNESS MATRICES

Because the program was written, in the first instance, as a research tool, it was necessary for it to be made as versatile as possible. The arbitrary coupling (or slaving) of some degrees of freedom and the dissociation of any mass from others, in particular, tend not to



a). No coupling of degrees of freedom - three degrees of freedom per joint.

b). Horizontal degrees of freedom at each floor are coupled together.

FIGURE 4-1 : NUMBERING PATTERNS FOR DEGREES OF FREEDOM SHOWING THE EFFECT OF COUPLING OR SLAVING.

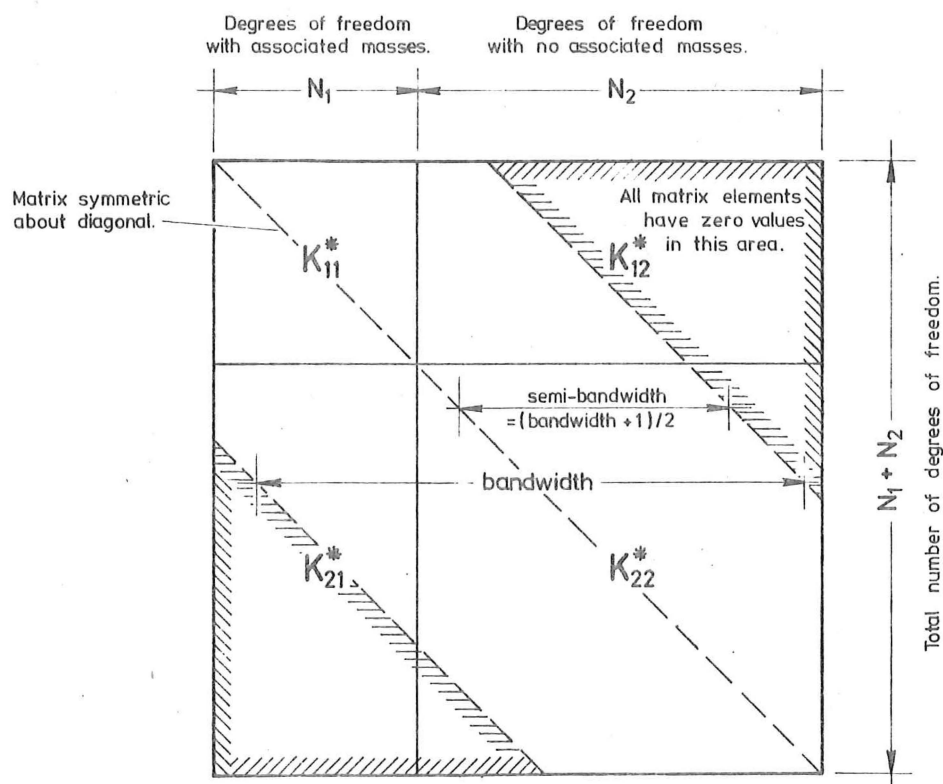


FIGURE 4-2 : THE PARTITIONING OF THE DYNAMIC STIFFNESS MATRIX.

provide the best conditioned static and dynamic stiffness matrices when these matrices are assembled by the Direct Stiffness method [21]. The accuracy of the solutions to the simultaneous equations of motion may be impaired when terms which are close together in the matrix (particularly those along the diagonal), have values which differ by many orders of magnitude. Artificial members introduced to provide rigid connections between joints will lead to this situation.

To provide better conditioned matrices, it was decided that the stiffness and associated matrices should be partitioned, even though this would result in increased computation. The partitioning and subsequent solution method were similar to those used by Felippa [22].

A solution is required for the incremental displacement,  $\{\Delta x\}$ , from...

$$[K^*]\{\Delta x\} = \{\Delta R\} \quad (4-i)$$

where  $[K^*]$  is the dynamic total stiffness matrix and

$\{\Delta R\}$  is the incremental force vector.

The stiffness matrix is assembled in such a way that the top left partition contains only terms relating to degrees of freedom which have mass associated with them. Equation 4-i can thus be expanded to...

$$\begin{bmatrix} K_{11}^* & K_{12}^* \\ K_{21}^* & K_{22}^* \end{bmatrix} \begin{bmatrix} \Delta x_1 \\ \Delta x_2 \end{bmatrix} = \begin{bmatrix} \Delta R_1 \\ \Delta R_2 \end{bmatrix} \quad (4-ii)$$

The upper triangle of the banded and symmetric dynamic stiffness matrix (figure 4-2) can then be reduced by a symmetric backward Gauss elimination technique so that...

$$\begin{bmatrix} K_{11}^* & K_{12}^* \\ K_{21}^* & K_{22}^* \end{bmatrix} \rightarrow \begin{bmatrix} K_A^* & S_{12} \\ - & - \\ - & - \\ D_2 & L_{22}^T \end{bmatrix}$$

where the backward Gauss decomposition of  $[K_{22}^*]$  gives...

$$\begin{bmatrix} K_{22}^* \end{bmatrix} = \begin{bmatrix} L_{22}^* \end{bmatrix} \begin{bmatrix} D_2 \end{bmatrix} \begin{bmatrix} L_{22}^T \end{bmatrix}$$

$$\text{Also} \quad \begin{bmatrix} S_{12} \end{bmatrix} = \left[ \begin{bmatrix} D_2 \end{bmatrix}^{-1} \begin{bmatrix} L_{22}^T \end{bmatrix}^{-1} \begin{bmatrix} K_{21}^* \end{bmatrix} \right]^T$$

$$\text{and} \quad \begin{bmatrix} K_A^* \end{bmatrix} = \begin{bmatrix} K_{11}^* \end{bmatrix} - \begin{bmatrix} K_{12}^* \end{bmatrix} \begin{bmatrix} L_{22}^* \end{bmatrix}^{-1} \begin{bmatrix} S_{12} \end{bmatrix}^T$$

The solution for  $\begin{Bmatrix} \Delta x_1 \\ \Delta x_2 \end{Bmatrix}$  in equation 4-ii is obtained after first performing

a backward substitution on each partition, in turn, of the incremental load vector  $\begin{Bmatrix} \Delta R_1 \\ \Delta R_2 \end{Bmatrix}$  to produce the modified vectors  $\{\Delta \bar{R}_1\}$ ,  $\{\Delta \bar{R}_2\}$  where...

$$\begin{aligned} \{\Delta \bar{R}_1\} &= \{\Delta R_1\} - \begin{bmatrix} \diagdown & L_{22}^T \\ & \diagdown \end{bmatrix}^{-1} [S_{12}] \{\Delta R_2\} \\ \text{and} \quad \{\Delta \bar{R}_2\} &= \begin{bmatrix} \diagdown & D_2 \\ & \diagdown \end{bmatrix}^{-1} \begin{bmatrix} \diagdown & L_{22}^T \\ & \diagdown \end{bmatrix}^{-1} \{\Delta R_2\} \end{aligned}$$

$\{\Delta x_1\}$  is then derived from a backward substitution solution to...

$$\{\Delta x_1\} = \{\Delta \bar{R}_1\}$$

and  $\{\Delta x_1\}$  from the transformation...

$$[K_A^*] \{\Delta x_2\} = \begin{bmatrix} \diagdown & \\ & L_{22} \end{bmatrix}^{-1} \left\{ \{\Delta \bar{R}_2\} - [S_{12}]^T \{\Delta x_1\} \right\}$$

If all those degrees of freedom left after the elimination of any 'fixed' by foundation boundary conditions each have a mass associated with them, the lower partition ceases to exist and the relevant Gaussian decompositions do not occur.

The effect of the partitioning on the computational effort required for the solution of (4-i) can be seen in the times taken by both the IBM 360/44 (with selected double precision employed) and the Burroughs B6718 (single precision) to solve the 54 equations of motion (18 joints, 3 per joint) once only for structure I (appendix A). Results for the three cases...

- a) masses associated only with horizontal degrees of freedom,
- b) horizontal and vertical masses, and
- c) mass associated with all degrees of freedom,

are given in table 4-I.

	Semi-bandwidth of non-zero terms	Order of the first partition	Order of the second partition	Time taken (seconds)			
				IBM 360/44		Burroughs B6718	
				Backward elimination	Solving	Backward elimination	Solving
a) Horizontal masses only	40	18	36	154.7	0.66	53.8	1.87
b) Horizontal and vertical masses	28	36	18	101.7	1.32	38.3	1.90
c) Masses on all degrees of freedom	12	54	0	7.68	1.20	4.12	0.86

TABLE 4-I : SOLUTION TIMES FOR PARTITIONED EQUATIONS.

It can be seen that, from a computational effort point of view, it is advantageous to have no second partition at all in inelastic frame analyses - where the dynamic stiffness may have to be reconstituted a number of times. Provided that an ill-conditioned matrix does not arise, it is possible to have a non-partitioned stiffness, as well as some degrees of freedom without mass, as long as an unconditionally stable numerical integration method (chapter 3.7) is being employed. Where this is not possible, an attempt should be made to associate some mass with every degree of freedom.

#### 4.4 THE DAMPING MODEL

To model the material and velocity damping present in a dynamically excited frame, a damping system proposed by Caughey [23] was set up to give damping forces proportional to both the mass and stiffness of the frame. All degrees of freedom are allowed to attract velocity-dependent damping forces based on the following algorithm which defines the damping matrix...

$$[C] = \alpha [M] + \beta [K]$$

$$\text{where } \alpha = - \frac{2\omega_1\omega_2(\omega_2\lambda_1 - \omega_1\lambda_2)}{\omega_1^2 - \omega_2^2}$$

$$\text{and } \beta = \frac{2(\omega_1\lambda_1 - \omega_2\lambda_2)}{\omega_1^2 - \omega_2^2}$$

in which  $\omega_1, \omega_2$  are any two natural circular frequencies and  $\lambda_1, \lambda_2$  are the respective fractions of critical damping applicable to modes with these frequencies. Although provision is made for any two frequencies to be input to the program, in default the first and second (lowest) natural frequencies will be accredited with the specified fractions of critical damping. In either case, all other modes are then forced to have amounts of damping given, for the  $n^{\text{th}}$  mode, by

$$\lambda_n = \frac{1}{2} \left( \frac{\alpha}{\omega_n} + \beta \omega_n \right)$$

An example of this relationship for a typical situation is illustrated in figure 4-3. As the damping matrix is not required in its entirety at any one time, it is convenient to calculate it term by term as required, thereby making it easy for it to change as the total stiffness alters.

#### 4.5 A NON-LINEAR BEAM MODEL

For the purposes of this study, it was required that the beam-model should be such that its critical sections had the ability to track any generalized moment-curvature function. In particular, it would be used to follow a Ramberg-Osgood [24] curvi-linear hysteretic function and those of the standard bi-linear type - a special case of the latter being the elastic/perfectly-plastic hysteresis. It was considered unnecessary to make provision for the loading of frame members with either distributed or point loads because of the emphasis being placed on lateral inertial loads. Such loads as do arise can be adequately dealt with by the inclusion of dummy nodes or joints at which loading is permitted. It follows that it can be assumed that the critical sections of all members occur at their interfaces with each other. A suitable model, therefore, need only simulate the correct moment-rotation and axial stiffness characteristics at these interfaces.

Giberson's [25] one-component model of a non-linear beam proves to be ideal for such a task. It is, simply, a one-dimensional prismatic beam with sprung hinges incorporated at infinitesimal distances from either end. By varying the rotational spring stiffness of the independent hinges, it is possible to model the full range of situations, from that of a pinned end to one in which the beam is linearly elastic along its entire length. Hence, the full spectrum of possibilities can be covered. A schematic diagram of the beam appears in figure 4-4. The spring rate of each of the hinges is expressed as a fraction of the bending stiffness of the beam,  $4EI/L$  ( $E$ , Young's modulus;  $I$ , moment of inertia;  $L$ , length).

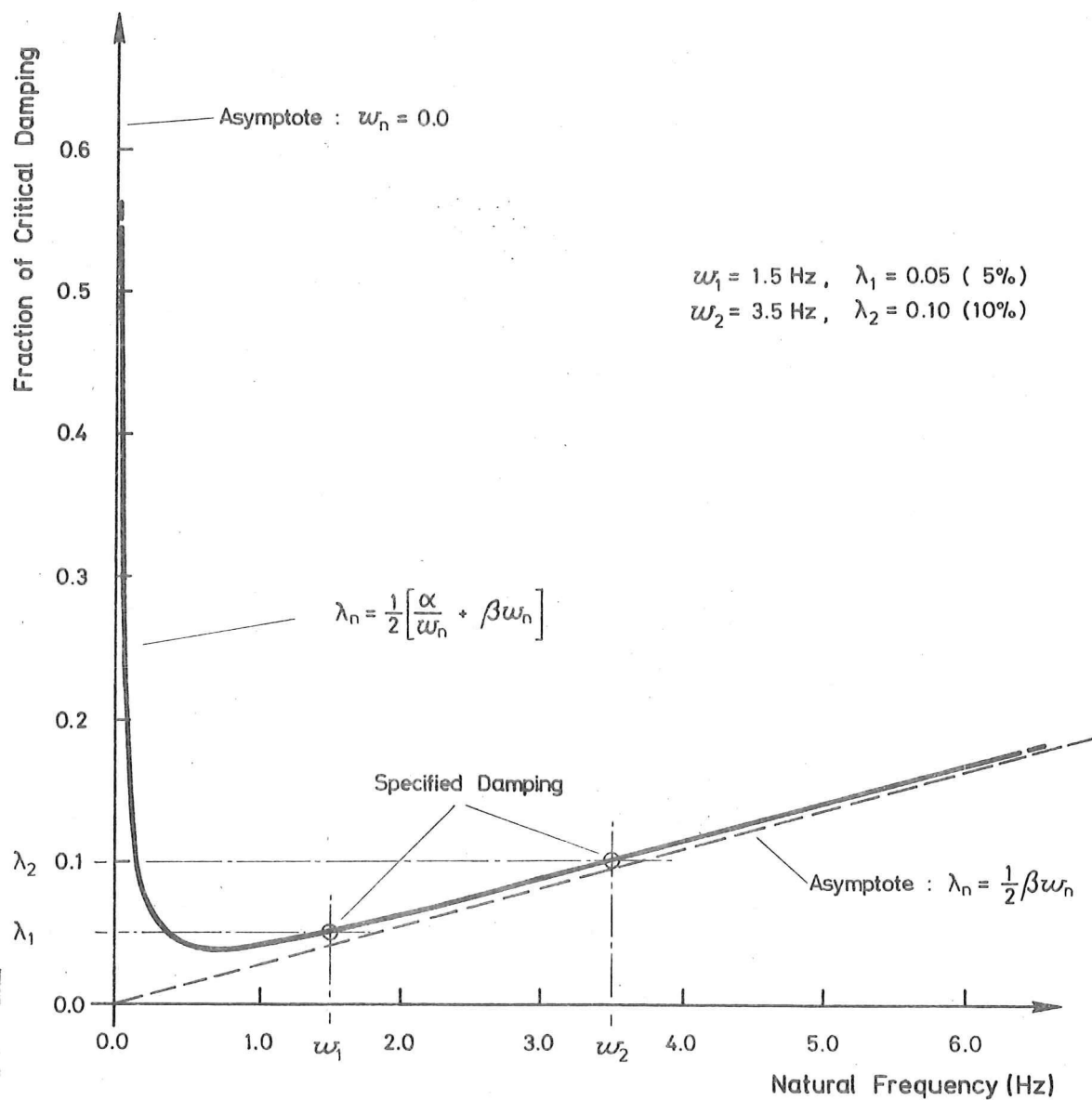
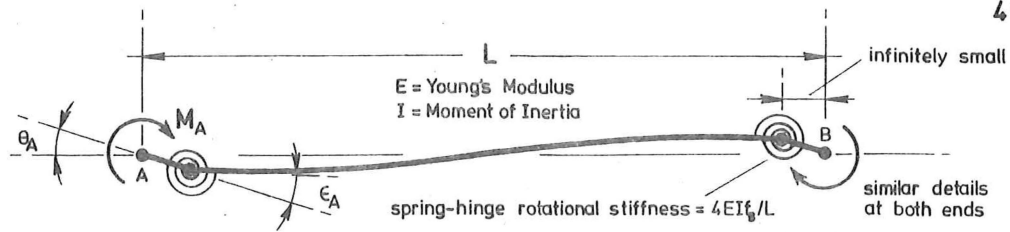


FIGURE 4-3 : TYPICAL CAUGHEY RELATIONSHIP BETWEEN DAMPING AND NATURAL FREQUENCY ARISING FROM THE SPECIFICATION OF THE DAMPING AT TWO PARTICULAR FREQUENCIES.



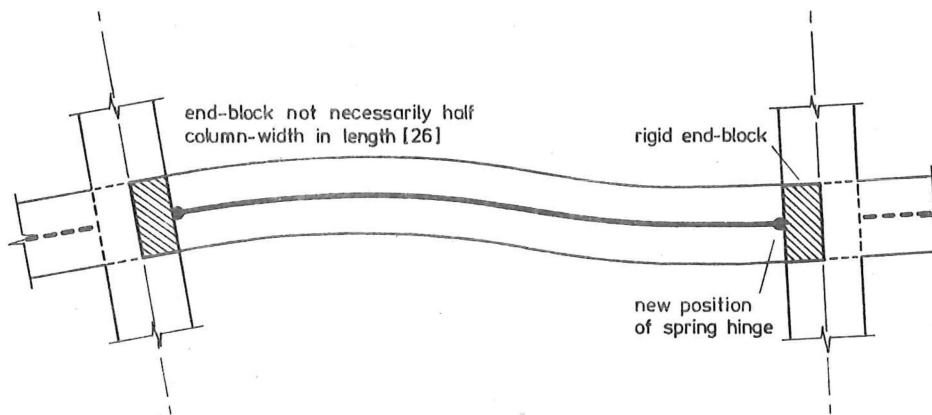
Case 1 : Hinges A and B both non-linear.

Case 2 : Hinge A non-linear, B linear.

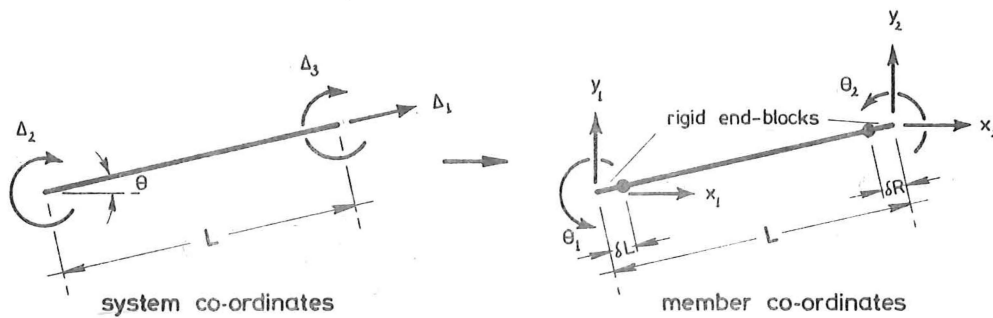
$$\begin{Bmatrix} \Delta M_A \\ \Delta M_B \end{Bmatrix} = \frac{4EI/L}{1 + \frac{4}{3}(\bar{f}_A + \bar{f}_B + \bar{f}_A \bar{f}_B)} \begin{bmatrix} \bar{f}_A(1 + \frac{4}{3}\bar{f}_B) & \frac{2}{3}\bar{f}_A \bar{f}_B \\ \frac{2}{3}\bar{f}_A \bar{f}_B & \bar{f}_B(1 + \frac{4}{3}\bar{f}_A) \end{bmatrix} \begin{Bmatrix} \Delta \theta_A \\ \Delta \theta_B \end{Bmatrix}$$

$$\begin{Bmatrix} \Delta M_A \\ \Delta M_B \end{Bmatrix} = \frac{4EI/L}{1 + \bar{f}_A} \begin{bmatrix} \bar{f}_A & \frac{1}{2}\bar{f}_A \\ \frac{1}{2}\bar{f}_A & \frac{3}{4} + \bar{f}_A \end{bmatrix} \begin{Bmatrix} \Delta \theta_A \\ \Delta \theta_B \end{Bmatrix}$$

a). Giberson's one-component non-linear beam model.



b). Beam model modified to incorporate rigid end-blocks which shift the position of the critical sections inwards.



$$\begin{Bmatrix} \Delta_1 \\ \Delta_2 \\ \Delta_3 \end{Bmatrix} = \begin{bmatrix} -\cos \theta & \sin \theta & 0 & \cos \theta & -\sin \theta & 0 \\ -\frac{\sin \theta}{L} & -\frac{\cos \theta}{L} & -1 - \frac{\delta L}{L} & \frac{\sin \theta}{L} & \frac{\cos \theta}{L} & -\frac{\delta L}{L} \\ -\frac{\sin \theta}{L} & -\frac{\cos \theta}{L} & -\frac{\delta L}{L} & \frac{\sin \theta}{L} & \frac{\cos \theta}{L} & -1 - \frac{\delta L}{L} \end{bmatrix} \begin{Bmatrix} x_1 \\ y_1 \\ \theta_1 \\ x_2 \\ y_2 \\ \theta_2 \end{Bmatrix}$$

c). The transformation from system- to member- co-ordinates.

FIGURE 4-4 : THE BEAM MODEL.



Because of the limited accuracy of any computer, it is possible to consider any hinge which has a rotational stiffness greater than a predetermined magnitude, to be non-existent. For an IBM 360/44 with a minimum single-precision floating-point accuracy of about 6.5 decimal digits, this value (of 'f') is approximately  $1 \times 10^7$  units.

In order that the critical sections may occur at the interface of the members rather than at the intersection of their centre-lines, a small modification is made to the transformation matrix which relates the co-ordinates of the member to those of the frame system. Based on small deflection theory, this allows a member to have small rigid end-blocks at either or both of its extremities. This transformation is also shown in figure 4-4.

The theoretical discontinuity, which occurs at the critical sections in the beam-model, extends over an infinitely small length. The rotation of the hinge at this point can only be related to the curvature at the same point in the real structure if the hinge is considered to have, in retrospect, some finite length. This plastic length is known to vary with both the amount of curvature and the type of material in which it occurs [27, 28]. If a constant value for this length is fed into the computer with the rest of that beam's data, then a relationship, again based on small deflection theory, can be derived to manufacture an equivalent curvature from the beam-model's hinge rotation. Using the notation of figure 4-5 and assuming the bending moment over the length of the hinge to be constant at that value being transmitted at the critical section, the finite plastic hinge is first considered to consist of two discontinuous parts. For each of these halves...

$$\frac{H}{2} = r\theta_1 \quad (4-iii)$$

$$\text{and} \quad M = \frac{EI}{r} \quad (4-iv)$$

For the equivalent continuous hinge A-C, which has constant curvature,...

$$H = \rho\theta_2$$

By definition, Giberson's beam gives...

$$M = \frac{4EI}{L} f\epsilon$$

where  $\epsilon$  is the angle of rotation of the infinitely small model hinge. The geometry of the model gives...

$$2\theta_1 + \epsilon = \theta_2$$

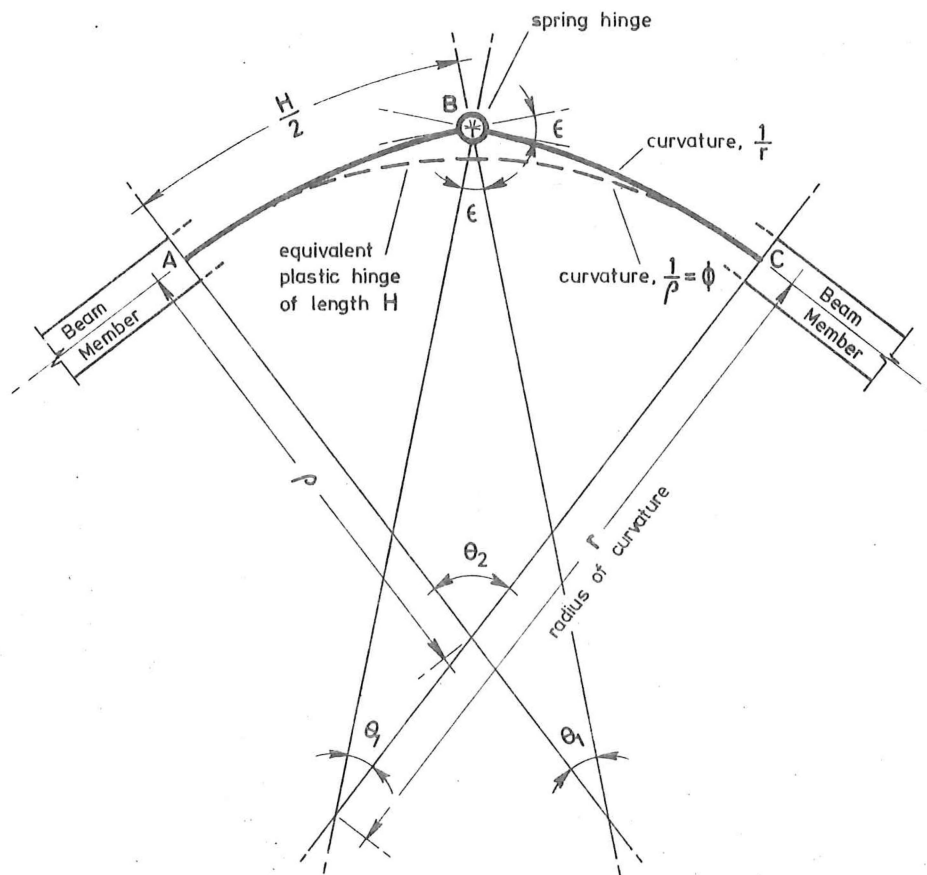


FIGURE 4-5 : BEAM PLASTIC HINGE MODEL (SMALL DEFLECTION THEORY).

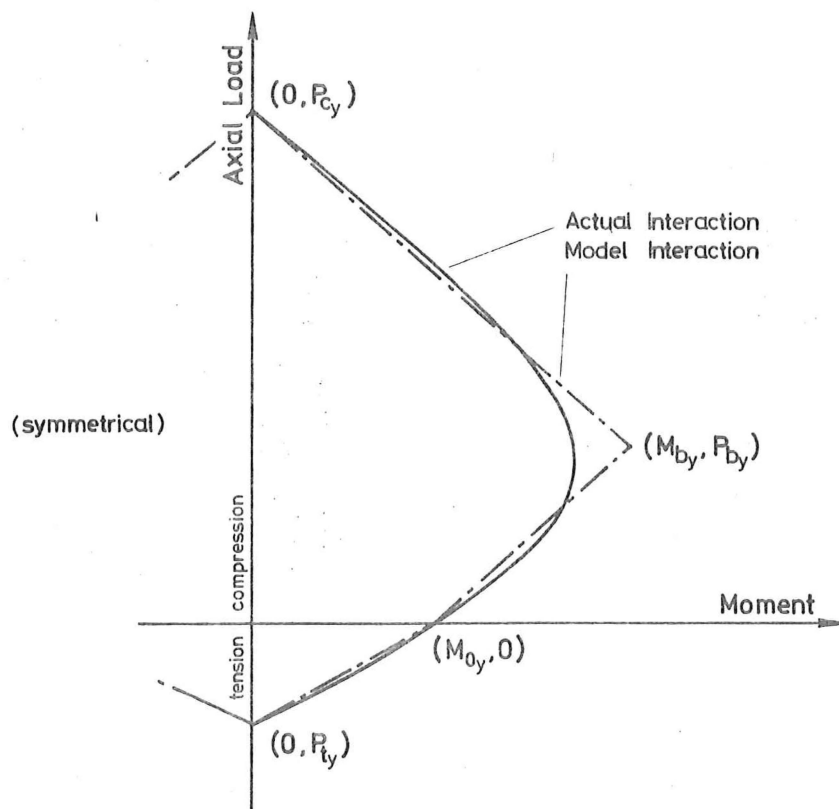


FIGURE 4-6 : COLUMN YIELD MOMENT-AXIAL LOAD INTERACTION MODEL.

It follows, from (4-iii) and (4-iv), that...

$$\begin{aligned}
 M &= EI \frac{2\theta_1}{H} \\
 &= EI \frac{(\theta_2 - \epsilon)}{H} \\
 &= EI \frac{1}{H} \left( \frac{H}{\rho} - \frac{ML}{4EIF} \right) \\
 \text{i.e.} \quad M &= EI \left( \frac{1}{1 + \frac{L}{4HF}} \right) \phi
 \end{aligned}$$

where  $\phi$  is the curvature of the equivalent plastic hinge ( $\phi = \frac{1}{\rho}$ ). In the incremental situation, the curvature of the plastic hinge can be then expressed as...

$$\frac{dM}{d\phi} = EI \left( \frac{1}{1 + \frac{L}{4HF}} \right)$$

This expression relies on the adoption of small deflection theory. This is consistent with similar assumptions made in the analysis of structural frames. Obviously, the selection of an unrealistically large plastic hinge length will invalidate the use of the expression.

#### 4.6 MEMBER DUCTILITY - A DEFINITION

Despite the proliferation of definitions of ductility, caused by each user formulating one to fit his own particular problem, no single definition seems to have found universal favour. This situation is compounded by the difficulty encountered in trying to apply some of the defining algorithms to the mathematical models used in analysis. In particular, it is common for the ductility of a beam element to be expressed in terms of end-rotation ratios, by using the generally invalid assumption that the element has deformed anti-symmetrically - as would be experienced in cases of symmetric structures under anti-symmetric loadings. Any realistic representation of the loading conditions on a frame at any one time does not produce such loadings (as was pointed out by Anderson and Bertero in a discussion on work by Walpole [12]).

The *raison d'être* for the quantifying of member ductility is to enable the designer to detail his structural members in such a way that they will withstand specified strains in the material fibres at a section. It is therefore, essentially, a measure of a member's curvature, unless specifically defined otherwise as an overall description of a frame's

inelastic behaviour (i.e. frame ductility).

Giberson [25] presents three alternative methods for defining the ductility of a member section and calculates the total energy dissipated in a complete symmetric force-deflection hysteresis for each. Two of these require a well defined yield level to make the definitions operable. The third definition is suitable for curvi-linear hystereses but, as he points out, the choice of definition can make an appreciable difference to the value obtained for the same response.

By taking a pragmatic approach, it is realized that the characteristics of the moment-curvature relationships, for most structural members that will be analysed, exhibit a reasonable well defined first yield point which can then be used for a calculation of ductility. Once this point has been defined, then the ductility is the simple ratio of the maximum curvature to that at first yield. For degrading members the bending moment at maximum curvature should also be quoted.

Columns, with their axial load dependent ultimate strength, pose a much more complex problem. In a typical design-checking analysis, the particular forces present at failure are normally of more importance to the designer than an artificially derived value of ductility. Accordingly, the ductilities given by the program in these situations are merely based on the curvature that would be present at the balanced yielding of the column section.

#### 4.7 COLUMN MOMENT - AXIAL LOAD INTERACTION

The most popular design philosophies suggest that the critical sections of columns be provided with an overstrength sufficiently large enough to ensure that virtually all a frame's plastic hinges form in the beam members. This forces as many plastic hinges as possible to be required to form before a catastrophic collapse mechanism is approached. There is the possibility, especially in frames with high overturning moments, that the variation in axial load in the columns will cause significant fluctuations in the ultimate strength of some column sections during an earthquake.

For common building materials, the relationship between axial load and ultimate moment of a section is far from linear and so an approximation must be sought to enable a simple numerical representation to be made. Figure 4-6 describes the interaction model chosen for this study. Under typical conditions it was found that the critical (yield) interaction occurs most often in one particular area covered by the relationship. Thus, it is considered sufficient to model the interaction curve by a

series of straight lines - providing that the most care in modelling is taken over that area where the relationship is likely to be most invoked. For a typical reinforced concrete column, this region will generally be between the point representing balanced yield (or failure) and that representing yielding in pure bending (i.e. with no axial load). Accurate representation of the rapidly changing section of the interaction curve, at either side of the point of balanced yield, would require a number of extra points to be specified, but this is not as important as the modelling of the general trends of the relationship. Hence, only five (easily measured) pieces of information need be elicited to define the interaction.

An example of the use of this yield criteria, and of the consequent sensitivity of a structure to its use, is discussed in chapter seven in the investigation into the dynamic behaviour of a bridge pier.

#### 4.8 TRACKING A MOMENT-CURVATURE RELATIONSHIP

##### 4.8.1 The 'moment overshoot' effect

As with many other factors affecting the results of a deterministic dynamic analysis, it is a matter of judgement as to whether the chosen time-step for the piece-wise integration procedure is small enough to allow sufficiently accurate tracking of the moment-curvature function specified. When the variation in moment, with respect to curvature, is large (as is the case when the plastic section of an elasto-plastic hysteresis is being followed), there is, inherent in the procedure when a change of stiffness is incurred, an often unavoidable over- or underestimation (figure 4-7) of the moment at a particular curvature. This arises from the necessary assumption of linear behaviour for the duration of each constant length time-step. Preliminary studies show that, for a simple multi-storey frame together with a realistic time-step, overshooting of about five per cent of the yield moment might be expected in the tracking of an elasto-plastic relationship.

##### 4.8.2 Counteracting moment overshoot

One way of getting around the problem of moment overshoot is, in effect, to ignore it. The excessive or (as in the converse case) deficient moment is reset to the value which correctly corresponds to the current curvature, without carrying out the relaxation of the frame which is physically implied by such an action. A second way, which is even more simple, is to not reset the moment which is in error and so let the

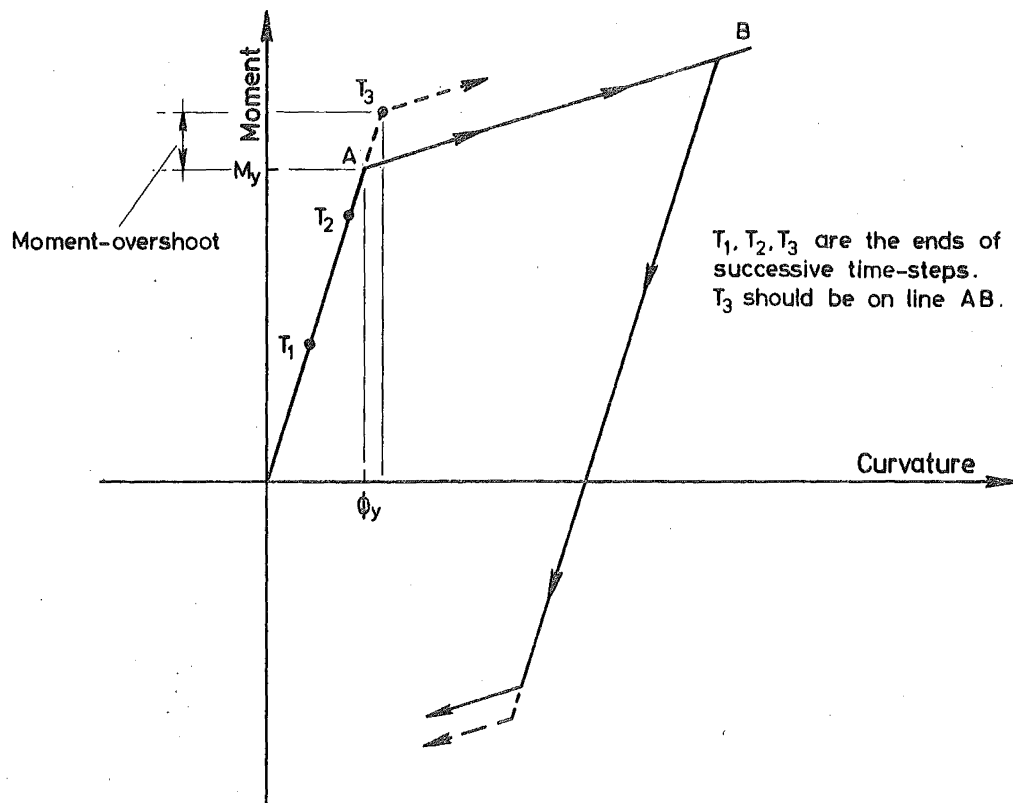


FIGURE 4-7 : AN EXAMPLE OF MOMENT-OVERSHOOT IN THE TRACKING OF A BI-LINEAR MOMENT-CURVATURE HYSTERESIS.

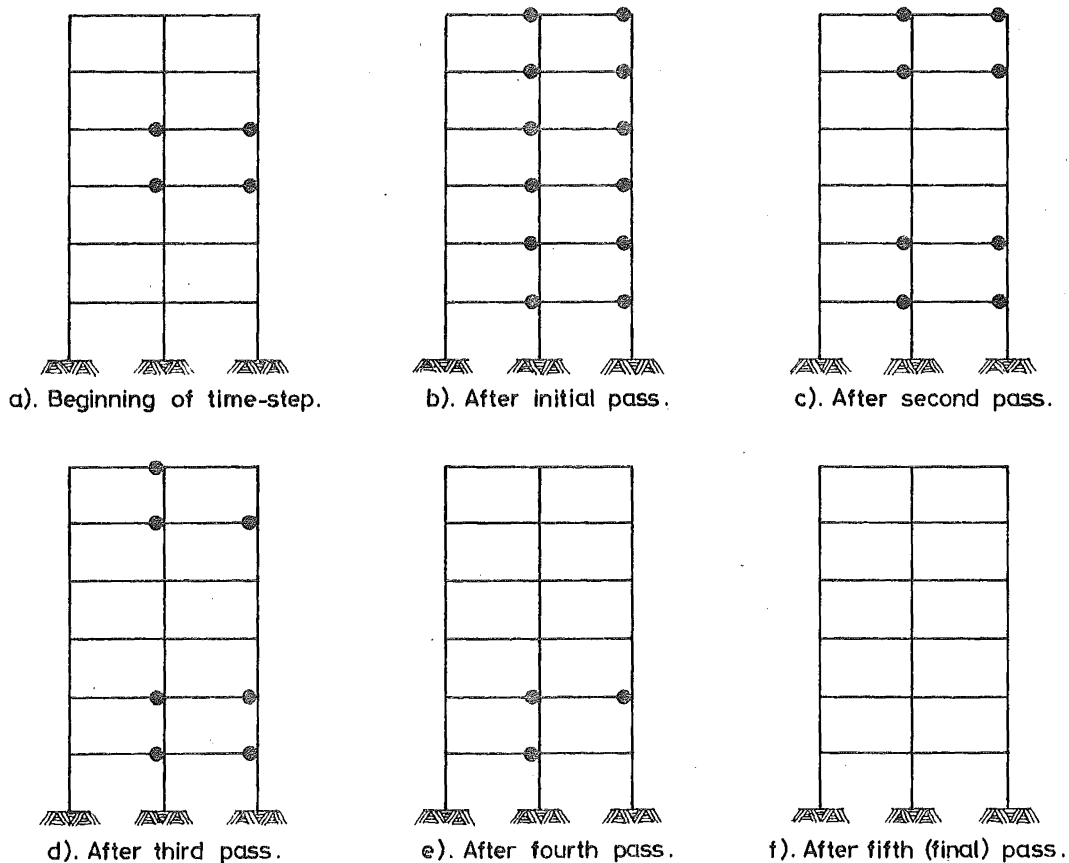


FIGURE 4-8 : TYPICAL ITERATIVE RELAXATION AT A TIME-STEP SHOWING THE ERRONEOUS DISAPPEARANCE OF PLASTIC HINGES.

analysis proceed using the erroneous value as an initial condition for the following time-step. This has the disadvantage of allowing a plastic hinge to be removed as soon as an incremental curvature opposite in sense to that causing the plastic hinge is encountered, even though the resultant moment carried by the section might be still greater than that theoretically required to force plasticity. A third approach consists of limiting the moment to that dictated by the moment-curvature relationship for the current curvature (as is done in the first method described) and applying the difference between these two values as a constant excessive load on the appropriate node for the duration of the next time-step. This then reflects the fact that during the current time-step the critical section at some stage reached its prescribed loading capacity for the curvature calculated, and then could be considered to be incrementally more flexible (in the case of an increasing load). Its stiffness was not altered at that stage, however, so the calculated incremental deflections that do occur will be smaller than what they should be. By applying the excess moment to the nodes which define the member in question, this erroneously prolonged stiffness is partially compensated for by the tendency for it to increase the deflections in the next time-step. Although this results in an out-of-phase loading, some effort is being made to provide a semblance of dynamic force equilibrium at the member joints.

The fourth scheme to be considered requires an iteration procedure over any time-step in which any moment overshoots. Any reaction of reluctance to the idea of implementing an iterative procedure within a piece-wise deterministic analysis should be tempered with the consideration that the process might be highly convergent. The method consists of applying a vector of excess moments, the same as that used in the previous scheme, to the dynamic flexibility applicable to the interval in which they arose. The incremental displacements thus produced are added to those already found for the time-step and the checking of the moment-curvature relationship again takes place - resulting in further plastic hinges being either recognized or removed and more moment overshoots occurring. The relaxation is then repeated until no more change takes place in the plastic hinge pattern - at which time the velocities and accelerations for the end of the time-step are calculated from the compounded incremental displacements. The necessary modifications to the stiffness are then made in preparation for the next time-step.

#### 4.8.3 Comparison of schemes to counteract moment overshoot

To test and compare the effectiveness of the various approaches

outlined in the previous section, their effect on the response of a six-storey, two-bay frame (structure I, appendix A) to the first ten seconds of the El Centro, May 18, 1940 earthquake (North-South component) was sought. An elasto-plastic hysteretic moment-curvature relationship was used in conjunction with the constant average acceleration ( $\beta = 1/4$ ) numerical integration technique at a time-step of one hundredth of a second as the basis for all the tests. A benchmark response was produced by carrying out a similar analysis (with  $\beta = 1/6$ ) at the very fine time-step of one four-hundredth of a second (c.f. a fundamental period of 0.74 seconds), with the over- and undershooting of the moments ignored and the yield moments set at the values of the excessive moments (i.e. as in the second scheme described). By choosing such a fine integration interval, the magnitude of the error accruing was minimized.

When yielding occurs in the model part of the way through a time-step, the frame does not lose stiffness instantly as the real structure would, but has to wait until the end of the interval for it to be modified. Hence, it could be expected that refined schemes would show a greater response occurring when the trend was for yielding to be initiated and a reduced response when plasticity was generally disappearing. Higher plastic deformations may then be a consequence. Because of this, the resulting responses are not necessarily best compared by plotting them one on top of another, but rather by studying of the peak-to-peak values for each half-cycle of the frame's oscillation. This latter method can then give a better indication of where plastic flow is occurring.

The iterative scheme was found to be unsatisfactory in its postulated form. The excess moment, when re-applied to the structure using the current dynamic stiffness, tended to cause a reversal in the direction of incremental loading of sections which, on the first pass of the iteration (or in a previous interval) had been found to be yielding. The program then deemed these to have become elastic again and an adjustment was made to the appropriate member stiffness but not, at that stage, to the total frame dynamic stiffness. These changes then produced a further relaxation with similar trends and the iterative process was continued until a stable situation was attained. The largest number of iterations required in the achieving of this was twenty-one. In general, the frame was left at the end of a time-step with less plastic hinges than could have been expected. Similarly, a number of critical sections were left with moments which were only just less than their yield values. A typical iteration in which this effect occurred is recorded pictorially in figure 4-8. In this particular example, the frame should have



approximately regained the plastic hinge status that it had reached after the first pass but, instead, the iteration procedure left it devoid of any plastic hinges, even though both the deflections and ground acceleration were continuing to increase.

While it does vary the frame deflections in the manner expected, this phenomenon indicated that the iterating procedure, although reasonably fast in relaxing the out-of-balance moments, does not parallel the physical model which it is attempting to portray. Whereas the deflections are due to inertial loadings being attracted proportionally throughout the frame, the iterated moment correction is applied in specific locations in a manner which does not mirror the equivalent inertial loading. Even if those members which changed their state of plasticity in the first cycle of the iteration were to be prevented from incurring opposite changes in subsequent cycles on that interval, the deflected shape which would be created would not necessarily converge on the correct solution.

At this stage, a variation on this iterative method was attempted by limiting the solution at the end of each time-step to the result of the initial pass plus one corrective iterative cycle. When calculating the relaxations to the incremental displacements, no attempt was made to calculate the corresponding moment corrections. This was justified, albeit crudely, on the grounds that the altered accelerations and velocities would compensate for the missing moment corrections when the solution for the following interval was initiated with a revised incremental force vector which would include contributions arising from viscous damping and inertia. The response generated using the technique is shown in figure 4-9. The most noticeable feature is that it causes considerably increased deflections in the initial peaks where plastic flow is taking place - resulting in an increased permanent drift later on. To provide further comparison with this scheme, a similar analysis, but with a time-step four times as small and with the corrective force vector zeroed, was carried out. It was thought desirable that it be seen whether the prediction, that a smaller time-step would be equivalent to having negligible moment overshooting, was viable. The excessive time required for this response resulted in it being prematurely terminated. Peak-to-peak values of the response from this analysis and those of the previously described benchmark were generally within one per cent of each other.

Table 4-II summarizes the salient features of the four comparative responses shown in figure 4-10. To obtain a more complete picture of the response variations, the amount of plasticity present at any one time should be taken into consideration. This is shown in figure 4-11 for that

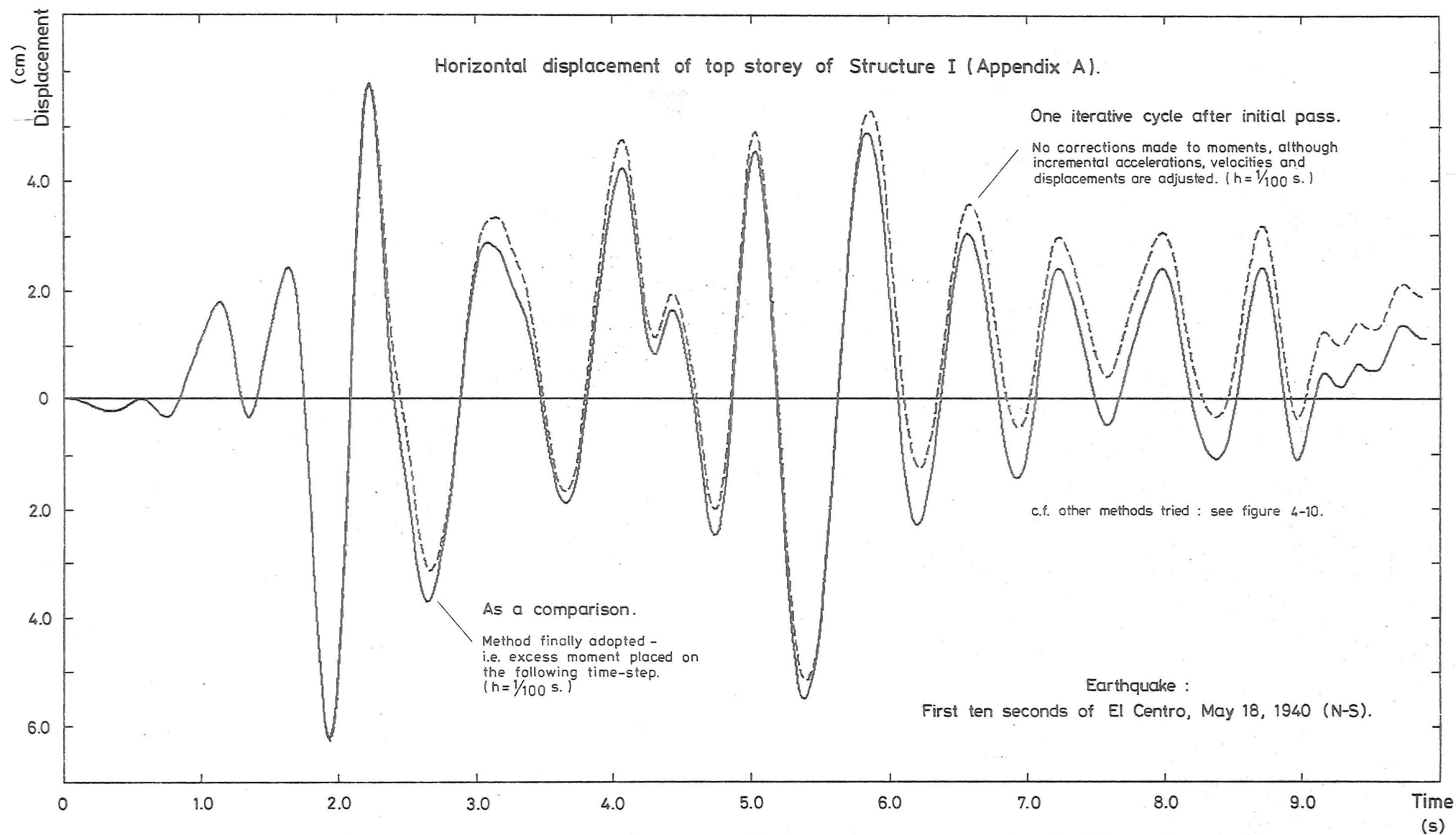


FIGURE 4-9 : THE EFFECT OF A REVISED ITERATIVE METHOD IN COUNTERING MOMENT-OVERSHOOT.

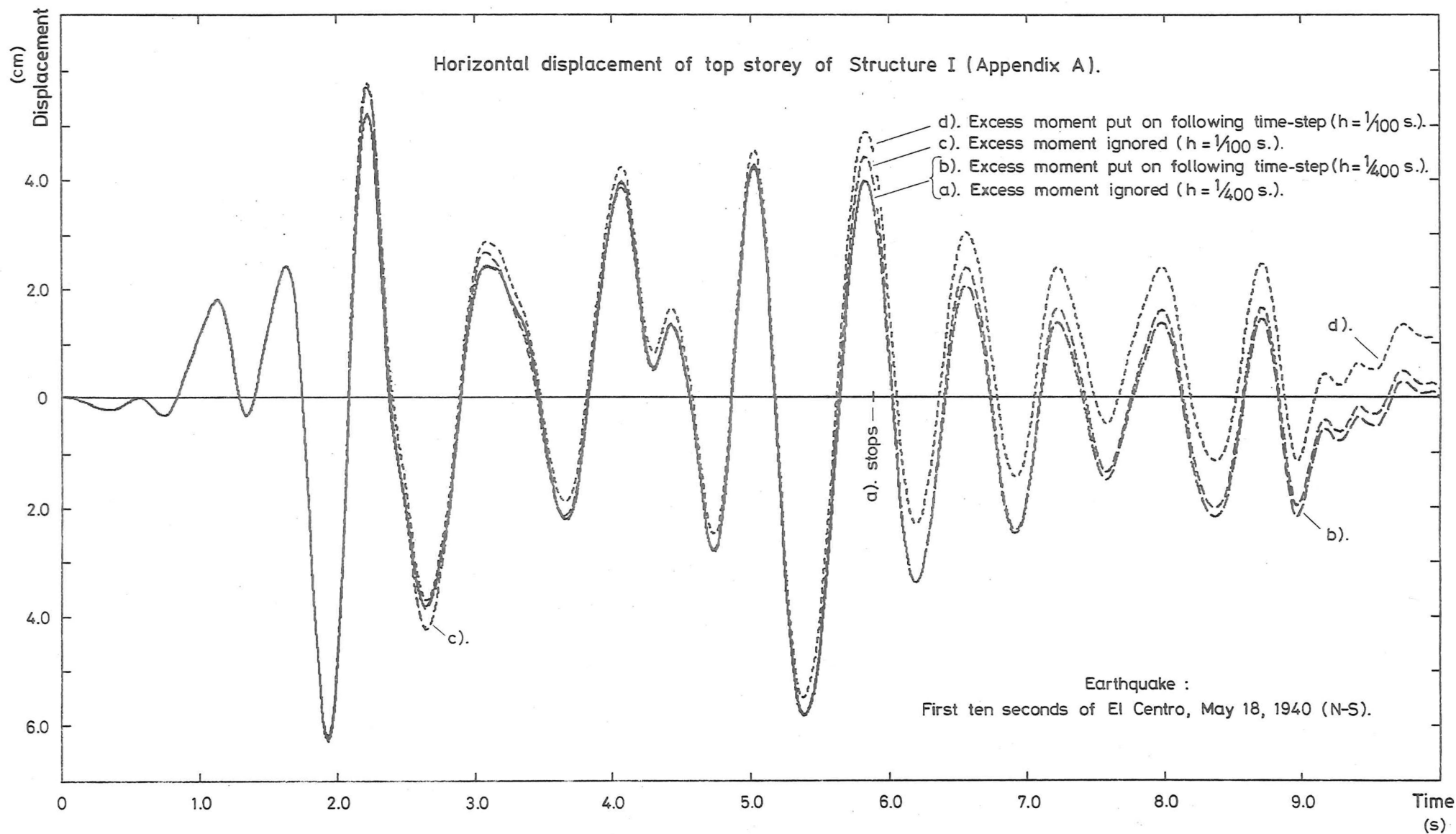


FIGURE 4-10 : THE EFFECT ON A RESPONSE OF DIFFERENT METHODS FOR COUNTERING MOMENT-OVERSHOOT.

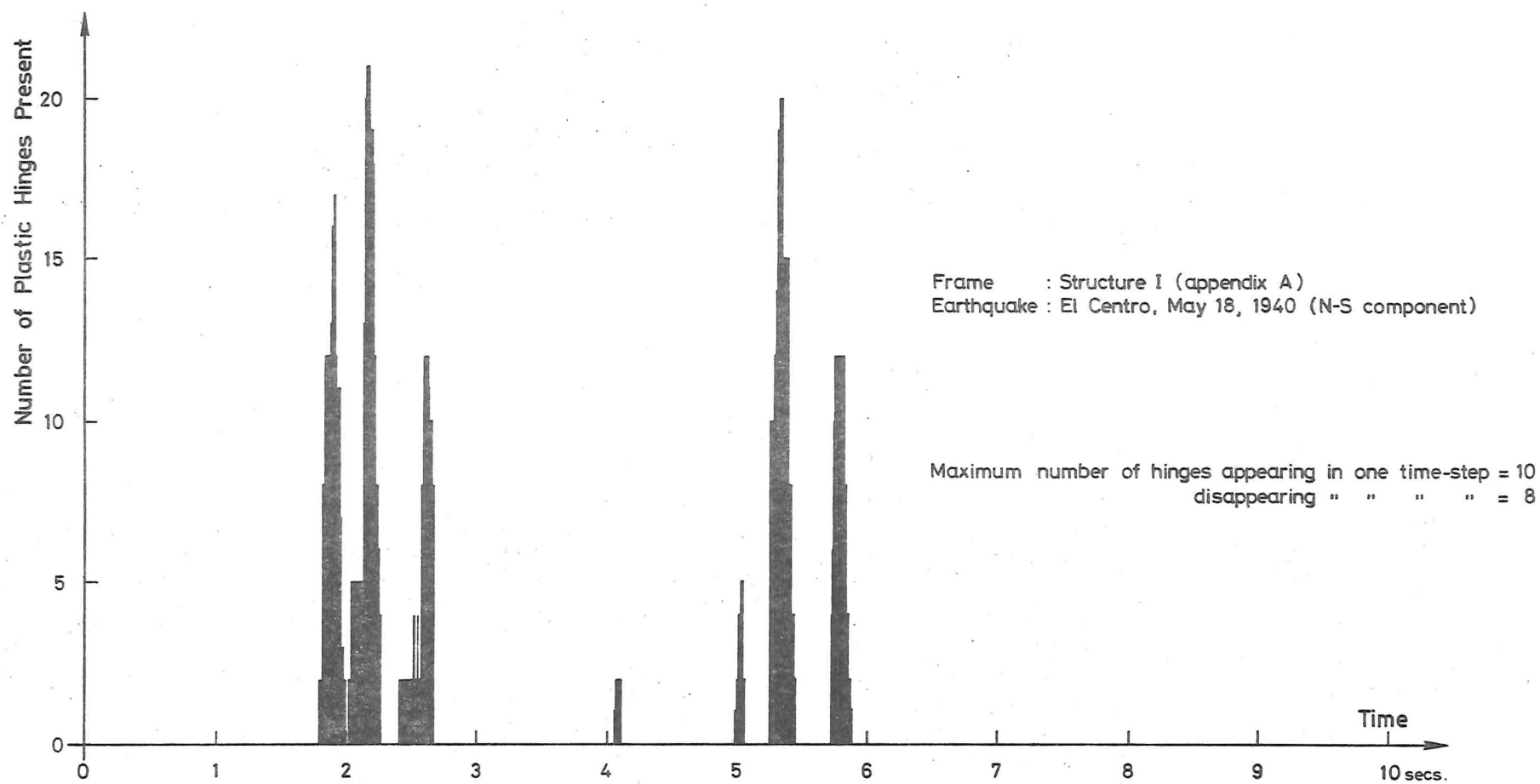


FIGURE 4-11 : NUMBER OF PLASTIC HINGES PRESENT DURING A TYPICAL INELASTIC ANALYSIS.

response in which the excess moment is reinvested on the next time-step.

Time (secs)	Time-step of 1/400 sec.				Time-step of 1/100 sec.			
	Excess moments ignored		Excess moments on following time-step		Excess moments ignored		Excess moments on following time-step	
	Peak values	Peak-to- peak	Peak values	Peak-to- peak	Peak values	Peak-to- peak	Peak values	Peak-to- peak
2.22	0.0509		0.0508		0.0567		0.0574	
		0.0893		0.0894		0.0994		0.0947
2.65	-0.0384		-0.0386		-0.0427		-0.0373	
		0.0625		0.0625		0.0688		0.0656
3.10	0.0241		0.0239		0.0261		0.0283	
		0.0450		0.0450		0.0460		0.0457
3.70	-0.0209		-0.0211		-0.0199		-0.0174	
		0.0605		0.0605		0.0584		0.0596
4.06	0.0396		0.0394		0.0385		0.0422	
		0.0665		0.0665		0.0656		0.0661
4.70	-0.0269		-0.0271		-0.0271		-0.0239	

TABLE 4-II : COMPARISON OF RESPONSE PEAK VALUES (METRES).

#### 4.8.4 Avoiding moment overshoot

A secant modulus approach, involving the possibility of extensive iteration of the member stiffnesses for the dynamic situation over a particular time-step, must be considered prohibitive for long excitations, because of the computational cost of the continual alterations (and consequent reductions) to both the static and dynamic total stiffness matrices. There are, however, several other approximate schemes worthy of future investigation, all of which are formulated so that moment overshooting does not occur.

The first of these methods is, quite simply, an attempt to make any abrupt changes in elasticity coincide with the end of a time-step, by permitting the interval to vary in length within certain bounds. For example, an analysis with a normal time-step (compatible with the integration technique being used) of length 'h' may be considered. At some stage of this analysis, on checking the critical sections at time

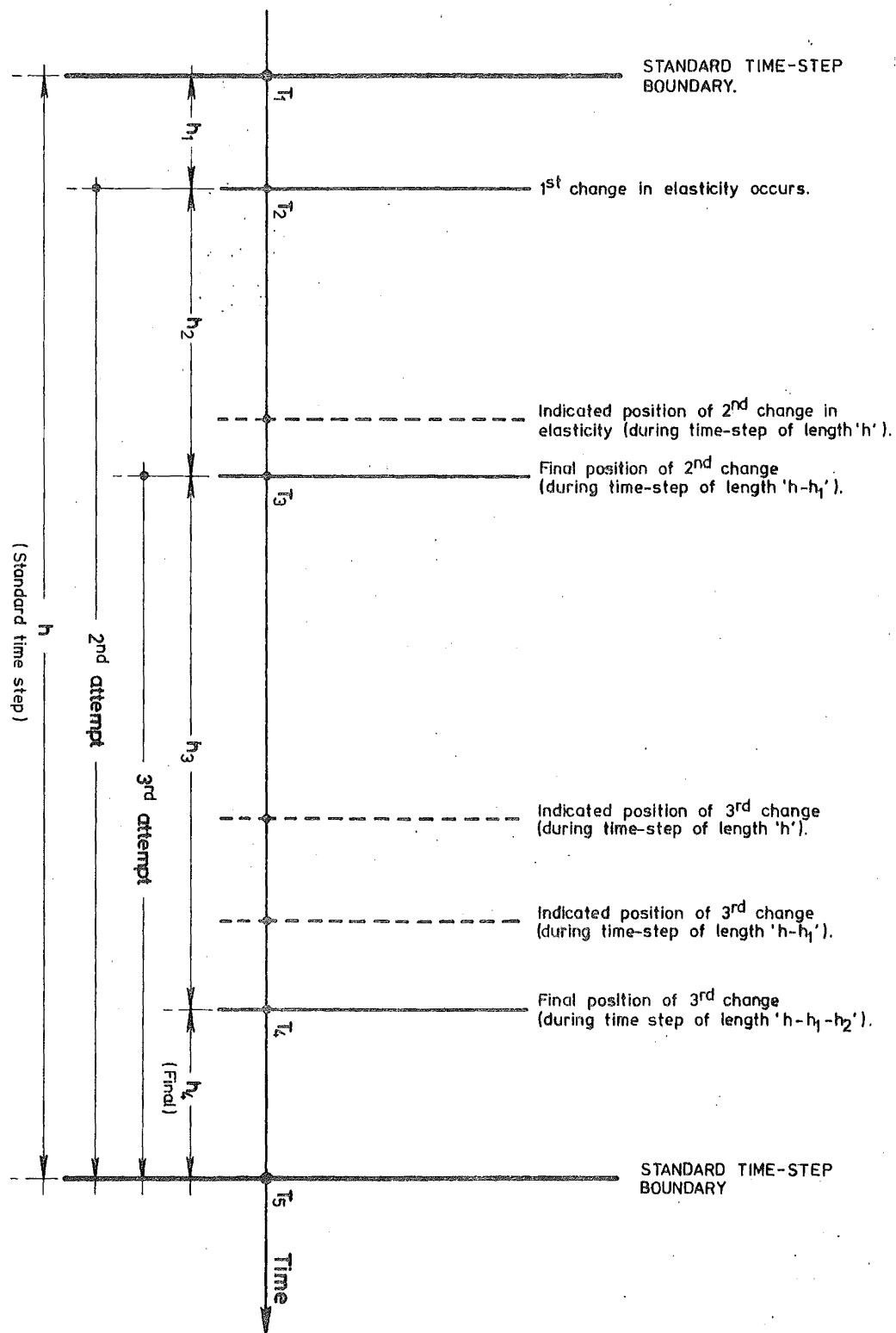
$T_4$  (figure 4-12), it is found that the criteria for a change in elasticity to occur has been exceeded at three different critical member sections during the current interval. Because it has been assumed that the frame remains linearly elastic throughout the interval, it is possible to calculate at what time the first section exceeded the stipulated criteria. The original time-step of length 'h' is then discarded and replaced by one (of length 'h<sub>1</sub>') which finishes at this earlier point and the normal updating of the accelerations, velocities, displacements, member reactions and overall stiffness is implemented for this position. The analysis then continues with a new time-step of 'h-h<sub>1</sub>' (see figure 4-12). It is then likely that the other two critical sections which yielded will again be observed to yield in this new time-step. If this is the case, the effective time-step will be reduced to coincide with the initial occurrence of yielding in the first of these. The procedure is then repeated until the original time  $T_4$  is reached - at which point another attempt is made to continue the analysis with a time-step of 'h'.

The advantages of this technique are that, at any boundary between time-steps, dynamic equilibrium is always attained throughout the frame. Both increasing and decreasing (multi-linear) stiffness can be accommodated in identical fashions. It has the disadvantages of requiring increased overheads in the program's book-keeping caused by the continual adjustment of the interval length, it cannot handle a curvi-linear relationship such as that of a Ramberg-Osgood moment-curvature hysteresis and it will result in a significantly higher number of time-steps. Each of these new time-steps implies the formation of a new static and dynamic stiffness - together with their subsequent reduction into a form suitable for a fast equation-solver.

Although, in a typical seismic analysis, the total time during which a frame contains anything other than linearly elastic sections may be small when compared with the length of the excitation, those time-steps within which plasticity changes do occur are (relatively) extremely expensive. For example, an inelastic analysis of structure I (appendix A) with a constant time-step, produced the following statistics...

a) Number of possibly critical member sections in frame	-	24
b) Number of time-steps in this analysis	-	1000
c) Number of time-steps in which plasticity changes occurred	-	69
d) Maximum number of sections with plasticity changes in any one time-step	-	10

FIGURE 4-12 : USING A VARIABLE TIME-STEP IN ORDER TO AVOID MOMENT-OVERSHOOT.



- e) Number of time-steps required to accommodate all the stiffness changes which did occur - but at one per time-step - 267
- f) Hence, extra number of the expensive time-steps required if only one section allowed to change per time-step - i.e. an increase of, approximately, 200% - 198
- g) Time taken for one time-step when no change in elasticity detected (s). - 0.748
- h) Typical time taken for one time-step when a number of changes detected (s). - 4.38

It is considered that this method is worthy of future consideration, particularly for use in those situations where there are relatively few critical sections and, hence, there exists a reduced probability of many changes of plasticity occurring in any one standard time-step. It is important to note, however, that the method is not applicable to systems where the force-displacement function takes the form of a continuous curve. The scheme selected for use in the rest of this study was that in which the moment overshoot was counteracted by reinvesting it on the following (constant length) time-step. In this way, bi-linear and curvi-linear relationships could be treated in a similar manner.

#### 4.9 THE RAMBERG-OSGOOD HYSTERESIS

Previous work by Goel [30] and Kaldjian [24, 31] has shown that the moment-curvature relationship for structural members can be modelled reasonably closely by one of a series of Ramberg-Osgood functions, a typical example of which appears in figure 2-2.

In moment-curvature terms, for the first curve through the origin, the relationship has the form

$$\frac{\phi}{\phi_y} = \frac{M}{M_y} \left( 1 + \left| \frac{M}{M_y} \right|^{r-1} \right)$$

where  $\phi$  is the curvature, 'M' is the moment, 'r' controls the abruptness of the loss in stiffness of the section and the subscript  $_y$  denotes an equivalent first-yield value. Because an explicit solution for the moment is difficult, a fast-converging iterative scheme such as Newton's method [32] is to be preferred. In general terms, where...

$$\begin{aligned} y &= F(x) \\ \text{and} \quad \frac{dy}{dx} &= F'(x) \end{aligned}$$

$$\text{this is... } x_1 = x_0 - \frac{F(x_0) - y}{F'(x_0)}$$



where  $x_1$  is a better solution than the previous approximation,  $x_0$ . For the case of the Ramberg-Osgood curve through the origin then, given an approximate moment, 'M', a better solution,  $M_1$ , is...

$$M_1 = M_0 - \frac{\frac{\phi_y}{M_y} \left[ 1 + \left| \frac{M_0}{M_y} \right|^{r-1} \right] - \phi}{\frac{\phi_y}{M_y} \left[ 1 + r \left| \frac{M_0}{M_y} \right|^{r-1} \right]}$$

If Giberson's non-linear single component beam (section 4.5) is to be made to follow the Ramberg-Osgood function as a moment-curvature relationship at the critical member sections, then it must be adapted to suit the form of equation 4-iii,

$$\text{i.e.} \quad f = \frac{L}{4H} \frac{1}{EI \frac{d\phi}{dM} - 1} \quad (4\text{-iv})$$

In the case of that function which begins at the origin, this reduces to...

$$f = \frac{L}{4H} \frac{1}{\frac{EI}{k} - 1}$$

as, by definition...

$$\frac{dM}{d\theta} = \frac{M_y}{\theta_y} = k$$

For the general Ramberg-Osgood curve beginning at the point  $(\phi_i, M_i)$ , which is...

$$\theta - \theta_i = \frac{\theta_y}{M_y} (M - M_i) \left[ 1 + \left| \frac{M - M_i}{2M_y} \right|^{r-1} \right]$$

it becomes

$$f = \frac{L}{4H} \frac{1}{EI \frac{\theta_y}{M_y} \left[ 1 + r \left| \frac{M - M_i}{2M_y} \right|^{r-1} \right] - 1}$$

The constant need to change each member's stiffness at each load increment or time-step is very expensive. For column behaviour, the yield values for moment and curvature depend on the axial force at the time and so the resulting surface is extremely complex. No attempt has been made, therefore, to combine these two functions.

#### 4.10 VERTICAL COMPONENTS OF EARTHQUAKES

As soon as the degree of complexity is reached at which moment-

axial load interaction is being considered it becomes essential to consider and incorporate the vertical component of the ground motion. This is simply achieved by accrediting mass to all the relevant vertical degrees of freedom and modifying the incremental load vector so that it will accrue vertical inertia terms based on an input digitised vertical accelerogram - in an identical manner to that for the horizontal motion.

#### 4.11 INERTIAL LOADS FROM JOINT ROTATIONS

If nodes are given rotational masses, based on the rotational inertia of the members framing into them, then the calculations referred to in the previous section (section 4.10) can be further extended to allow the acceleration of the rotational degrees of freedom to cause inertial resistance to be attracted. This mass may be calculated so as to produce a consistent mass matrix [33], which is an upper limit to the allocation, or may be input as single (lumped) values. The allocation of rotational mass will also bring into play the viscous damping of these degrees of freedom. Mass is not considered to be time-dependent in this program.

#### 4.12 VISUAL OUTPUT

Both the presence of member sections at which a yield criteria has been exceeded and the initial checking of frame-geometry data are made obvious by having the computer assemble its own centre-line line-printer sketches showing the frame. It is then possible, when a change in the elasticity of a member occurs, to show the position of the critical section, conveniently and explicitly. The precise form of this output is described further in appendix C.

#### 4.13 COMPARISON OF RESULTS WITH OTHER KNOWN RESULTS

Because of the refinements initiated in this program, it is difficult to compare directly results obtained from it with those of previous studies. By instituting suitable modifications, the program was degraded to the level of that used by Walpole [12] and identical analyses carried out with each. In particular, it was necessary to adjust the damping matrix formulation in order to match that of Walpole. His was constant with respect to time and acted on the lateral stiffness matrix only. The difference in the responses of a multi-storey frame calculated by each program was negligible.

## CHAPTER FIVE

SENSITIVITY OF MODELLING5.1 INTRODUCTION

When the abstraction of data is commenced in preparation for the dynamic analysis of a frame which has either already been constructed or is still in the design stage, the question invariably arises as to what degree of complexity and accuracy is necessary in the numerical representation of the structure in order that meaningful results might be achieved. Both the shape and size of the frame will influence the analyst's choice of degree of accuracy. A tall and narrow frame, for example, will need more attention paid to the axial properties of its columns than will a frame with an aspect ratio at the other extreme. Although many of the factors involved in these decisions can be tested for sensitivity by applying them to a single-degree of freedom system and observing the resulting trends, information on their quantitative effect on real-size frames is much harder to obtain, because of the difficulty in assessing whether the resulting changes in a member's load history are directly attributable to the local changes in the element or whether they are the same as those inherent in any equivalent modification to the overall structure's dynamic stiffness. For the same reasons it follows that a relatively small alteration in an element's character may have a disproportionately-large effect on the overall response of the frame. In order to obtain a feeling for the sensitivity of frames to some of the more common variables, a limited study (restricted in size by the high cost of deterministic inelastic analyses) was made using a small selection of frames.

5.2 AXIAL AND SHEAR DEFORMATION

When a computer program for frame analyses is being written, it is a simple matter to incorporate the effects of both axial and shear deformation in that section which assembles the initial member-stiffnesses. The engineer, however, when contemplating an analysis which will take these parameters into account, is less worried about the complexities of mathematically accommodating these than he is in deciding to what levels of accuracy he should go in reducing his design into a set of numerical values for input as data to the program. With reinforced concrete members, for example, he is faced with the decisions as to whether the cross-sectional areas should include the concrete outside the shear-

reinforcement cage, whether he should assume cracked or uncracked sections and as to how accurate his conversion of steel areas into equivalent concrete areas should be. Alternatively, he may be worried as to whether his choice for some other parameter would be so critical as to make a decision about cross-sectional areas trivial.

The three frames used in the study are all described elsewhere in this thesis. The thirteen-storey frame (appendix A), being tall and slender, could be expected to behave in a manner somewhat akin to that of an equivalent vertically cantilevered beam. In contrast, the bending action of the six-storey, two-bay frame (appendix A) is most likely to be less accentuated than that exhibited by the taller two-bay frame. The bridge pier (chapter seven), because of its simple geometry, is likely to have its behaviour largely determined by the axial characteristics of its very slender piles. The first few undamped natural frequencies of these frames, for a number of variations in axial and shearing conditions, are listed in table 5-I. The control values are obtained from the case for which axial deformation, shear deformation and both horizontal and vertical masses are included. By preventing all the vertical degrees of freedom of the frame's joints from moving, it is possible to eliminate all column axial deformation and thereby simulate very large cross-sectional areas. If the rotational degrees of freedom were to be fixed similarly, the frames would adopt rigid-floor modes of vibration (i.e. the columns alone would carry all the horizontal deformation in shear and bending). By carrying out modal analyses in which all forms of deformation were allowed, but with the axial areas of the vertical members arbitrarily halved, it was expected that the degree of sensitivity of the frame stiffness to variations in axial areas would become apparent. Varying of the cross-sectional areas used in the calculation of the members' shear deformation was also tried, the most severe (stiffest) case being when no shear deformation was allowed in any member.

As expected, the thirteen-storey frame was found to be considerably more sensitive to alterations in the column properties than was the six-storey one. Whereas the inclusion of infinite axial area in the column properties resulted in the taller frame enduring a sixty-five per cent increase in the magnitude of its first natural (undamped) mode's frequency, only a sixteen per cent increase was experienced in that of the smaller example. For similar variations, the bridge structure attracted a twenty-five per cent increase in its fundamental natural frequency. It, too, has a relatively slender structural form. An examination of the

NATURAL (UNDAMPED) FREQUENCIES (HZ)		- CONTROL - Axial and shear deformation, rigid end- blocks	No axial deformation of columns allowed	No vertical masses	No column shear deformation. Column axial areas halved	No shear deformation in any member	Shear areas of columns halved	No rigid end-blocks
13 storey, 2 bay frame. (Structure II, appendix A)	1 2 3 4 5 6	1.076 1.906 2.156 2.363 2.440 2.492	1.724 2.156 2.342 2.440 2.471 2.571	1.079 1.907 2.156 2.364 2.440 2.492	0.841 1.740 2.225 2.268 2.438 2.528	1.138 2.170 2.229 2.535 2.742 2.818	1.069 1.889 2.101 2.361 2.403 2.490	0.805 1.402 1.673 1.758 1.855 1.914
6 storey, 2 bay frame. (Structure I, appendix A)	1 2 3 4 5 6 7 8	1.359 4.116 7.338 10.76 14.27 16.27 ↑ 16.97	1.381 4.161 7.355 10.78 14.28 - 16.98	1.359 4.118 7.339 10.77 14.28 - 16.98	1.348 4.105 7.397 10.86 11.66 ↑ 13.26 ↑ 13.90 ↑ 14.55	1.378 4.176 7.452 10.94 14.53 16.28 ↑ 17.31	1.348 4.081 7.261 10.62 14.04 16.27 ↑ 16.66	1.142 3.447 6.078 8.793 11.45 13.42 14.94 16.70
Auckland upper harbour crossing. (chapter seven)	1 2 3 4 5	0.6529 3.413 8.493 ↑ 36.64 ↑ 53.92 ↑	0.8184 3.674	0.6530 3.414	0.5661 3.354 6.006 ↑ 25.91 ↑ 46.75 ↑	0.6585 3.456 8.493 ↑ 36.64 ↑ 54.42 ↑	0.6475 3.371 8.493 ↑ 36.64 ↑ 53.45 ↑	0.6248 3.208 8.055 ↑ 34.76 ↑ 51.80 ↑

(↑ = vertical mode)

TABLE 5-I : SENSITIVITY OF NATURAL FREQUENCIES TO AXIAL AND SHEAR DEFORMATION.

higher modal frequencies of all the frames showed the effect of a lack of axial deformation to become rapidly less significant with the increasing mode number. Again, this trend was more marked in the less slender regular frame. The effect is still seen to be discernible at the fifth and sixth lateral modes of the thirteen-storey frame, but to be insignificant at the corresponding stage in the six-storey frame.

A restriction on the occurrence of shear deformation in the members had a less telling effect than that of variations in the axial area of column members. Making the shear areas infinitely large (i.e. not allowing any shear deformation) naturally caused the flexible frames to stiffen, but in all three cases an increase of less than five per cent in the lowest natural frequencies was noticed. Higher modes, however, were seen to retain the effect to a greater degree than they did in the similar study of axial areas. This is because the behaviour of modes with the higher frequencies depends more on relative nodal movement than does that of the fundamental mode. Shear forces, influenced by the greater moment-gradients induced, are higher and so shear deformation is more significant. The presence of short, deep beams (i.e. length-to-depth ratio less than about ten) in a frame are, therefore, an indication that shear deformation should be considered in any stiffness-modelling that is proposed. This modelling will become critical if the idealization of a coupled shear wall as an assemblage of members with large rigid end-blocks is attempted as the coupling elements are designed to transmit large shearing forces. For the same reason, care should be taken when modelling spandrel beams.

If any member is not permitted to deform in shear, it must, in order to be able to connect nodes with certain rotations, endure higher curvatures (see figure 5-1) than the corresponding member in which a contribution from shear deformation is allowed. (All other factors being equal, it could be expected that a frame, assembled from members devoid of shear deformation, would sustain higher section ductilities during a deterministic dynamic analysis.) However, it is difficult to distinguish between the sensitivity of the ductilities to the increased stiffness of the frame and that due to the increased curvature requirements of the members. In an analysis performed to investigate this effect, the stiffer (i.e. no shear deformation) frame incurred a twenty per cent decrease in the maximum recorded top-storey displacement of the six-storey frame for the first ten seconds of the El Centro, May 18, 1940 (North-South) accelerogram. The ductility requirements reflected the smaller deflections which took place, although the plastic hinge patterns

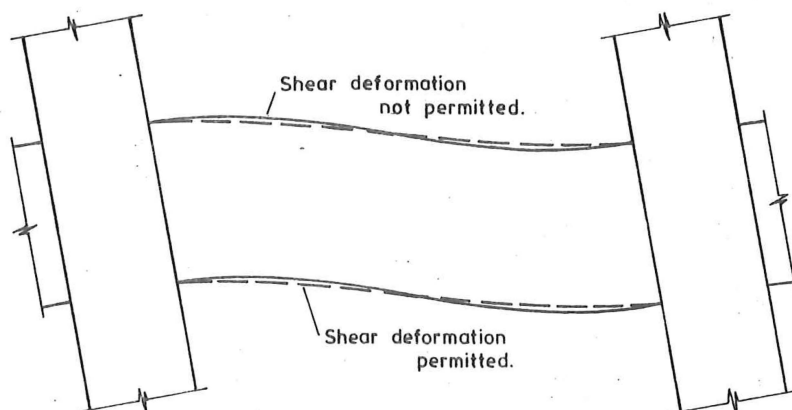


FIGURE 5-1 : THE EFFECT OF SHEAR DEFORMATION ON THE ELASTIC LINE OF A BEAM.

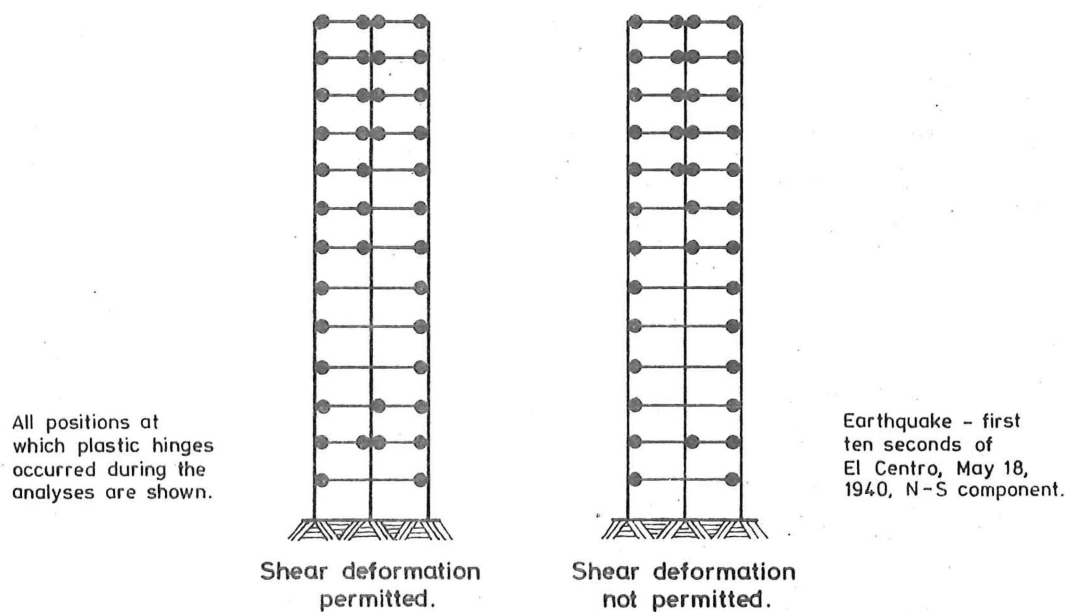


FIGURE 5-2 : THE EFFECT OF SHEAR DEFORMATION ON A PLASTIC HINGE PATTERN.

(figure 5-2) varied a little - in such a way that a few critical sections in the frame without shear deformation had greater plastic deformations than their counterparts in the standard frame. Figure 5-3 shows an example of this.

It appears that, by careful inspection of the frame to be analysed, it should be possible to conclude as to whether there is much error to be incurred by ignoring the deformation of members in shear in the proposed analysis. The ability for an accurate representation of axial stiffness in column members to be made is essential as the quantitative sensitivity of the frame to this stiffness is harder to predict. Any new analysis programs being written should definitely include both these stiffness capabilities because of the ease with which they can be incorporated.

### 5.3 ALLOWANCES FOR JOINT SIZE

In any real structural frame there is a difference between the centre-line length of idealized members and that clear length over which deformation can take place. It is self-evident that the exclusion of the rigid blocks at the ends of a member will appreciably alter its stiffness, particularly as some of the stiffness terms are dependent on up to the third power of the member's flexible length. A glance at table 5-I will show that the effect of neglecting the size of the rigid joint can be drastic if the overall natural frequencies are used as an indication of a frame's stiffness. The bridge, because it consists of members which are relatively slender in the plane of the motion, suffers the least. The inclusion of an allowance for joint size is, therefore, elementary - particularly in those frames in which shear deformation (because of the member length-to-depth ratio) must be considered. When inelastic analysis programs are being written, it is again simple to take advantage of the rigid end-block to place a member's critical sections (or plastic hinges) at a more realistic distance from the intersection of the centre-lines of the framing members.

### 5.4 THE SHAPE OF THE MOMENT-CURVATURE HYSTERESIS

The importance of modelling a realistic moment-curvature relationship for the critical sections of a member has been dealt with (analytically) in chapter two. In trying to adhere to the recommendations which arose from that study a conflict is encountered. Briefly, any relationship which is to be included economically in a deterministic analysis must be essentially simple in its concept.



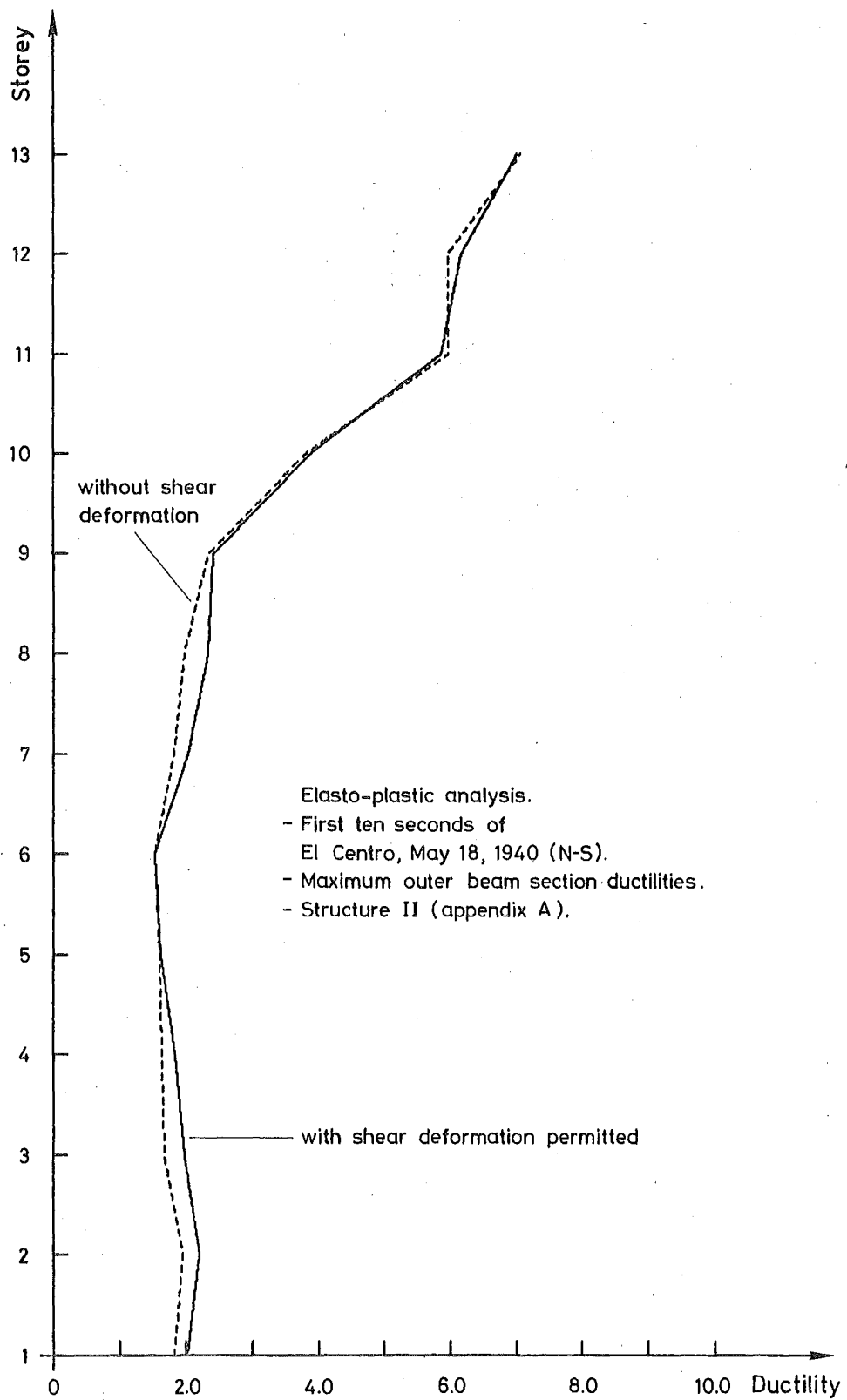


FIGURE 5-3 : THE EFFECT OF SHEAR DEFORMATION ON BEAM DUCTILITIES.

At the present stage of the development of dynamic inelastic analyses, the inclusion of procedures for the self-generation of moment-curvature curves from input details of the section properties of the member can not always be justified, because of the inordinate computation time they require. Although a complete study of the effectiveness of matching the modelling of the behaviour of different construction materials to certain relationships is not the intention of this section, such studies have been well advanced by many independent researchers, typified by Park [34]. For the case of a reinforced concrete section, for example, they have been able to attain good agreement between experimental moment-curvature paths and those derived by assuming suitable individual concrete and steel stress-strain relationships and iteratively varying the distribution of stress across a cracked section until a balanced condition is reached at each load increment.

The level of fidelity that can be reached through such a modelling procedure is high when it is compared with those reached in other contributory sections of a dynamic analyses. Hence, it was intended that a brief investigation be made of the differences which would arise from the selection of any one of three, relatively simple, approximate moment-curvature relationships. The relationships chosen were those most likely to be offered at present to the prospective user of a commercial inelastic analysis program.

Elasto-plastic, bi-linear and Ramberg-Osgood functions were used alternatively to control the moment-curvature at the critical sections of beam members when analysing deterministically the six-storey, two-bay frame of appendix A for the first five seconds of the familiar North-South component of the El Centro, May 18, 1940 earthquake. Column behaviour was assumed to be linearly elastic. The top-storey lateral displacement (figure 5-5) and the moment at the outer end of a second-floor beam (figure 5-6) were recorded to provide a basis for the comparison. A short excitation was chosen because of the expense involved in running the Ramberg-Osgood analysis (because the stiffness-changing procedure must be invoked at every time-step). This particular analysis, with a processing time of thirty-seven minutes, took twice as long as either of the bi-linear or elasto-plastic analyses to complete. All three hysteretic loops had the same initial slope. In order to produce a Ramberg-Osgood function that would, apparently, be similar to that of a bi-linear one in which the gradient of the second branch was one-tenth of that of the initial part, the input characteristic yield moments were increased by five per cent. The consequent matching of these two functions is

illustrated in figure 5-4. Only for curvatures in excess of about three did the Ramberg-Osgood function again parallel, in gradient, that of the bi-linear curve. The complexity of the resulting moment-curvature track for the Ramberg-Osgood function is clearly shown in figure 5-7. Each reversal, after the initial few, results in a slightly different version of the function being followed, whereas the bi-linear and elasto-plastic plots show the reversals of moment generally to leave the section stiffness unchanged. Both of the straight-line plots show irregularities at the junctions of the linear branches. These arise from the integrating procedure only being capable of recognizing a change in the direction and/or rate of increase of curvature at the end of a time-step, even though it may have, in reality, occurred part-way through the interval.

The time-histories of both the displacements and moments show similar, but reversed, trends. The maximum deflection occurred when the Ramberg-Osgood hysteresis was used (after 2.2 seconds of excitation). At the same point in time, however, the bi-linear case gave the selected beam moment as being greater than that recorded in the Ramberg-Osgood case. This apparent incongruity partly reflects the effect of the preceding history of the member section. The frame, having endured higher levels of plasticity at a previous peak in the Ramberg-Osgood response, proceeds to incur larger curvatures at reduced levels of moment. Because the Ramberg-Osgood hysteresis offers a more gradual deterioration of the increasing stiffness, the response generated by its use tends to have some of the abruptness exhibited by the other two responses smoothed out of it. This is particularly noticeable (figure 5-6) in the first second of the analysis and again after a total of 2.6 seconds have elapsed.

As was seen in the study of tracking methods in the preceding chapter, the apparent permanent plastic drift of a frame is most sensitive to the form of the moment-curvature hysteresis. The responses, for those periods of time when the frame is enduring a linearly elastic state, are merely displaced amplitude-wise with respect to each other. The final (plastic) drifts for the excitation being used are, of course, subject to the effects of the remaining part of the earthquake and cannot be properly ascertained until the frame has finally come to rest.

The matching of the Ramberg-Osgood function to that with a bi-linear form was not particularly successful. The motion of the earthquake was such that deformation along the initial branch of the Ramberg-Osgood hysteresis did not continue far into what would normally be designated as the plastic range. Subsequent motion in this analysis then took place in accordance with the second form of the Ramberg-Osgood

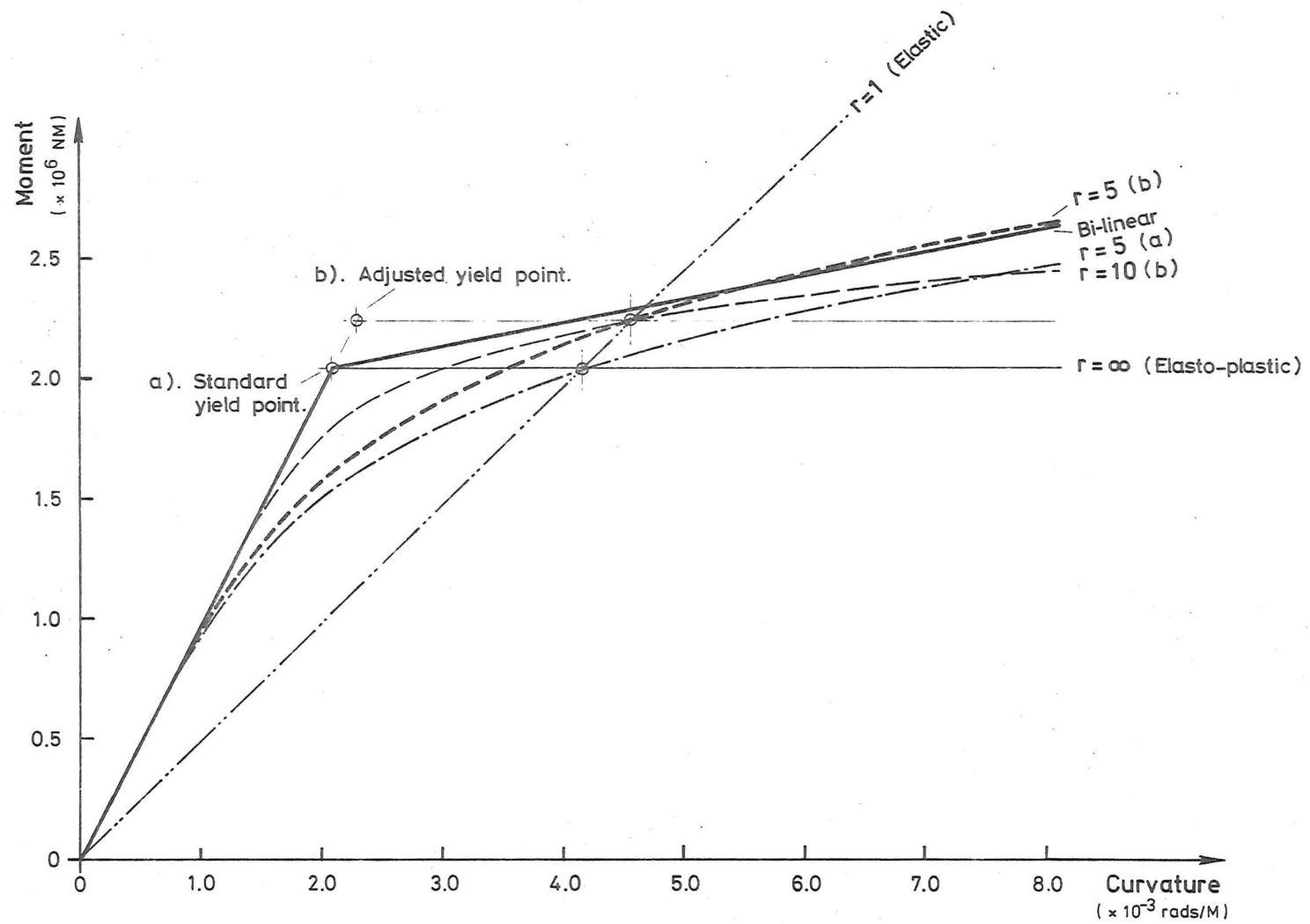


FIGURE 5-4 : MATCHING A RAMBERG-OSGOOD FUNCTION WITH A BI-LINEAR HYSTERESIS.

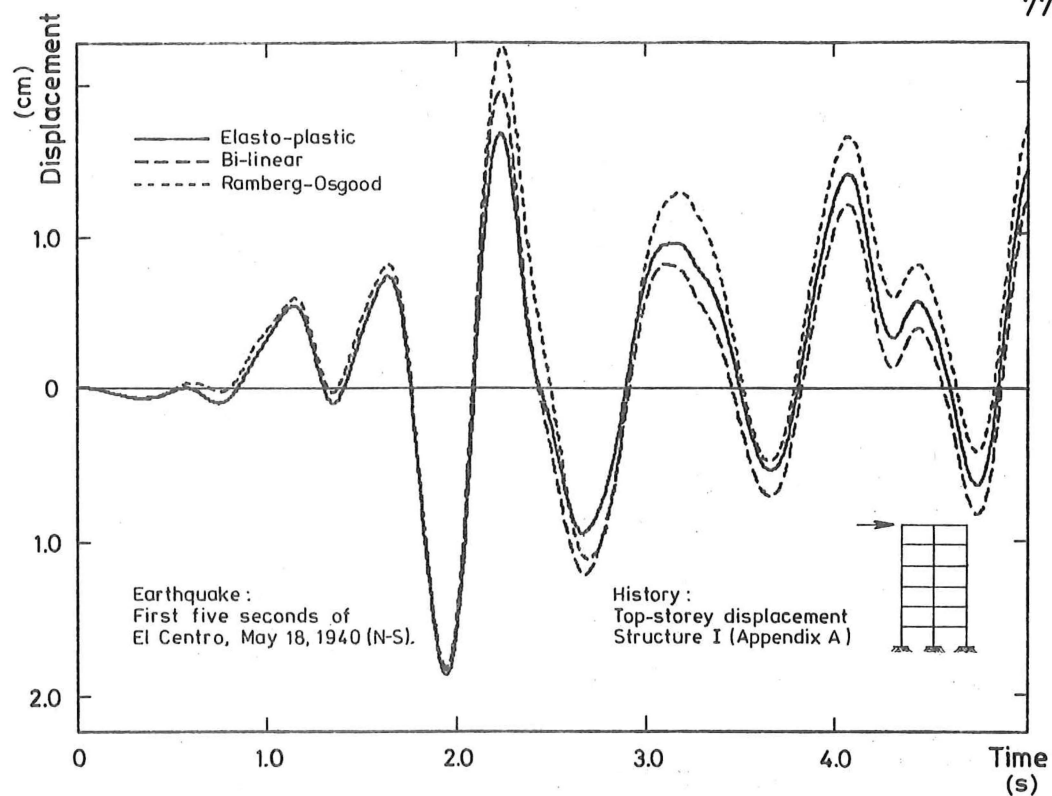


FIGURE 5-5 : COMPARATIVE DISPLACEMENT RESPONSES ARISING FROM THE USE OF DIFFERENT BEAM MOMENT-CURVATURE RELATIONSHIPS.

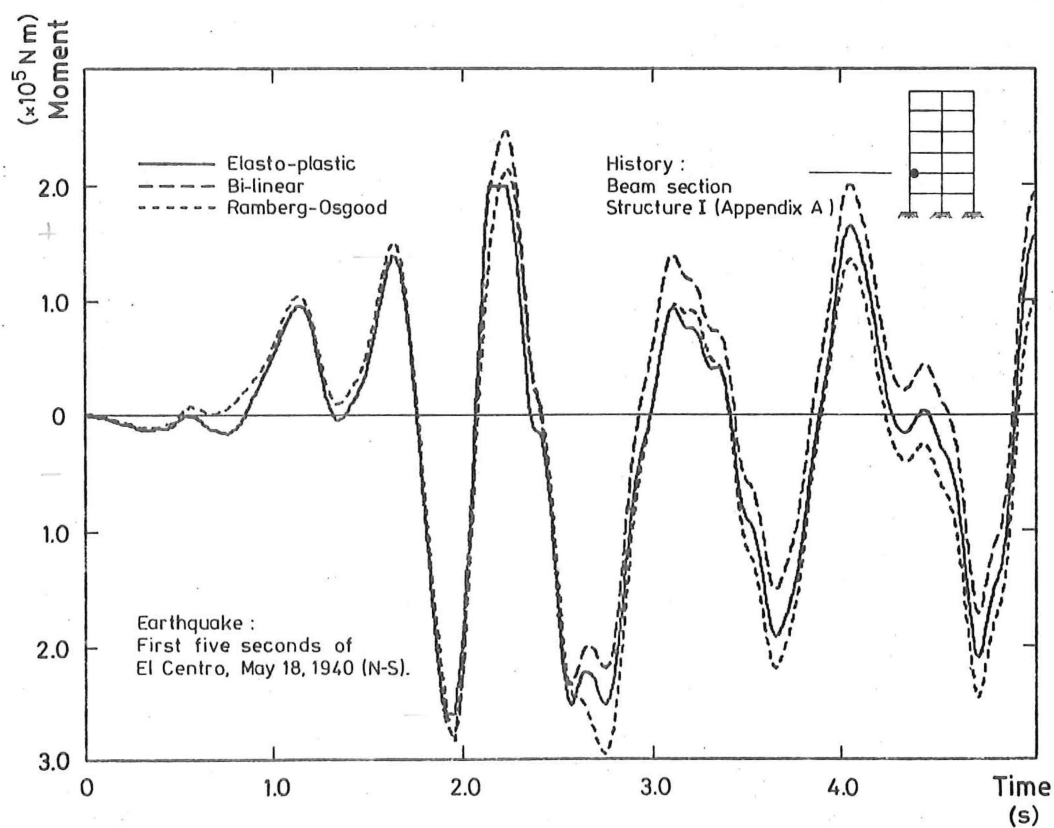


FIGURE 5-6 : COMPARATIVE MOMENT HISTORIES ARISING FROM THE USE OF DIFFERENT BEAM MOMENT-CURVATURE RELATIONSHIPS.

function (see chapter 4.9) which defines a flatter profile. The moment-curvature response plots have tended to show that the bi-linear schemes are essentially quite different in performance to the curvi-linear example, although they provided a similar type of reaction. If this study is to be taken up and extended then it is suggested that it take the form of an effort to distinguish between moment-curvature relationships which are more basically similar to each other than these are. There are, obviously, some structural materials which exhibit a behaviour more in the nature of bi-linear hysteresees than those of the curvi-linear Ramberg-Osgood family. Such a fact will, to some extent, restrict the choice of hysteresees to be made by the analyst. Others have been prepared to make a comparison. Goel and Berg[30] noted that elasto-plastic behaviour tended to over-estimate the response when compared with that formed by using a Ramberg-Osgood function. They also found that an elasto-plastic structure may be expected to show larger permanent distortion. Neither of these views could be absolutely supported by this study. The magnitude of the maximum displacement achieved depends partly on the history of previous plastic excursions of the frame's members during the earthquake. It is thus also dependent on both the amount of energy being dissipated by the plastic flow and the effect this is having on the frame by both damping it and altering its natural frequencies. The rates of energy-absorption of two systems, one exhibiting an elasto-plastic hysteresis and the other a Ramberg-Osgood function, could only be exactly compared if they were suffering a forced vibration of constant amplitude. As can be seen from figure 5-7, the hysteretic nature of the Ramberg-Osgood function's tracking is of a vastly different nature to that of the other two and, in this particular case, would lead to a higher amount of energy being absorbed.

Before the use of a Ramberg-Osgood hysteresis for moment-curvature representation is decided upon, the analyst must be sure that it is truly representative of the material that he is modelling. Because of the expense its use involves, if he can not justify its use and he merely wants an 'inelastic' frame analysis, a more simple form of hysteresis will most likely be satisfactory. The adaption of more complex multi-linear (rather than curvi-linear) hysteretic functions to inelastic dynamic analyses is the most logical development for this area. The conflict between the proven need for accurate representation of the moment-curvature function and the possible expense of the highly-refined schemes would then be partly resolved.

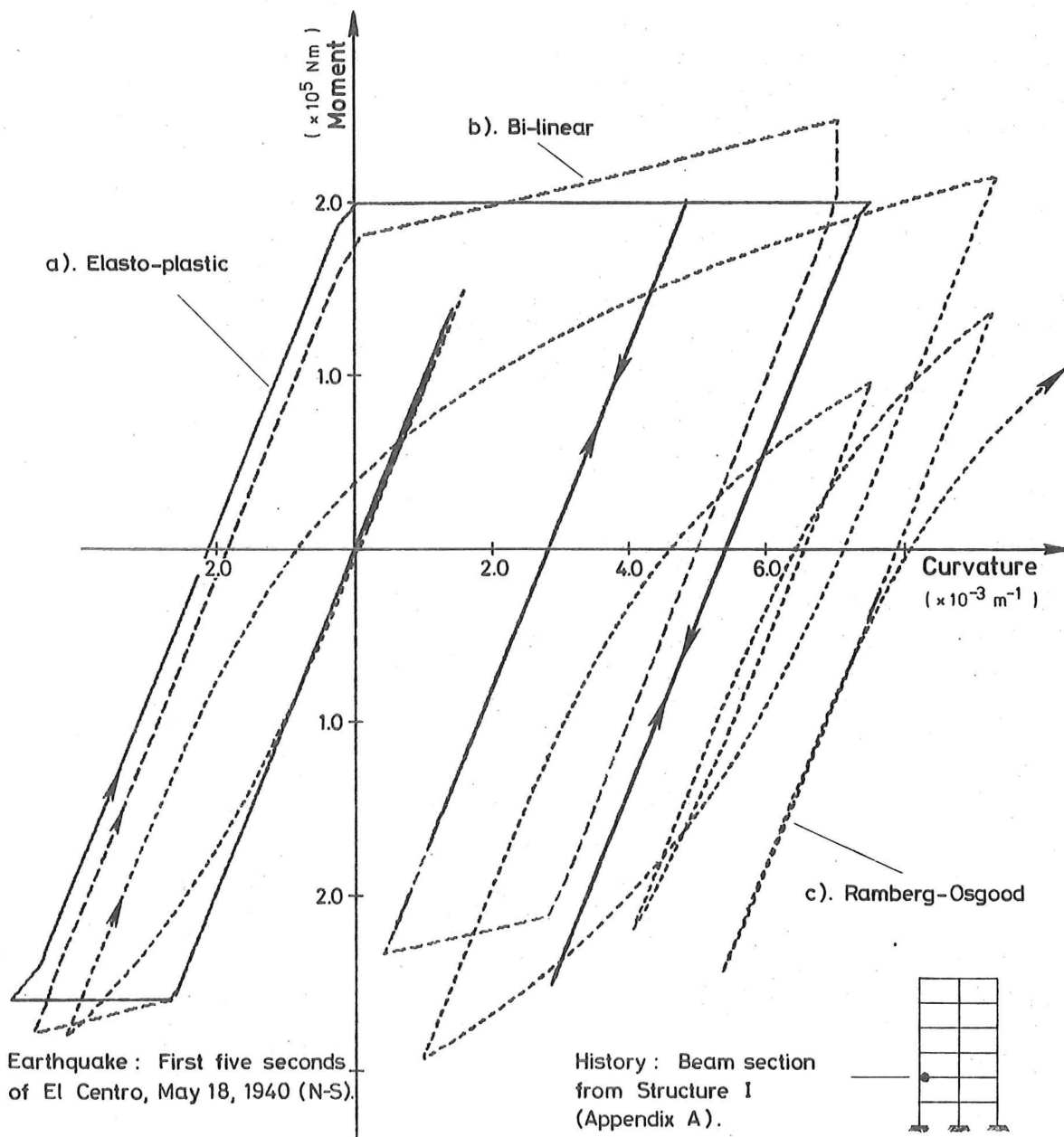


FIGURE 5-7 : TYPICAL MOMENT-CURVATURE TRACKS FOR DIFFERENT HYSTERETIC FUNCTIONS.

## 5.5 THE REPRESENTATION OF MASS

Although no sensitivity studies were initiated exclusively to find the effect of the different forms of the mass representation that could be adopted, general conclusions were made as to which aspects of the representations are the most important. Basically, the mass of a structure can be modelled in either an equivalent lumped or a consistently (Archer [33]) distributed form.

If a lumped form is used, it is recommended that the associating of mass with vertical degrees of freedom be now considered intrinsic to the analysis of all frames in which vertical displacements or accelerations could be important. In particular, if an axial load-dependent yield criteria for columns or a vertical ground excitation is applied, the incorporation of vertical mass becomes essential. Tall, slender frames, in which the axial displacement of external columns plays a significant role, should be equipped with vertical mass in order to model faithfully their cantilever action. Formulation of the vertical lumped mass is normally without problems as the same mass distribution as that for horizontal mass is normally used.

The criteria for the use of lumped rotational mass at the joints have the same basis as those for vertical mass. Where there is likely to be considerable rotation of a joint (or bending of a member), it is worth-while considering the placing of lumped rotational masses. Again, if a frame is extraordinarily flexible or the members framing into some of the joints are relatively slender, then a rotational lumped mass distribution should be considered. The selection of a value for a lumped rotational mass is not straightforward, however, and is best dealt with by reference to the consistent mass formulation.

Use of a consistent mass matrix, adequately described by Archer [33], enables the components of acceleration at one node or joint to apply realistic inertial loads to interconnected nodes in a similar way to that in which the displacement of one node is inextricably related to the stiffnesses of the other nodes to which it is connected. It also enables the distribution of mass along a member to be taken into account when inertial effects are being considered. The formulation referenced previously provides an upper-bounded solution for the dynamic stiffness of the frame and thus tends to give natural frequencies which are slightly higher than they should be. An inspection of the appropriate rotational terms of the consistent mass matrices which affect a particular joint will give an analyst the limits within which his choice of rotational mass for a lumped distribution can be made.



It then falls on the analyst to make a decision as to how much emphasis he wants to place upon the rotational degrees of freedom by varying the magnitude of the associated lumped masses.

Either when analysing simple structures, or in cases where it is not economic to spend time in investigating the sensitivity of such a decision, it becomes expedient to specify a unit mass for each type of element and accept that the solution will be bounded. This avoids having to make any further assumption as to the formulation of the lumped rotational mass.

## CHAPTER SIX

CHOOSING AN EARTHQUAKE6.1 INTRODUCTION

A limited attempt has been made to find some correlation between the damaging potential of various digitised earthquakes and their relative strengths which have been calculated in a variety of ways.

Although practitioners of the art of dynamic analysis have had access to a variety of both actually recorded and artificially produced digitised earthquake accelerograms for a number of years, the North-South component of the El Centro, May 18, 1940 earthquake is still the favourite choice. Because of a lack of knowledge of the comparative effects and strengths of the others available, use of that component has become, by default, firmly entrenched in the repertoire of both designer and analyst. The relationship between code requirements and the ability of a particular frame to withstand such a digitised earthquake have always been vague, because of the uncertainty as to the criteria with which to gauge the strength of an earthquake in absolute terms. For example, measurement of the maximum ground acceleration is not, by itself, a true indication of the 'size' of an earthquake unless the duration of this acceleration can be incorporated into the assessment. Jennings [35] and others have electronically generated artificial earthquake records to meet predetermined criteria for spectral response so that they are characteristic of the type of motion that might be expected at various distances from the epicentre. Penzien and Liu [36] subjected a non-linear single-degree of freedom model to a wide range of these artificial records and attained good correlation between the peak responses for similar earthquakes. Again, however, this gives little indication of the extent of the correlation that could be expected for multi-degree of freedom systems in which varying amounts of non-linearity occur.

It was, therefore, decided to make an attempt to gain an appreciation of what the principal earthquake parameter was in the amount of damage sustained by a tall frame when it was subjected to various earthquakes.

6.2 THE FRAME

A thirteen-storey, two-bay frame (structure II, appendix A) was chosen for the comparative study. Because of the frame's reasonably large number of members, it was ensured that diverse patterns of plasticity would

be set up by different excitations, thus avoiding the all or nothing radicalism of the sensitive single-degree of freedom system. The frame, designed to the load factors of the proposed revision to Chapter 8, NZSS 1900 [1] was considered to have elasto-plastic moment-curvature characteristics at the critical sections in its beams. Trial analyses, using the North-South and vertical components of the El Centro, May 18, 1940 earthquake accelerogram, confirmed that, even with a moment - axial load interaction yield criteria being used in the columns, the likely occurrence of column-hinging for such a strong-motion earthquake was small. The formation of these hinges would be transitory by nature and would not significantly alter the overall response of the frame. As the computer program was capable of desisting from the checking of vertical (i.e. column) members for possible hinge formation (for a saving of time, in this case, of about ten per cent), it was decided to assume that no plastic hinges would occur in the columns. Another trial analysis, using this assumption and the same ground excitation as before, confirmed the validity of this as, on the few excursions when the interaction yield criteria would have been exceeded, a maximum increase of four per cent in the section's ultimate strength would have prevented the formation of column hinges.

### 6.3 EARTHQUAKE SCALING

The most important attribute of a particular earthquake record is its damaging potential. To describe two earthquakes as being comparable is, therefore, to imply that their damaging potential is similar. The very nature of an earthquake is such that it will affect different structures in different ways - as the random study of any response spectrum will testify. In this attempt to compare and scale earthquakes it is, therefore, necessary to limit severely the extent of the range of frames and earthquakes that can be considered. By choosing a tall, slender frame of a type quite likely to be built in New Zealand, an expedient compromise is reached between the size of the problem and the resources available. Similarly, because of both the exceedingly large computing times required for non-linear dynamic analyses and the variations in the lengths of those earthquake accelerograms available, only the first ten seconds of each record was considered throughout this study.

Various criteria for the scaling of earthquake records are easy to evolve. These range in complexity from that of the simple scaling of the maximum ground accelerations to that of a factor produced from the ratio of the integrals of the spectral velocity from a period of 0.1 seconds to

one of 2.5 seconds (Housner [37]). In order to gain an appreciation of the significance and scatter of these various scaling factors, a large number of spectral responses were calculated. Those vertical components available were included in the range used so that their significance could be established. Table 6-I lists the factors by which each component needs to be multiplied for it to be comparable with the designated standard - El Centro, May 18, 1940 (North-South component). The percentages of critical viscous damping used were chosen so as to encompass the extremes likely in practice. The particular El Centro component was chosen as a standard because, as well as being a good example of a strong motion excitation, it has an acceptance which has arisen from a familiarity engendered by its frequent use.

An examination of table 6-I shows that there is no obvious correlation between the scale factors and the method by which they were derived. It could be expected that the scaling produced under higher percentages of damping would have an asymptotic tendency as the damping was increased. However, the differences between the scale factors derived using similar methods, but for different levels of damping, show as much variability as do those of factors which have been derived using entirely different criteria. In some isolated cases, such as that of the East-West component of the El Centro, May 18, 1940 earthquake, the factors are remarkably constant for many of the criteria. In this particular case, this is most likely attributable to the fact that two variations of what is, essentially, the same earthquake, are being compared. It is also of interest that, in this particular series of comparisons, the maximum spectral acceleration ratios stand out as being the most inconsistent.

Despite the wide variations in the magnitude of the scaling factors produced for each earthquake and the undoubted influence that particular intrinsic properties of the control earthquake will have on these values, a macroscopic inspection can justify the making of some approximate comparisons. For example, the artificial earthquakes C1 and C2 are apparently of the order of five times as intense as the control one - regardless of which criteria is used in the comparison.

#### 6.4 MEASURING AN EARTHQUAKE'S DAMAGE POTENTIAL

To the observer of the aftermath of a major earthquake, the severity of the damage caused is quantified in terms of the financial cost of the subsequent repairs. It could be expected, therefore, that a highly developed dynamic analysis may, in the future, give a likewise estimate of the costs to be expected. A large part of the cost of the damage to a

Ratios given as Benchmark* E/Q component	Component	Maximum acceleration	Maximum spectral accel.	Maximum spectral velocity	Sp. vel. integral 0.0-3.0s	Sp. vel. integral 0.1-2.5s	Maximum spectral accel.	Maximum spectral velocity	Sp. vel. integral 0.0-3.0s	Sp. vel. integral 0.1-2.5s	Maximum spectral accel.	Maximum spectral velocity	Maximum spectral displ.	Sp. vel. integral 0.1-2.5s	Average		
			0% damping					5% damping					20% damping				
El Centro, Dec. 30, 1934	N-S	1.24	1.67	1.61	2.24	1.98	2.00	1.88	2.02	1.74	1.81	1.36	2.82	1.46	1.83		
	E-W	2.42	2.09	2.18	2.23	2.31	2.51	1.80	1.93	2.01	2.54	1.27	1.27	1.51	2.01		
El Centro, May 18, 1940	N-S*	1.00	1.00	1.00	1.00	1.00	1.00	1.00	1.00	1.00	1.00	1.00	1.00	1.00	1.00		
	E-W	1.47	0.963	1.46	1.44	1.45	1.54	1.47	1.46	1.46	1.49	1.34	1.34	1.39	1.41		
Olympia, April 13, 1949	N80°E	1.91	1.29	1.83	1.90	2.17	1.47	1.37	1.76	1.94	1.78	1.47	1.46	1.72	1.70		
	N10°W	1.72	0.851	2.20	3.15	2.74	1.65	2.52	2.98	2.56	2.04	2.80	3.96	2.55	2.44		
Taft, July 21, 1952	N69°W	2.03	1.48	2.02	2.14	1.94	1.90	2.14	2.15	1.94	2.15	2.03	2.02	1.71	1.97		
	S21°W	1.79	1.36	1.70	2.62	2.34	1.62	2.42	2.67	2.33	2.23	2.48	3.52	2.08	2.24		
Olympia, April 29, 1965	S86°W	1.59	1.02	2.78	4.26	3.86	1.53	4.02	4.10	3.71	1.97	4.26	4.53	3.61	3.17		
	S04°E	1.98	0.781	2.44	5.42	4.57	1.53	3.43	5.34	4.46	2.22	4.56	7.31	4.24	3.71		
Seattle, April 29, 1965	S58°W	3.89	4.19	4.30	6.12	5.38	3.93	4.80	5.47	4.70	5.08	4.02	7.28	4.30	4.88		
	S32°E	6.02	4.46	5.00	11.9	10.8	4.49	6.76	11.0	9.99	6.25	8.39	10.0	8.92	8.00		
Artificial (Jennings')	A1	0.947	0.971	0.811	0.842	0.715	1.01	0.689	0.817	0.696	1.16	0.798	0.995	0.764	0.863		
	A2	0.707	0.807	0.967	0.950	0.919	0.953	0.958	0.894	0.864	0.894	0.911	0.910	0.683	0.878		
	A3	0.927	0.782	1.02	1.17	1.28	1.02	0.992	1.20	1.05	1.05	1.15	1.75	1.09	1.11		
	A4	1.04	0.810	0.955	0.845	0.768	1.07	0.747	0.779	0.707	1.05	0.815	0.896	0.773	0.866		
	B1	0.848	0.830	1.07	1.11	1.10	0.932	0.915	1.03	1.02	1.15	0.958	0.958	0.832	0.981		
	B2	1.01	0.848	1.12	1.18	1.06	1.10	1.02	1.16	1.04	1.11	1.13	1.46	1.06	1.10		
	C1	4.69	4.03	4.62	5.92	4.95	4.63	5.65	5.76	4.71	4.81	4.91	9.45	4.82	5.30		
	C2	5.50	5.16	5.46	6.88	5.80	4.61	6.65	7.08	5.89	5.35	6.92	11.8	6.09	6.40		
	D1	0.656	0.789	1.05	1.45	1.24	0.715	1.18	1.48	1.27	0.690	1.19	2.01	1.33	1.16		
	D2	0.648	0.915	1.35	1.62	1.37	0.745	1.22	1.44	1.19	0.726	1.21	2.43	1.19	1.23		

TABLE 6-I : SCALING FACTORS FOR ACCELEROGRAMS.

building is incurred in the repairing of non-structural items. If the problem is limited to that concerning only the structural members, it appears reasonable that the cost of repairs will be, qualitatively, a function of the size of the member, the maximum member ductility reached and the accessibility of the damage. Other factors likely to be involved in the assessment are the number of excursions of the critical sections into their plastic ranges and the total time for which this occurs. Together, these two give a measurement of the energy absorbed at a section.

The selection of a scheme by which the damaging potential of several different scaled earthquakes acting on a non-linear frame must, at this stage, be limited to one related to a measurement of member ductilities achieved. The maximum top-storey deflection of a tall multi-storey frame provides only limited information about the severity of the earthquake because the overall motion of this type of frame is unlikely to be dominated by the first natural mode of vibration.

#### 6.5 USING MAXIMUM MEMBER DUCTILITIES TO COMPARE RESPONSES

Having decided that the structural damage to a frame could only be measured, at this stage, in terms of the maximum ductilities achieved by the damaged members, a series of investigatory analyses were carried out on the frame previously described. Of all those available, four earthquake accelerograms (each ten seconds long) were chosen as being, on visual inspection, of a roughly similar type. The earthquakes chosen were...

- a) El Centro, December 30, 1934, North-South component,
- b) Taft, July 21, 1952, N69°W component,
- c) Seattle, April 29, 1965, S58°W component,
- d) Al - Jennings' [35] artificial earthquake suite.

Although an inspection of the various means of scaling does not help in the decision as to whether any particular scaling methods are more applicable than others, it was decided to scale the components according to some of the methods already discussed in order to gauge the success of the methods. In order to provide a standard against which to compare the results, the North-South component of the very familiar El Centro, May 18, 1940 accelerogram was used, its magnitude scaled linearly by factors of 0.7, 1.0 and 1.3.

The first type of scaling, used in a series of analyses with the selected earthquakes, was that based on the ratios of the maximum ground accelerations. This method gave a wide range of factors for the four selected components. The second method of scaling employed was that

arising from a comparison of the integral of the linear spectral velocity relationships, from a 0.1 seconds period to that of 2.5 seconds, with five per cent damping. The difficulty in quantitatively comparing responses becomes immediately clearer. Although the maximum top-storey displacement during analysis (a) was fifty per cent higher than that of the control earthquake, the resulting various ratios of corresponding member ductility varied widely, from 0.642 to 1.74. Tables 6-II and 6-III give further comparisons between the various analyses. In table 6-IV, which contains comparisons between the three strengths of the control earthquake, it can be seen that a decrease in the magnitude of the ground accelerations will not necessarily result in a decrease in the ductility requirements of every member. In this same case, the left-hand (outer) end of a twelfth-floor beam member obtained a plastic deflection sixteen per cent greater in the analysis in which the excitation was factored by 0.7 than in the standard. This is an example of the threshold effect of the yield plateau. In this member the maximum ductility occurred when the section was carrying a positive moment, whereas a negative moment existed when the lower maximum was reached in the standard excitation analysis. The lack of a more prolonged excursion by the critical section into the plastic region, when it was carrying a negative moment in a previous cycle, allowed the less severe excitation to cause more plastic flow when the positive yield criteria was reached later.

In figure 6-1, all the positions at which plastic hinges formed during the analyses are shown, both for the three standard analyses and for those employing the four selected earthquakes scaled by the two different methods. Without exception, the critical sections at the outermost end of the beams yielded at some stage of each analysis. The difference between them is indicated by the number of hinges forming at the inner ends. The patterns are all reasonably similar and fall, approximately, in to that range represented by the difference between that of the standard earthquake with a scaling factor of 0.7 and the one with a 1.3 scaling factor. The artificial earthquake A1, in particular, has very similar hinge patterns to those standards with similar scale factors - although the scale factors for A1 were supposed to be attempts at scaling the excitation to that of the level of the unscaled standard.

An interesting observation was made when an inspection of the printed output was in progress. It has been suspected, for some time, that the current ultimate strength design philosophy, which requires the bottom storey of a frame to resist an overturning moment compatible with plastic hinges occurring concurrently in all the frames' beams, is overtly

		E/Q scale factor $\left[ \frac{E/Q}{\text{Benchmark}^*} \right]$	Max. top-storey displacement ratio	Max. ductility recorded in any beam	Max. ductility recorded in any beam - ratio	Max. ductility recorded at position 1†	Max. ductility recorded at pos. 1 - ratio	Max. ductility recorded at position 2	Max. ductility recorded at pos. 2 - ratio	Max. ductility recorded at position 3	Max. ductility recorded at pos. 3 - ratio
El Centro, May 18, 1940	N-S*	1.00	1.00	6.99	1.00	5.85	1.00	6.99	1.00	4.23	1.00
El Centro, Dec. 30, 1934	N-S	1.24	1.54	7.36	1.05	5.08	0.868	4.49	0.642	7.36	1.74
Taft, July 21, 1952	N69°W	2.03	1.26	6.41	0.918	6.41	1.10	5.42	0.775	5.52	1.31
Seattle, April 29, 1965	S58°W	3.89	1.44	6.02	0.862	4.36	0.747	5.25	0.751	6.02	1.42
Artificial (Jennings')	A1	0.947	1.18	4.95	0.708	4.95	0.846	3.94	0.564	4.40	1.04

† Structure II (appendix A) used with first ten seconds of each accelerogram;  
 Position 1 at outer end of 11<sup>th</sup> level beam; position 2 at outer end of 13<sup>th</sup> level beam;  
 Position 3 at inner end of 11<sup>th</sup> level beam

**TABLE 6-II : DUCTILITY RATIOS - EARTHQUAKE SCALINGS BY MAXIMUM GROUND ACCELERATIONS.**

		E/Q scale factor $\left[ \frac{E/Q}{\text{Benchmark}^*} \right]$	Max. top-storey displacement ratio	Max. ductility recorded in any beam	Max. ductility recorded in any beam - ratio	Max. ductility recorded at position 1	Max. ductility recorded at pos. 1 - ratio	Max. ductility recorded at position 2	Max. ductility recorded at pos. 2 - ratio	Max. ductility recorded at position 3	Max. ductility recorded at pos. 3 - ratio
El Centro, May 18, 1940	N-S*	1.00	1.00	6.99	1.00	5.85	1.00	6.99	1.00	4.23	1.00
El Centro, Dec. 30, 1934	N-S	1.74	2.32	10.6	1.52	7.26	1.24	6.01	0.861	10.6	2.51
Taft, July 21, 1952	N69°W	1.94	1.21	5.77	0.828	5.77	0.987	5.25	0.752	5.20	1.23
Seattle, April 29, 1965	S58°W	4.70	1.73	7.24	1.04	5.26	0.900	5.70	0.816	7.24	1.71
Artificial (Jennings')	A1	0.696	0.878	4.34	0.621	3.30	0.564	3.17	0.455	4.37	1.02

See table 6-II for details of positions monitored.

**TABLE 6-III : DUCTILITY RATIOS - EARTHQUAKE SCALINGS BY SPECTRAL VELOCITY INTEGRAL.**

		E/Q scale factor $\left[ \frac{E/Q}{\text{Benchmark}^*} \right]$	Max. top-storey displacement ratio	Max. ductility recorded in any beam	Max. ductility recorded in any beam - ratio	Max. ductility recorded at position 1	Max. ductility recorded at pos. 1 - ratio	Max. ductility recorded at position 2	Max. ductility recorded at pos. 2 - ratio	Max. ductility recorded at position 3	Max. ductility recorded at pos. 3 - ratio
El Centro, May 18, 1940	N-S	1.30	1.24	9.95	1.42	9.95	1.70	9.79	1.40	7.88	1.86
	*	1.00	1.00	6.99	1.00	5.85	1.00	6.99	1.00	4.23	1.00
		0.70	0.837	5.21	0.746	4.00	0.685	5.21	0.746	4.89	1.16

See table 6-II for details of positions monitored.

**TABLE 6-IV : DUCTILITY RATIOS - BENCHMARKS.**



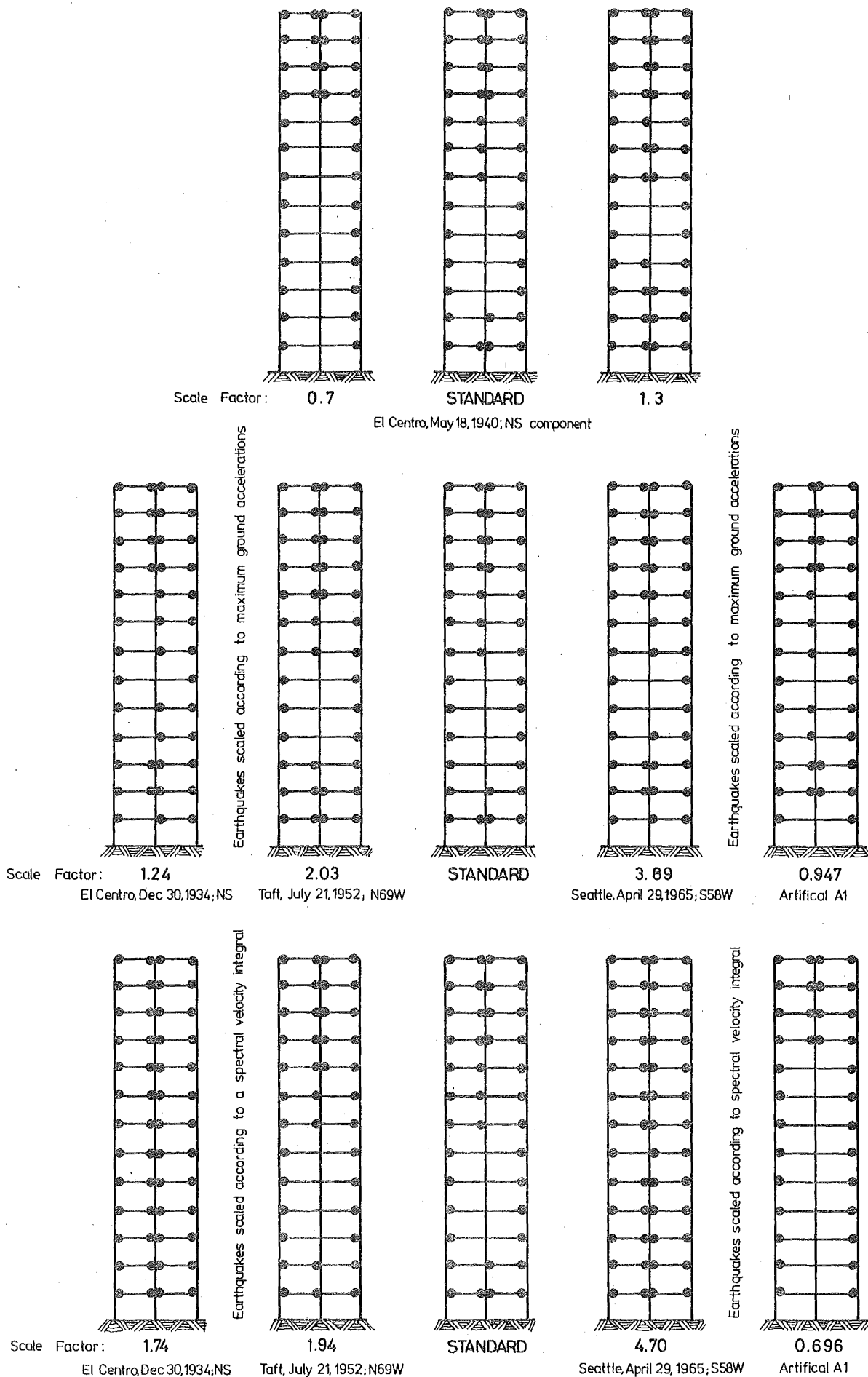


**FIGURE 6-1: POSITIONS AT WHICH PLASTIC HINGES FORMED DURING THE COMPARATIVE ANALYSES.**

conservative. The inspection of the hinge patterns of the thirteen-storey frame disclosed that there was normally a three-storey wave of plastic hinges migrating up the building. An example of this is shown in figure 6-2. Even when two such waves were present, there was still a band, free of beam hinges, between them. Furthermore, it is quite possible for some of the plastic hinges in one wave to be undergoing plastic rotation in an opposite sense to those in another. It could be, therefore, that an immediate use of such elasto-plastic analyses is in the justification of designing for much reduced ultimate overturning moments in tall buildings.

Figures 6-3, 6-4 and 6-5 show the maximum ductility demands at the outermost critical sections of the beam members for the previously described analyses. Again, no simple trend is obvious. The non-linearity of the ductility with respect to the maximum ground acceleration can again be seen from the relative positions of those lines representing the control responses (figure 6-3). Scaling by maximum ground acceleration has given less scatter of ductilities than that by scaling with respect to a spectral velocity integral. The varying effect of different earthquakes is visually emphasized by the crossing and re-crossing of ductility plots. The corresponding maximum lateral displacement envelopes, shown in figures 6-6, 6-7 and 6-8, also exhibit a seemingly unrelated scatter of magnitudes. Although these envelopes do look amenable to some form of scaling, it should be remembered that these maximum displacements, because they are envelopes, do not give any indication of the dynamic deformation and so are not reliable indicators of ductility levels reached.

## 6.6 CONCLUSIONS

Even if only the action of a limited number of earthquake accelerograms on a single frame is taken, there does not seem to be a simple criterion by which the strengths of these excitations can be scaled to give equivalent damage. The scope of this approach to the problem is severely limited by the expense of carrying out even this small number of inelastic analyses. Before further work in this field is attempted, a more comprehensive method of measuring the structural damage inflicted by a particular excitation needs to be found. Ductility factors, although valuable to the designer when detailing his structure, need to be combined with an integrating procedure in order to connect the length of time in which plastic flow takes place with the subsequent energy absorption.

The problem, which the designer encounters in trying to find a digitised earthquake that will cover a required code specification, has not been solved. The 'standard' earthquake does not exist. Any attempt

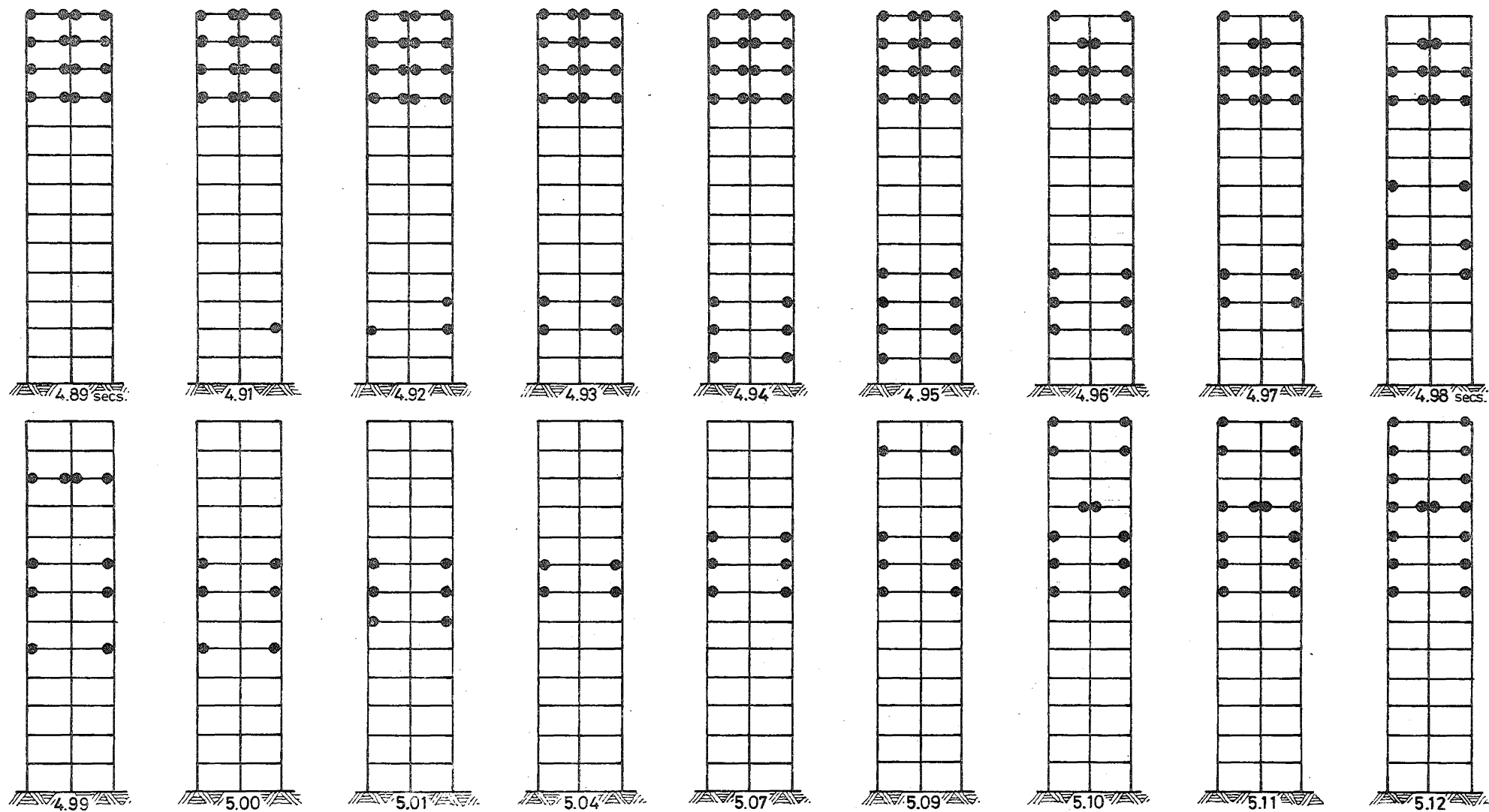


FIGURE 6-2: AN EXAMPLE OF THE MIGRATION OF PLASTIC HINGES UP A FRAME DURING AN EARTHQUAKE (EL CENTRO, MAY 18, 1940, N-S).

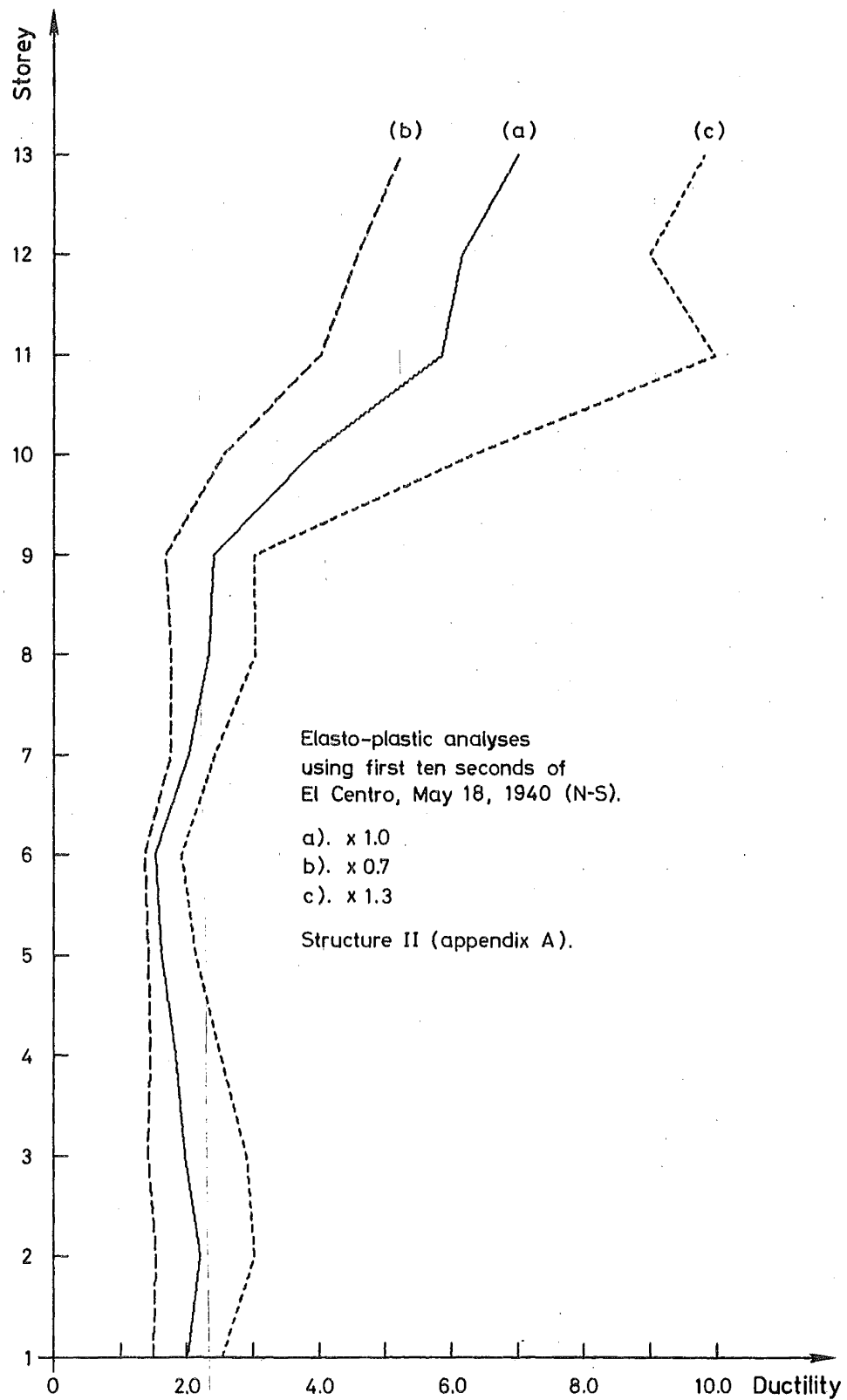


FIGURE 6-3 : MAXIMUM DUCTILITIES OF OUTER BEAM SECTIONS - BENCHMARKS.

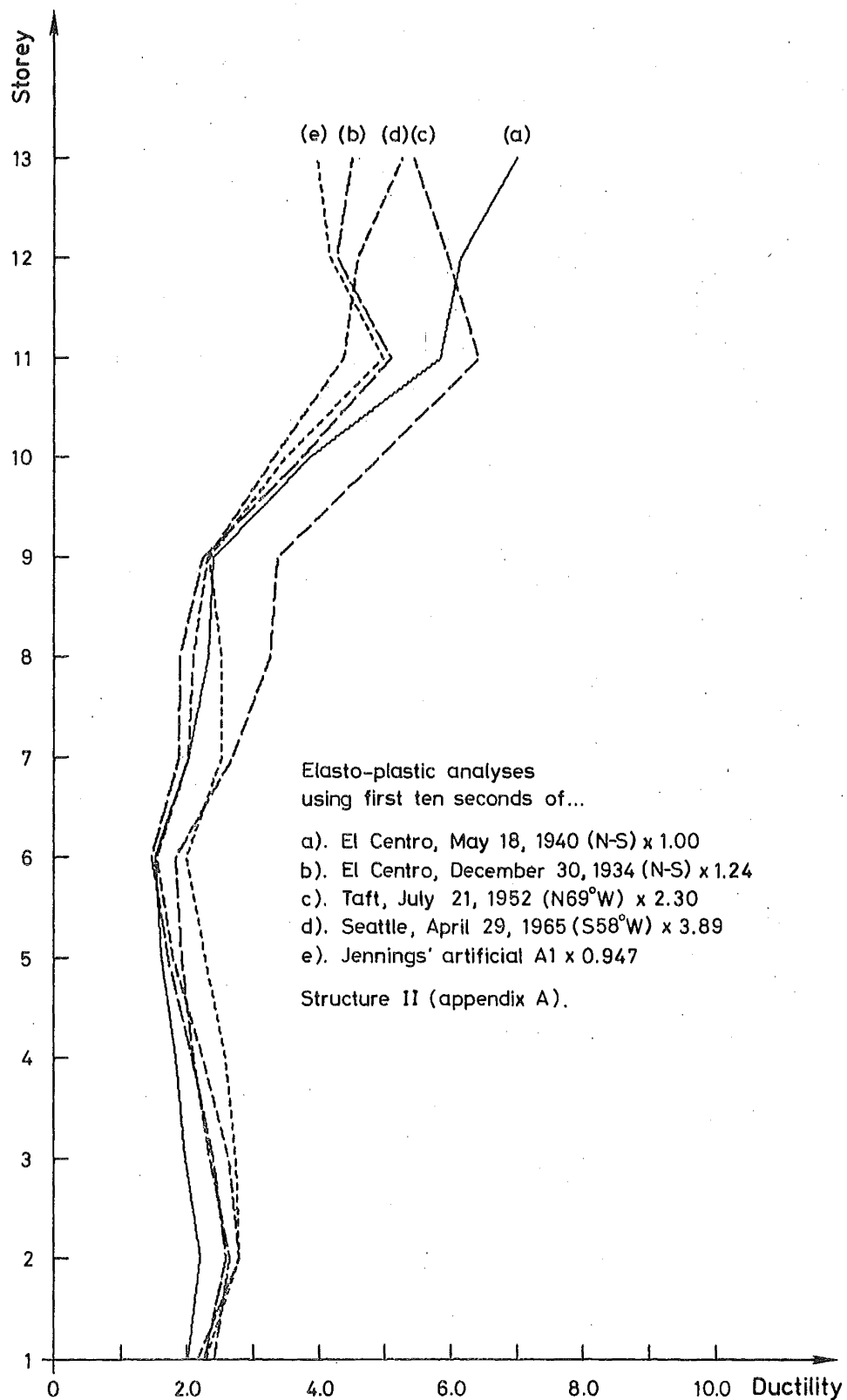


FIGURE 6-4 : MAXIMUM DUCTILITIES OF OUTER BEAM SECTIONS - SCALING  
BY MAXIMUM GROUND ACCELERATIONS.

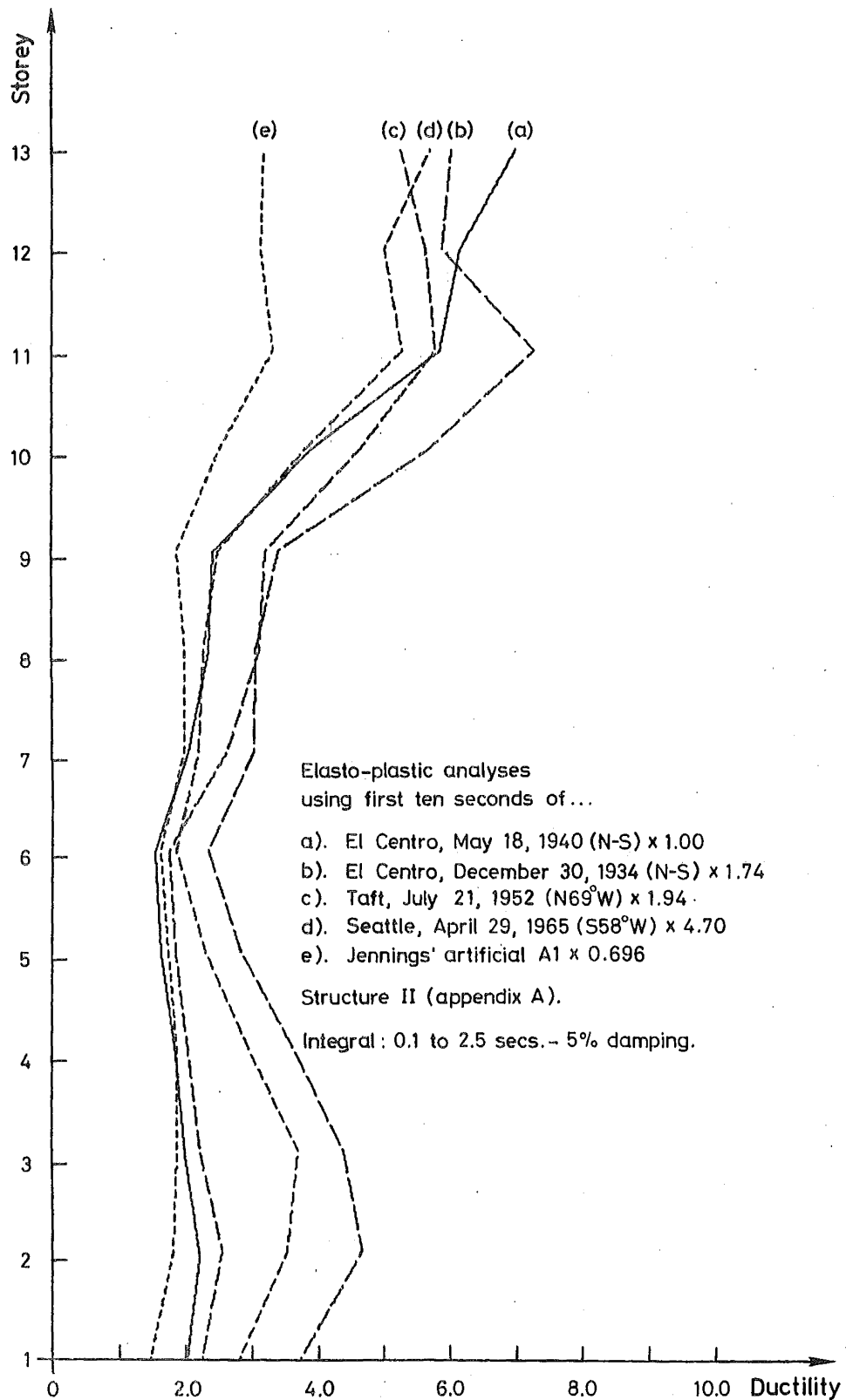


FIGURE 6-5 : MAXIMUM DUCTILITIES OF OUTER BEAM SECTIONS - SCALING BY A SPECTRAL VELOCITY INTEGRAL.

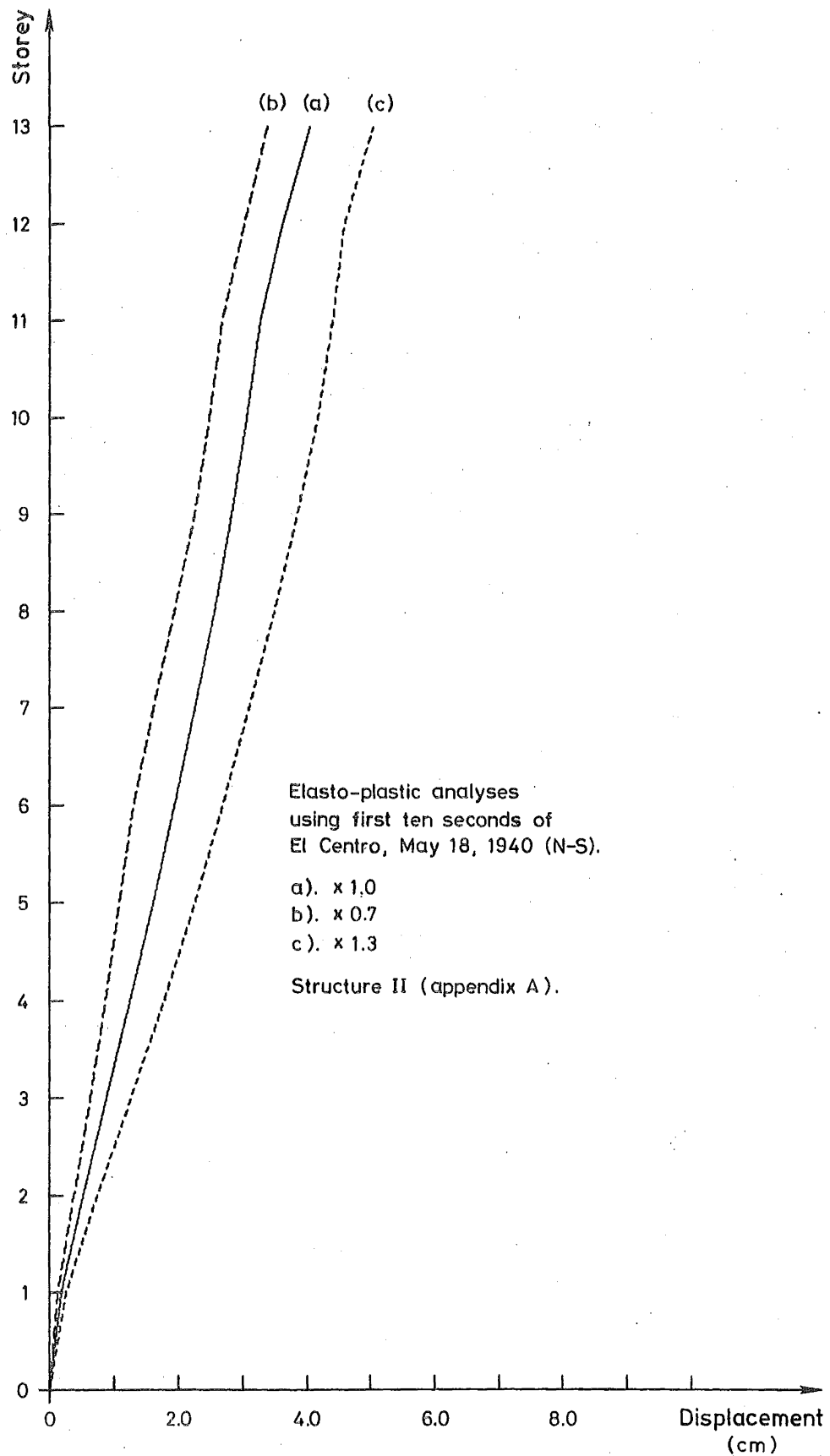


FIGURE 6-6 : MAXIMUM HORIZONTAL DISPLACEMENTS - BENCHMARK RESPONSES.

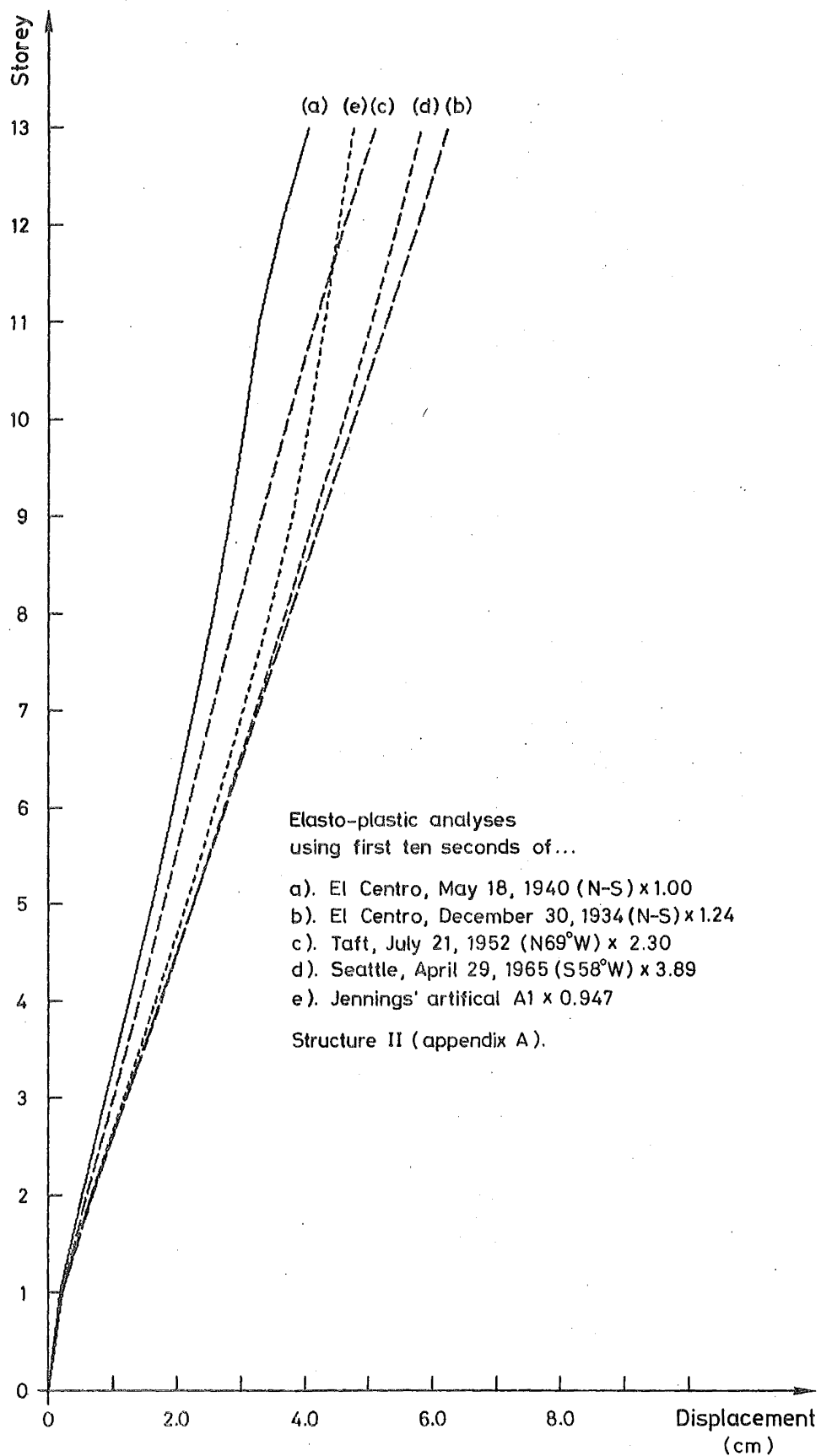


FIGURE 6-7 : MAXIMUM HORIZONTAL DISPLACEMENTS - SCALING BY MAXIMUM GROUND ACCELERATIONS.



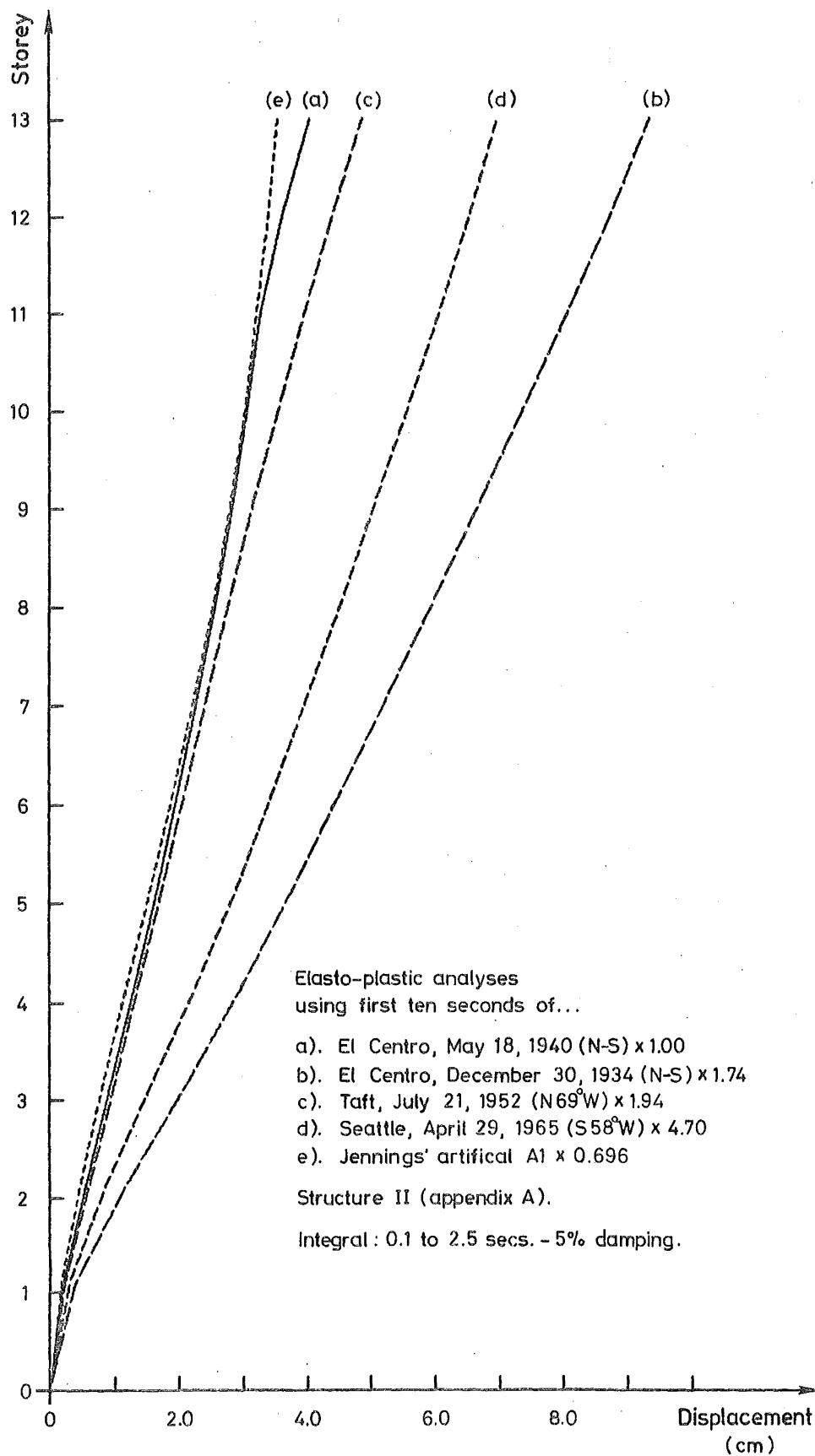


FIGURE 6-8 : MAXIMUM HORIZONTAL DISPLACEMENTS - SCALING BY A SPECTRAL VELOCITY INTEGRAL.

by a building code to specify too rigorously a set of conditions that must be met by the proposed excitation would tend to imply that such a standard does exist. Unfortunately, in the absence of a quantified input excitation, it is difficult then to demand that the resulting dynamic inelastic behaviour meet specific criteria. The role of codes of practice in this field should therefore be to lay down the values of some of the more obvious parameters (such as the percentage damping to be associated with different building materials), while stating general principles that must be met. There is an obvious temptation for designers to treat these codes as design manuals, but there is an inherent danger in this approach when the recommendations are applied to situations for which they were not intended.

If deterministic, inelastic, dynamic analyses are to be conducted it is necessary for more than one excitation to be tried. Scaling of the accelerograms so that their response spectra look similar over the range of the important frequencies is as satisfactory as any other scaling method at this stage. Only by seeing the results of such a series of analyses will a designer gain a feel for the sensitivity of his structure to a dynamic excitation.

## CHAPTER SEVEN

THE ANALYSIS OF TWO BRIDGE STRUCTURES7.1 INTRODUCTION

This chapter deals with the successful application of the dynamic inelastic analysis computer program to two actual problems. Each of the structures analysed required the use of special features of the program in different ways. In both cases, the analyses performed were considered to be well within the range of economic viability for their particular project. Bridge structures, because of their simple geometry, do not offer the same opportunities for the incorporation of energy-absorbent members as do multi-storey frames. Also, for the same reason, they may require only a very small number of critical member sections to yield in order to produce a catastrophic collapse mechanism. Both structures have an irregular geometry and, hence, could not be dealt with (except with doubtful modelling) by a program with a rectangular frame capability only.

In the first analysis - that of the proposed Durham Street railway overbridge - the design engineers were primarily interested in obtaining an estimate of the likely relative deflections of the deck sections with respect to both each other and the bridge abutments, whereas in the second analysis - that of a pier of the Auckland upper harbour crossing - they were more interested in the possible occurrence and position of plastic hinges.

7.2 THE DURHAM STREET RAILWAY OVERBRIDGE7.2.1 The structure

The bridge deck, simply-supported on piers formed on piles driven into alluvial material, will carry vehicular traffic over a series of important main-trunk railway tracks. Built of reinforced and prestressed concrete in two sections, it will be approached from either end by way of artificially-constructed embankments. In order that the two deck sections, when dynamically excited by an earthquake, should neither butt each other nor be interfered with by the positioning of the abutments, an attempt was made to predict a suitable width for the three seismic- and expansion-gaps incorporated in the structure.

Initial-condition moments due to shrinkage, temperature and creep were supplied by the engineer as were yield moments for the bases of the piers. Apart from the question of the adequacy of the assumed earthquake forces used in the static equivalent earthquake analysis, the engineer

also required information as to whether relative vertical displacement of the deck, with respect to the piers, was thought to be possible under earthquake loadings.

### 7.2.2 The idealization

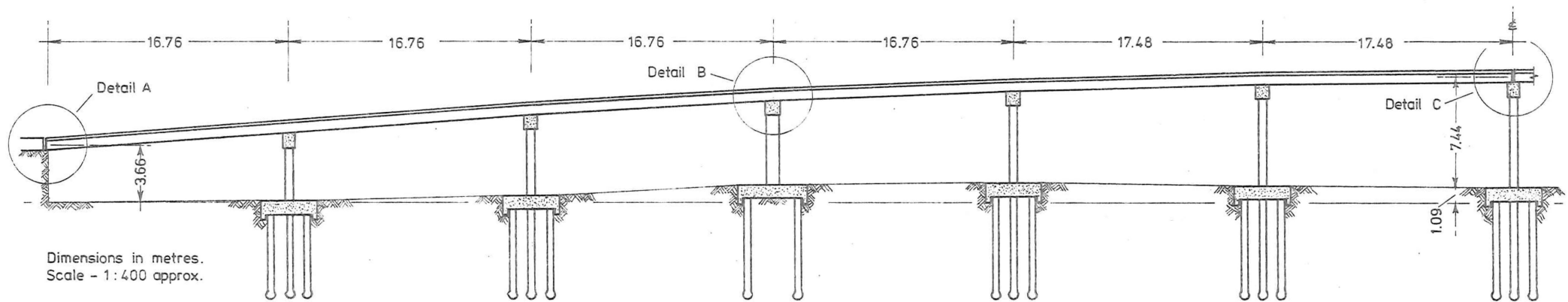
The bridge was reduced to the centre-line frame depicted in figure 7-1. An initial assumption was made that the deck would not lift off any of its supports. The model sliding bearings, shown in details (a) and (c) of figure 7-1, are idealized to the extent that they allow infinite movement in a horizontal direction and (detail (c)) allow the opposing ends of the two deck spans to slide through each other without interference at the centre of the bridge. The seismic gap necessary in the real structure, to avoid butting of the two deck sections, is then at least the peak-to-peak amplitude of the relative motion. The deck, being simply-supported at the top of the piers, did not require the possibility that it might develop plastic hinges to be considered. The only possible collapse modes were then those in which plastic hinges had to form at the bases of all the piers.

The ability of the program to handle an irregular nodal geometry eliminated the need for any approximations to be made as to the heights of fixity of the pier bases. These varied by up to 1.4 metres from the horizontal line through the base of the abutments. The two halves of the bridge are not symmetrically identical and so could most certainly be expected to oscillate out of phase with each other when dynamically excited.

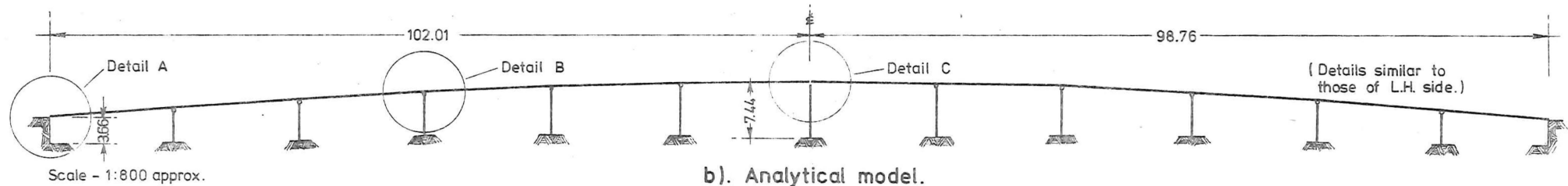
Equivalent viscous damping was set at five per cent of critical for the first two modes - with the other much less significant modes thus automatically attracting damping according to the extrapolation by Caughey (see chapter 4.4). The highest mode (the twenty-sixth) was, thus, credited with a damping of fifty per cent of critical.

### 7.2.3 The analyses

The left and right halves of the bridge were found to have frequencies of 2.789 and 2.879 Hz, respectively, for their undamped fundamental modes. This three per cent difference confirmed the possibility of the two deck sections eventually oscillating out of phase. For example, if they were given similar and coincident initial impulses, the two (undamped) halves of the bridge could then be expected to be one half-cycle out of phase after 5.55 seconds of free vibration (i.e. well



a). One half of proposed bridge.



b). Analytical model.

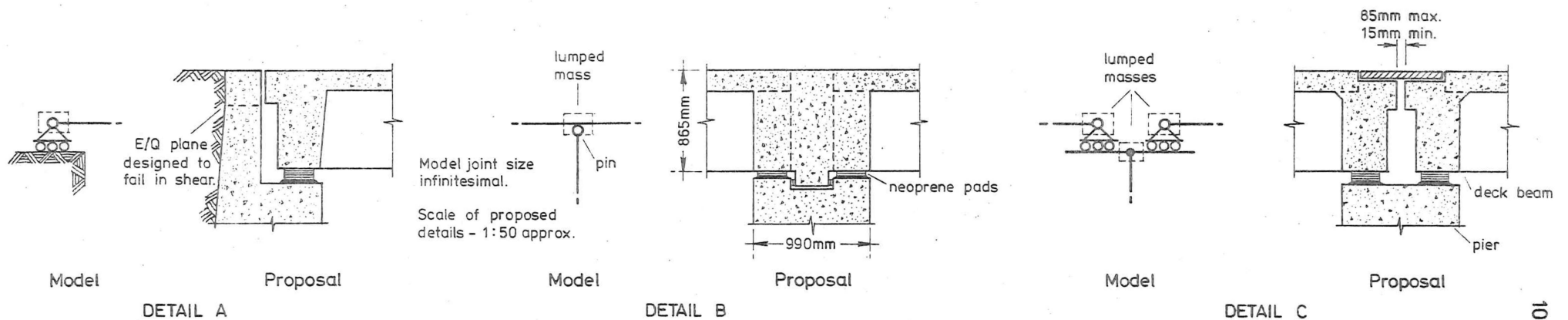


FIGURE 7-1 : DURHAM STREET RAILWAY OVERBRIDGE, CHRISTCHURCH.

within the realistic time-scale for the length of a seismically induced vibration).

A purely elastic dynamic analysis was performed using the first ten seconds of the North-South and vertical components of the El Centro, May 18, 1940 earthquake which was scaled, at the request of the engineer, to give a maximum horizontal ground acceleration of 0.23 g. The displacement responses of the two halves, measured horizontally at the top of the central pier and with respect to the ground, are shown plotted in figure 7-2a. The initial displacements, due to the initial moments introduced to represent the effects of shrinkage in the prestressed deck, have been eliminated from the plot (figure 7-3a) of the relative displacements of the two decks. Hence, the study as to the gap required between the deck sections was confined to a measure of the 'dynamic' gap alone.

The second analysis attempted was of a non-linear type, with only the columns being permitted to develop perfectly plastic hinges at their bases when the predicted yield moments were reached. The geometry of the structure is such that big variations in the piers' axial loads are not expected and so the abstraction of the data required for incorporating moment-axial load, interactive, ultimate strength criteria was not justifiable. For a collapse mechanism, it is only necessary for all the piers of either half of the bridge to yield at ground level. However, the formation of a collapse mechanism is not, in itself, a sufficient condition for a dynamically excited structure to become unstable and collapse. Even though a collapse mechanism may have formed, recovery is possible if the velocities of the collapsing structure are sufficiently small enough to enable an incremental ground acceleration in the prevailing direction of collapse to cause the supports to catch up with, and overtake, the (horizontally) collapsing deck.

With the same earthquake as used in the elastic analysis, the left half of the bridge formed a collapse mechanism after 1.72 seconds, followed by that of the right at 1.99 seconds. Both halves recovered briefly from this state before finally entering their respective collapse mechanisms at 2.20 and 2.15 seconds of earthquake. The corresponding horizontal deflections of the decks at these latter times were -14.6 and 11.2 mm. It is interesting to note the effect that the history of the bridge's plasticity has on the final collapse for, although the two sections of the bridge are reasonably similar, they formed collapse mechanisms at different times when their displacements were of opposite sign but, eventually, both collapsed in the same direction. The

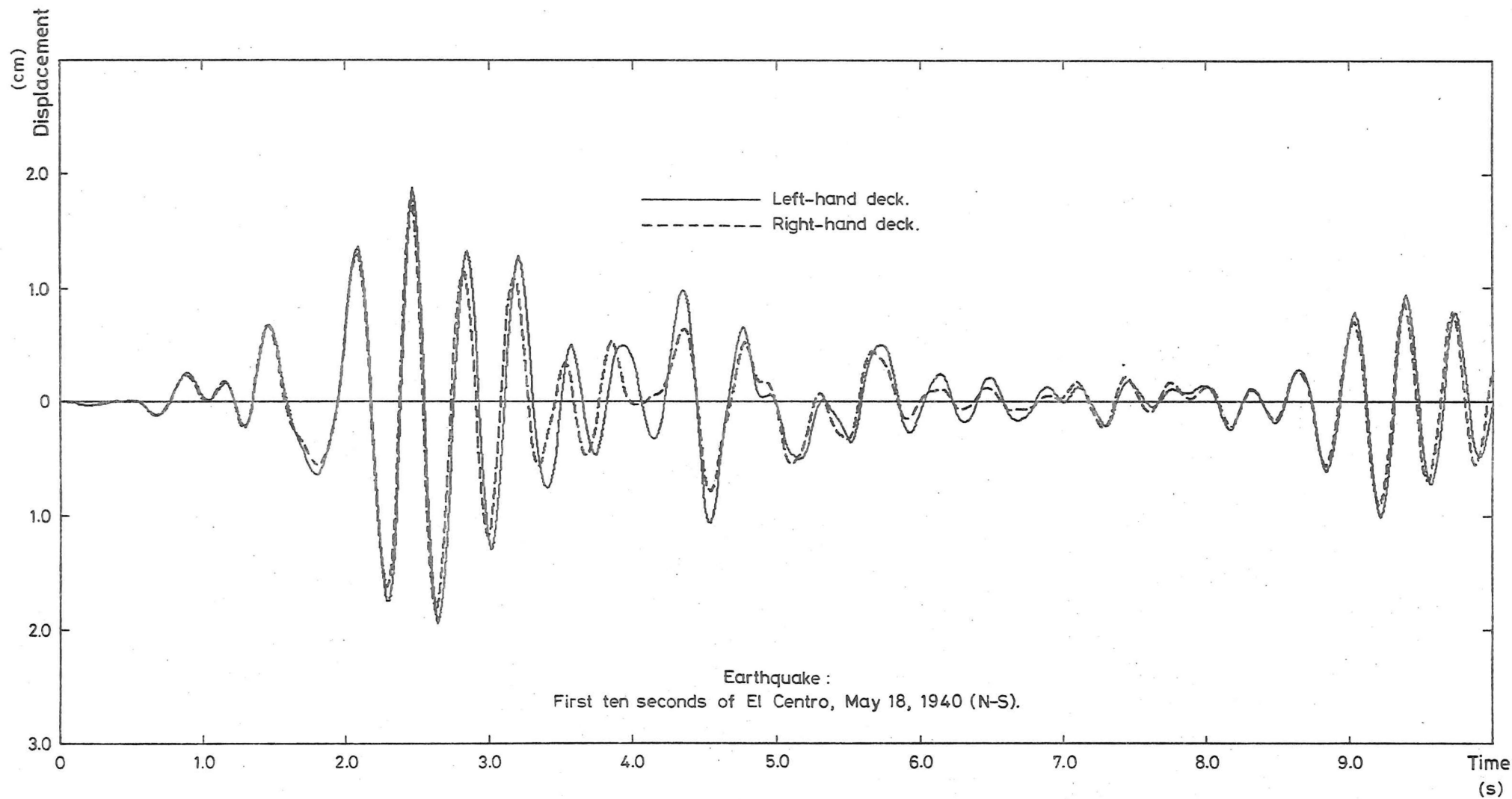


FIGURE 7-2a : HORIZONTAL DISPLACEMENT RESPONSES OF RAILWAY OVERBRIDGE DECKS - ELASTIC.

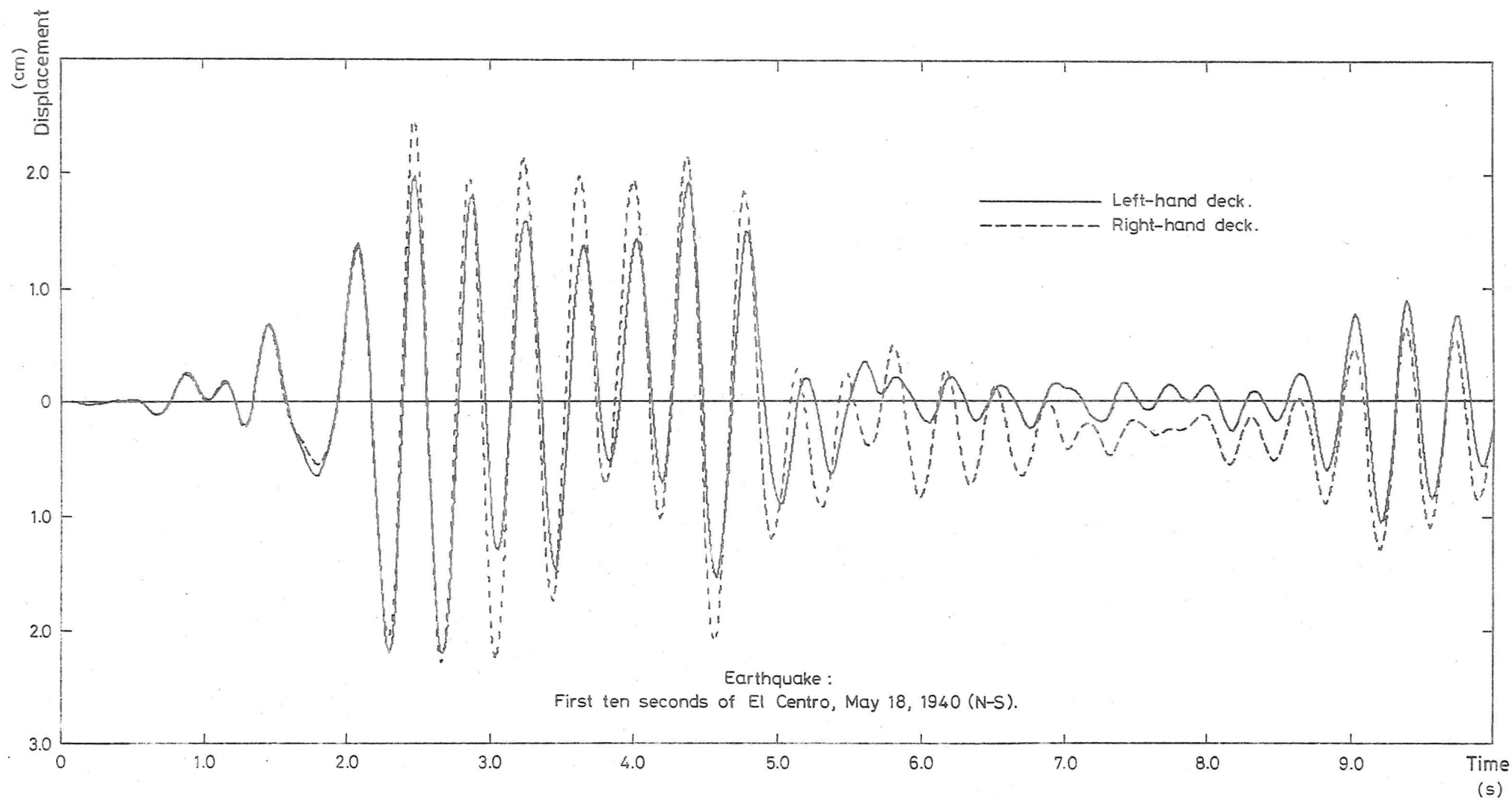


FIGURE 7-2b : HORIZONTAL DISPLACEMENT RESPONSES OF RAILWAY OVERBRIDGE DECKS - BI-LINEAR.



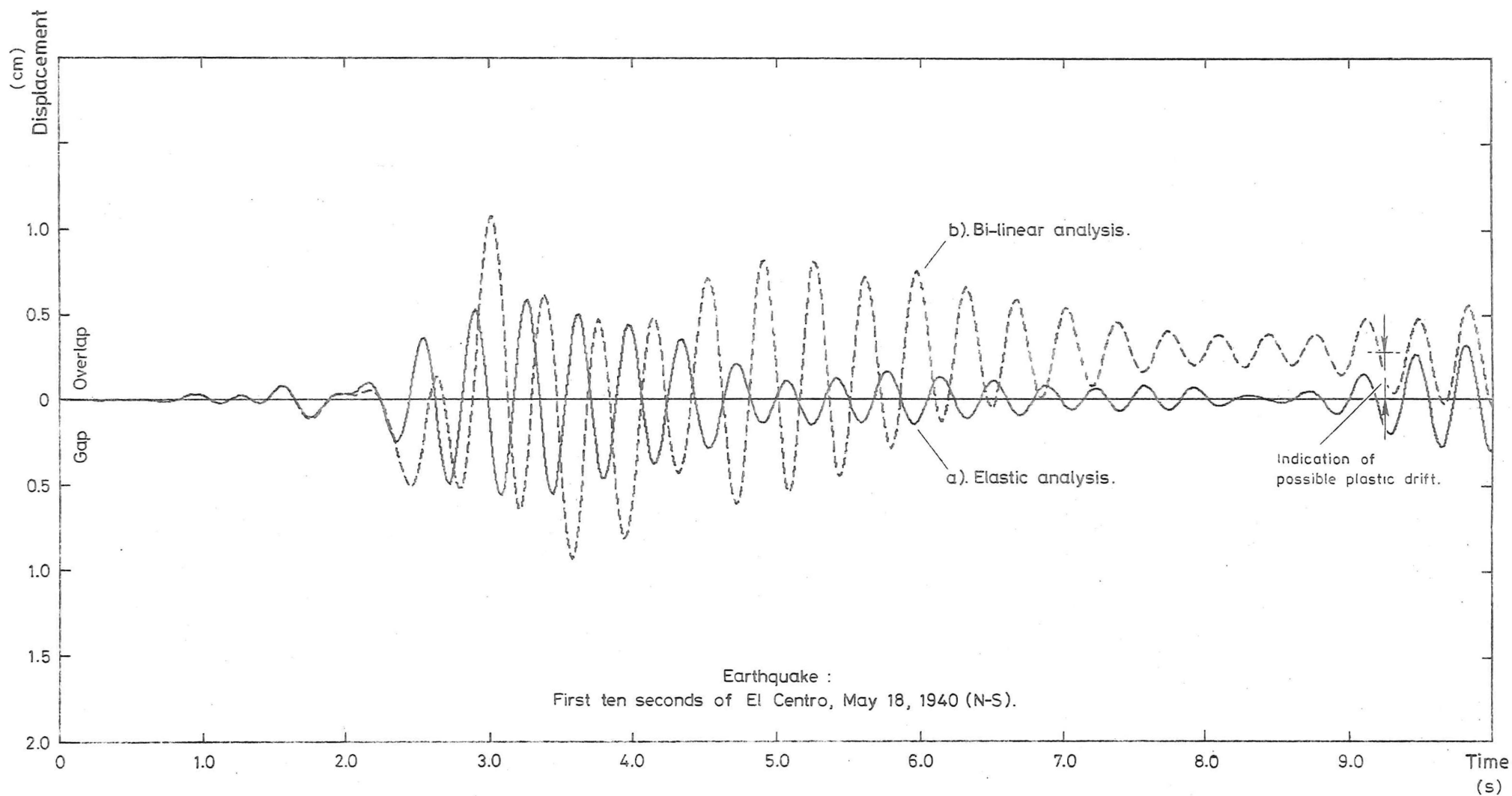


FIGURE 7-3 : RELATIVE HORIZONTAL DISPLACEMENT RESPONSES OF RAILWAY OVERBRIDGE DECKS.

sensitivity of this particular structure to its collapse mechanism can be seen from the fact that an identical non-linear analysis on the less accurate IBM 360/44 computer showed the bridge as being able to recover from the collapse mechanisms and ride out the full ten seconds of the earthquake without incurring what might be considered as fatally high deflections.

In order to confirm that the previous analysis had, by chance, shown the bridge just reaching the sensitive critical stage, a further deterministic inelastic analysis, using the same yield moments and earthquake, was implemented. The moment-curvature relationship to be followed at the pier bases was changed to that of a bi-linear hysteretic function in which the initial section remained the same as before. The second branch of the function was allocated a slope of ten per cent of the initial stiffness, in an attempt to simulate approximately the residual stiffness that might be left after the formation of a plastic hinge at a section. As a result, both bridge-sections again reached the stage where all the pier-bases had plastic hinges present concurrently, but catastrophic collapse was prevented from occurring by the presence of the small residual stiffness. Figures 7-2b and 7-3b show this response, both as a plot of the concurrent deck displacement and of the relative deck movement. A summary of the quantitative results is given in table 7-I. The maximum section ductility recorded at any of the pier-bases was approximately 6 - which indicates that only moderate yielding took place.

Both sides of the bridge experienced some permanent drift under the applied seismic action which, in this particular case, would have tended to widen permanently any seismic gap incorporated at the time of construction. It might have, just as easily (e.g. if the earthquake's direction was reversed), been of the opposite effect. The real structure is not in as much danger of total collapse under the design earthquake as these initial analyses would tend to indicate. The need for continuity in the road surface would ensure that further restraints on the horizontal movement of the deck would be imposed if a sufficiently severe earthquake was encountered. The inclusion of deliberate restraining devices, such as rubber buffering and sacrificial shear pins, is becoming more popular and would, if the abutments did not collapse, significantly decrease the response.

	Elastic analysis		Bi-linear analysis	
	Left deck	Right deck	Left deck	Right deck
Natural frequency of undamped fundamental mode (Hz)	2.789	2.879	2.789	2.879
Maximum deck displacement (horizontally) (mm)	20.2	18.3	23.1	25.4
Maximum amplitude of deck displacement (mm)	38.4	36.1	58.0	38.9
Maximum relative displacement of deck ends (mm)	11.5		25.0	
Maximum seismic gap required to prevent butting (mm)	5.9		9.4	

TABLE 7-I : SUMMARY OF RESULTS FOR DURHAM STREET RAILWAY OVERBRIDGE.

Because of the simplicity of the structure it could not be expected that the displacements of the non-linear frame would be approximately the same as those for the equivalent purely elastic frame. For the left deck section, the non-linear analysis gave a fourteen per cent increase in the maximum horizontal displacement experienced, whereas the right deck received a thirty-nine per cent boost. The widths of the minimum seismic gaps required are seen to approximately double.

The permanent plastic horizontal drift, which is becoming apparent in the last five seconds of the non-linear response, is significant if the possibility of an eventual failure, due to repeated stress-relief and incremental collapse, is to be considered. A purely elastic analysis, on the other hand, will give no indication of the permanent drift likely.

The final recommendations to the engineer suggested a minimum seismic gap of 38 mm (1.5 inches) between the two decks and, in order to allow for embankment earth pressure, 150 mm (6 inches) at the abutments. An examination of the axial loads in the piers showed that the deck was (as expected) unlikely to rise off its supports.

### 7.3 THE AUCKLAND UPPER HARBOUR CROSSING

#### 7.3.1 The structure

The Auckland upper harbour crossing provides a good example of a bridge structure in which there are very few members or places at which energy-absorption, through plastic work, can take place. The analysis

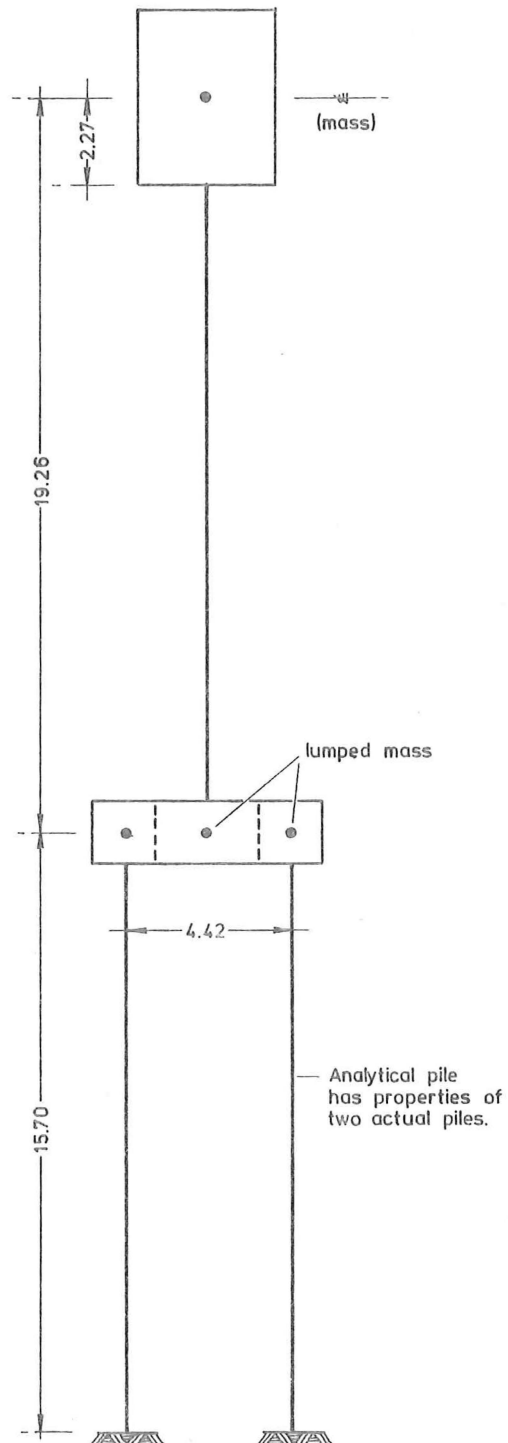
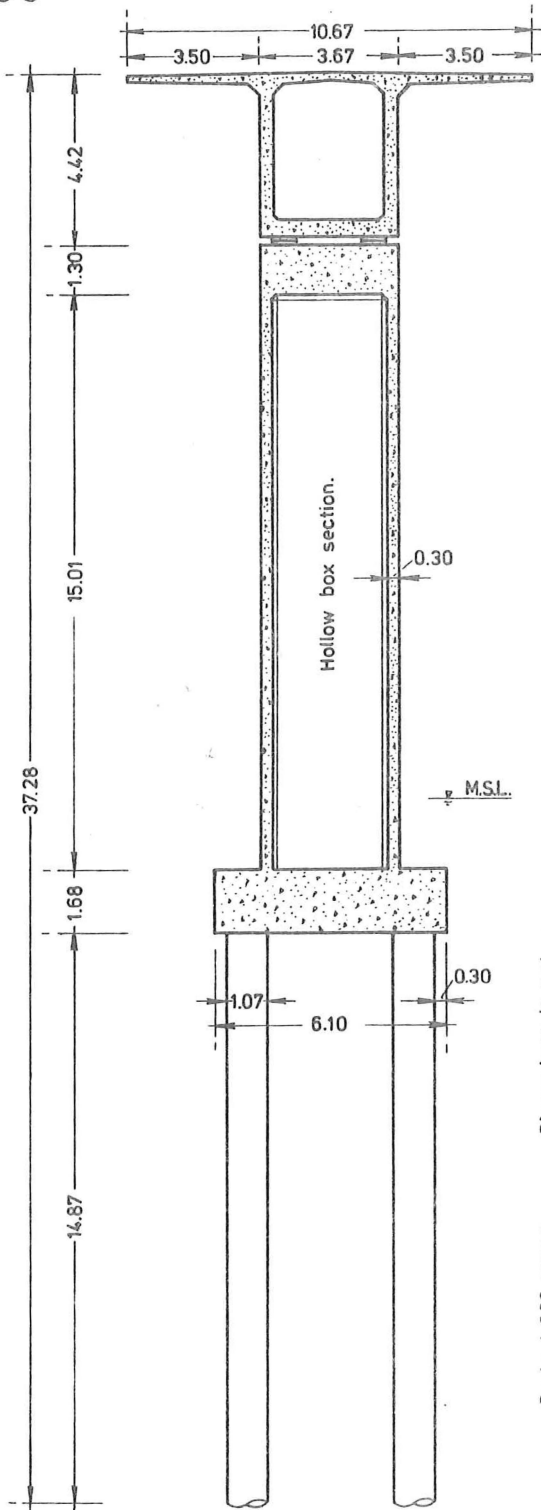
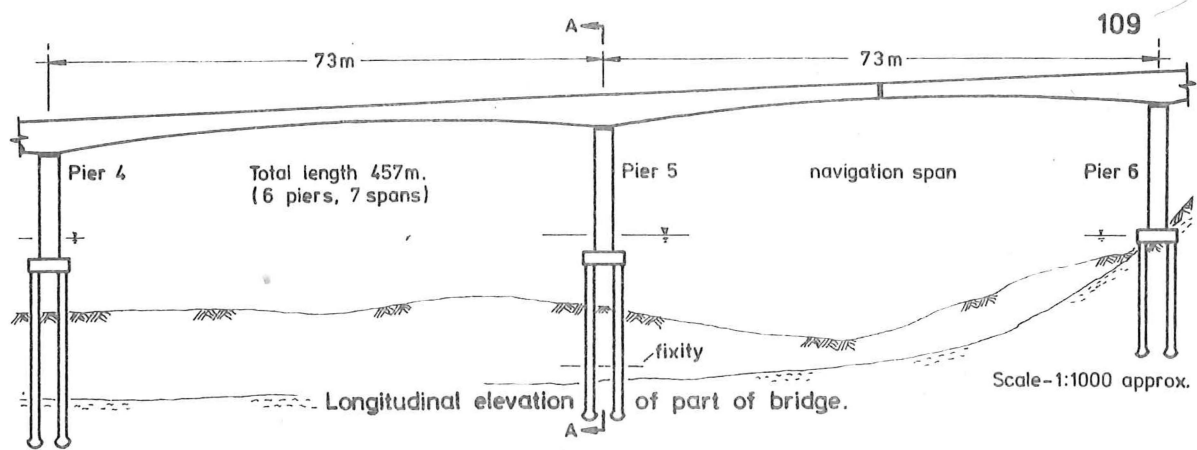
described below is that of pier 'five' - in a direction perpendicular to that of the bridge axis. This particular pier was selected as being probably the most critical of those supporting the bridge deck. Other analyses, not reported here, covered similar analyses of this pier in the longitudinal plane of the bridge. The structure, as sketched in figure 7-4, consists of a hollow, thin-walled, reinforced concrete pier which supports the box-girder deck. The pier is mounted on an almost square and relatively inflexible pile-cap which is, in turn, supported by four identical circular piles driven vertically for some distance into the harbour floor. At the request of the design engineer, the North-South and vertical components of the El Centro, May 18, 1940 earthquake accelerogram were used for all the analyses on this structure.

### 7.3.2 The idealization

The symmetrical nature of the plane-frame model of the pier enabled the four piles to be analytically replaced by two with twice the individual strength. The program could have coped with two co-linear pairs of members, but this would have unnecessarily introduced extra kinematic degrees of freedom and members at extra cost, without any compensating increase in accuracy being obtained. The assumption that the pile-cap was infinitely stiff meant that the horizontal degrees of freedom associated with the tops of the piles and the bottom of the pier could all be coupled together. To further stiffen the pile-cap, the associated rotations were also coupled. This latter coupling implies that the rotations will be identical at the relevant nodes and the rotational masses summed and made to act on one common degree of freedom. It cannot be inferred, as with some structural analysis programs, that the longitudinal axis of the member between the coupled rotations is, consequently, kept straight. The ability of the program to handle rigid end-blocks meant that the considerable differences between the interfaces and the centre-line intersections could be accounted for in both the stiffness calculations and the positioning of the possible plastic hinge sections. Both horizontal, vertical and rotational mass was lumped at the intersections of all members. The basic moment-curvature relationship employed was elasto-plastic in form. Damping was estimated (perhaps over-estimated) to be ten per cent of critical for the first two modes.

### 7.3.3 The analyses

Three different analyses, using the first ten seconds of the earthquake record, were carried out. They were...



a). Proposed structure

b). Analytical model

FIGURE 7-4 : AUCKLAND UPPER HARBOUR CROSSING - PIER 5.

- a) an elastic analysis,
- b) an elasto-plastic analysis in which the critical sections had only one constant value for the yield moment,
- c) an elasto-plastic analysis in which the moment - axial load interaction criteria was permitted to control the ultimate strength of the vertical members.

The first (i.e. lowest) two, natural, undamped frequencies were calculated to be 0.65 and 3.4 Hz, respectively. The highest of the six natural frequencies was 463 Hz and this mode's response was rendered virtually non-existent (and certainly non-oscillatory) by being accredited, using the previously described extrapolation, with 11 400% critical damping. This mode represents the vertical motion of the base of the pier with respect to the top of the columns and so it was expected that it would be non-existent because of the rigidity of the pile-cap.

The horizontal displacement responses of the deck (figure 7-5) in the three analyses illustrate how the formation of the plastic hinges has allowed sufficient energy to be absorbed to reduce noticeably the deck displacement. This is particularly evident in the last four seconds of the responses. The maximum non-linear response was decreased by approximately seven per cent. Examination of the printed time-history showed that significant plasticity was not encountered until after 5.4 seconds of earthquake. The effect of the energy-absorption did not show up in the plotted response (figure 7-5) until its next peak at about one second later - even though the former peak was also that at which the maximum response occurred. Accompanying the major excursions into the plastic range, there can be seen a slight increase in the dominant period over that of the initial elastic one. This is exactly as would normally be expected if there were an increase in some form of the damping.

The sensitivity of the structure to a changed criteria for the development of plastic hinges can be seen by an inspection of the differences in response between that using the obviously more correct moment - axial load interaction criteria and that in which the members' yield moments were fixed at a constant value. The response for the latter of these two cases (figure 7-5c) shows a very marked curtailment in the response after about seven seconds of excitation, resulting in the appearance of a significant permanent drift of the same magnitude as the curtailment.

An examination of the moment - axial load histories for the critical section at the top of the left-hand pile (figure 7-6) and at the base of the pier (figure 7-7) shows how the need for the interacting yield criteria

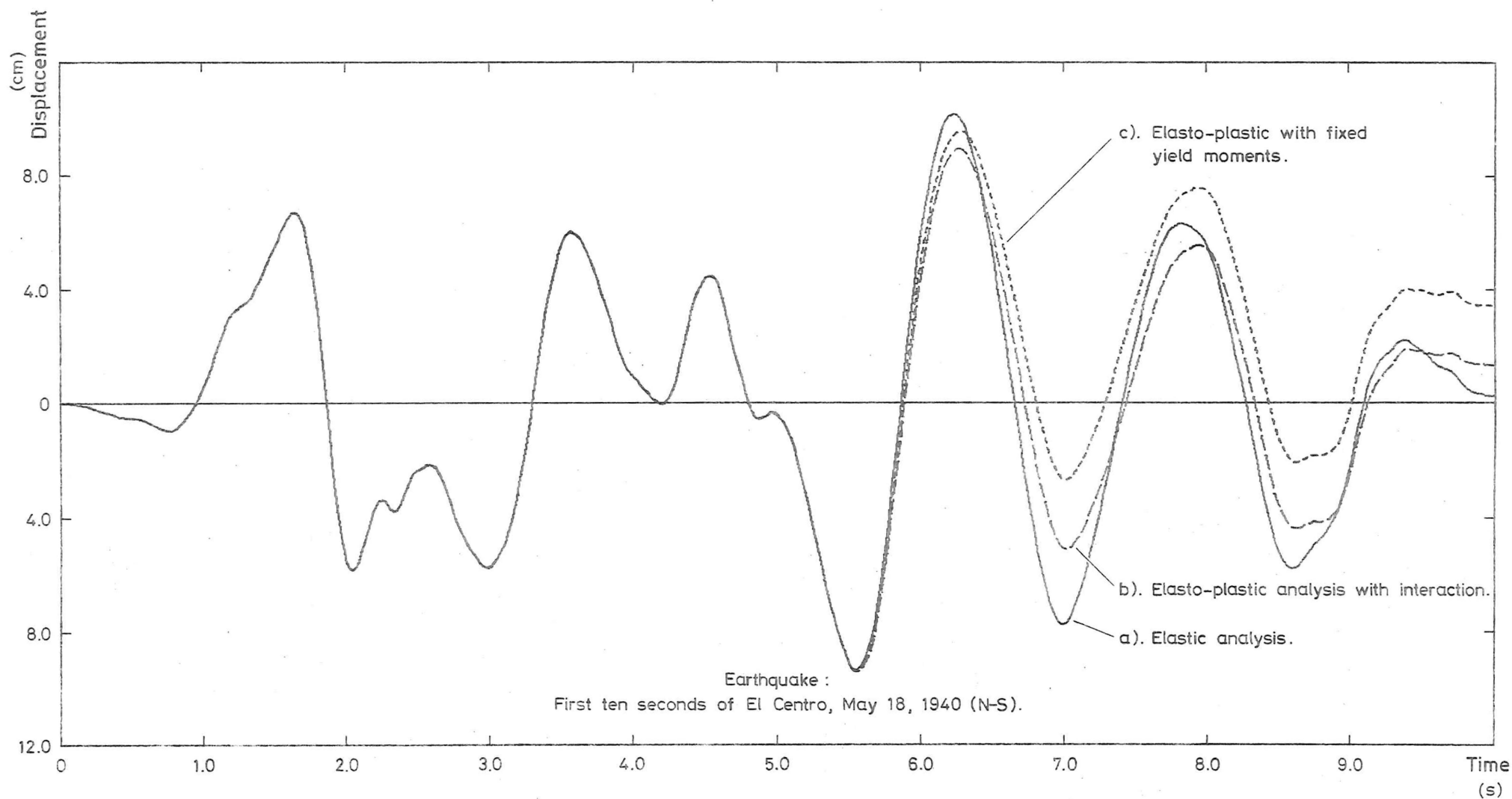


FIGURE 7-5 : HORIZONTAL DISPLACEMENT RESPONSES OF HARBOUR-CROSSING DECK.

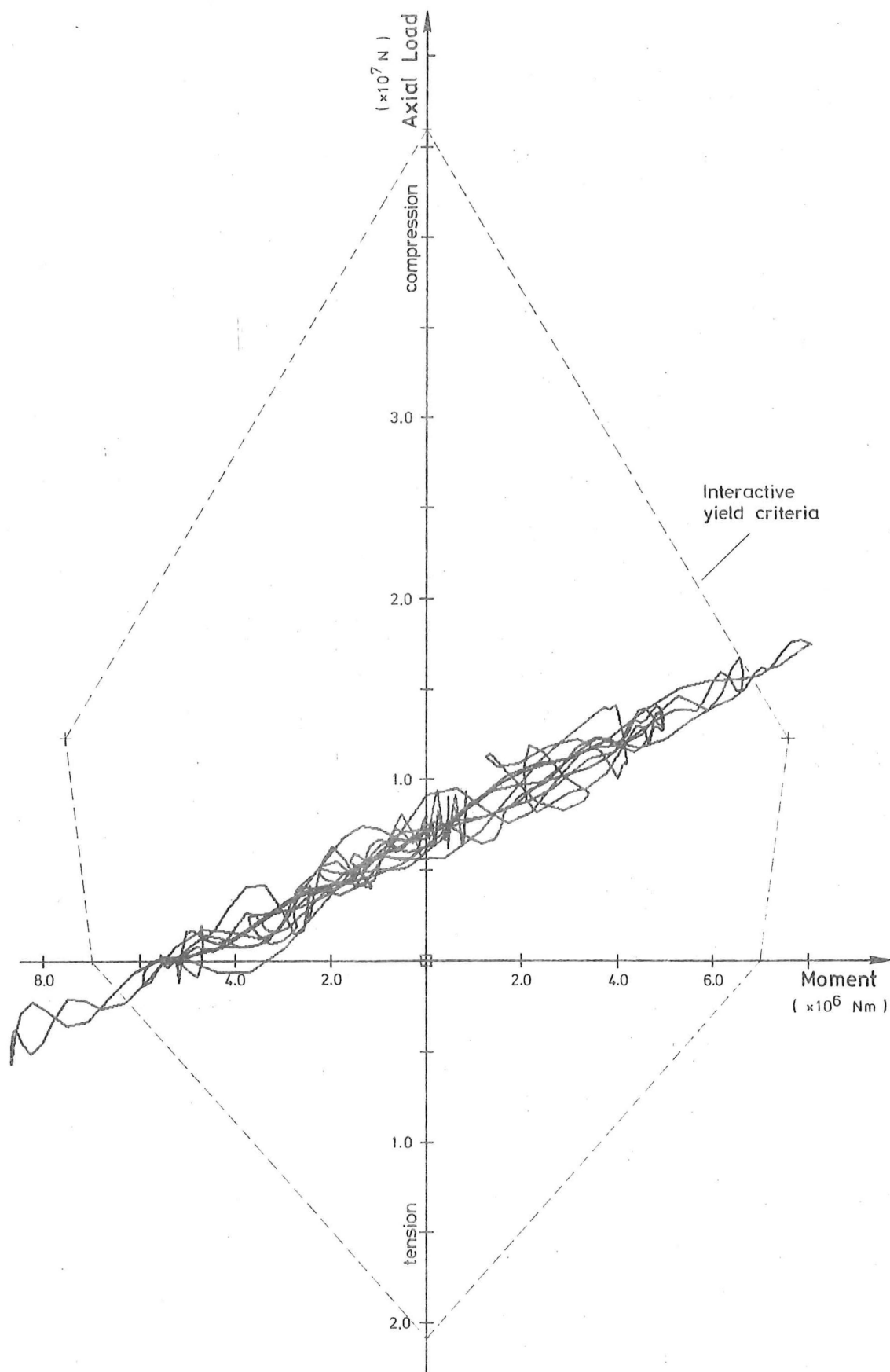


FIGURE 7-6a : MOMENT - AXIAL LOAD HISTORIES AT TOP OF LEFT-HAND PILE,  
ELASTIC ANALYSIS.



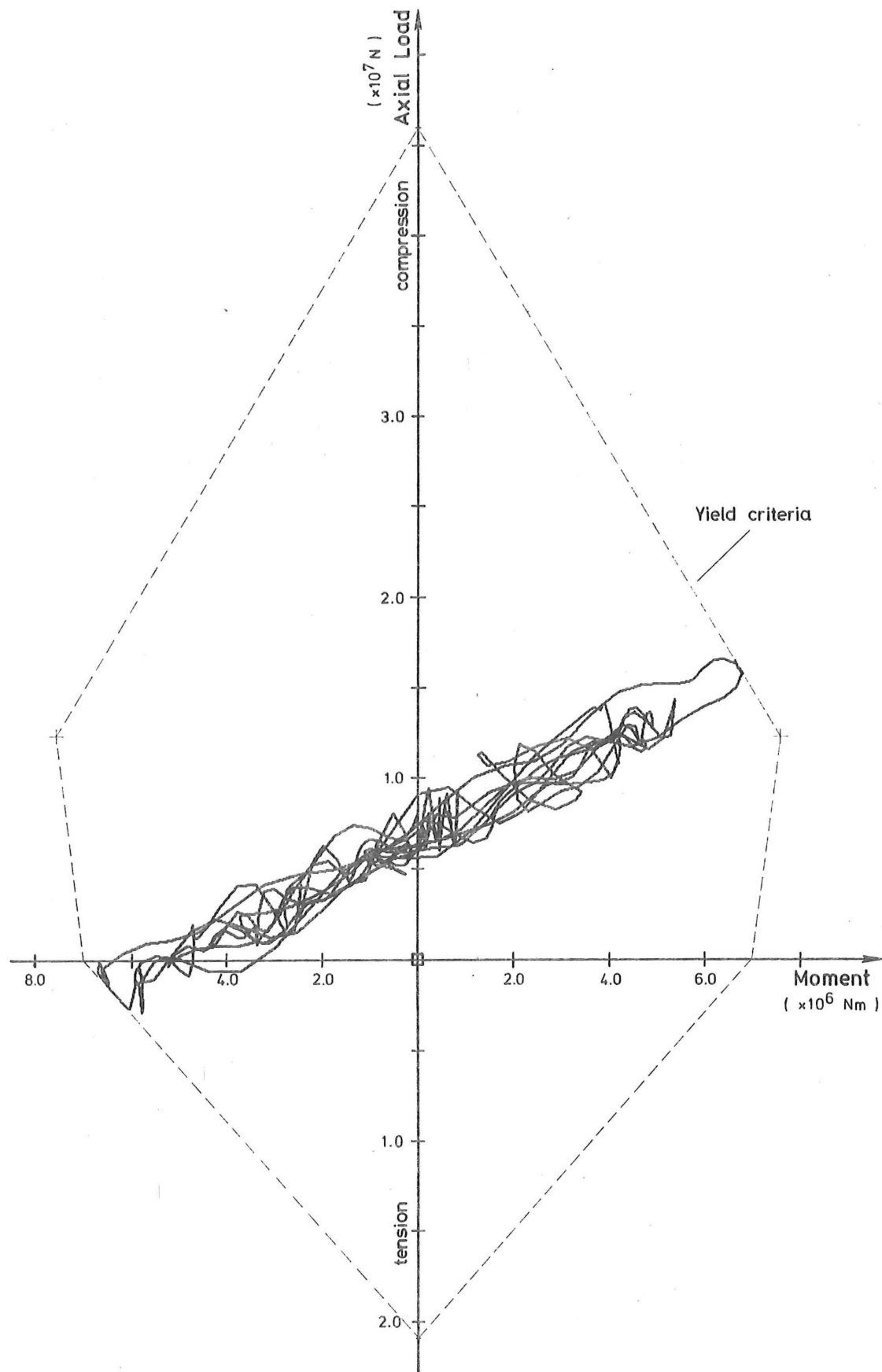


FIGURE 7-6b : MOMENT - AXIAL LOAD HISTORIES AT TOP OF LEFT-HAND PILE,  
ELASTO-PLASTIC WITH INTERACTION.

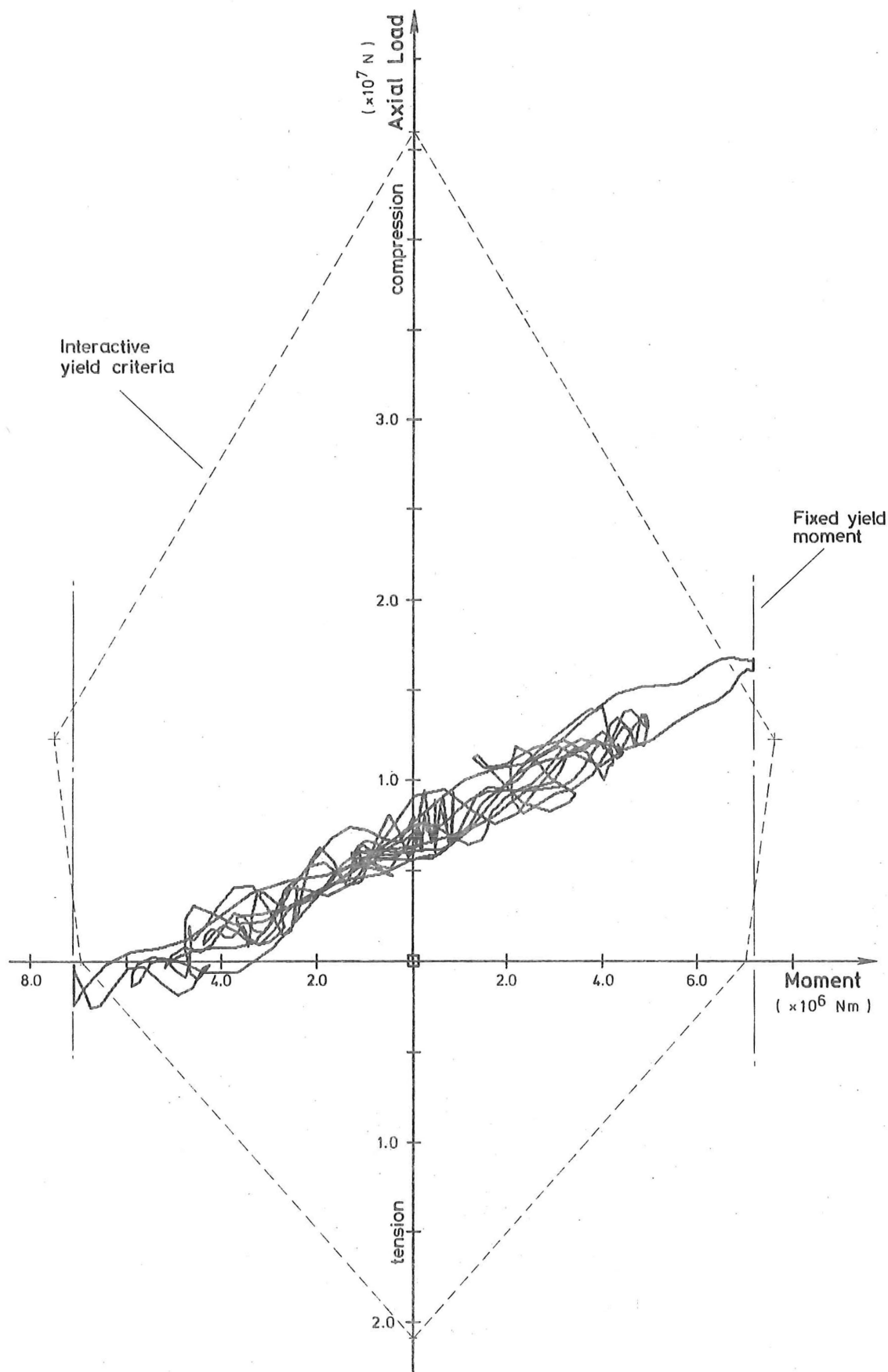
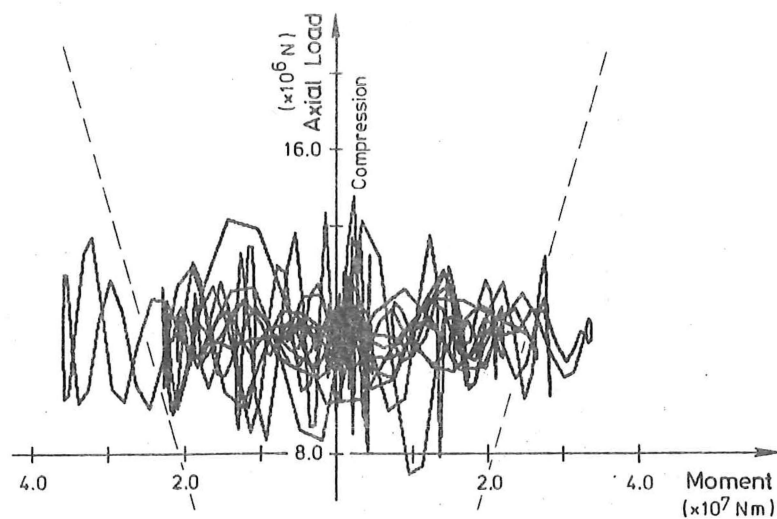
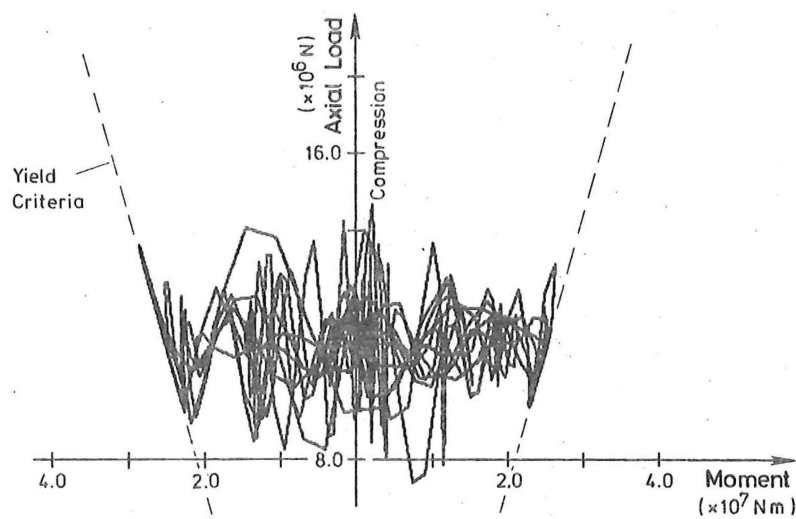


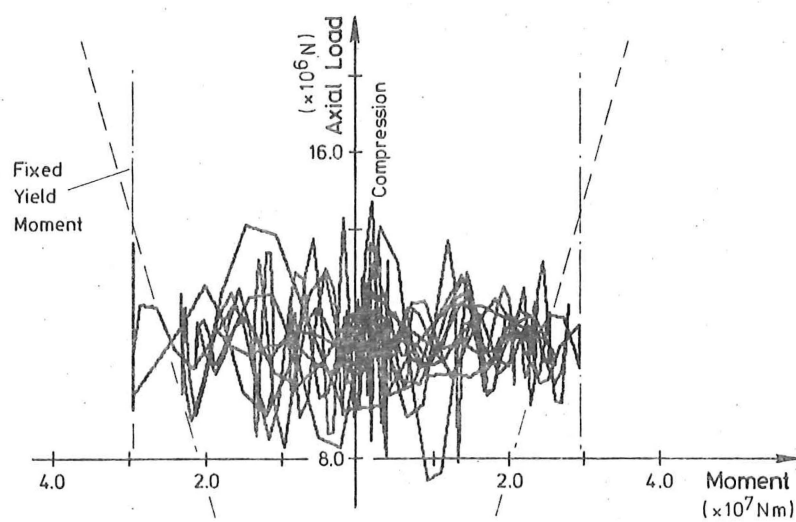
FIGURE 7-6c : MOMENT - AXIAL LOAD HISTORIES AT TOP OF LEFT-HAND PILE,  
ELASTO-PLASTIC WITH FIXED YIELD MOMENTS.



a). Elastic analysis.



b). Elasto-plastic with interaction.



c). Elasto-plastic with fixed yield moments.

FIGURE 7-7 : MOMENT - AXIAL LOAD HISTORIES AT BASE OF PIER.

can vary from column to column in the same structure. The overall geometry of the structure results in the bending moment in the piles being an almost linear function of the axial load. The heavily banded nature of the graphed relationship confirms this, the vertical width of the band reflecting the response of the bridge-deck and pile-cap to the vertical component of the earthquake. The imposition of either type of yield criteria on the pile moments is seen to be not very severe in the case of this excitation. In the absence of the ability for the yield criteria to be stipulated in terms of such interaction curves, provided that a linear prediction could be made (as in the case of these piles), a simple calculation would seem to be sufficient for an estimation of single positive and negative yield moments.

The moment - axial load interaction for the pier member's base section is similarly very strongly banded, but differs from that of the piles in that the imposed yield criteria is much more severe. Again, it can be seen that the choosing of more accurate single yield moments for the non-interaction analysis (admittedly, much easier with hind-sight) should, because of the narrow banding of the actual path of the moment - axial load response, give results which are similar to those of the analysis which had an interactive capability.

In order to confirm this a fourth analysis, incorporating these modified yield moment values, was carried out. Yield moments of  $6.51 \times 10^6$  N m for the double pile and  $25.1 \times 10^6$  N m for the pier were specified. These were, approximately, ten per cent smaller than those for the previous similar analysis (i.e. analysis b.). When compared to the analysis, the ductility required doubled for an increase in maximum horizontal deck displacement, from 95.7 mm to 108 mm. The permanent drift, estimated from the apparent offset of the response after ten seconds of excitation, more than doubled. A comparative summary of all the results is given in table 7-II.

The sensitivity of the structure to small changes in the member yield criteria is most noticable. This is understandable when it is realized that the dynamic system is working in the region of a boundary condition plateau - namely, the yield criteria. The small number of members (effectively, three) means that the loss of incremental stiffness at one or two critical member sections proportionately alters the total incremental stiffness of the structure much more significantly than the same number of changes in, for example, a ten-storey, four-bay frame with ninety members.

	Maximum horizontal deck displacement (mm)	Maximum horizontal pile-cap displacement (mm)	Maximum plastic rotation of hinge of pier base (rads)	Maximum plastic rotation of hinge at top of left pile (rads)	Estimated permanent horizontal drift of deck (mm)
a) Elastic analysis	102.	49.7	-	-	-
b) Elasto-plastic with no interaction	95.7	-46.3	$-1.53 \times 10^{-3}$	$3.66 \times 10^{-4}$	30
c) Elasto-plastic with interaction	-94.8	-46.6	$-0.73 \times 10^{-3}$	$4.39 \times 10^{-4}$	8
Elasto-plastic (no interaction) revised yield values	108.	-49.7	$-3.6 \times 10^{-3}$	$8.30 \times 10^{-4}$	64

TABLE 7-II: SUMMARY OF RESULTS OF ANALYSES OF PIER 5, TRANSVERSE  
DIRECTION, AUCKLAND UPPER HARBOUR CROSSING.

The only time that a collapse mechanism formed in the piles was after 5.54 seconds in that analysis in which the re-calculated yield moments were used instead of an interaction criteria. It was present for only 0.04 seconds. However, the formation of a plastic hinge at the base of the pier member also constitutes a collapse mechanism - this being observed in all the inelastic analyses. Again, this hinge was never present for any significant length of time.

#### 7.4 CONCLUSIONS

Both bridge structures are seen to be sensitive to the characteristics of their plastic hinges. The nature of the differences between the linear and non-linear responses is not predictable because of this

sensitivity. It is interesting to note that the formation of a potential collapse mechanism in a structure is a necessary (but not sufficient) condition for a failure under dynamic loading - because of the frame's ability to recover if the accelerations and velocities of the mass representation are not too large when compared with those of the ground motion. In both cases, the analyses benefitted the designers by showing them the range in which they could expect their structures to respond if modelled with non-linear elements.

## CHAPTER EIGHT

A SUMMARY WITH SUGGESTIONS FOR FUTURE STUDIES

It has become apparent during the course of this study that, although the designer of an inelastic frame may obtain quantitative and definitive answers from a deterministic analysis of that frame, he will find it most difficult to relate his structure's response to some arbitrary excitation to those criteria laid down by the relevant parts of the building code of practice which he must satisfy. His interpretation of the results must also be skilfully made in terms of the modelling procedures he has used.

Having decided to commission an inelastic seismic analysis of his frame, the engineer must ensure that the various modelling procedures, which are integral parts of such an analysis, are suitable for the representation of his particular structure. It is upon the choice of these procedures that this study concentrated.

The modelling of the stiffness and mass distributions were the first areas of concern. It was found that costly partitioning of stiffness matrices could be dispensed with - in order to save computational time - if a stable numerical integration scheme was used. The stiffness method of analysis, using one-dimensional finite-elements, enabled a generalized formulation of the frame model to be achieved. Slaving (or coupling) of similar degrees of freedom must be judiciously carried out so that unnecessary increases in computation times are not enforced by the consequent increases in the bandwidth of the stiffness matrices. Where possible, all degrees of freedom should be given at least an associated lumped mass, as this, too, both improves the conditioning of the stiffness matrix and allows a better distribution of inertial loads to accrue. The use of a consistent mass matrix, however, is not so necessary, for it provides an upper-bound solution by slightly increasing the frame's dynamic stiffness. Nevertheless, apart from a little extra storage space being required, the extra computation associated with a consistent mass formulation is not great and may be considered a small price to pay for not having to make some estimate of the equivalent lumped rotational mass at a node.

Giberson's mathematical model of a non-linear beam [25] was found to be a particularly versatile tool. The incorporation of a moment - axial load interaction capability for determining the failure or yield levels of a column is simple and must be used for all structures

in which there are fluctuating axial loads. Many of the simple improvements to the modelling of a beam, such as the inclusion of allowances for the existence of rigid end-blocks and shear deformation, must now, at this stage of the development of the art, be considered as essential options to be provided in any new programs being written, for their inclusion costs virtually nothing. The use of computer programs which are devoid of these options should not be contemplated if there is the likelihood of such refinements having a significant effect on the response of the particular frame under study.

It has been shown, by considering the work done by an oscillating inelastic system, that the shape of the moment-curvature hysteresis chosen may have a profound effect on the response of a dynamically excited single-degree of freedom system. Furthermore, if this system is allowed to weaken, the displacements required to maintain at least a constant rate of energy-absorption increase rapidly. A limited study of the sensitivity of the deterministic dynamic response of a multi-storey frame to different moment-curvature functions showed that, at this stage of the development of the use of inelastic analyses, a simple hysteresis exhibiting a bi-linear relationship will suffice for most analyses as long as only the general trends of inelasticity are being sought. Future research into this aspect should concentrate on the production of an improved multi-linear approximate relationship.

Whichever moment-curvature function is chosen as being applicable to the frame under analysis, there still remains the major difficulty of satisfactorily tracking the relationship during a piece-wise integration. The extent of this problem is compounded by the unsuitability of the straightforward iterative procedures of predictor-corrector methods used for static loading cases. In an effort to minimize the computational work required when a frame's stiffness is being constantly modified, it was found that the most expedient scheme consisted of adding those amounts by which a member's reactions were under- or over-estimated in one time-step on to the vector of incremental dynamic loads for the following time-step. A number of other schemes were put forward as being worthy of future investigation.

It was confirmed that care must be exercised in the choosing of a suitable piece-wise scheme for the numerical integration of the kinematic equations, for it remains an art to select a time-step which will complement the chosen procedure. The linear acceleration approximation (i.e. Newmark's ' $\beta=1/6$ ' method), which has been very popular because of its realistic form, has a numerical stability criteria which



requires too fine a time-step for refined inelastic analyses. Apart from period-errors, which are usually negligible for those modes which contribute most to a frame's response, the constant average acceleration ( $\beta=1/4$ ) assumption stands out as being the most reliable. Being unconditionally stable, it allows a time-step of about one-hundreth of a second to be used for most structures and accelerograms. Wilson's schemes, unfortunately, were found to imply the presence of intolerable increased levels of damping, although they, too, have the advantage of being unconditionally stable. It is recommended, however, that any computer programs which are to be made widely available should incorporate a check on the length of the input time-step (based on the stability criteria for the linear acceleration method), in order to ensure that an unwise choice of an unconditionally stable integration approximation does not result in the inexperienced user persisting with an inaccurate analysis. It is mathematically shown that these numerical stability criteria, developed by Newmark, are basically unaffected by the existence of supercritically damped (non-oscillatory) modes of vibration. It was also found that kinematic degrees of freedom whose associated masses are allowed to tend to zero will upset conditionally stable integration schemes, because they imply the presence of natural modes with infinitely small periods.

Explicit integration schemes, which up to now have only been used for the deterministic analysis of short-duration loadings (c.f. shock loads) because of the very short time-step they require, need to be investigated as a way of eliminating the large amounts of computation necessary when the stiffness matrix is being reduced at each change of plasticity. The dimensions of the matrices associated with three-dimensional analyses will magnify the size of the problem to be faced.

'Ductility' has been found to be a most useful description if its use is left exclusively to that of describing the curvature at a section of a member. In the inelastic analysis developed in this study, it corresponds to the measure of the curvature at a theoretical plastic hinge with respect to some first-yield (or equivalent) curvature at the same section. When the results of deterministic dynamic analyses are being considered, 'frame ductility' or 'displacement ductility' have no meaning and the use of such terms should be strictly left to their use in describing equivalent static uni-directional loadings. In both theoretical inelastic analyses and the detailing of a frame's structure, the use of the terms 'curvature' and 'ductility'

implies that the engineer must estimate the length of the plastic hinge which he is permitting to form. This study has highlighted the need for increased research into means of determining practical values for this length.

One of the most difficult problems facing the designer is that of deciding which earthquake accelerogram will best match the static loading conditions stipulated by the relevant building code of practice. Most codes do not lay down any standard conditions for deterministic dynamic analyses. There is a need for them to provide some criteria for the choosing of the type of excitation that a structure should resist and, in the absence of any better knowledge being available, indicate the likely values of some of the more obvious parameters (e.g. damping) to be used. In the same way, in order to assist those who compile building codes, many more experimental values of the parameters for typical buildings are required.

A need has been shown for further research into the measurement of the damage potential of an earthquake to a particular frame. Although, on a very broad scale, one earthquake can be described as being some fraction of the size of another, no simple criterion was found to give any degree of correlation over a selection of accelerograms. Until the statistical likely-earthquake has been developed, all deterministic analyses must be described with reference to the actual properties of the accelerogram used. The time has come for the development of a method by which the measurement of the integral of the inelastic behaviour of a member can be related to the likely cost of damage sustained by the load-resisting structure. An extension of this principle would be the use of the displacement response to give an estimate of the damage likely to be inflicted on non-structural items.

The use of vertical components of the earthquakes was found to be essential because of the possible effect of vertical accelerations on column axial loads and deflections. Special non-regular frames may often be susceptible to these effects and this was proven in the case of the tall bridge-pier investigated.

It became apparent, during the execution of many inelastic analyses, that it was unlikely that tall slender frames would develop plastic hinges at all their critical sections simultaneously. Examination of the visually-output plastic hinge patterns showed the presence of bands of inelastic behaviour migrating upward through the frames. This is evidence that code requirements for the calculation of the design base-overturning moment to be resisted by a frame should be reduced in severity

from that level indicated by 'equivalent' static loadings. Confirmation of these findings was made by Row[20], who used the inelastic program, developed by the author, to investigate the occurrence of plastic hinges in the columns of a three-dimensional, skew-loaded, frame.

Now that the benefit of such designs can be analytically evaluated, there is a need for the development of new structural members and joints (e.g. those which will exhibit rising spring-rates) which will enhance the energy-absorption of a frame at low levels of deflection, thus helping to deter the frame from increasing its response. These features may need to be sacrificial and, therefore, easily accessed for repair or replacement.

For certain structures there has been seen a need for the investigation and eventual analytical recognition of the consequences of large deflections. If these were to be incorporated in an inelastic frame analysis program, the possibility of some structures collapsing by either overturning, 'shaking-down' or developing large eccentricities of loading during long or consecutive earthquakes could be studied.

Work on minimizing the quantity and improving the presentation of the results with, perhaps, maximum moment, displacement and shear force envelopes being developed and incorporated in programs, would help to make designers understand the dynamic behaviour of their buildings - in the same way as the displays of plastic hinge patterns have helped this study. These improvements are simple in concept, but time-consuming to incorporate.

The immediate future in the art of dynamic inelastic analysis lies in helping engineers to develop a qualitative understanding of the behaviour of their already designed structure, so that they might more expertly detail its load-resisting elements - rather than in just finding absolute quantitative results which may be pertinent for only one particular excitation.

## REFERENCES

1. "Basic Design Loads", New Zealand Standard Model Building Bylaw, NZSS 1900, Draft Revision of Chapter 8, 1973.
2. "Proposed Building Code Amendments", Department of Building and Safety, City of Los Angeles, California, April, 1972.
3. Clough, R.W., "Effect of Stiffness Degradation on Earthquake Ductility Requirements", Structures and Materials Research Report, Department of Civil Engineering, University of California, Berkeley, Report No. 66-16, October, 1966.
4. Liu, S-C., "Earthquake Response Statistics of Nonlinear Structures", Journal of the Engineering Mechanics Division, ASCE, Vol. 95, No. EM2, Proc. Paper 6507, April, 1969, pp. 397-419.
5. Nickell, R.E., "On the Stability of Approximation Operators in Problems of Structural Dynamics", International Journal of Solids and Structures, Pergamon Press, Vol. 7, 1971, pp. 301-319.
6. Nickell, R.E., "A Survey of Direct Integration Methods in Structural Dynamics", Technical Report, Office of Naval Research, U.S.A. Navy, No. 9, April, 1972.
7. Weeks, G., "Temporal Operators for Nonlinear Structural Dynamics Problems", Journal of the Engineering Mechanics Division, ASCE, Vol. 98, No. EM5, Proc. Paper 9260, October, 1972, pp. 1087-1105.
8. Cheng, F.Y., "Vibrations of Timoshenko Beams and Frameworks", Journal of the Structural Division, ASCE, Vol. 96, No. ST3, Proc. Paper 7155, March, 1970, pp. 551-571.
9. Goel, S.C., "P- $\Delta$  and Axial Column Deformation in Aseismic Frames", Journal of the Structural Division, ASCE, Vol. 95, No. ST8, Proc. Paper 6738, August, 1969, pp. 1693-1711.
10. Shinozuka, M., "Maximum Structural Response to Seismic Excitations", Journal of the Engineering Mechanics Division, ASCE, Vol. 96, No. EM5, Proc. Paper 7620, October, 1970, pp. 729-738.
11. Clough, R.W., and Benuska, K.L., "F.H.A. Study of Seismic Design Criteria for High-Rise Buildings", U.S. Department of Housing and Urban Development Report, Federal Housing Administration, Washington, HUD TS-3, August, 1966.
12. Walpole, W.R., "The Response of Structures to Earthquake Loading", Unpublished Ph.D. thesis, University of Canterbury, Christchurch, New Zealand, 1968.
13. Garden, R.J.P., Shepherd, R. and Sharpe, R.D., "Notes on the Representation of Plastic Hinge Behaviour in Dynamic Analyses", New Zealand Engineering, NZIE, Vol. 24, No. 12, December, 1969, pp. 386-391.

14. MacNeal, R.H., and McCormick, C.W., "The NASTRAN Computer Program for Structural Analysis", Computers and Structures, Pergamon Press, Vol. 1, 1971, pp. 389-412.
15. Newmark, N.M., "A Method of Computation for Structural Dynamics", Journal of the Engineering Mechanics Division, ASCE, Vol. 85, No. EM3, Proc. Paper 2094, July, 1959, pp. 67-94.
16. Dunham, R.S., Nickell, R.E., and Stickler, D.C., "Integration Operators for Transient Structural Response", Computers and Structures, Pergamon Press, Vol. 2, 1972, pp. 1-15.
17. Brand, L., "Differential and Difference Equations", John Wiley & Sons Inc., New York, 1966, pp. 379.
18. Fox, L., and Mayers, D.F., "Computing Methods for Scientists and Engineers", Oxford University Press, Oxford, 1968, pp. 37.
19. Clough, R.W., and Wilson, E.L., "Dynamic Finite Element Analysis of Arbitrary Thin Shells", Computers and Structures, Pergamon Press, Vol. 1, 1971, pp. 33-56.
20. Row, D.G., "The Effects of Skew Seismic Response on Reinforced Concrete Frames", Unpublished M.E. Report, Department of Civil Engineering, University of Canterbury, January, 1973.
21. Rubinstein, M.F., "Matrix Computer Analysis of Structures", Prentice-Hall Inc., New Jersey, 1966, pp. 224.
22. Felippa, C.A., "Refined Finite-Element Analysis of Linear and Nonlinear Two-Dimensional Structures", U.C. SEL Report, University of California, Berkeley, Report No. 66-22, 1966.
23. Caughey, T.K., "Classical Normal Modes in Damped Linear Dynamic Systems", Journal of Applied Mechanics, ASME, Vol. 27, No. 2, Paper 59-A-62, June, 1960, pp. 269-271.
24. Kaldjian, M.J., "Moment-Curvature of Beams as Ramberg-Osgood Functions", Journal of the Structural Division, ASCE, Vol. 93, No. ST5, Proc. Paper 5488, October, 1967, pp. 53-65.
25. Giberson, M.F., "Two Nonlinear Beams with Definitions of Ductility", Journal of the Structural Division, ASCE, Vol. 95, No. ST2, Proc. Paper 6377, February, 1969, pp. 137-157.
26. Muto, K., "Seismic Analysis of Reinforced Concrete Buildings", Shokoku-sha Publishing Company, Tokyo, Japan, 1965, pp. 116.
27. Baker, A.L.L., and Amarakone, A.M.N., "Inelastic Hyperstatic Frames Analysis", Proceedings of the International Symposium, Flexural Mechanics of Reinforced Concrete, Miami, Florida, 1964, pp. 85-135.
28. Corley, W.G., "Rotational Capacity of Reinforced Concrete Beams", Journal of the Structural Division, ASCE, Vol. 92, No. ST5, October, 1966, pp. 121-146.

29. Walpole, W.R., and Shepherd, R., "Elasto-Plastic Seismic Response of Reinforced Concrete Frame", Journal of the Structural Division, ASCE, Vol. 95, No. ST10, October, 1969, Proc. Paper 6813, pp. 2031-2055.
30. Goel, S.C., and Berg, G.V., "Inelastic Earthquake Response of Tall Steel Frames", Journal of the Structural Division, ASCE, Vol. 94, No. ST8, Proc. Paper 6061, August, 1968, pp. 1907-1934,
31. Kaldjian, M.J., and Fan, W.R.S., "Earthquake Response of a Ramberg-Osgood Structure", Journal of the Structural Division, ASCE, Vol. 94, No. ST10, Proc. Paper 6196, October, 1968, pp. 2451-2465.
32. Heading, J., "Mathematical Methods in Science and Engineering", Edward Arnold Ltd., London, 1963, pp. 295.
33. Archer, J.S., "Consistent Mass Matrix for Distributed Mass Systems", Journal of the Structural Division, ASCE, Vol. 89, No. ST4, Proc. Paper 3591, August, 1963, pp. 161-178.
34. Park, R., "Theorisation of Structural Behaviour with a View to Defining Resistance and Ultimate Deformability", Bulletin of the New Zealand Society for Earthquake Engineering, N.Z. Society for Earthquake Engineering, Vol. 6, No. 2, June, 1973, pp. 52-70.
35. Jennings, P.C., Housner, G.W., and Tsai, N.C., "Simulated Earthquake Motions for Design Purposes", Proceedings of the Fourth World Conference on Earthquake Engineering, Santiago, Chile, Vol. 1, January, 1969, pp. A1 145-160.
36. Penzien, J., and Liu, S-C., "Nondeterministic Analysis of Nonlinear Structures Subjected to Earthquake Excitations", Proceedings of the Fourth World Conference on Earthquake Engineering, Santiago, Chile, Vol. 1, January, 1969, pp. A1 114-129.
37. Housner, G.W., "Behaviour of Structures During Earthquakes", Journal of the Engineering Mechanics Division, ASCE, Vol. 85, No. EM4, Proc. Paper 2220, October, 1959.
38. Çakiroğlu, A., and Özmen, G., "Numerical Integration of Forced-Vibration Equations", Journal of the Engineering Mechanics Division, ASCE, Vol. 94, No. EM3, Proc. Paper 5968, June, 1968, pp. 711-729.

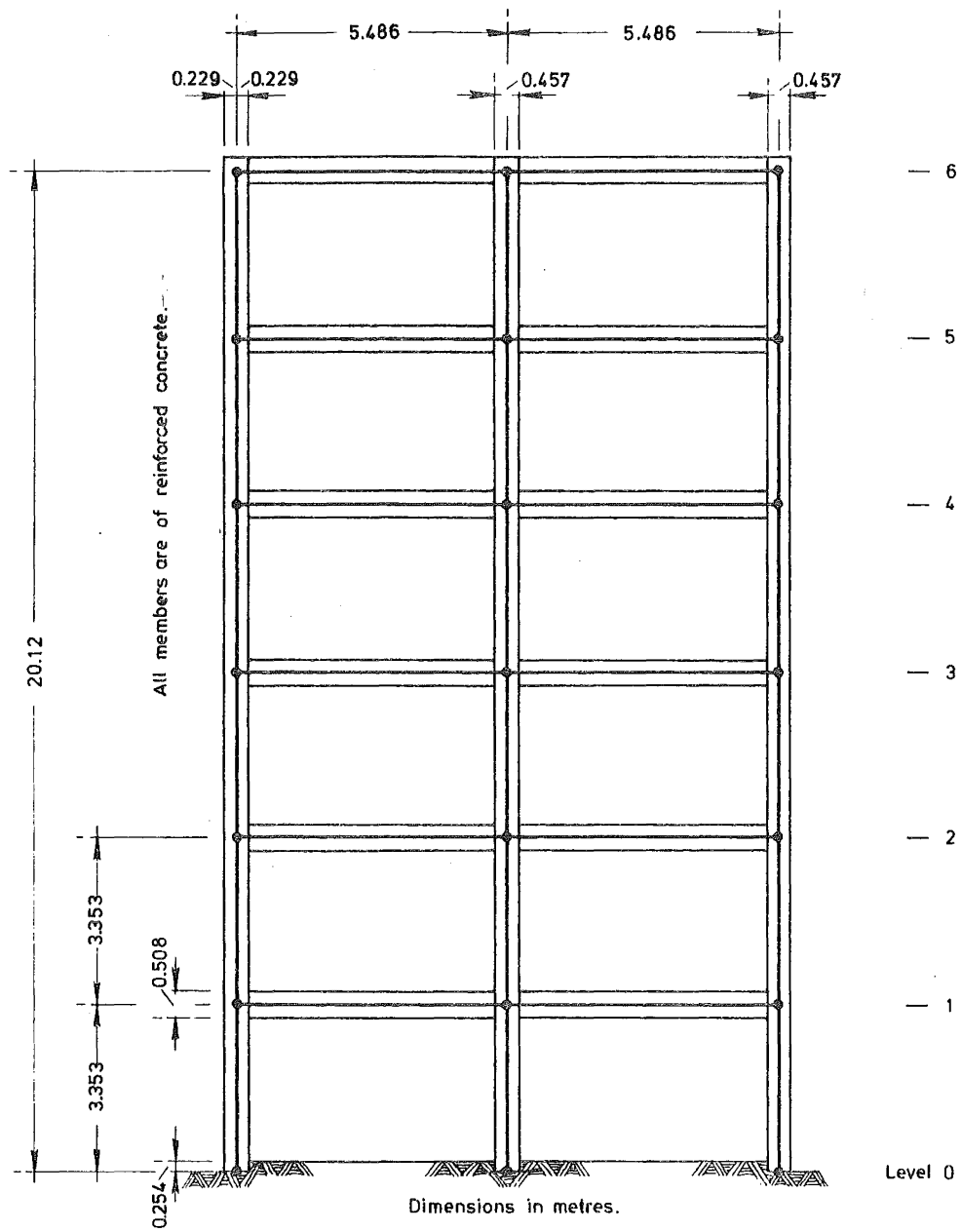
## APPENDIX A

ANALYSIS MODELSA.1 STRUCTURE I

A six-storey, two-bay exterior frame based on that used by Row [20] that is designed to the proposed revision to Chapter 8, NZSS 1900 [1].

A.1.1 Data

Elastic modulus	$2.622 \times 10^{10} \text{ N m}^{-2}$
Shear modulus	$1.104 \times 10^{10} \text{ N m}^{-2}$
Axial and shear areas - exterior columns	
Levels 0 - 6	$0.1652 \text{ m}^2$
	- interior columns
Levels 0 - 3	$0.2323 \text{ m}^2$
3 - 6	$0.2090 \text{ m}^2$
	- beams
Levels 1 - 3	$0.1806 \text{ m}^2$
4 - 6	$0.1626 \text{ m}^2$
Moment of inertia	- exterior columns
Levels 0 - 6	$1.915 \times 10^{-3} \text{ m}^4$
	- interior columns
Levels 0 - 3	$2.830 \times 10^{-3} \text{ m}^4$
3 - 6	$2.539 \times 10^{-3} \text{ m}^4$
	- beams
Levels 1 - 3	$3.746 \times 10^{-3} \text{ m}^4$
4 - 6	$3.205 \times 10^{-3} \text{ m}^4$
Rigid end-blocks	- columns
	$0.2540 \text{ m}$
	- beams
	$0.2286 \text{ m}$
Weight per unit beam length	-
	$2.229 \times 10^4 \text{ N m}^{-1}$
Plastic hinge lengths - exterior columns	
	$0.203 \text{ m}$
	- interior columns
	$0.229 \text{ m}$
	- beams
	$0.356 \text{ m}$
Natural frequencies	-
$\omega_1$	$1.359 \text{ Hz}$
$\omega_2$	$4.116 \text{ Hz}$
Percentage critical damping in first two modes	-
	$10.0$

FIGURE A-1 : STRUCTURE I.



Ultimate strengths -

	$M_1$	$M_2$	$M_b$	$P_b$	$P_{yc}$	$P_{yt}$
	$\times 10^5 \text{Nm}$	$\times 10^5 \text{Nm}$	$\times 10^5 \text{Nm}$	$\times 10^6 \text{N}$	$\times 10^6 \text{N}$	$\times 10^6 \text{N}$
Ext. cols. -						
Level 0 - 1	2.092		3.494	-1.625	-3.606	1.202
1 - 2	1.651		3.234	-1.603	-4.808	0.957
2 - 3	1.470		3.076	-1.603	-4.585	0.824
3 - 6	1.289		2.974	-1.603	-4.452	0.712
Int. cols. -						
Level 0 - 1	2.827		5.823	-2.359	-7.390	1.781
1 - 2	2.601		5.043	-2.226	-6.722	1.336
2 - 3	2.578		5.009	-2.226	-6.700	1.304
3 - 6	2.556		4.975	-2.226	-6.678	1.269
Beams -						
Level 1	2.239	-2.955				
2	2.177	-2.873				
3	1.891	-2.562				
4	1.418	-2.090				
5	0.790	-1.467				
6	0.426	-0.827				

The dimensions of this frame are given in figure A-2.

## A.2 STRUCTURE II

A thirteen-storey, two-bay exterior frame based on that used by Walpole [12]. That frame was derived from a North-East frame of the Jerningham Apartments, Wellington.

### A.2.1 Data

Elastic modulus	$2.760 \times 10^{10} \text{ N m}^{-2}$	
Shear modulus	$1.200 \times 10^{10} \text{ N m}^{-2}$	
Axial areas, Shear areas - exterior columns		
Levels 0 - 4	0.6580	0.5550 $\text{m}^2$
4 - 8	0.6070	0.5050 $\text{m}^2$
8 -13	0.5560	0.4540 $\text{m}^2$
- interior columns		
Levels 0 - 4	0.5660	0.4630 $\text{m}^2$
4 - 8	0.5410	0.4380 $\text{m}^2$
8 -13	0.5150	0.4130 $\text{m}^2$
- beams		
Levels 1 - 4	0.4350	0.3600 $\text{m}^2$
5 - 9	0.3800	0.3150 $\text{m}^2$
10 -13	0.3250	0.2700 $\text{m}^2$
Moment of inertia - exterior columns		
Levels 0 - 4	$2.900 \times 10^{-2} \text{ m}^4$	
4 - 8	$2.720 \times 10^{-2} \text{ m}^4$	
8 -13	$2.460 \times 10^{-2} \text{ m}^4$	

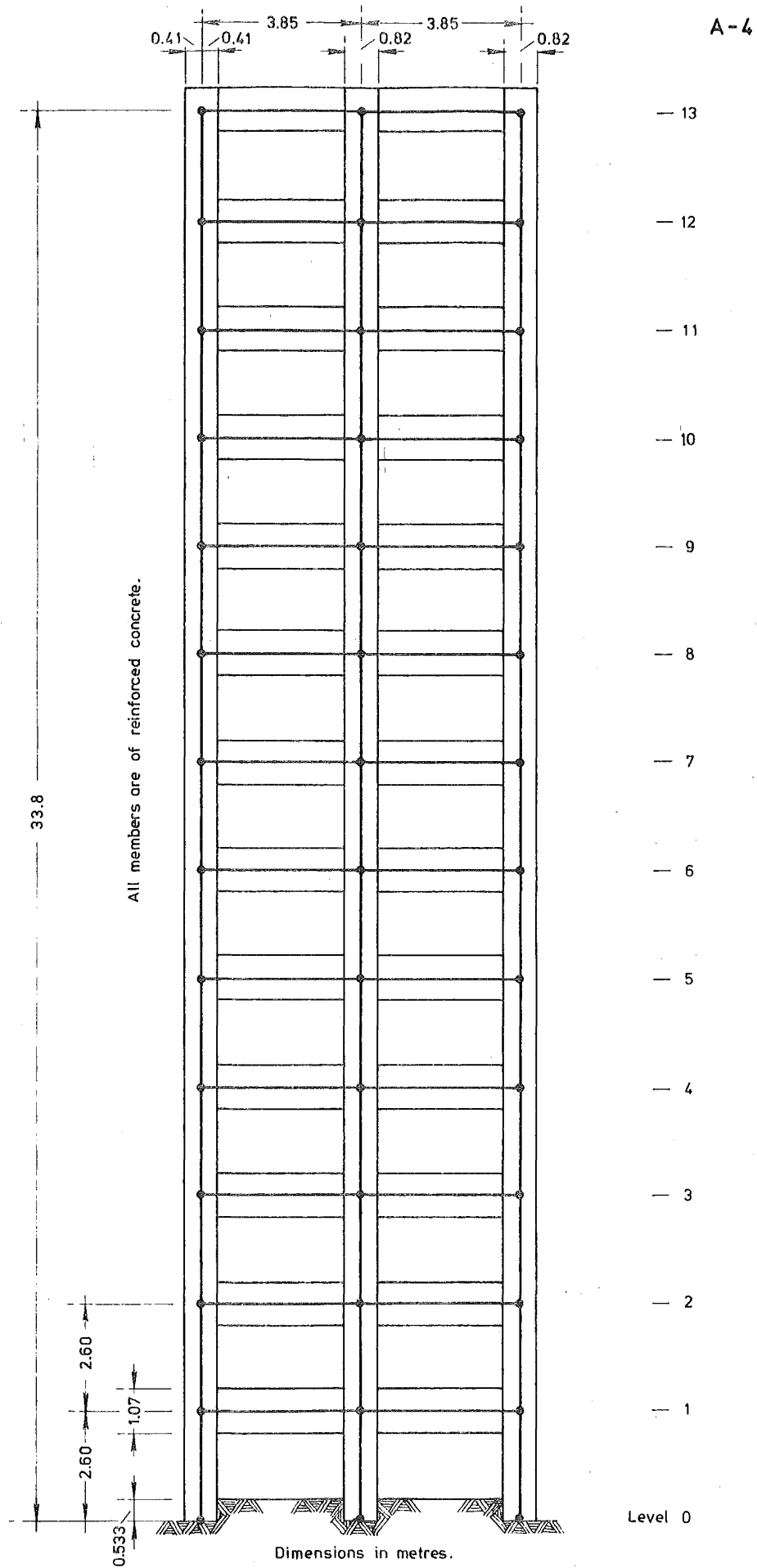


FIGURE A-2 : STRUCTURE II.

		- interior columns				
Levels	0 - 4		$4.320 \times 10^{-2} \text{ m}^4$			
	4 - 8		$3.930 \times 10^{-2} \text{ m}^4$			
	8 -13		$3.770 \times 10^{-2} \text{ m}^4$			
		- beams				
Levels	1 - 4		$4.705 \times 10^{-2} \text{ m}^4$			
	5 - 9		$4.370 \times 10^{-2} \text{ m}^4$			
	10 -13		$3.920 \times 10^{-2} \text{ m}^4$			
Rigid end-blocks		- columns				
			0.533 m			
		- beams				
			0.410 m			
Weight per unit beam length		-				
			$1.250 \times 10^5 \text{ N m}^{-1}$			
Plastic hinge lengths		- exterior columns				
			0.320 m			
		- interior columns				
			0.420 m			
		- beams				
			1.06 m			
Natural frequencies		-				
	$\omega_1$		1.076 Hz			
	$\omega_2$		1.906 Hz			
Percentage critical damping in first two modes		-				
			5.00			
Ultimate strengths		-				
	$M_1$	$M_2$	$M_b$	$P_b$	$P_{y_c}$	$P_{y_t}$
	$\times 10^6 \text{ Nm}$	$\times 10^6 \text{ Nm}$	$\times 10^6 \text{ Nm}$	$\times 10^6 \text{ N}$	$\times 10^7 \text{ N}$	$\times 10^6 \text{ N}$
Ext. cols. -						
Level 0 - 4	1.450		1.850	-3.740	-1.540	7.790
4 - 8	1.060		1.520	-4.010	-1.340	5.250
8 -13	0.583		1.230	-3.740	-1.090	2.670
Int. cols. -						
Level 0 - 4	1.330		1.800	-3.230	-1.460	5.340
4 - 8	1.030		1.610	-2.880	-1.300	3.920
8 -13	0.706		1.430	-3.160	-1.140	2.630
Beams						
Level 1 - 4	1.040	1.980				
5 - 6	1.030	1.970				
7	0.790	1.500				
8	0.724	1.440				
9	0.679	1.290				
10	0.550	0.506				
11 -13	0.421	0.785				

The dimensions of this frame are given in figure A-2.

## APPENDIX B

DERIVATIONSB.1 THE CONVERGENCE CRITERIA FOR A DAMPED SINGLE-DEGREE OF FREEDOM SYSTEM (EQUATION 3-X)

For convergence to be possible in the iterative solution for the acceleration at the end of the time-step then...

$$\frac{\text{error in derived acceleration}}{\text{error in assumed acceleration}} \leq 1$$

$$\text{i.e.} \quad \frac{\ddot{\hat{x}}_{t+1} - \ddot{\ddot{x}}_{t+1}}{\ddot{\ddot{x}}_{t+1} - \ddot{\ddot{x}}_{t+1}} \leq 1 \quad (\text{B-i})$$

where  $\ddot{\hat{x}}_{t+1}$  is the derived acceleration at the end of the time-step,  $\ddot{\ddot{x}}_{t+1}$  is the assumed acceleration and  $\ddot{\ddot{x}}_{t+1}$  is the actual acceleration. By initially assuming the acceleration at the end of the time-step to be  $\ddot{\ddot{x}}_{t+1}$ , values for the displacement and velocity can be derived from equations (3-viii) and (3-ix)...

$$\hat{x}_{t+1} = x_t + \dot{x}_t h + \left(\frac{1}{2} - \beta\right) \ddot{x}_t h^2 + \beta \ddot{\ddot{x}}_{t+1} h^2 \quad (\text{B-ii})$$

$$\dot{\hat{x}}_{t+1} = \dot{x}_t + \ddot{x}_t \frac{h}{2} + \ddot{\ddot{x}}_{t+1} \frac{h}{2} \quad (\text{B-iii})$$

where  $x_t$ ,  $\dot{x}_t$ ,  $\ddot{x}_t$  are the known values at the beginning of the time-step. Equation (3-vi) is then used to calculate the derived acceleration...

$$\ddot{\hat{x}}_{t+1} = - \frac{K \hat{x}_{t+1} + C \dot{\hat{x}}_{t+1}}{M}$$

The same equation (3-vi) also gives the true solution...

$$\ddot{\ddot{x}}_{t+1} = - \frac{K x_{t+1} + C \dot{x}_{t+1}}{M}$$

(in the iteration process the derived acceleration would then become the new assumed acceleration and the procedure would be repeated.)

(B-i) then gives the convergence criterion to be...

$$\frac{\left[ -\frac{K}{M}(x_t + \dot{x}_t h + (\frac{1}{2} - \beta)\ddot{x}_t h^2 + \beta\ddot{x}_{t+1} h^2) - \frac{C}{M}(\dot{x}_t + \ddot{x}_t \frac{h}{2} + \ddot{x}_{t+1} \frac{h}{2}) \right] + \frac{K}{M}(x_t + \dot{x}_t h + (\frac{1}{2} - \beta)\ddot{x}_t h^2 + \beta\ddot{x}_{t+1} h^2) + \frac{C}{M}(\dot{x}_t + \ddot{x}_t \frac{h}{2} + \ddot{x}_{t+1} \frac{h}{2})}{\ddot{x}_{t+1} - \ddot{x}_t} \leq 1$$

i.e. 
$$\left| \frac{(\ddot{x}_{t+1} - \ddot{x}_t) \left( -\frac{K}{M} \beta h^2 - \frac{C}{M} \frac{h}{2} \right)}{\ddot{x}_{t+1} - \ddot{x}_t} \right| \leq 1$$

Defining damping as  $C = 2\lambda\omega M$  (equation 3-vii)

$$\left| -\omega^2 \beta h^2 - 2\lambda\omega \frac{h}{2} \right| \leq 1$$

Neglecting negative damping and assuming  $\beta > 0$ ,  $\omega > 0$  and  $h > 0$ ,

then...

$$\omega^2 \beta h^2 + \lambda\omega h \leq 1$$

If 'T' is the natural period, then  $\omega = \frac{2\pi}{T}$ . Therefore...

$$4\pi^2 \beta \frac{h^2}{T^2} + 2\lambda\pi \frac{h}{T} - 1 \leq 0$$

Solving for the quadratic in  $\frac{h}{T}$ ...

$$\left[ \frac{h}{T} + \frac{\lambda}{4\pi\beta} - \frac{1}{2\pi} \sqrt{\frac{\lambda^2}{4\beta^2} + \frac{1}{\beta}} \right] \left[ \frac{h}{T} + \frac{\lambda}{4\pi\beta} + \frac{1}{2\pi} \sqrt{\frac{\lambda^2}{4\beta^2} + \frac{1}{\beta}} \right] \leq 0$$

The solution for positive values of 'h', 'T' is...

$$\frac{h}{T} \leq -\frac{\lambda}{4\pi\beta} + \frac{1}{2\pi} \sqrt{\frac{\lambda^2}{4\beta^2} + \frac{1}{\beta}}$$

i.e. 
$$\frac{h}{T} \leq \frac{1}{2\pi} \sqrt{\frac{1}{\beta}} \left[ \frac{1}{2} \sqrt{\frac{1}{\beta}} \left[ -\lambda + \sqrt{\lambda^2 + 4\beta} \right] \right] \quad (3-x)$$

B.2 THE DIFFERENCE EQUATION FOR A DAMPED SINGLE DEGREE OF FREEDOM SYSTEM (EQUATION 3-XI)

Equations (3-vi), (3-vii), (3-viii) and (3-ix) are used recursively to produce the following relationships

$$x_t = x_{t-1} + \dot{x}_{t-1}h + \left(\frac{1}{2} - \beta\right)\ddot{x}_{t-1}h^2 + \beta\ddot{x}_th^2 \quad (\text{B-iv})$$

$$x_{t+1} = x_t + \dot{x}_th + \left(\frac{1}{2} - \beta\right)\ddot{x}_th^2 + \beta\ddot{x}_{t+1}h^2 \quad (\text{B-v})$$

$$\dot{x}_t = \dot{x}_{t-1} + \frac{1}{2}\ddot{x}_{t-1}h + \frac{1}{2}\ddot{x}_th \quad (\text{B-vi})$$

$$\dot{x}_{t+1} = \dot{x}_t + \frac{1}{2}\ddot{x}_th + \frac{1}{2}\ddot{x}_{t+1}h \quad (\text{B-vii})$$

$$\ddot{x}_{t-1} = -2\omega\lambda\dot{x}_{t-1} - \omega^2 x_{t-1} \quad (\text{B-viii})$$

$$\ddot{x}_t = -2\omega\lambda\dot{x}_t - \omega^2 x_t \quad (\text{B-ix})$$

$$\ddot{x}_{t+1} = -2\omega\lambda\dot{x}_{t+1} - \omega^2 x_{t+1} \quad (\text{B-x})$$

Making the substitution  $\theta = \omega h$ , where possible, and eliminating  $\ddot{x}_{t-1}$ ,  $\ddot{x}_t$ ,  $\ddot{x}_{t+1}$  from equations (B-iv) to (B-x)...

$$x_t = x_{t-1} + \dot{x}_{t-1}h + h^2\left(\frac{1}{2} - \beta\right)(-2\omega\lambda\dot{x}_{t-1} - \omega^2 x_{t-1}) + \beta h^2(-2\omega\lambda\dot{x}_t - \omega^2 x_t) \quad (\text{B-xi})$$

$$x_{t+1} = x_t + \dot{x}_th + h^2\left(\frac{1}{2} - \beta\right)(-2\omega\lambda\dot{x}_t - \omega^2 x_t) + \beta h^2(-2\omega\lambda\dot{x}_{t+1} - \omega^2 x_{t+1}) \quad (\text{B-xii})$$

$$\dot{x}_t = \dot{x}_{t-1} + \frac{1}{2}h(-2\omega\lambda\dot{x}_{t-1} - 2\omega\lambda\dot{x}_t - \omega^2 x_{t-1} - \omega^2 x_t) \quad (\text{B-xiii})$$

$$\dot{x}_{t+1} = \dot{x}_t + \frac{1}{2}h(-2\omega\lambda\dot{x}_t - 2\omega\lambda\dot{x}_{t+1} - \omega^2 x_t - \omega^2 x_{t+1}) \quad (\text{B-xiv})$$

Eliminating  $\dot{x}_t$  and  $\dot{x}_{t+1}$  from (B-xi), (B-xiii) and (B-xii), (B-xiv) respectively, gives...

$$x_t = x_{t-1} + \dot{x}_{t-1}h + h^2\left(\frac{1}{2} - \beta\right)(-2\omega\lambda\dot{x}_{t-1} - \omega^2 x_{t-1}) + \beta h^2\left[-\omega^2 x_t - \frac{2\omega\lambda}{1+\theta\lambda}(\dot{x}_{t-1} - \theta\lambda\dot{x}_{t-1} - \frac{\theta\omega}{2}x_{t-1} - \frac{\theta\omega}{2}x_t)\right]$$

$$\begin{aligned} \text{i.e. } 0 &= x_{t-1}\left(1 + \theta\lambda - \frac{\theta^2}{2} - \frac{\theta^3\lambda}{2} + \beta\theta^2 + 2\beta\theta^3\lambda\right) \\ &\quad - x_t(1 + \theta\lambda + \beta\theta^2) + \dot{x}_{t-1}h(1 - \theta^2\lambda^2 + 4\theta^2\lambda^2\beta) \end{aligned} \quad (\text{B-xv})$$

$$\begin{aligned}
\text{and } x_{t+1} &= x_t - h^2 \left( \frac{1}{2} - \beta \right) \omega^2 x_t + \beta h^2 \left[ -\omega^2 x_{t+1} - \frac{2\omega\lambda}{1+\theta\lambda} \left( -\frac{\theta\omega}{2} x_t - \frac{\theta\omega}{2} x_{t+1} \right) \right] \\
&+ \frac{1}{1+\theta\lambda} \left( \dot{x}_{t-1} - \theta\lambda \dot{x}_{t-1} - \frac{\theta\omega}{2} x_{t-1} - \frac{\theta\omega}{2} x_t \right) \{ h - 2\omega\lambda h^2 \left( \frac{1}{2} - \beta \right) \\
&+ \beta h^2 \left[ -\frac{2\omega\lambda}{1+\theta\lambda} (1 - \theta\lambda) \right] \}
\end{aligned}$$

$$\begin{aligned}
\text{i.e. } 0 &= x_{t-1} \frac{-\theta^2}{2} (1 - \theta^2 \lambda^2 + 4\theta^2 \lambda^2 \beta) \\
&+ x_t (1 - \theta^2 + \beta\theta^2 + 2\theta\lambda - \theta^3 \lambda + \beta\theta^3 \lambda + \theta^2 \lambda^2) \\
&- x_{t+1} (1 + \theta^2 \lambda^2 + 2\theta\lambda + \beta\theta^2 + \beta\theta^3 \lambda) \\
&+ \dot{x}_{t-1} h (1 - \theta\lambda - \theta^2 \lambda^2 + \theta^3 \lambda^3 + 4\theta^2 \lambda^2 \beta + 4\theta^3 \lambda^3 \beta) \quad (\text{B-xvi})
\end{aligned}$$

Eliminating  $\dot{x}_{t-1}$  from (B-xv), (B-xvi)...

$$\begin{aligned}
0 &= x_{t-1} (1 + \beta\theta^2 - \theta\lambda) + x_t (\theta^2 - 2 - 2\beta\theta^2) + x_{t+1} (1 + \beta\theta^2 + \theta\lambda) \\
&= x_{t-1} \left( 1 - \frac{\theta\lambda}{1 + \beta\theta^2} \right) + x_t \left( \frac{\theta^2}{1 + \beta\theta^2} - 2 \right) + x_{t+1} \left( 1 + \frac{\theta\lambda}{1 + \beta\theta^2} \right) \\
\text{i.e. } &\left( 1 + \frac{\alpha^2 \lambda}{\theta} \right) x_{t+1} - (2 - \alpha^2) x_t + \left( 1 - \frac{\alpha^2 \lambda}{\theta} \right) x_{t-1} = 0 \quad (3-xi)
\end{aligned}$$

$$\text{where } \alpha^2 = \frac{\theta^2}{1 + \beta\theta^2}$$

## APPENDIX C

NOTES ON THE USE OF THE INELASTIC  
FRAME DYNAMIC ANALYSIS COMPUTER PROGRAM

C.1 INTRODUCTION

This program is designed to produce a piece-wise time-history response of a non-linear general two-dimensional frame subjected to an horizontal and/or vertical ground acceleration record. It has been written with an accent on providing flexibility of approach, with the frame members being treated as one-dimensional finite elements. Because it has been produced foremostly as a research tool, it has been found necessary, in some parts, to sacrifice a little computational efficiency for the sake of achieving generality. Its structure is amenable to future refinements.

C.2 THE PROGRAMMING LANGUAGE

Although first written in FORTRAN IV to suit an 128k byte IBM 360/44 computer, the coding was kept as independent of marque as possible. Subsequent to a faster and bigger Burroughs B6718 computer becoming available, it was required that the program be adapted expeditiously to the new computer. Consequently, the program structure, which was dictated to some extent by the hardware limitations and characteristics of the smaller IBM 360/44, was basically unaltered in the adapted version.

Whereas selected double-precision accuracy was found to be necessary for the IBM 360/44 version, the B6718's single precision was sufficient for the corresponding tasks. The accuracy and speed of the two machines are:-

	Accuracy (decimal digits)		Single precision word length (bytes)	Approximate relative average speed
	Single precision	Double precision		
IBM 360/44	7.2	16.8	4	1.0
B6718	11.	23.0	6	3.5

The floating-point word structure of the IBM 360/44 is hexadecimal, whereas that of the B6718 is binary orientated. The version listed (appendix D) is that for use on the B6718.

C.3 HARDWARE REQUIREMENTS

The basic program uses two sequential data scratch (disk)



files large enough to store...

- a) the upper half of the non-zero band of the vectorised stiffness matrix, and
- b) a card-image file of the vertical acceleration record.

Frame data is input on standard 80 column punched cards and the output formatting is suitable for an 132 character line-printer. If adequate core memory is economically available, a simple modification would eliminate the need for the scratch files.

#### C.4 GENERAL PROCEDURES

##### C.4.1 Free-formatted input

All data for this program is read in under free-format control - a blank column providing field definition. Integer and real fields may be mixed on the one card, as long as the fields of each type are in order within that type. No provision has been made in this version for data specified for one card to be continued on subsequent cards, although the free-formatting routine is capable of handling such requirements. Trailing zero-value fields (of both integer and real types) may be omitted. The maximum field-size for an integer, and each of the mantissa and exponent parts of a real number, is limited to the maximum integral number of significant digits carried by the user's machine for representing an integer. Both fixed point and 'E' (floating point) format may be used for real-type data. The 'E' format follows normal rules, except that an imbedded blank is not allowed between the mantissa and the 'E'.

Any card containing a field with an invalid format will be displayed on the line-printer - with a dollar sign beneath the character to which the routine has objected. Control will then pass to the next executable statement, although the program will terminate after reading and listing all the data if the detected error does not cause it to terminate before this.

##### C.4.2 Dimensions check

On successfully completing the reading of the input data (provided that a serious dimensioning violation has not already caused a premature termination of the program), a check will be initiated to ensure that the array and vector dimensioning, for the current compilation of the FORTRAN code, is sufficient to accommodate the particular frame about to be analysed. On an inadequate dimension being detected, execution will be terminated.

#### C.4.3 Data echo

Whatever the value of the data-echo option, an initial page containing a basic description and options for the analysis will be printed, together with a further page detailing the dimensions check. The data-echo option also controls the printing of the natural frequencies of the frame - whether calculated or read in as data. The printing of an approximate picture of the frame on the line-printer is independent of this same option.

#### C.4.4 Units

Any consistent set of absolute units may be used. Particular care should be taken in the expressing of weight units where these are used to define masses.

#### C.4.5 Numbering

A finite-element approach requires that all nodes and members be exclusively numbered. For efficient computation, the nodes should be numbered in such a way that the difference in number between any two nodes connected by a member is minimized. This will, in turn, minimize the width of the non-zero band of the stiffness matrix.

### C.5 THE FORM OF THE RESULTS

#### C.5.1 Initial static analysis

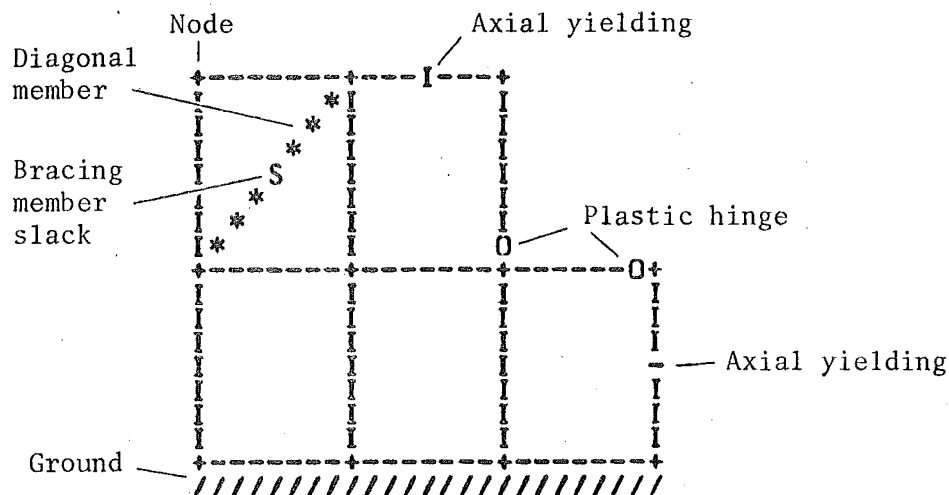
If a static analysis of the dead loads initially imposed on the frame has been requested, then the displacements (horizontal, vertical and rotational) of all nodes and deformations (end rotations and axial extensions) will be printed, together with the member end moments and axial forces.

#### C.5.2 Natural frequencies

If they are calculated by the program, then as many natural frequencies and mode shapes as there are dynamic (i.e. with mass) degrees of freedom, may be printed. The extrapolated percentage of the assumed equivalent viscous critical damping associated with the mode would then be also printed. If the first two (lowest) natural frequencies are read as data, then only they may be printed out.

### C.5.3 The time-history

Details of selected node displacements and member forces can be printed throughout the analysis, at any regular interval, beginning with those at the end of the first time-step completed. At the end of every time-step in which a change in the frame stiffness is detected (except when a Ramberg-Osgood moment-curvature relationship is employed - in which case the regular interval is maintained), an extra module of this node and member information will be printed. In addition, the amount by which the selected section curvatures exceed the curvature at first yield will also be given, followed by a picture showing the positions where the elasticity of the members is different from those at the beginning of the analysis. The following notation is used for these...

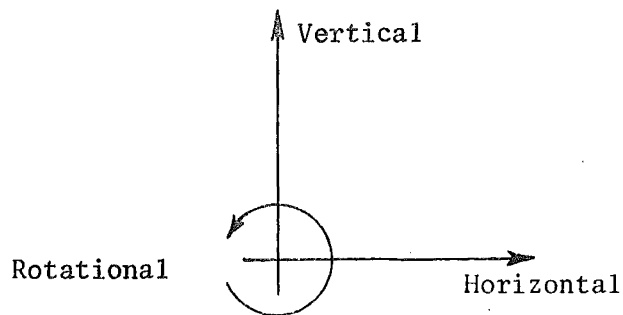


At the conclusion of the time-history, a summary of maximum displacements, moments and plastic displacements (including the moments at the time of these maximum plastic displacements) is produced in a form similar to that for the static analysis. Finally, there is an option allowing for member section ductilities to be calculated and printed.

## C.6 SIGN CONVENTIONS

### C.6.1 Nodes

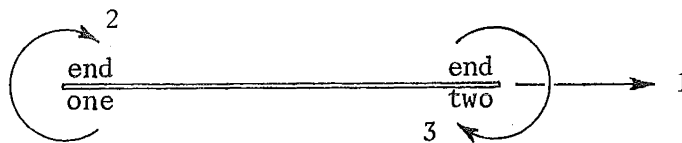
The geometry co-ordinates, displacements, velocities, accelerations and external forces of all the nodes (i.e. member joints) have a sign convention based on the right-handed cartesian co-ordinate system.



Horizontal displacements are therefore positive to the right, vertical movements positive upwards and rotations positive when anti-clockwise.

#### C.6.2 Members

In the member system of co-ordinates three degrees of freedom adequately describe the member



Axial elongation (and therefore tension also) is positive. Applied moments, together with fixed-end and yield moments, are clockwise-positive. A positive rotation of the equivalent plastic hinge is the result of a positively applied moment.

C.7 THE DATA DECK

## Section Card Format

1 1  
(DESCRIPTION  
OF ANALYSIS)

A	Description of frame being analysed. All 80 columns may be used for any characters with valid card codes.
---	---

2 1  
(PRINCIPAL  
ANALYSIS  
OPTIONS)

I	Analysis option	0 = Static (initial) analysis only. 1 = Natural frequencies and mode shapes only. 2 = Dynamic (time-history) analysis with optional static analysis.
I	Data-echo option	0 = Essential data-echo only. 1 = Full data-echo.
I	Picture option	0 = No picture of frame. 1 = Full page picture on line-printer to assist checking of data.
I	Node numbering option	0 = No numbering on picture. 1 = All nodes numbered.
I	Hysteresis type	0 = Elastic analysis only. 1 = Elastic/perfectly-plastic. 2 = Bi-linear. 3 = Ramberg-Osgood function.
The remaining options on this card need not be specified if a static analysis alone is attempted.		
I	Mass option	0 = Only input nodal masses used. 1 = Only input member masses used. 2 = Both types of masses to be summed and used.
I	Mass matrix option	0 = Lumped mass matrix. 1 = Consistent mass matrix.
The remaining options on this card need not be specified when natural frequencies alone are required.		
I	Natural frequencies option	0 = All natural frequencies calculated. 1 = Natural frequencies (first two) to be read in.

## Section Card Format

1 (EARTHQUAKE DESCRIPTION)	I	Vertical earth- quakes option	0 = No vertical earthquakes. n = Vertical earthquake acceleration record factored by the integer 'n' in addition to being factored by the general earthquake factor.	
	I	Plasticity- checking option for vertical members	0 = All members checked for possible yielding. 1 = All vertical members remain purely elastic.	
	I	Ductility option	0 = Member ductilities not calculated. 1 = Ductilities calculated using plastic hinge lengths.	
	The following card is required only if a dynamic (time- history) analysis is attempted.			
	A	Description of horizontal earthquake being used (up to 80 characters).		
	The following card is required only if a vertical earthquake has been specified.			
	2	A	Description of vertical earthquake being used (up to 80 characters).	
	4	1	A	Reason for this run (up to 80 characters) - printed on the title page to help identify the output.
	5 (FRAME & ANALYSIS CONTROL)	1	I	Number of nodes.
			I	Number of members.
		I	Number of types of members.	
The remaining items on this card are not necessary if only a static analysis is required.				
		F	Local value of the acceleration of gravity.	
		F	Percentage of critical damping to be applied to first mode.	
		F	Percentage of critical damping to be applied to second mode.	
		I	Number of mode shapes required (only if natural frequencies calculated).	
The remaining items on this card are unnecessary if a dynamic analysis not required.				

## Section Card Format

F	Newmark's $\beta$ for integration technique (normally set to $\frac{1}{4}$ ).
F	Inverse of the integration time-step interval.
F	Inverse of Wilson's integration technique time-step, set to 0. if not being considered.
F	Length of earthquake acceleration record to be used (seconds).
F	Earthquake magnification factor (applied to ground accelerations).
I	Number of time-steps to be inserted before time 'zero' on the earthquake record. This is to eliminate an impulse due to the earthquake record having a finite acceleration at time 'zero'.
I	Sequence number of first ('Berg' formatted) card of earthquake acceleration record to be used.
I	Period of printout during time-history analysis (in number of time-steps). A zero value will be treated as unity.
I	Period of the calculating of member forces (in number of time-steps). For an elastic analysis this need not be smaller than the printout period. A zero value will be treated as unity.
I	Period of the calling of the user's auxiliary output routine 'AUXØUT' (see section C.8) during the time-history analysis. A zero value will result in no call being made.
The following six cards (which may be blank) must only be included if the dynamic analysis option has been selected.	
1	I The numbers of up to 30 nodes for which a history of horizontal node displacements is required.
2	I As above - but for vertical node displacements.
3	I As above - but for nodal rotations (output in radians).
4	I The numbers of up to 30 members for which a history of moments and plastic displacements is required for end 'one'.
5	I As above - but for end 'two'.
6	I As above - but for axial forces and plastic displacements.

6  
(HISTORY  
OUTPUT  
CONTROL)

## Section Card Format

7

1

One card required per node - except that the presence of sequential nodes with one or both co-ordinates regularly spaced need only be implied by the presence of the first and the last cards of the sequence. Coupling and fixity will be taken (for all except the last card defining the sequence) as being identical to those of the first node of the sequence.

I	Node number - numbering being such as to produce the smallest interval between any two connected nodes.
F	Horizontal co-ordinate of node - measured from an arbitrary datum.
F	Vertical co-ordinate of node - measured from the same datum.
I	Boundary condition option = 0 if horizontal degree of freedom of this node is not fixed in relation to the co-ordinate datum. = 1 if fixed.
I	As above - but for vertical degree of freedom of this node.
I	As above - but for the rotational degree of freedom.
I	Coupling option = number of node, if any, which has its horizontal degree of freedom coupled to the horizontal degree of freedom of this node. (If coupled, both nodes will share the same static and dynamic d.o.f. masses will be added).
	= 0, (or a blank if it is a trailing zero) otherwise the user should be aware of the effect of coupling on the non-zero bandwidth of the stiffness and mass matrices. The coupling should preferably be specified in one direction only.
I	As above - but for the vertical degree of freedom.
I	As above - but for the rotational degree of freedom. This does <u>not</u> imply compensatory vertical and horizontal movements of nodes in order to keep a straight member connecting the coupled nodes straight.



## Section Card Format

8 (MEMBER GEOMETRY)	1-	One card per member - except that sequential members with sequential end numbering may be implied by the presence of the first and last cards in the series. Member type for all interpolated members will be as for the first member of the sequence.
	I	Member number.
	I	Node at end number one - hence end 'one' is defined.
	I	Node at end 'two'.
	I	Number of the member type - refers to the following section of member properties.
9 (MEMBER-TYPE PROPERTIES)		One card per member-type if the analysis is purely elastic - a second card per member-type must be inserted if (and only if) the analysis is an inelastic one.
	1-	I Member-type number.
	F	Axial area of member (for axial stiffness).
	F	Shear area (setting shear area to zero stops shear deformation occurring).
	F	Moment of inertia.
	F	Length of rigid end-block, end 'one'. Inclusion of a value for the end-block allows for the difference between the node-to-node member length and the clear length in stiffness calculations. Also, it allows the critical member sections to be displaced from the end nodes.
	F	Length of rigid end-block, end 'two'.
	F	Young's modulus.
	F	Shear modulus.
	F	Weight per unit centre-line length of member - converted internally to mass units. Required only if mass option non-zero.
	I	Pin option = 0 for no pin at end 'one'. = 1 for perfect pin at member side of rigid end-block to end 'one'.
	I	Pin option for end 'two' - as above.
	I	Brace option = 1 for member being able to take no compression. For member to be a true brace the pin option must be set for each end otherwise the ends will attract moment without being able to yield. = 0, otherwise.

## Section Card Format

F	Initial moment at end 'one'. This may be the initial fixed end moment as the initial static analysis will relax it correctly. Clockwise moments acting on the beam ends are positive.
F	Initial moment at end 'two'. As above.
F	Initial axial load (tension in the member is positive).

2- This card, if necessary, must follow immediately after the previous card pertaining to this particular member-type.

F	Length over which plastic hinge assumed to occur - end 'one'. A zero value will be replaced internally by unity.
F	Plastic hinge length - end 'two'.
F	Yield moment ' $M_1$ ' of ' $M_0$ ' - see below.
F	<p>Yield moment '<math>M_2</math>'.</p> <p>If <math>M_2 = 0</math> - then member is assumed to act as a column. An interaction curve is used to find one yield moment value which is used at both ends of the member. <math>M_1</math> is taken to be the yield moment for no axial load.</p> <p><math>M_2 + ve</math> - member acts in beam fashion (on axial load - moment interaction and has yield moments of <math>\pm M_1</math> at end 'one'; <math>\pm M_2</math> at end 'two'.</p> <p><math>M_2 - ve</math> - member acts in beam fashion with yield moments of <math>M_1, M_2</math> at end 'one'; <math>-M_2, -M_1</math> at end 'two'.</p>
F	Balanced failure yield moment (only used by column type members) ' $M_b$ '.
F	Balanced failure axial load (normally negative as it is a compression load) ' $P_b$ '.
F	Axial load for compression (negative) yielding (beams and columns), ' $P_{yc}$ '.
F	Axial load for tension (positive) yielding (beams and columns), ' $P_{yt}$ '.

## Section Card Format

F	Curve family indicator 'r' for Ramberg-Osgood function hysteresis or fraction of original stiffness for second arm of bi-linear hysteresis moment-curvature curve. A non-zero value of hinge length must be entered to enable the program to convert curvatures to spring-hinge rotations. In default a hinge length of unity is used for this purpose. If this latter case exists, then the stiffness fraction should be divided by the hinge length before inputting.
<p>The interaction curve for a column member-type is...</p> <p>The diagram shows a closed interaction curve on a coordinate system where the vertical axis is 'Axial Load (-ve)' and the horizontal axis is 'Moment'. The curve is a closed loop with vertices at <math>(0, P_{yc})</math>, <math>(M_b, P_b)</math>, <math>(M_0, 0)</math>, <math>(0, P_{yt})</math>, and back to <math>(0, P_{yc})</math>. The origin is marked with a small square.</p>	

10  
(EXTERNAL  
NODE  
FORCES)

1	One card required per node - unless sequential nodes have identical values when omitted nodes will be assumed to have values as for the last node in the series. The card for the highest numbered node must always be included.
I	Node number.
F	External static loading on node in horizontal direction.
F	External static loading on node in vertical (up = +ve) direction.
F	External static applied moment on node.
F	Lumped nodal weight for horizontal degree of freedom of node.
F	Lumped nodal weight for vertical degree of freedom of node.
F	Lumped nodal weight for rotational degree of freedom of node. These weights (converted internally to mass) may be omitted if only a static analysis is ordered.

(LUMPED  
WEIGHT  
AT NODE)

## Section Card Format

11	This section is included only if a vertical earthquake has been called.	
1	I	Number of vertical earthquake record cards - 'nc'.
2-nc	I	Card sequence number
(VERTICAL ACCELERATION RECORD)	F	Four sets of time/ground-acceleration co-ordinates. This card is essentially in 'Berg' format - see details of horizontal acceleration record.
12	This card is included only if natural frequencies are to be read, not calculated.	
(NATURAL 1 FREQUENCIES)	F	First (smallest) natural frequency (Hz).
	F	Second natural frequency (Hz).
13	The following cards are in 'Berg' format (I3, F8.4, F9.6).	
1-	13	Card sequence number.
(HORIZONTAL ACCELERATION RECORD)	F8.4 F9.6	Four pairs of time/ground-acceleration co-ordinates with the time in seconds and the accelerations as a fraction of gravitational acceleration.

## C.8 THE PROGRAM STRUCTURE

The following are brief descriptions of the functions of the subroutines which make up the program:

MAIN	:	Controls overall analysis; contains dimensions and file information.
ALTRMX	:	Adds or subtracts a member stiffness or mass matrix to (or from) the total stiffness or mass matrix.
AUXOUT	:	This subroutine can be completed by the user in order to access moment, displacement and plastic displacement information for possible permanent storage during the dynamic analysis.
BINARY	:	A function to extract nodal fixity information from a single integer word.
DFORCE	:	Sets up the incremental dynamic force vector and reduces it into a two-partitioned form.
DIGAC	:	Progressively supplies incremental ground accelerations at constant time intervals from a record stored in 'Berg' format on either a real or pseudo card reader.
DIMEOK	:	Checks actual dimensions allowed for against the dimensioning requirements of the frame under consideration and terminates the job if they are insufficient.
DSTIFF	:	Sets up the dynamic stiffness matrix, reduces it into a two-partition form ready for a backward elimination equation solver and recovers the static stiffness matrix from a sequential disk file.
DUCTIL	:	Calculates member-section ductilities based on the maximum rotation of the spring-hinge model and the input length over which the actual plastic hinge is allowed to form.
ECHØ	:	Prints out the input information about the analysis.
HQRW	:	Standard subroutine (Felippa, University of California) which provides the eigenvalues and -vectors of a real symmetric matrix.
INPUT	:	Reads, interpolates and checks (changing where necessary) the input information.
JUGGLE	:	Re-numbers and partitions the degrees of freedom of the frame; calculates the non-zero semi-bandwidths of the stiffness matrices.
MCURV	:	Controls the moment-curvature and axial load-displacement relationships for a member.
MFORCE	:	Given the incremental displacements of the nodes at both ends of a member it calculates the incremental member forces (in member sign convention).

MMASS : Calculates the member mass matrix from a mass/unit length.  
 MØDES : Calculates (or reads) and prints the natural frequencies and mode shapes (where required); calculates the damping coefficients from the lowest two natural frequencies.  
 MØTION : Controls the dynamic analysis.  
 MSTIFF : Forms the member stiffness in the frame co-ordinate system; forms the member to frame co-ordinate transformation matrix.  
 ØUTPUT : Provides a complete printout of the state of the frames moments and displacements for all nodes and members.  
 PDATE : A machine-dependent subroutine for providing the Julian date in 5A4 format.  
 PHØTØ : Draws a full page line-printer sketch of the frame, with the nodes optionally numbered.  
 PIKCHA : Draws a small sketch of frame on line-printer and shows positions of plasticity and/or slackness of bracing members.  
 PRINTR : Prints (on line-printer) selected moments, forces, rotations and displacements at the desired interval throughout the history of the dynamic analysis.  
 RAMØSG : Solves, iteratively, the Ramberg-Osgood function for a given curvature.  
 READR : Free-format reading routine - (A.J. Carr, University of Canterbury, 1971).  
 RECØV : Recovers the incremental displacements from the solution to the partitioned equations.  
 STATAN : Controls the initial static analysis of the frame.  
 SYMSØL : In-core equation solver for case where the matrix is stored as a vector, the upper band only being stored diagonal by diagonal - each diagonal being shorter than the previous.  
 SYMS8L : Same as SYMSØL except that the upper rectangular band is stored as an array (e.g. the principal diagonal forms the first column of the array).  
 TMASS : Forms the total mass matrix, either as a lumped mass diagonal or an upper triangular consistent matrix (stored as a vector).  
 TSTIFF : Forms the total stiffness matrix (partitioned - with the upper triangle alone stored as a vector).  
 YIELD : Provides the appropriate yield moments for a section - interrogates the moment/axial load interaction curve for a column.

The inter-relation of the subroutines is shown in figure C-1.

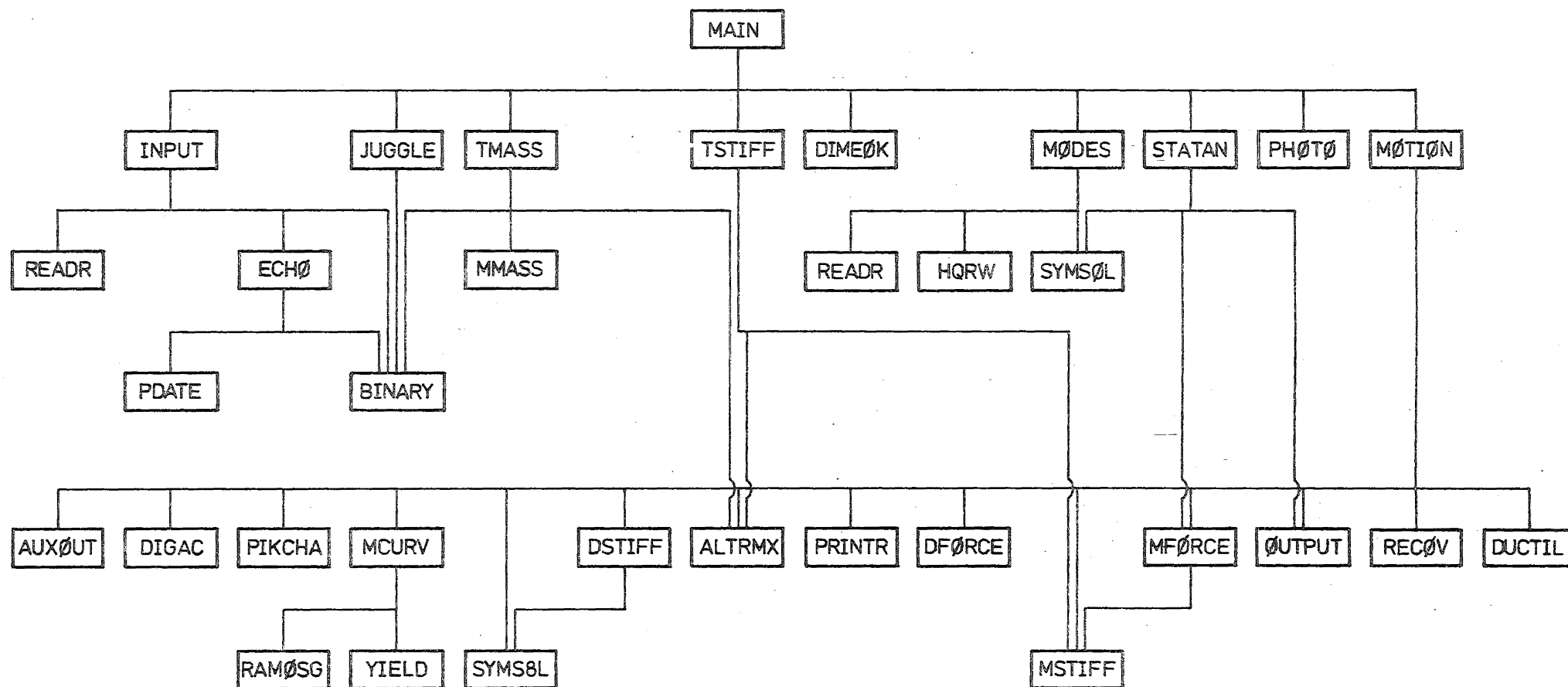


FIGURE C-1: SUBROUTINE STRUCTURE OF PROGRAM.

APPENDIX D

COMPUTER PROGRAM LISTING

FORTRAN IV LISTING OF THE INELASTIC FRAME DYNAMIC ANALYSIS  
COMPUTER PROGRAM - AS RUN ON A BURROUGHS' B6718 COMPUTER



\*\*\*\*\*

A PROGRAM FOR THE DYNAMIC ANALYSIS OF TWO-DIMENSIONAL INELASTIC  
FRAMES SUBJECTED TO GROUND EXCITATION RECORDS.

WRITTEN BY RICHARD D. SHARPE,  
C/- DEPARTMENT OF CIVIL ENGINEERING,  
UNIVERSITY OF CANTERBURY,  
PRIVATE BAG,  
CHRISTCHURCH, NEW ZEALAND.

IT IS NOT PURPORTED THAT THIS PROGRAM HAS BEEN DEVELOPED TO A  
STAGE AT WHICH IT CAN BE OFFERED AS A COMMERCIAL PACKAGE - FULLY  
TESTED AND GUARANTEED FREE OF LATENT FAULTS.  
AS IT IS AN EXPERIMENTAL PROGRAM, THE AUTHOR WOULD BE PLEASED TO  
BE NOTIFIED OF ITS USE AND WILL ENDEAVOUR, WHERE POSSIBLE, TO  
ADVISE INTERESTED PERSONS ON ITS CORRECT USE. IT IS RECOMMENDED  
THAT BOTH CHAPTER FOUR AND APPENDIX C BE READ THOROUGHLY BEFORE  
AN ATTEMPT IS MADE TO CARRY OUT AN ANALYSIS.

THE VERSION LISTED BELOW IS DESIGNED TO RUN ON A BURROUGHS B6718.

THE FRAME CO-ORDINATE SYSTEM USED IS A RIGHT-HANDED CARTESIAN  
ONE IN WHICH --  
X IS POSITIVE TO THE RIGHT HORIZONTAL,  
Y UPWARDS VERTICAL,  
Z ANTI-CLOCKWISE ROTATION, IN THAT ORDER.

\*\*\*\*\*

MAIN PROGRAM UNIT.

\*\*\*\*\*

```

COMMON/ CONST/ NNP,NMEM,NE,NEQ,NREQ,NSEQ,NBW1,NBW2,NBW3,NTYPE
1 / DIME/ ND1,ND2,ND3,ND4,NPROP,MSSMA,NM,NADOF,NSDOF,MMMA,
2 MDSMA,MTSMA
3 /SYSTEM/ INP,LNP,IPCH,NDS1,NDS2,NDS3
4 / ECCO/ IPNODE,IPDATA,IPNF,IPANAL,IPLAS,IPVERT,IPHO,
5 IPVM,IPHL,IPMASS,IPCONM

```

```

1 DIMENSION S(6000),DYSTIF(6000),PROPS(30,20),
2 COORD(100,2),NPFIX(100),CUP(100,3),S12(6000),
3 FLEX(200,200),W(200),W1(200),W2(200),W3(200),W4(201),
4 W5(200),W6(200),MASS(6000),DR(200),SD(200),TSD(200),
5 XTSD(200),JUG(200),SDE(200),ACC(200),VEL(200),AA(200),
6 LUMAS(200),AXIAL(100),MTYPE(100),AMOM(100,2),
7 MEMNP(100,2),XAXIAL(100),XAMOM(100,2),C(100,6),
CMAX(100,6),F(100,6),E(200,200)

```

```

INTEGER CUP
LOGICAL W6
REAL LUMAS,MASS

```

```

INP = 5
LNP = 6
IPCH = 7
NDS1 = 1
NDS3 = 3
ND1 = 100
ND2 = 100
ND3 = 30
ND4 = 200
NPROP = 20
MSSMA = 6000
NM = 200
NADOF = 200
NSDOF = 200

```

```

MMMA = 6000
MDSMA = 6000
MTSMA = 6000

```

WHERE ...

```

INP = SYSTEM NUMBER FOR THE CARD READER.
LNP = FOR THE LINE-PRINTER.
IPCH = FOR THE CARD-PUNCH.
NDS1 = OF A SEQUENTIAL DATA-SET.
NDS3 = OF A SEQUENTIAL DATA-SET.
ND1 = DIMENSION FOR NO. OF NODES.
ND2 = NO. OF MEMBERS.
ND3 = NO. OF TYPES OF MEMBERS.
ND4 = FLEXIBILITY MATRIX.
NPROP = NO. OF PROPERTIES/TYPE.
MSSMA = STIFFNESS MATRIX.
NM = NUMBER OF MODE SHAPES.
NADOF = NUMBER OF APPARENT DEGREES OF FREEDOM.
NSDOF = NUMBER OF ACTUAL STATIC D.O.F.'S.
MMMA = THE CONSISTENT MASS MATRIX.
MDSMA = THE DYNAMIC STIFFNESS MATRIX.
MTSMA = THE TRANSFORMED DYNAMIC STIFFNESS MATRIX.

```

THE COMPOSITION OF THE DIMENSION STATEMENT IS, THEREFORE ...

```

1 DIMENSION S(MSSMA),DYSTIF(MDSMA),PROPS(ND3,NPROP),
2 COORD(ND1,2),NPFIX(ND1),CUP(ND1,3),S12(MSSMA),
3 FLEX(ND4,ND4),W(ND4),W1(ND4),W2(ND4),W3(ND4),W4(ND4+1),
4 W5(ND4),W6(ND4),MASS(MMMA),DR(NSDOF),SD(NSDOF),
5 TSD(NSDOF),XTSD(NSDOF),JUG(NSDOF),SDE(NSDOF),ACC(NSDOF),
6 VEL(NSDOF),AA(NSDOF),LUMAS(NSDOF),AXIAL(ND2),MTYPE(ND2),
7 AMOM(ND2,2),MEMNP(ND2,2),XAXIAL(ND2),XAMOM(ND2,2),
CMAX(ND2,6),F(ND2,6),E(ND4,NM)

```

POSSIBLE EQUIVALENCING - IF NECESSARY, THAT AREA USED BY FLEX,W,  
W1,W2,W3,W4,W5,W6 CAN BE SHARED WITH  
DYSTIF,AA,ACC,VEL,SD,TSD,SDE,XTSD,XAXIAL,  
XAMOM,P,PMAX.  
ALSO, TSD CAN BE EQUIVALENCED TO CUP.

SET DIMENSIONS OF (DYSTIF) AND (S12) TO MSSMA UNTIL VALUES CAN BE  
ACQUIRED FROM 'DIMENSIONS CHECK' PRINTOUT.

IF(IPANAL.GT.1) REWIND NDS1

READ, EDIT AND PRINT DATA.  
CALL INPUT (COORD,PROPS,LUMAS,DR,MEMNP,MTYPE,F,CUP,NPFIX,AMOM,  
AXIAL)

IF(IPHOTO.EQ.0) GO TO 2

PRINT APPROXIMATE PICTURE OF FRAME.  
CALL PHOTO (COORD,MEMNP)

2 CONTINUE

IF(IPANAL.EQ.0) GO TO 4

SET UP THE UNCONDENSED LUMPED MASS MATRIX.  
CALL TMASS (MASS,LUMAS,JUG,MEMNP,MTYPE,F,COORD,PROPS,NPFIX,1)

PRODUCE A SHUFFLING VECTOR FOR THE NUMBERING OF THE D'S OF FREEDOM  
CALL JUGGLE (LUMAS,NPFIX,MEMNP,JUG,CUP)

CHECK DIMENSIONING REQUIREMENTS AND TERMINATE IF INSUFFICIENT.  
CALL DIMEOK

SET UP THE STATIC STIFFNESS MATRIX (S).

```

C CALL TSTIFF (S,JUG,MEMNP,MTYPE,COORD,PROPS,F)
C
C II=3
C IF(IPANAL.EQ.0) GO TO 10
C IF(IPANAL.EQ.1) GO TO 9
C
C SAVE THE STATIC STIFFNESS MATRIX IN A SEQUENTIAL DATA SET.
C
C II=2
C IF(IPNF.EQ.1) II=3
C NS=(NBW2*(2*NE+1-NBW2))/2
C WRITE(NDS1) (S(I),I=1,NS)
C REWIND NDS1
C
C FIND THE CONDENSED MASS MATRICES.
C 9 CALL TMASS (MASS,LUMAS,JUG,MEMNP,MTYPE,F,COORD,PROPS,NPFI,2)
C
C FIND THE NATURAL MODES OF THE FRAME.
C CALL MODES (S,FLEX,MASS,TSD,JUG,E,W,W1,W2,W3,W4,W5,W6)
C IF(IPANAL.EQ.1) GO TO 50
C
C 10 IS=0
C
C CARRY OUT A STATIC ANALYSIS WITH THE DEAD-LOADS.
C CALL STATAN (S,SD,TSD,DR,JUG,MTYPE,MEMNP,COORD,F,PROPS,AXIAL,
C 1 AMOM,II,IS)
C
C IF(IPANAL.EQ.0) GO TO 50
C
C READ(NDS1) (S(I),I=1,NS)
C IF(IPLAS.NE.0) REWIND NDS1
C
C CARRY OUT A DYNAMIC ANALYSIS.
C 15 CALL MOTION (COORD,DR,SD,PROPS,S,DYSTIF,ACC,VEL,AA,TSD,SDE,
C 1 MASS,AXIAL,AMOM,C,CMAX,MEMNP,MTYPE,JUG,S12,
C 2 XAXIAL,XAMOM,XTSD,F,IS)
C
C 50 CALL EXIT
C END
C
C SUBROUTINE ALTRMX (S,SM,JUG,NODE,N)
C *****
C SUBROUTINE TO ADD OR SUBTRACT MEMBER STIFFNESSES FROM THE TOTAL
C STIFFNESS MATRIX.
C THE TOTAL STIFFNESS MATRIX IS STORED AS THE UPPER BAND, IN VECTOR
C FORM, LEADING DIAGONAL FIRST.
C *****
C COMMON/ CONST/ NNP,NMEM,NE,NEQ,NREQ,NSEQ,NBW1,NBW2
C
C DIMENSION S(1),SM(6,6),NODE(2),JUG(1)
C
C THE FOLLOWING POSITION FUNCTION WORKS ONLY FOR J.GE.I .
C LOC(I,J)=I+(J-I)*(1+I-J+2*NE)/2
C
C N IS +1 OR -1 DEPENDING ON WHETHER THE MEMBER STIFFNESS IS TO BE
C ADDED OR SUBTRACTED.
C
C DO 10 II=1,2
C NOD1=(NODE(II)-1)*3
C DO 10 JJ=1,3
C NF1=JUG(NOD1+JJ)
C IF(NF1.EQ.0) GO TO 10

```

```

C I=(II-1)*3+JJ
C
C DO 9 KK=1,2
C NOD2=(NODE(KK)-1)*3
C DO 9 LL=1,3
C NF2=JUG(NOD2+LL)
C J=(KK-1)*3+LL
C
C IF(NF2.EQ.0.OR.NF1.GT.NF2) GO TO 9
C IJ=LOC(NF1,NF2)
C S(IJ)=S(IJ)+N*SM(I,J)
C 9 CONTINUE
C 10 CONTINUE
C
C RETURN
C END
C
C SUBROUTINE AUXOUT (TIME,AXIAL,AMOM,C,CMAX,TSD,K)
C *****
C DUMMY SUBROUTINE TO REPLACE A NON-EXISTANT SUBROUTINE.
C
C THE USER MAY WRITE HIS OWN SUBROUTINE TO REPLACE THIS ONE IN ORDER
C TO OUTPUT TO A NOMINATED DEVICE A HISTORY (AT A SELECTED TIME
C INCREMENT) OF MEMBER AXIAL FORCES, MOMENTS, CURVATURES, MAXIMUM
C CURVATURES TO DATE AND TOTAL FRAME DISPLACEMENTS. 'K' IS A COUNTER
C WHICH IS UPDATED BY THE SUBROUTINE 'MOTION'.
C *****
C DIMENSION AXIAL(1),AMOM(1,1),C(1,1),CMAX(1,1),TSD(1)
C RETURN
C END
C
C FUNCTION BINARY (NUM,I)
C *****
C THIS FUNCTION ACCESSES NODAL FIXITY CONDITIONS STORED IN A BINARY
C FORM IN AN INTEGER VECTOR.
C *****
C INTEGER BINARY
C N=NUM/2**I
C N=N*2
C NN=NUM/2**(I-1)
C BINARY=NN-N
C RETURN
C END
C
C SUBROUTINE DFORCE (DACC,DACCV,A,ACC,VEL,DR,S,S12,AMASS,JUG,IT)
C *****
C SUBROUTINE TO FORM THE INCREMENTAL FORCING FUNCTION.
C VECTOR (A) PROVIDES WORKING AREA ONLY, OF LENGTH NE.
C *****
C COMMON / CONST/ NNP,NMEM,NE,NEQ,NREQ,NSEQ,NBW1,NBW2
C COMMON / INTEG/ D1,D2,D3,D4

```

```

C DIMENSION A(1),ACC(1),VEL(1),DR(1),AMASS(1),S(1),JUG(1),S12(1)
C LOC(I,J)=I+((J-I)*(1+I-J+2*NE))/2
C LOK(I,J)=(J-1)*NREQ+(J*(J-1))/2+I
C NBW1 IS THE SEMI-BANDWIDTH OF THE MASS STIFFNESS MATRIX.
C NBW2
C IF(IT.EQ.2) GO TO 10
C D5=DACC
C D6=DACC*V
C DO 1 I=1,NNP
C DO 1 J=1,3
C IJ=(I-1)*3+J
C JIJ=JUG(IJ)
C IF(JIJ.EQ.0) GO TO 1
C A(JIJ)=0.0
C IF(J.EQ.1) A(JIJ)=D5
C IF(J.EQ.2) A(JIJ)=D6
C 1 CONTINUE
C DO 2 I=1,NE
C 2 A(I)=A(I)+D1*VEL(I)+D2*ACC(I)
C DO 5 I=1,NE
C D7=DR(I)
C DO 4 J=1,NE
C IF(IABS(J-I)+1.GT.NBW1) GO TO 3
C IF(J.GT.I) D6=AMASS(LOC(I,J))
C IF(J.LE.I) D6=AMASS(LOC(J,I))
C GO TO 4
C 3 D6=0.0
C 4 D7=D7-D6*A(J)
C 5 DR(I)=D7
C DO 6 I=1,NE
C 6 A(I)=D3*VEL(I)+D4*ACC(I)
C DO 9 I=1,NE
C D7=0.0
C DO 8 J=1,NE
C IF(IABS(J-I)+1.GT.NBW2) GO TO 7
C IF(J.GT.I) D6=S(LOC(I,J))
C IF(J.LE.I) D6=S(LOC(J,I))
C GO TO 8
C 7 D6=0.0
C 8 D7=D7-D6*A(J)
C 9 DR(I)=DR(I)+D7
C TRANSFORM 'DR' FOR TWO-PARTITION SOLUTION.
C 10 IF(NSEQ.EQ.0) RETURN
C DO 12 II=1,NSEQ
C K=NE-II
C L=K+1
C MM=NSEQ+1-II
C D7=S12(LOK(MM+NREQ,MM))
C DO 11 I=1,K
C D6=S12(LOK(I,MM))
C 11 DR(I)=DR(I)-D6*DR(L)
C 12 DR(L)=DR(L)/D7
C RETURN
C END

```

```

C SUBROUTINE DIGAC (*)
C *****
C SUBPROGRAM TO READ DIGITIZED ACCELERATION RECORDS
C AND SUPPLY INCREMENTALLY INTERPOLATED ACCELERATIONS.
C *****
C COMMON / DIGIT/ DACC,TIME,INP,LNP,KC,IT,ICC,DACC2,PP,T(5),G(5)
C 1 /EQUAKE/ DT,IPAD,ISTART
C IF(KC.NE.0) GO TO 2
C ICC=ISTART
C KC=0
C PP=0
C T(5)=0.0
C G(5)=0.0
C IT=5
C 2 KC=KC+1
C IF(TIME.GT.T(IT+1).OR.KC.EQ.1) GO TO 3
C DACC=DACC2
C PP=PP+DACC
C RETURN
C 3 IF(IT.GE.4) GO TO 4
C IT=IT+1
C GO TO 10
C 4 IT=1
C G(1)=G(5)
C T(1)=T(5)
C READ, STORE + CHECK SEQUENCE OF NEXT RECORD CARD.
C 5 READ(INP,6,END=13) ISEQ,(T(I),G(I),I=2,5)
C 6 FORMAT(I3,4(F8.4,F9.6))
C IF(ISEQ.EQ.ICC) GO TO 9
C K=0
C K=K+1
C WRITE(LNP,8) ISEQ,INP,ICC
C 8 FORMAT(1H0,22HDIGITIZED E/Q CARD NO.,I3,9H ON SYS00,I1,18H IS WHER
C 1E CARD NO.,I3,11H SHOULD BE.)
C IF(K.EQ.5) RETURN 1
C GO TO 5
C 9 ICC=ICC+1
C IF(KC.NE.1) GO TO 10
C T(1)=T(2)-IPAD*DT
C TIME=T(1)+DT
C IF(IPAD.EQ.0) PP=G(2)
C 10 TT=TIME-T(IT)
C TS=T(IT+1)-T(IT)
C IF(.NOT.TS.GT.0.0.OR.TIME.GT.T(IT+1)) GO TO 3
C GS=G(IT+1)-G(IT)
C GG=GS*TT/TS
C DACC2=GS*DT/TS
C DACC =G(IT)+GG-PP
C PP=G(IT)+GG
C RETURN
C 13 RETURN 1
C END

```

```

SUBROUTINE DIMEOK
*****
SUBROUTINE TO CHECK DIMENSIONING REQUIREMENTS AGAINST ACTUAL
DIMENSIONS AND TO DETERMINE WHETHER TO PROCEED WITH THE ANALYSIS.
*****
COMMON / CONST/ NNP,NMEM,NE,NEQ,NREQ,NSEQ,NBW1,NBW2,NBW3,NTYPE
1 / DIME/ ND1,ND2,ND3,ND4,NPROP,MSSMA,NM,NADOF,NSDOF,MMMA,
2 / ECCO/ MDSMA,MTSMA
3 / IPDATA,IPNF,IPANAL,IPLAS,IPVERT,IPHOTO,
4 / IPVM,IPHL,IPMASS,IPCONM
5 / FREQ/ C1,C2,M
6 / SYSTEM/ INP,LNP

N=NBW3
NBW3=NBW2
NBW2=N

ND1, ND2, ND3, ND4, MSSMA, M, NADOF, NSDOF, MMMA, MDSMA, MTSMA,
ARE THE DIMENSIONING RESTRICTIONS ON THE NO. OF NODES, MEMBERS,
MEMBER TYPES, DYNAMIC D.O.F.'S, STATIC STIFFNESS MATRIX, MODE
SHAPES, APPARENT D.O.F.'S, STATIC D.O.F.'S, MASS MATRIX, DYNAMIC
STIFFNESS MATRIX, TRANSFORMED STIFFNESS MATRIX. M IS THE ACTUAL
NO. OF MODE SHAPES FOUND.
NBW1, NBW2, NBW3 ARE THE BANDWIDTHS OF THE MASS, STATIC STIFFNESS
AND DYNAMIC STIFFNESS MATRICES.

ISTOP=0
NDSMA=0
NTSMA=0
NMMA=0
NBW1=NBW3
IF(IPCONM.EQ.0) NBW1=1
NBW2=MAX0(NBW2,NBW3)
NSSMA=(NBW2*(2*NE+1-NBW2))/2
IF(IPANAL.EQ.0) GO TO 1
NMMA=(NBW1*(2*NE+1-NBW1))/2
IF(IPANAL.EQ.1) GO TO 1
NDSMA=NREQ*NBW3
NTSMA=NREQ*NSEQ+(NSEQ*NSEQ+NSEQ)/2

1 IF( NNP.GT. ND1) ISTOP=1
IF( NEQ.GT.NADOF) ISTOP=1
IF( NE.GT.NSDOF) ISTOP=1
IF( NMEM.GT. ND2) ISTOP=1
IF( NTYPE.GT. ND3) ISTOP=1
IF( NSSMA.GT.MSSMA) ISTOP=1
IF( IPANAL.EQ.0) GO TO 5
IF( M.GT. NM) ISTOP=1
IF( NREQ.GT. ND4) ISTOP=1
IF( NMMA.GT. MMMA) ISTOP=1
IF( IPANAL.EQ.1) GO TO 5
IF( NDSMA.GT.MDSMA) ISTOP=1
IF( NTSMA.GT.MTSMA) ISTOP=1

5 WRITE(LNP,10) NNP,ND1,NEQ,NADOF,NE,NSDOF,NREQ,ND4,NMEM,ND2,NTYPE,
1 ND3,NPROP,NPROP,M,NM,NSSMA,MSSMA,NDSMA,MDSMA,NTSMA,
2 MTSMA,NMMA,MMMA,NBW2,NBW3,NBW1
10 FORMAT(1H1,16HDIMENSIONS CHECK,44X,6HACTUAL,12X,9HALLOWABLE/1X,
1 16(1H-))/20X,15HNUMBER OF NODES,25X,16,13X,16//
2 20X,40HNUMBER OF APPARENT DEGREES OF FREEDOM ,16,13X,16//
3 20X,40HNUMBER OF STATIC DEGREES OF FREEDOM ,16,13X,16//
4 20X,40HNUMBER OF DYNAMIC DEGREES OF FREEDOM ,16,13X,16//
5 20X,17HNUMBER OF MEMBERS,23X,16,13X,16//
6 20X,22HNUMBER OF MEMBER TYPES,18X,16,13X,16//
7 20X,27HNUMBER OF PROPERTIES/MEMBER,13X,16,13X,16//
8 20X,32HNUMBER OF MODE SHAPES CALCULATED,8X,16,13X,16//

```

```

9 20X,28HSTATIC STIFFNESS MATRIX AREA,12X,16,13X,16//
A 20X,29HDYNAMIC STIFFNESS MATRIX AREA,11X,16,13X,16//
B 20X,34HTRANSFORMED DYNAMIC STIFFNESS AREA,6X,16,13X,16//
C 20X,16HMASS MATRIX AREA,24X,16,13X,16//32X,4(2H* )//
D 20X,34HSEMI-BANDWIDTH OF STATIC STIFFNESS,6X,16//
E 38X,17HDYNAMIC STIFFNESS,5X,16//
F 38X,11HMASS MATRIX,11X,16)

C IF(ISTOP.EQ.0) RETURN
C
C WRITE(LNP,21)
21 FORMAT(1H0,39(1H-),5X,44HALLOWABLE DIMENSIONS EXCEEDED - JOB ABORT
1ED.,5X,39(1H-))
C
C CALL EXIT
END

SUBROUTINE DSTIFF (S,SD,DYSTIF,S12,JUG,AMASS,A1,B1)
*****
SUBROUTINE TO SET UP THE DYNAMIC STIFFNESS MATRIX AND THEN REDUCE
IT TO A FORM SUITABLE FOR A TWO-PARTITIONED SOLUTION.
BEFORE EXITING, STIFFNESS MATRIX IS RE-READ FROM SEQUENTIAL D-S.
*****
COMMON /SYSTEM/ INP,LNP,IPCH,ND51
COMMON / CONST/ NNP,NMEM,NE,NEQ,NREQ,NSEQ,NBW1,NBW2,NBW3

DIMENSION S(1),SD(1),DYSTIF(NREQ,1),S12(1),JUG(1),AMASS(1)

LOC(I,J)=I+((J-I)*(1+I-J+2*NE))/2
LOK(I,J)=(J-1)*NREQ+(J*(J-1))/2+I

REWIND NDS1
NS=(NBW2*(2*NE+1-NBW2))/2

MASS MATRIX 'AMASS' IS ASSUMED TO BE IN CONDENSED FORM.

DO 3 I=1,NS
3 S(I)=S(I)*B1

IJ=(NBW1*(2*NE+1-NBW1))/2
DO 5 I=1,IJ
5 S(I)=S(I)+AMASS(I)*A1

IF(NSEQ.EQ.0) GO TO 50

NS12=LOK(NE,NSEQ)
DO 30 I=1,NS12
30 S12(I)=0.0
DO 40 KK=1,NSEQ
K=NE+1-KK
KM1=K-1
KS12=K-NREQ
SKK=S(LOK(K,K))
DO 40 J=1,KM1
CKJ=0.0
IF(K-J+1.LE.NBW2) CKJ=S(LOK(J,K))/SKK
DO 39 I=J,KM1
SIK=0.0
IF(K-I+1.LE.NBW2) SIK=S(LOK(I,K))
JI=LOK(J,I)
SJI=S(JI)
IF(CKJ.EQ.0.0.OR.SIK.EQ.0.0) GO TO 39
SJI=SJI-CKJ*SIK

```

```

      S(JI)=SJI
39 IF(I.GT.NREQ) S12(LOK(J,I-NREQ))=SJI
40 S12(LOK(J,KS12))=CKJ
   NI=NREQ+1
   DO 41 I=NI,NE
C   S12(LOK(I,I-NREQ))=S(LOC(I,I))
50 CONTINUE
   DO 52 I=1,NREQ
   DO 51 J=1,NBW3
   L=I+J-1
   IF(L.GT.NREQ) GO TO 52
51 DYSTIF(I,J)=S(LOC(I,L))
52 CONTINUE
C
C   CALL SYMS8L (NREQ,NBW3,DYSTIF,SD,NREQ,1)
C
C   READ(NDS1) (S(I),I=1,NS)
C   REWIND NDS1
C
C   RETURN
C   END

SUBROUTINE DUCTIL (MTYPE,MEMNP,COORD,CMAX,PROPS)
*****
SUBROUTINE TO CALCULATE AND PRINT THE MAXIMUM DUCTILITIES OR
PLASTIC DISPLACEMENTS FOR A MEMBER WHICH HAS HAD SOME PLASTIC
DEFORMATION.
DUCTILITIES ARE BASED ON HINGE LENGTHS INPUT AS DATA.
*****
COMMON / CONST/ NNP,NMEM
/ DIME/ ND1,ND2,ND3
/ ECCO/ DUM(4),IPLAS,DAM(3),IPHL
/ SYSTEM/ INP,LNP
/ YIELDS/ PAX,P(6),YMP(2),YMN(2)
C
C   DIMENSION COORD(ND1,1),CMAX(ND2,1),PROPS(ND3,1),
C   MTYPE(1),MEMNP(ND2,1)
C
C   WRITE(LNP,2)
C   FORMAT(1H1,50X,30HMAXIMUM PLASTIC DISPLACEMENTS./51X,30(1H-))//
1 28X,5HEND 1,40X,5HEND 2,40X,5HAXIAL/
2 5X,6HMEMBER,7X,2(9HCURVATURE,7X,6HMOMENT,23X),9HEXTENSION,
3 6X,9HAX. FORCE/5X,6(1H-))
   DO 10 I=1,NMEM
   IF(CMAX(I,1).EQ.0..AND.CMAX(I,2).EQ.0..AND.CMAX(I,3).EQ.0.)GOTO 10
   WRITE(LNP,9) I,(CMAX(I,J),CMAX(I,J+3),J=2,3),CMAX(I,1),CMAX(I,4)
9  FORMAT(6X,I3,4X,1P2E15.5,2(15X,2E15.5))
10 CONTINUE
   IF(IPHL.EQ.0) GO TO 40
C
C   WRITE(LNP,15)
C   FORMAT(1H1,34X,62HMAXIMUM MEMBER DUCTILITIES - BASED ON REALISTIC
1 HINGE LENGTHS./35X,62(1H-))//
2 28X,5HEND 1,40X,5HEND 2,40X,5HAXIAL/
3 5X,6HMEMBER,7X,2(9HDUCTILITY,7X,6HMOMENT,23X),9HDUCTILITY,
4 6X,9HAX. FORCE/5X,6(1H-))
   DO 35 I=1,NMEM
   N=MTYPE(I)
C
C   THIS SECTION CONSIDERS ALL COLUMNS TO HAVE THEIR MAXIMUM CURVATURE
C   AT THEIR BALANCED-FAILURE AXIAL LOAD.
C
C   ONE=1.

```

```

C   IF(IPLAS.EQ.3) ONE=0.
C
C   DO 16 K=1,6
16 P(K)=PROPS(N,13+K)
   PAX=P(4)
   CALL YIELD
   DO 21 J=2,3
   JM1=J-1
   IF(CMAX(I,J)) 17,21,18
17 YM=YMN(JM1)
   GO TO 19
18 YM=YMP(JM1)
19 IF(YM.NE.0.) GO TO 20
   CMAX(I,J)=0.
   GO TO 21
20 CMAX(I,J)=ONE+CMAX(I,J)*PROPS(N,6)*PROPS(N,3)/YM
21 CONTINUE
   IF(CMAX(I,1)) 22,34,23
22 P19=P(5)
   GO TO 24
23 P19=P(6)
24 IF(P19.EQ.0.) GO TO 34
   XL=COORD(MEMNP(I,1),1)-COORD(MEMNP(I,2),1)
   YL=COORD(MEMNP(I,1),2)-COORD(MEMNP(I,2),2)
   CL=SQRT(XL*XL+YL*YL)-PROPS(N,4)-PROPS(N,5)
   CMAX(I,1)=1.0+CMAX(I,1)*PROPS(N,6)*PROPS(N,1)/(CL*P19)
34 IF(CMAX(I,1).LE.ONE.AND.CMAX(I,2).LE.ONE.AND.CMAX(I,3).LE.ONE)
1 GO TO 35
   WRITE(LNP,9) I,(CMAX(I,J),CMAX(I,J+3),J=2,3),CMAX(I,1),CMAX(I,4)
35 CONTINUE
C
C   RETURN
C   END

SUBROUTINE ECHO (COORD,NPFX,CUP,MEMNP,MTYPE,PROPS,DR,MASS,AMOM,
1 AXIAL)
*****
SUBROUTINE TO PRINT ECHO OF ALL DATA ON LINE-PRINTER.
*****
COMMON/ANSWER/ NXT,NYT,NZT,M1T,M2T,AXT,NX,NY,NZ,M1,M2,AX
1 / CONST/ NNP,NMEM,NE,NEQ,NREQ,NSEQ,NBW1,NBW2,NBW3,NTYPE
2 / DIME/ ND1,ND2,ND3,ND4,NPROP
3 / ECCO/ IPNODE,IPDATA,IPNF,IPANAL,IPLAS,IPVERT,IPHOTO,
4 IPVM,IPHL,IPMASS,IPCONM
5 /EQUAKE/ DT,IPAD,ISTART,TIME,TR,GFACTR,GRAV,TOR,B,KP,KMF,KPA
6 / FREQ/ C1,C2,M
7 /LABELS/ DESCR,EARTHQ,EARTVQ,OTHER
8 /SYSTEM/ INP,LNP,IPCH,NDS1,NDS2,NDS3
C
C   DIMENSION COORD(ND1,1),PROPS(ND3,1),MASS(1),AMOM(ND2,1),AXIAL(1),
1 DESCR(20),EARTHQ(20),EARTVQ(20),OTHER(20),DR(1),NODE(3),
2 NX(30),NY(30),NZ(30),M1(30),M2(30),AX(30),YN(4),DATE(5)
C
C   REAL MASS
C   INTEGER MEMNP(ND2,1),MTYPE(1),CUP(ND1,1),NPFX(1),AX,AXT,BINARY
C   DATA YN(1)/3H NO/,YN(2)/3HYES/,YN(3)/3HYES/,YN(4)/3H NO/
C
C   EQUIVALENCE (IDUM1,RDUM1),(IDUM2,RDUM2),(IDUM3,RDUM3)
C
C   CALL PDATE(1)
C   WRITE(LNP,2) DATE
2  FORMAT(1H1,51X,30HTWO-DIMENSIONAL FRAME ANALYSIS/52X,30(1H-))//
1 35X,52H.D.SARPE, UNIVERSITY OF CANTERBURY, CHRISTCHURCH, ,

```

```

2      11HNEW ZEALAND/35X,63(1H-)//25H TYPE OF ANALYSIS - ELAST,
3      85X,5A4)
4      IF(IPLAS.EQ.0) WRITE(LNP,3)
5      IF(IPLAS.GT.0) WRITE(LNP,4)
6      FORMAT(1H+,24X,2HIC)
7      FORMAT(1H+,24X,9H0-PLASTIC,9X,5HWITH )
8      IF(IPANAL.EQ.0) WRITE(LNP,5)
9      IF(IPANAL.EQ.1) WRITE(LNP,6)
10     IF(IPANAL.EQ.2) WRITE(LNP,7)
11     FORMAT(1H+,34X, 6HSTATIC)
12     FORMAT(1H+,34X,30HDETERMINATION OF NATURAL MODES)
13     FORMAT(1H+,34X, 7HDYNAMIC)
14     IF(IPANAL.EQ.1.OR.IPLAS.EQ.0) GO TO 11
15     IF(IPLAS.EQ.1) WRITE(LNP,8)
16     IF(IPLAS.EQ.2) WRITE(LNP,9)
17     IF(IPLAS.EQ.3) WRITE(LNP,10)
18     FORMAT(1H+,47X,36HELASTIC/PERFECTLY-PLASTIC HYSTERESIS)
19     FORMAT(1H+,47X,20HBI-LINEAR HYSTERESIS)
20     FORMAT(1H+,47X,25HHRAMBERG-OSGOOD HYSTERESIS)
21     WRITE(LNP,12) DESCR
22     FORMAT(6HOF FRAME,12X,2H- ,20A4)
C
23     IF(IPANAL.LT.2) GO TO 17
24     WRITE(LNP,13) EARTHQ
25     FORMAT(20HORIZONTAL E/Q - ,20A4)
26     WRITE(LNP,14)
27     FORMAT(20HVERTICAL E/Q - )
28     IF(IPVERT.EQ.0) WRITE(LNP,15)
29     FORMAT(1H+,19X,4HNONE)
30     IF(IPVERT.GT.0) WRITE(LNP,16) EARTVQ
31     FORMAT(1H+,19X,20A4)
C
32     WRITE(LNP,18) OTHER
33     FORMAT(9HOTHIS RUN,9X,2H- ,20A4)
34     WRITE(LNP,19) NNP,NEQ,NMEM,NTYPE
35     FORMAT(11H INPUT DATA,9X,15HNUMBER OF NODES,25X,I6,16X,
36     40HNUMBER OF APPARENT DEGREES OF FREEDOM ,I6/I1X,10(1H-)/
37     20X,17HNUMBER OF MEMBERS,23X,I6,16X,26HNUMBER OF MEMBER TYPE
38     14X,I6)
39     IF(IPANAL.GT.0) WRITE(LNP,20) C1,GRAV,C2,M
40     FORMAT(2(32X,4(2H* ),22X)//20X,
41     33HPERCENT CRIT. DAMPING IN 1ST MODE,7X,F6.2,16X,
42     22HLOCAL VALUE OF GRAVITY,18X,F6.2//
43     20X,33HPERCENT CRIT. DAMPING IN 2ND MODE,7X,F6.2,16X,
44     30HNUMBER OF MODE SHAPES REQUIRED,10X,I6)
45     IF(IPANAL.LE.1) GO TO 25
C
46     WRITE(LNP,21) GFACTR,IPAD,TR,ISTART,DT,B
47     FORMAT(2(32X,4(2H* ),22X)//20X,
48     31HEARTHQUAKE MAGNIFICATION FACTOR,9X,F6.3,16X,
49     38HNO. OF TIME-STEPS BEFORE 'ZERO' OF E/Q,18//
50     20X,37HLENGTH OF E/Q RECORD TO BE RUN (SECS),F9.2,16X,
51     30HSEQUENCE NO. OF FIRST E/Q CARD,10X,I6//2(32X,4(2H* ),22X)
52     //20X,32HINVERSE OF INTEGRATION TIME-STEP,8X,F6.1,16X,
53     23HVALUE OF NEWMARK'S BETA,16X,F7.5)
54     IF(TOR.NE.DT) WRITE(LNP,22) TOR
55     FORMAT(20X,29HINVERSE OF WILSON'S TIME-STEP,11X,F6.1)
56     WRITE(LNP,23) KP,KMF
57     FORMAT(2(32X,4(2H* ),22X)//20X,
58     37HNO. OF TIME-STEPS BETWEEN PRINT-OUTS ,I9,16X,
59     38HNO. OF TIME-STEPS BETWEEN FORCE CALCS.,I8)
60     IF(KPA.NE.0) WRITE(LNP,24) KPA
61     FORMAT(20X,40HNO. OF TIME-STEPS BETWEEN AUXIL. OUTPUT ,I6)
C
62     WRITE(LNP,26) YN(IPDATA+1),YN(IPHOTO+1)
63     FORMAT(2(32X,4(2H* ),22X)//20X,
64     24HPRINT ECHO-CHECK OF DATA,19X,A3//20X,
65     22HPRINT PICTURE OF FRAME,21X,A3)
66     IF(IPHOTO.NE.0) WRITE(LNP,27) YN(IPNODE+1)

```

```

27     FORMAT(1H+,81X,23HNUMBER NODES ON PICTURE,20X,A3)
28     IF(IPANAL.EQ.0) GO TO 40
C
29     WRITE(LNP,28) YN(IPNF+1)
30     FORMAT(20X,35HREAD, NOT CALCULATE, NATURAL FREQS.,8X,A3)
31     IF(IPLAS.NE.0) WRITE(LNP,29) YN(IPHL+1)
32     FORMAT(1H+,81X,34HDUCTILITIES BASED ON HINGE-LENGTHS,9X,A3)
33     WRITE(LNP,30) YN(IPMASS+1),YN(IPCONM+1)
34     FORMAT(20X,31HINCLUDE DISTRIBUTED MEMBER MASS,12X,A3,16X,
35     29HCONSISTENT LUMPED MASS MATRIX,14X,A3)
36     IF(IPLAS.NE.0) WRITE(LNP,31) YN(IPVM+3)
37     FORMAT(20X,37HCHECK VERTICAL MEMBERS FOR PLASTICITY,6X,A3)
38     IF(IPANAL.EQ.1) GO TO 40
C
39     WRITE(LNP,33) (NX(I),I=1,NXT)
40     FORMAT(10HOPRINT-OUT/1X,9(1H-)/22HODISPLACEMENT OF - X ,30I3)
41     WRITE(LNP,34) (NY(I),I=1,NYT)
42     FORMAT(14H NODES (NODES)/18X,4H- Y ,30I3)
43     WRITE(LNP,35) (NZ(I),I=1,NZT)
44     FORMAT(18X,4H- OZ/1H+,19X,2H- ,30I3)
45     WRITE(LNP,36) (M1(I),I=1,M1T)
46     FORMAT(22HOMEMBER FORCES - M1,30I3)
47     WRITE(LNP,37) (M2(I),I=1,M2T)
48     FORMAT(10H (MEMBERS)/18X,4H- M2,30I3)
49     WRITE(LNP,38) (AX(I),I=1,AXT)
50     FORMAT(18X,4H- AX,30I3)
C
51     IF(IPDATA.EQ.0) RETURN
C
52     WRITE(LNP,41)
53     FORMAT(1H+,21X,17HPOSITION OF NODES,24X,11HNODE FIXITY,18X,
54     13HCOUPLED NODES/22X,17(1H-),24X,11(1H-),18X,13(1H-)//
55     6X,4HNODE,9X,8HX CO-ORD,7X,8HY CO-ORD,21X,11HX Y OZ,
56     19X,11HX Y OZ/1H+,71X,1H-,29X,1H-/6X,4(1H-)//)
57     DO 43 I=1,NNP
58     NFIX=NPFIX(I)
59     DO 42 J=1,3
60     NODE(J)=BINARY(NFIX,4-J)
61     WRITE(LNP,44) I,COORD(I,1),COORD(I,2)
62     IF(NODE(1).NE.0) WRITE(LNP,48) NODE(1)
63     IF(NODE(2).NE.0) WRITE(LNP,49) NODE(2)
64     IF(NODE(3).NE.0) WRITE(LNP,50) NODE(3)
65     IF(CUP(I,1).NE.0) WRITE(LNP,45) CUP(I,1)
66     IF(CUP(I,2).NE.0) WRITE(LNP,46) CUP(I,2)
67     IF(CUP(I,3).NE.0) WRITE(LNP,47) CUP(I,3)
68     FORMAT(6X,I3,8X,1PE11.4,4X,E11.4)
69     FORMAT(1H+,90X,I3)
70     FORMAT(1H+,95X,I3)
71     FORMAT(1H+,100X,I3)
72     FORMAT(1H+,60X,I3)
73     FORMAT(1H+,65X,I3)
74     FORMAT(1H+,70X,I3)
C
75     WRITE(LNP,51)
76     FORMAT(1H+,10X,2(8X,7HNODE AT)/5X,6HMEMBER,9X,5HEND 1,10X,5HEND 2,
77     11X,4HTYPE/5X,6(1H-)//)
78     WRITE(LNP,52) (I,MMNP(I,1),MEMNP(I,2),MTYPE(I),I=1,NMEM)
79     FORMAT(4(6X,I3,6X))
C
80     KH=0
81     DO 60 I=1,NTYPE
82     RDUM1=PROPS(I,9)
83     RDUM2=PROPS(I,10)
84     RDUM3=PROPS(I,11)
85     KH=KH+IDUM1+IDUM2+IDUM3
86     WRITE(LNP,63)
87     FORMAT(1H+,53X,28HMEMBER PROPERTIES TABLE (1)/54X,28(1H-)//21X,
88     5HAXIAL,10X,5HSHEAR,27X,16HEND BLOCK LENGTH,11X,7HYOUNG'S,
89     9X,5HSHEAR,7X,10HMASS (WT.)/6X,4HTYPE,11X,5H-AREA,10X,

```

```

3      5H-AREA,8X,8HM. OF I.,8X,6H-END 1,9X,6H-END 2,9X,7HMODULUS,
4      8X,7HMODULUS,7X,7H/LENGTH/6X,4H----/)
WRITE(LNP,64) I,(PROPS(I,J),J=1,8),I=1,NTYPE)
64     FORMAT(6X,I3,4X,1P3E15.4)
IF(KH.EQ.0.AND.IPLAS.EQ.0) GO TO 80

C
WRITE(LNP,65)
65     FORMAT(1H1,53X,28HMEMBER PROPERTIES TABLE (2)/54X,28(1H-)/
1       25X,11HPINNED ENDS,13X,7HBRACING,16X,
2       22H- INITIAL CONDITIONS -)
IF(IPLAS.NE.0) WRITE(LNP,66)
66     FORMAT(1H+,113X,13HHINGE LENGTHS)
WRITE(LNP,67)
67     FORMAT(6X,4HTYPE,10X,6H-END 1,9X,6H-END 2,8X,7H-MEMBER,11X,2HM1,
1       13X,2HM2,11X,5HAXIAL)
IF(IPLAS.NE.0) WRITE(LNP,68)
68     FORMAT(1H+,109X,6H-END 1,9X,6H-END 2)
WRITE(LNP,69)
69     FORMAT(6X,4H----/)
DO 72 I=1,NTYPE
RDM1=PROPS(I,9)
RDM2=PROPS(I,10)
RDM3=PROPS(I,11)
DO 70 J=1,NMEM
K=J
70     IF(MTYPE(J).EQ.I) GO TO 71
71     WRITE(LNP,73) I,YN(IDUM1+1),YN(IDUM2+1),YN(IDUM3+1),
1       AMOM(K,1),AMOM(K,2),AXIAL(K)
72     IF(IPLAS.NE.0) WRITE(LNP,74) PROPS(I,12),PROPS(I,13)
73     FORMAT(6X,I3,3(12X,A3),4X,1P3E15.4)
74     FORMAT(1H+,102X,1P2E15.4)
IF(IPLAS.EQ.0) GO TO 80
WRITE(LNP,75)
75     FORMAT(1H1,45X,44HMEMBER PROPERTIES TABLE - ULTIMATE STRENGTHS/
1       46X,44(1H-)/16X,15HMOM. FOR NO AX.,11X,2(7X,8HBALANCED),
2       6X,11HCOMPRESSION,6X,23HTENSION RAM-OSG 'R'/6X,4HTYPE,
3       7X,12HLOAD (OR M1),7X,4H(M2),10X,7HMOMENT ,3(7X,8HAX. LOAD)
4       ,19H OR BI-LIN FACT./6X,4H----/)
DO 76 I=1,NTYPE
76     WRITE(LNP,64) I,(PROPS(I,J),J=14,20)

C
80     WRITE(LNP,81)
81     FORMAT(1H1,30X,14HSTATIC LOADING,36X,
1       34HLUMPED MASS (WEIGHT UNITS) AT NODE/31X,14(1H-),36X,
2       34(1H-)//6X,4HNODE,9X,8HX D.O.F.,7X,8HY D.O.F.,6X,
3       9HMZ D.O.F.,22X,8HX D.O.F.,7X,8HY D.O.F.,6X,9HOZ D.O.F./1H+
4       107X,1H-//6X,4H----/)
DO 84 I=1,NNP
84     WRITE(LNP,85) I,(DR(I*3-3+J),J=1,3),(MASS(I*3-3+J),J=1,3)
85     FORMAT(6X,I3,4X,1P3E15.4,15X,3E15.4)

C
RETURN
END

```

SUBROUTINE HQRW (N,NM,M,G,E,V,A,B,P,W,Q,INT)

\*\*\*\*\*  
SUBROUTINE TO COMPUTE EIGENVALUES AND EIGENVECTORS OF A  
SYMMETRIC REAL MATRIX STORED AS A TWO-DIMENSIONAL ARRAY  
THIS ROUTINE IS COMPUTER DEPENDENT.  
PRECS=1.0E(-NDIG) WHERE NDIG IS THE NUMBER OF DECIMAL DIGITS OF  
ACCURACY IN A FLOATING-POINT WORD.  
BASE\*\*(ILIM+4) IS OF THE ORDER OF BUT DOES NOT EXCEED WORD SIZE  
WHERE BASE IS THE BASE TO WHICH THE MACHINE WORKS  
E.G. 2. FOR A BINARY COMPUTER.

```

C      HOV=BASE**(ILIM/2)
C      *****
C
C      DIMENSION G(NM,1), E(1), V(NM,1), A(1), B(1), P(1), W(1), Q(1)
REAL LAMBDA
LOGICAL INT(1)

C
IF (N.LE.0.OR.N.GT.NM) GO TO 1000
PRECS=1.0E-11
BASE = 2.0
ILIM=224
HOV=BASE**(ILIM/2)
B(1) = 0.
SQRT2 = SQRT(2.)
N1 = N - 1
DO 100 I = 1,N
E(I) = G(I,1)
IF (N-2) 900,280,110

C
C      TRI-DIAGONALIZE MATRIX G BY HOUSEHOLDERS PROCEDURE
C
110 DO 250 K = 2,N1
K1 = K - 1
KJ = K + 1
Y = G(K,K1)
SUM = 0.0
DO 120 I = KJ,N
SUM = SUM + G(I,K1)**2
120 IF (SUM.EQ.0.) GO TO 230
S = SQRT(SUM+Y**2)
B(K) = SIGN(S,-Y)
W(K) = SQRT(1.+ABS(Y)/S)
X = SIGN(1./S*W(K),Y)
DO 150 I = K,N
IF (I.GT.K) W(I) = X*G(I,K1)
P(I) = 0.
150 G(I,K1) = W(I)
DO 180 I = K,N
Y = W(I)
IF (Y.EQ.0.) GO TO 180
I1 = I + 1
DO 160 J = K,I
P(J) = P(J) + Y*G(I,J)
IF (I1.GT.N) GO TO 180
DO 170 J = I1,N
170 P(J) = P(J) + Y*G(J,I)
180 CONTINUE
190 X = 0.
DO 200 J = K,N
X = X + W(J)*P(J)
X = 0.5*X
DO 210 J = K,N
P(J) = X*W(J) - P(J)
DO 220 J = K,N
DO 220 I = J,N
220 G(I,J) = G(I,J) + P(I)*W(J) + P(J)*W(I)
GO TO 250
230 G(K,K1) = SQRT2
B(K) = -Y
DO 240 I = KJ,N
240 G(I,K) = -G(I,K)
250 CONTINUE
280 DO 290 I = 1,N
A(I) = G(I,I)
290 G(I,I) = E(I)
B(N) = G(N,N1)

C
C      GET EIGENVALUES OF TRI-DIAGONAL FORM BY KAHAN-VARAH Q-R METHOD
C

```

```

TOL = PRECS/(10.*FLOAT(N))
BMAX = 0.
TMAX = 0.
W(N+1) = 0.
DO 300 I = 1,N
  BMAX = AMAX1(BMAX,ABS(B(I)))
  TMAX = AMAX1(TMAX,ABS(A(I)),TMAX)
  SCALE = 1.0
  IF (BMAX.EQ.0.) GO TO 520
DO 310 I = 1,ILIM
  IF (SCALE*TMAX.GT.HOV) GO TO 320
310 SCALE = SCALE*BASE
320 DO 330 I = 1,N
  E(I) = A(I)*SCALE
330 W(I) = (B(I)*SCALE)**2
  DELTA = TMAX*SCALE*TOL
  EPS = DELTA**2
  K = N
  L = K
350 IF (L.LE.0) GO TO 460
  L1 = L - 1
  DO 360 I = 1,L
  K1 = K
  K = K - 1
360 IF (W(K1).LT.EPS) GO TO 380
380 IF (K1.NE.L) GO TO 400
  W(L) = 0.
  GO TO 350
400 T = E(L) - E(L1)
  X = W(L)
  Y = 0.5*T
  S = SQRT(X)
  IF (ABS(T).GT.DELTA) S = (X/Y)/(1.+SQRT(1.+X/Y**2))
  E1 = E(L) + S
  E2 = E(L1) - S
  IF (K1.NE.L1) GO TO 430
  E(L) = E1
  E(L1) = E2
  W(L1) = 0.
  GO TO 350
430 LAMBDA = E1
  IF (ABS(T).LT.DELTA.AND.ABS(E2).LT.ABS(E1)) LAMBDA = E2
  S = 0.
  C = 1.
  GG = E(K1)-LAMBDA
  GO TO 450
440 C = F/T
  S = X/T
  X = GG
  GG = C*(E(K1)-LAMBDA) - S*X
  E(K) = (X-GG) + E(K1)
450 IF (ABS(GG).LT.DELTA) GG = GG + SIGN(C*DELTA,GG)
  F = GG**2/C
  K = K1
  K1 = K + 1
  X = W(K1)
  T = X + F
  W(K) = S*T
  IF (K.LT.L) GO TO 440
  E(K) = GG + LAMBDA
  GO TO 350
460 DO 470 I = 1,N
470 E(I) = E(I)/SCALE
  Y = ISIGN(1,M)
  DO 500 L = 1,N1
  K = N - L
  DO 500 I = 1,K
  IF (Y*(E(I)-E(I+1)).GT.0.) GO TO 500
  X = E(I)

```

```

E(I) = E(I+1)
E(I+1) = X
500 CONTINUE
520 IF (M.EQ.0) GO TO 1000
C
C
C
COMPUTE EIGENVECTORS BY INVERSE ITERATION
NVEC = IABS(M)
IF (NVEC.GT.N) NVEC = N
F = SCALE/HOV
IF (BMAX*F.LT.PRECS) GO TO 830
DO 530 I = 1,N
  A(I) = A(I)*F
530 B(I) = B(I)*F
  SEP = 25.*TMAX*PRECS
  X1 = 0.
  X2 = SQRT2
  DO 800 NV = 1,NVEC
  IF (NV.EQ.1) GO TO 539
  IF (ABS(E(NV)-E(NV-1)).LT.SEP) GO TO 550
539 DO 540 I = 1,N
540 W(I) = 1.0
  GO TO 570
550 DO 560 I = 1,N
  X = AMOD(X1+X2,2.0)
  X1 = X2
  X2 = X
560 W(I) = X - 1.0
570 EV = E(NV)*F
  X = A(1) - EV
  Y = B(2)
  J = N1
  DO 600 I = 1,N1
  C = A(I+1) - EV
  S = B(I+1)
  IF (ABS(X).GE.ABS(S)) GO TO 580
  P(I) = S
  Q(I) = C
  INT(I) = .TRUE.
  Z = -X/S
  X = Y + Z*C
  IF (I.LT.N1) Y = Z*B(I+2)
  GO TO 600
580 IF (ABS(X).LT.TOL) X = TOL
  P(I) = X
  Q(I) = Y
  INT(I) = .FALSE.
  Z = -S/X
  X = C + Z*Y
  Y = B(I+2)
600 V(I,NV) = Z
  IF (ABS(X).LT.TOL) X = TOL
  NITER = 0
620 NITER = NITER + 1
  W(N) = W(N)/X
  SUM = W(N)**2
  DO 640 L = 1,N1
  I = N - L
  Y = W(I) - Q(I)*W(I+1)
  IF (INT(I)) Y = Y - B(I+2)*W(I+2)
  W(I) = Y/P(I)
640 SUM = SUM + W(I)**2
  S = SQRT(SUM)
  DO 660 I = 1,N
660 W(I) = W(I)/S
  IF (NITER.GE.2) GO TO 760
  DO 700 I = 1,N1
  Z = V(I,NV)
  IF (INT(I)) GO TO 680

```



```

      W(I+1) = W(I+1) + Z*W(I)
      GO TO 700
680  Y = W(I)
      W(I) = W(I+1)
      W(I+1) = Y + Z*W(I)
700  CONTINUE
      GO TO 620
730  L = J
      J = J - 1
      X = 0.
      DO 740 I = L,N
740  X = X + G(I,J)*W(I)
      DO 750 I = L,N
750  W(I) = W(I) - X*G(I,J)
760  IF (J.GT.1) GO TO 730
      DO 800 I = 1,N
800  V(I,NV) = W(I)
      DO 820 I = 1,N
820  A(I) = A(I)/F
      B(I) = B(I)/F
      GO TO 860
830  DO 850 NV = 1,NVEC
      DO 840 I = 1,N
840  V(I,NV) = 0.
850  V(NV,NV) = 1.0
860  DO 880 I = 2,N
      K = I - 1
      DO 880 J = 1,K
880  G(I,J) = G(J,I)
      GO TO 1000
900  V(1,1) = 1.0
      A(1) = E(1)
1000 RETURN
      END

```

```

      SUBROUTINE INPUT (COORD,PROPS,MASS,DR,MEMNP,MTYPE,F,CUP,NPFI,
1  AMOM,AXIAL)
      *****

```

```

      SUBROUTINE TO LOAD PROGRAM WITH DATA AND ECHO-PRINT IT.
      ALL INPUT IS FREE-FORMATTED UNDER CONTROL OF SUBROUTINE 'READR'.
      *****

```

```

      COMMON/ANSWER/ IANS
1  / CARD/ NSTOP,NTRAP,INFO
2  / CONST/ NNP,NMEM,NE,NEQ,NREQ,NSEQ,NBW1,NBW2,NBW3,NTYPE
3  / DIME/ ND1,ND2,ND3,ND4,NPROP
4  / ECCO/ IPNODE,IPDATA,IPNF,IPANAL,IPLAS,IPVERT,IPHOTO,
5  /EQUAKE/ DT,IPAD,ISTART,TIME,TR,GFACTR,GRAV,TOR,B,KP,KMF,KPA
6  / FREQ/ C1,C2,M
7  / LABELS/ DESCR,EARTHQ,EARTVQ,REASON
8  / SYSTEM/ INP,LNP,IPCH,NDS1,NDS2,NDS3
9

```

```

      DIMENSION COORD(ND1,1),PROPS(ND3,1),MASS(1),DR(1),DCORD(2),
1  AXIAL(1),AMOM(ND2,1),F(ND2,1),
2  DESCR(20),EARTHQ(20),EARTVQ(20),REASON(20),BLAB(60),
3  RRDR(20),IRDR(30),IANS(186),CI(4),INFO(80),
4  MEMNP(ND2,1),MTYPE(1),CUP(ND1,1),NPFI(1)

```

```

      REAL MASS
      INTEGER BINARY

```

```

1  EQUIVALENCE (EARTHQ(1),BLAB(1)),(EARTVQ(1),BLAB(21)),
      (REASON(1),BLAB(41)),(RDUM,IDUM)

```

```

      N.B. 'MASS' IS 'LUMAS' (I.E. LUMPED MASS VECTOR) OF MAINLINE.

```

```

      NSTOP=0
      NTRAP=1

```

```

      CALL READR(0,0,-1,RRDR,IRDR)
      REWIND NDS3
      WRITE(NDS3,1)(INFO(I),I=1,80)
      REWIND NDS3
      READ(NDS3,2)(DESCR(I),I=1,20)
1  FORMAT(80A1)
2  FORMAT(20A4)
      REWIND NDS3

```

```

      CALL READR(0,11,0,RRDR,IRDR)
      IPANAL=IRDR(1)
      IPDATA=IRDR(2)
      IPHOTO=IRDR(3)
      IPNODE=IRDR(4)
      IPLAS=IRDR(5)
      IPMASS=IRDR(6)
      IPCONM=IRDR(7)
      IPNF=IRDR(8)
      IPVERT=IRDR(9)
      IPVM=IRDR(10)
      IPHL=IRDR(11)
      IF(IPANAL.EQ.1) IPLAS=0
      IF(IPANAL.EQ.1) IPNF=0
      IF(IPANAL.LT.2) IPVERT=0
      IF(IPMASS.EQ.0) IPCONM=0
      DO 5 K=1,3
      IF(IPANAL.LT.2.AND.K.LT.3) GO TO 5
      IF(IPVERT.EQ.0.AND.K.EQ.2) GO TO 5
      CALL READR(0,0,-1,RRDR,IRDR)
      KI=(K-1)*20
      WRITE(NDS3,1)(INFO(I),I=1,80)
      REWIND NDS3
      READ(NDS3,2)(BLAB(KI+1),I=1,20)
      REWIND NDS3
5  CONTINUE

```

```

      READ IN THE NO. OF NODAL POINTS, NO. OF MEMBERS, NO. OF MEMBER TYPE
      GRAVITY, ACCELERATION FACTOR, PERCENTAGE DAMPING FOR
      GRAVITY, PERCENTAGE DAMPING FOR MODE 1, MODE 2, NO. OF
      MODES, NEWMARK'S BETA, INVERSE OF TIME-STEP, INVERSE OF
      WILSON'S TIME-STEP, LENGTH OF E/Q, ACCELERATION FACTOR
      NUMBER OF TIME-STEPS BEFORE 'ZERO' OF E/Q RECORD,
      SEQUENCE NUMBER OF FIRST E/Q CARD, NUMBER OF TIME-STEP
      BETWEEN PRINTOUTS, NUMBER OF STEPS BETWEEN UPDATING
      AND CHECKING FORCES, NUMBER OF TIME-STEPS BETWEEN
      AUXILIARY OUTPUT.

```

```

      CALL READR(8,9,0,RRDR,IRDR)
      NNP=IRDR(1)
      NMEM=IRDR(2)
      NTYPE=IRDR(3)
      GRAV=RRDR(1)
      C1=RRDR(2)
      C2=RRDR(3)
      M=IRDR(4)
      B=RRDR(4)
      DT=RRDR(5)
      TOR=RRDR(6)
      TR=RRDR(7)
      GFACTR=RRDR(8)
      IPAD=IRDR(5)
      ISTART=IRDR(6)
      KP=IRDR(7)

```

საქართველო

[illegible]

24

26

22

555

10

“

53

```

55 IF(N.GE.NNP) GO TO 57
56 NLAST=N
57 CONTINUE
IF(IPVERT.EQ.0) GO TO 70

READ VERTICAL COMPONENT OF E/Q ON TO THE PSEUDO CARD READER
WHICH IS SEQUENTIAL DATA SET NDS3.

REWIND NDS3
CALL READR(0,1,0,RRDR,IRDR)
ISTOP=ISTOP+NSTOP
NCARDS=IRDR(1)
DO 62 I=1,NCARDS
CALL READR(8,1,0,RRDR,IRDR)
62 WRITE(NDS3,63) IRDR(1), (RRDR(J), J=1,8)
63 FORMAT(I3,4(F8.4,F9.6))
REWIND NDS3

70 CALL ECHO(COORD,NPFX,CUP,MEMNP,MTYPE,PROPS,DR,MASS,AMOM,AXIAL)
IF(NSTOP.EQ.1) STOP 1

ZERO THE LUMPED MASS FOR ANY DEGREE OF FREEDOM WHICH IS FIXED.
IF(IPANAL.EQ.0) GO TO 86
DO 84 I=1,NTYPE
84 PROPS(I,8)=PROPS(I,8)/GRAV
DO 85 I=1,NNP
NFX=NPFX(I)
DO 85 J=1,3
II=3*(I-1)+J
NFX=BINARY(NFX,4-J)
85 MASS(II)=(1-NFX)*MASS(II)/GRAV

86 IF(IPLAS.EQ.0) GO TO 88
DO 87 N=1,NTYPE
IF(IPLAS.EQ.1) PROPS(N,20)=0.0
IF(PROPS(N,12).EQ.0.) PROPS(N,12)=1.
87 IF(PROPS(N,13).EQ.0.) PROPS(N,13)=1.

88 DO 90 I=1,3
II=(I-1)*30+6
DO 90 J=1,30
IJ=II+J
90 IANS(IJ)=(IANS(IJ)-1)*3+I
DO 91 I=1,NNP
DO 91 J=1,3
IJ=CUP(I,J)
IF(IJ.EQ.1) IJ=0
IF(IJ.EQ.0) GO TO 91
CUP(I,J)=3*(IJ-1)+J
91 CONTINUE

INITIALIZE MATRIX (F) WHICH CARRIES FACTORS DESCRIBING EQUIVALENT
HINGE ACTION IN MEMBER.

DO 95 I=1,NMEM
MT=MTYPE(I)
F(I,1)=1.0
F(I,2)=2.0E7
F(I,3)=2.0E7
RDUM=PROPS(MT,9)
IF(IDUM.NE.0) F(I,2)=0.0
RDUM=PROPS(MT,10)
95 IF(IDUM.NE.0) F(I,3)=0.0
IF(IPANAL.LT.2) RETURN

DT=1.0/DT
TOR=1.0/TOR

```

```

C
C RETURN
C END

SUBROUTINE JUGGLE (AMASS,NPFX,MEMNP,JUG,CUP)
*****

SUBROUTINE TO PRODUCE A JUGGLING VECTOR WHICH WILL CATALOGUE THE
POSITIONS OF VARIOUS DEGREES OF FREEDOM FOR A PARTITIONED
STIFFNESS AND WILL FIND THE SEMI-BANDWIDTHS OF THE PARTITIONS.
*****

COMMON/ CONST/ NNP,NMEM,NE,NEQ,NREQ,NSEQ,NBW1,NBW2,NBW3
COMMON/ DIME/ ND1,ND2
COMMON/SYSTEM/ INP,LNP

DIMENSION AMASS(1),NF(6),NPFX(1),MEMNP(ND2,1),JUG(1)
INTEGER BINARY,CUP(ND1,1)

M=0
L=0
DO 10 J=1,NNP
NFX=NPFX(J)
DO 10 K=1,3
I=(J-1)*3+K
JUG(I)=0
NFX=BINARY(NFX,4-K)
IF(NFX.EQ.1) GO TO 10
IF(CUP(J,K).NE.0) GO TO 4
IF(AMASS(I).EQ.0.0) GO TO 3
L=L+1
JUG(I)=L
GO TO 10
3 M=M+1
JUG(I)=-M
GO TO 10
4 JUG(I)=10000+CUP(J,K)
10 CONTINUE

NREQ=L
NSEQ=M
NE=L+M
DO 20 I=1,NEQ
JI=JUG(I)
IF(JI.GE.0.AND.JI.LE.NEQ) GO TO 20
IF(JI.GT.NEQ) GO TO 13
JUG(I)=NREQ-JI
GO TO 20
13 JI=JUG(JI-10000)
IF(JI.GE.0) GO TO 14
JUG(I)=NREQ-JI
GO TO 20
14 IF(JI.GT.NEQ) GO TO 13
JUG(I)=JI
20 CONTINUE

FIND THE SEMI-BANDWIDTH OF BOTH SECTIONS OF THE STIFFNESS MATRIX.
NBW2, NBW3 ARE THE SEMI-BW'S OF THE 1ST + 2ND PARTITIONS.

NBW2=0
NBW3=0
DO 40 I=1,NMEM
N1=(MEMNP(I,1)-1)*3

```

```

N2=(MEMNP(I,2)-1)*3
DO 25 J=1,3
NF(J)=JUG(N1+J)
25 NF(J+3)=JUG(N2+J)
DO 30 K=1,6
N1=NF(K)
IF(N1.EQ.0) GO TO 30
DO 29 J=1,6
N2=NF(J)
IF(N2.EQ.0) GO TO 29
NB=IABS(N2-N1)+1
IF(N1.GT.NREQ) GO TO 28
NBW2=MAX0(NBW2,NB)
GO TO 29
28 NBW3=MAX0(NBW3,NB)
29 CONTINUE
30 CONTINUE
40 CONTINUE

C RETURN
END

SUBROUTINE MCURV (AXIAL,AMOM,TSO,DRM,PROPS,F,C,CMAX,XS)
*****
SUBROUTINE TO CONTROL THE MOMENT/CURVATURE AND AXIAL LOAD/DEFLECTION CHARACTERISTICS OF A MEMBER.
NON-LINEARITY IS ATTAINED BY INTRODUCING, WHEN NECESSARY, SPRING HINGES WITH A SPRING RATE OF 4*F*E*I/L AND AXIAL SPRINGS WITH SPRING RATES OF F*E*A/L. THE HINGES ARE DEEMED TO EXIST ONLY IF F.LE.1.E7.
*****

COMMON / DIME/ ND1,ND2,ND3
1 / ECCO/ DUMMY(4),IPLAS,DUM1,DUM2,IPVM
2 / MEMBER/ TRANS,CL,BETA,XL,YL,AREA,GAREA,ERTIA,END1,END2,
3 / YIELDS/ EMOD,GMOD,SMA,F1,F2,F3,SDM,N1,N2,MT,N,ITRIG
4 / PAX,PY(6),YMP(2),YMN(2)
5 / CURVE/ AM,AMO,AMY,CO,CY,R,CONV,CYC,DMDC,LNPI

DIMENSION AXIAL(1),AMOM(ND2,1),PROPS(ND3,1),TSO(1),C(ND2,1),
1 CMAX(ND2,1),F(ND2,1),TRANS(3,6),SMA(54),FN(2),XS(3),
2 SDM(6),DRM(3)

EQUIVALENCE (FNEW,R),(F2,FN(1)),(F3,FN(2)),(APIN,IPIN),
1 (ABRACE,IBRACE)

ITRIG=0
DO 1 I=1,3
1 XS(I)=0.
PAX=AXIAL(N)+DRM(1)
AXIAL(N)=PAX

CHECK AS TO WHETHER MEMBER IS A BRACE.
ABRACE=PROPS(MT,11)
IF(ABRACE.EQ.1) GO TO 25

IF(IPLAS.NE.0) GO TO 2
100 AMOM(N,1)=AMOM(N,1)+DRM(2)
AMOM(N,2)=AMOM(N,2)+DRM(3)
RETURN

2 IF(PROPS(MT,15).EQ.0..AND.IPVM.NE.0) GO TO 100

```

```

DO 3 I=1,6
3 PY(I)=PROPS(MT,13+I)
LNPI=6
FEXIST=1.E7
FNONE=2.E7

C FIND THE CURRENT YIELD MOMENTS.
C CALL YIELD
C DO 22 I=2,3
C IM1=I-1
C CHECK AS TO WHETHER THIS END OF MEMBER IS PINNED.
C APIN=PROPS(MT,7+I)
C IF(IPIN.EQ.1) GO TO 22
C
C AM =AMOM(N,IM1)
C DM =DRM(I)
C AMO =F(N,I+3)
C AMI =AM+DM
C DC =0.
C HDL =PROPS(MT,10+I)/CL
C EI =EMOD*ERTIA
C HK =4.*EI*HDL
C FOLD=F(N,I)
C FNEW=PROPS(MT,20)
C IF(IPLAS.EQ.2) FNEW=FNEW*.25/(HDL*(1.-FNEW))
C IF(PY(2).EQ.0.) AMO=0.
C TC =C(N,I)
C DMY=0.
C KOLY=0

C CALCULATE THE SPRING HINGE'S INCREMENTAL ROTATION AND CHECK
C WHETHER IT HAS CHANGED ITS DIRECTION.
C
C IF(FOLD.LE.FEXIST.AND.PY(2).EQ.0.) KOLY=1
C IF(FOLD.EQ.0.) GO TO 4
C DC=DM*(1./EI+1./HK*FOLD)
C IF(FOLD.GT.FEXIST.AND.IPLAS.NE.3) DC=0.
C IF(DC*(AM-AMO).GE.-0.) GO TO 10
C GO TO 6
C 4 DO 5 J=1,6
C 5 DC=DC+TRANS(I,J)*SDM(J)/PROPS(MT,10+I)
C IF(KOLY.EQ.1) GO TO 11
C IF(DC*AM.GE.-0.) GO TO 10
C
C CORNER IN HYSTERESIS INTRODUCED - CALCULATE MOMENT UNDERSHOOT.
C
C 6 F(N,I+3)=AM
C CO=TC
C TC=CO+DC
C IF(IPLAS.EQ.3) GO TO 7
C ** BI-LINEAR **
C AMI =AM+EI*DC
C IF(KOLY.EQ.1) AMI=AM
C IF(KOLY.NE.1) XS(I)=EI*DC-DM
C FNEW=FNONE
C GO TO 17
C ** RAMBERG-OSGOOD **
C 7 AMO =AM
C CONV=.001
C AMY =YMP(IM1)
C CYC=2.
C IF(DC.LT.-0.) AMY=YMN(IM1)
C IF(ABS(CMAX(N,I)).GT.ABS(.15*AMY/EI)) GO TO 8
C AMO =0.
C F(N,I+3)=AMO

```

```

      CO =0.
      CYC =1.
8     CY =AMY/EI
      AM1 =RAMDSG (TC)
      XS(1)=AM1-AM+DM
      DIV=(EI-DMDC)*4.*HDL
      FNEW=FNONE
      IF(DIV.NE.0.) FNEW=DMDC/DIV
      GO TO 17
C
C     NO CHANGE IN DIRECTION OF INCREMENTAL CURVATURE.
C
10    IF(IPLAS.EQ.3) GO TO 15
      ** BI-LINEAR ** (INSERT A SPRING HINGE IF NECESSARY)
      IF(FOLD.LE.FEXIST) GO TO 18
      IF(AMO.EQ.0.) GO TO 11
      IF(AMO.GE.AM) DMY=AMO-YMP(IM1)
      IF(AMO.LT.AM) DMY=AMO-YMN(IM1)
11    YMPI=YMP(IM1)+DMY
      YMNI=YMN(IM1)+DMY
      IF(AM1.GE.YMPI) GO TO 12
      IF(AM1.LE.YMNI) GO TO 13
      IF(KOLY.EQ.1) GO TO 6
      GO TO 18
12    YM=YMPI
      GO TO 14
13    YM=YMNI
14    DDM=PROPS(MT,20)*(AM1-YM)
      AM2=AM1
      AM1=YM+DDM
      XS(1)=AM2-YM-DDM
      TC1=TC
      TC=TC+DC
      IF (KOLY.EQ.1) GO TO 16
      DC=(AM2-YM)/EI
      TC=TC1+DC
      GO TO 17
C
      ** RAMBERG-OSGOOD **
15    CYC=1.
      IF(AMO.NE.0.) CYC=2.
      CONV=.001
      AMY =YMP(IM1)
      IF(DC.LT.-0.) AMY=YMN(IM1)
      CY =AMY/EI
      CO =TC-(AM-AMO)*[1.+ABS((AM-AMO)/(CYC*AMY))]*(R-1.)/EI
      TC =TC+DC
      AM1 =RAMDSG (TC)
      XS(1)=AM+DM-AM1
      IF(AM1.EQ.AMO) GO TO 16
      DIV=(EI-DMDC)*4.*HDL
      FNEW=FNONE
      IF(DIV.NE.0.) FNEW=DMDC/DIV
      GO TO 17
16    FNEW=FOLD
C
17    FN(IM1)=FNEW
      F(N,I)=FNEW
      GO TO 19
18    TC=TC+DC
      FNEW=FOLD
19    C(N,I)=TC
      AMOM(N,IM1)=AM1
C
      IF(FOLD.EQ.FNEW) GO TO 20
      IF(FOLD.GT.FEXIST.AND.FNEW.GT.FEXIST) GO TO 20
      ITRIG=1
C
20    IF(ABS(TC).LT.ABS(CMAX(N,I))) GO TO 22
      CMAX(N,I)=TC

```

```

      CMAX(N,I+3)=AM1
C
22    CONTINUE
C
      CHECK BRACING AND/OR AXIAL CHARACTERISTICS OF MEMBER.
C
25    FBRACE=-1.
      FAX=F(N,I)
      TC=C(N,I)
      IF(IPLAS.EQ.0) GO TO 30
      P18=PROPS(MT,18)
      P19=PROPS(MT,19)
      IF(FAX.NE.0.) GO TO 27
C
      AXIAL (ELASTOPLASTIC), YIELDING OCCURRING - IS IT CONTINUING.
C
      SDL=0.
      DO 26 I=1,6
      SDL=SDL+TRANS(1,I)*SDM(I)
26    IF(SDL.LT.0.) GO TO 29
      TC=TC+SDL
      IF(SDL.LT.0..AND.PAX.EQ.P19) GO TO 29
      IF(SDL.GT.0..AND.PAX.EQ.P18) GO TO 29
      IF(ABS(TC).GT.ABS(CMAX(N,I))) CMAX(N,I)=TC
      GO TO 50
C
      CHECK FOR THE ONSET OF YIELDING.
C
27    IF(PAX.LE.P19.AND.PAX.GE.P18) GO TO 30
      IF(PAX.GT.P19) YP=P19
      IF(PAX.LT.P18) YP=P18
      AXIAL(N)=YP
      XS(1)=PAX-YP
      FNEW=0.
      ITRIG=1
      GO TO 49
C
      STOP YIELDING.
C
29    FNEW =1.
      ITRIG=1
      XS(1)=SDL*FNEW*EMOD*AREA/CL
      GO TO 35
C
      CHECK AS TO WHETHER BRACE ALREADY SLACK.
C
30    IF(IBRACE.EQ.0) RETURN
      IF(FAX.LT.-0.) GO TO 40
C
      CHECK AS TO WHETHER BRACE GOING SLACK.
C
35    IF(IBRACE.EQ.0) GO TO 49
      IF(PAX.GT.0.) GO TO 49
      XS(1)=XS(1)+PAX
      ITRIG=1
      FNEW =FBRACE
      GO TO 49
C
      CHECK AS TO WHETHER MEMBER BECOMING TAUT.
C
40    HL=CL+END1+END2
      TL=(TSD(N2*3-2)-TSD(N1*3-2))*XL/HL+(TSD(N2*3-1)-TSD(N1*3-1))*YL/HL
      IF(TL.LE.TC) GO TO 50
      FNEW =1.
      ITRIG=1
      XS(1)=(TC-TL)*EMOD*AREA*FNEW/CL
C
49    F1=FNEW
      F(N,I)=FNEW

```

```

50 C(N,1)=TC
   RETURN
   END

```

```

SUBROUTINE MFORCE (COORD,F,PROPS,SD,DRM)

```

```

SUBROUTINE TO TRANSFORM INCREMENTAL DISPLACEMENTS IN SYSTEM
COORDINATES INTO INCREMENTAL MEMBER FORCES.

```

```

COMMON/ DIME/ ND1,ND2,ND3,ND4
1 MEMBER/ TRANS,CL,BETA,XL,YL,AREA,GAREA,ERTIA,END1,END2,
2 EMOD,GMOD,SM,A,F1,F2,F3,SDM,MN1,MN2,MT,N
1 DIMENSION DRM(1),SDM(6),TRANS(3,6),SM(6,6),A(3,6),P(7),
1 COORD(ND1,1),F(ND2,1),PROPS(ND3,1),SD(1)
1 EQUIVALENCE (AREA,P(1)),(GAREA,P(2)),(ERTIA,P(3)),(END1,P(4)),
1 (END2,P(5)),(EMOD,P(6)),(GMOD,P(7))

```

```

XL =COORD(MN2,1)-COORD(MN1,1)
YL =COORD(MN2,2)-COORD(MN1,2)

```

```

DO 5 I=1,7
5 P(I)=PROPS(MT,I)
F1=F(N,1)
F2=F(N,2)
F3=F(N,3)

```

```

CALL MSTIFF (4)

```

```

FORM THE MEMBER INCREMENTAL DEFLECTION VECTOR (SDM).

```

```

MNP1=(MN1-1)*3
MNP2=(MN2-1)*3
DO 10 I=1,3
SDM(I)=SD(MNP1+I)
10 SDM(I+3)=SD(MNP2+I)

```

```

FORM THE MEMBER INCREMENTAL FORCES VECTOR (DRM).

```

```

DO 11 I=1,3
D1=0.0D0
DO 11 J=1,6
D2=A(I,J)
D3=SDM(J)
D1=D1+D2*D3
11 DRM(I)=D1

```

```

RETURN
END

```

```

SUBROUTINE MMASS (MM,UNIMAS)

```

```

MEMBER MASS MATRIX FORMATION.
THIS SUBROUTINE IS FOR THREE DEGREES OF FREEDOM PER NODE
PROPER PROVISION HAS NOT BEEN MADE FOR THE POSSIBILITY OF A PIN AT
EITHER END AT THIS STAGE OF PROGRAM DEVELOPMENT.

```

```

COMMON/MEMBER/ TRANS,CL,BETA,XL,YL,AREA,GAREA,ERTIA,END1,END2,
1 EMOD,GMOD,AA,A,F1,F2,F3

```

```

DIMENSION MM(6,6),TRANS(3,6),AA(6,6),A(18)
REAL MM

```

```

DO 2 I=1,6
DO 1 J=1,6
1 MM(I,J)=0.
DO 2 J=1,3
2 TRANS(J,I)=0.

```

```

HL=SQRT(XL*XL+YL*YL)
CL=HL-END1-END2
SINE =YL/HL
COSINE=XL/HL
BETA=0.
IF(GAREA.NE.0.0) BETA=6.0*EMOD*ERTIA/(CL**2*GAREA*GMOD)
BZ=HL**3/(1.0+BETA)**2

```

```

SET UP THE MEMBER MASS MATRIX FOR MEMBER CO-ORDINATES.

```

```

MM(1,1)=.333333333*HL
MM(4,4)= MM(1,1)
MM(1,4)=.166666667*HL
IF(F2.EQ.0.0.OR.F3.EQ.0.0) GO TO 4

```

```

MM(2,2)= HL*13./35.
MM(2,3)= HL*HL*11./210.
MM(2,5)= HL*9./70.
MM(2,6)=HL*HL*13./420.
MM(3,3)= BZ*(1./105.+BETA/60.+BETA*BETA/120.)
MM(3,5)=-MM(2,6)
MM(3,6)=-BZ*(1./140.+BETA/60.+BETA*BETA/120.)
MM(5,5)= MM(2,2)
MM(5,6)=-MM(2,3)
MM(6,6)= MM(3,3)
GO TO 6

```

```

4 IF(F2.NE.0.0) GO TO 5
MM(6,6)= 32.*HL**3/(105.*(4.+BETA)**2)
5 IF(F3.NE.0.0) GO TO 6
MM(3,3)= 32.*HL**3/(105.*(4.+BETA)**2)

```

```

6 DO 7 I=1,6
DO 7 J=1,6
MM(I,J)=MM(I,J)*UNIMAS
7 IF(I.NE.J) MM(J,I)=MM(I,J)
IF(SINE.EQ.0..AND.COSINE.EQ.1.) RETURN

```

```

APPLY CO-ORDINATE TRANSFORMATION TO MEMBER MASS MATRIX.

```

```

TRANS(1,2)= SINE
TRANS(1,5)= SINE
TRANS(2,1)= COSINE
TRANS(2,2)= COSINE
TRANS(2,3)= 1.
TRANS(2,4)= COSINE
TRANS(2,5)= COSINE
TRANS(2,6)= 1.
TRANS(3,1)=-SINE
TRANS(3,4)=-SINE

```

```

DO 9 I=1,6
DO 9 J=1,6
AIJ=0.
DO 8 K=1,3
KJ=J-2+K
IF(KJ.EQ.0.OR.KJ.EQ.7) GO TO 8
AIJ=AIJ+MM(I,KJ)*TRANS(K,J)
8 CONTINUE

```

```

C 9 AA(I,J)=AIJ
DO 11 I=1,6
DO 11 J=1,6
AMIJ=0.
DO 10 K=1,3
KI=I-2+K
IF(KI.EQ.0.OR.KI.EQ.7) GO TO 10
AMIJ=AMIJ+TRANS(K,I)*AA(KI,J)
10 CONTINUE
11 MM(I,J)=AMIJ

C MATRIX (MM) IS THE MEMBER MASS.
C
C RETURN
C END

C
C SUBROUTINE MODES (S,FLEX,LUMAS,DR,JUG,E,W,W1,W2,W3,W4,W5,W6)
C *****
C THIS VERSION OF MODES CALLS ON A HOUSEHOLDER TRI-DIAGONALIZING
C EIGENVALUE SUBROUTINE TO FIND ALL THE NATURAL FREQUENCIES
C AND NORMAL MODE SHAPES OF A 3 DEGREE OF FREEDOM PER NODE FRAME.
C HENCE THE DAMPING FACTORS ARE FOUND - USING THE FIRST TWO
C NATURAL FREQUENCIES ONLY.
C *****
C COMMON/ CONST/ NNP,NMEM,NE,NEQ,NREQ,NSEQ,NBW1,NBW2
C 1 / DIME/ ND1,ND2,ND3,ND4
C 2 / ECCO/ IPNODE,IPRINT,IPNF
C 3 / FREQ/ C1,C2,M,ALPHA,BETA
C 4 / SYSTEM/ INP,LNP
C
C DIMENSION S(1),LUMAS(1),DR(1),FLEX(ND4,1),W(1),E(ND4,1),JUG(1),
C 1 W1(1),W2(1),W3(1),W4(1),W5(1),W6(1),IDUM(1)
C LOGICAL W6
C REAL LUMAS
C
C IF(IPNF.NE.0) GO TO 19
C
C FORM THE FLEXIBILITY MATRIX FOR NREQ DEGREES OF FREEDOM.
C ALSO, ASSUMING THAT THE MASS VECTOR HAS BEEN ALREADY 'JUGGLED',
C FORM THE SQUARE ROOT OF THE LUMPED MASS MATRIX.
C
C CALL SYMSOL (NE,NBW2,S,DR,NE,1)
C
C DO 2 I=1,NREQ
C W(I)=SQRT(LUMAS(I))
C DO 1 J=1,NE
C 1 DR(J)=0.0
C DR(I)=1.0
C
C CALL SYMSOL (NE,NBW2,S,DR,NE,2)
C
C DO 2 K=1,NREQ
C 2 FLEX(K,I)=DR(K)
C
C FIND THE EIGENVALUES (I.E. NATURAL FREQUENCIES) OF (FLEX).
C
C FIRST MAKE (FLEX)*(LUMAS) SYMMETRICAL BY PRE- AND POST-
C MULTIPLYING (FLEX) BY (LUMAS)**1/2.
C
C DO 16 I=1,NREQ
C DO 16 J=1,NREQ
16 FLEX(I,J)=FLEX(I,J)*W(I)*W(J)

```

```

C MAKE SURE THAT THE NEW (FLEX) IS ABSOLUTELY SYMMETRICAL.
C
C N1=NREQ-1
C DO 17 I=1,N1
C 11=I+1
C DO 17 J=I1,NREQ
C FLEX(I,J)=(FLEX(I,J)+FLEX(J,I))/2.0
17 FLEX(J,I)=FLEX(I,J)
C
C CALL HQRW (NREQ,ND4,M,FLEX,W,E,W1,W2,W3,W4,W5,W6)
C
C DO 18 I=1,NREQ
C W(I)=ABS(W(I))
18 W(I)=1.0/SQRT(W(I))
C GO TO 20
C
C 19 CALL READR(2,0,0,W,IDUM)
C W(1)=6.28318*W(1)
C W(2)=6.28318*W(2)
C
C 20 BETA=.02*(C2*W(2)-C1*W(1))/(W(2)*W(2)-W(1)*W(1))
C ALPHA=.02*C1*W(1)-BETA*W(1)*W(1)
C
C IF (IPRINT.EQ.0) RETURN
C
C WRITE ON THE LINE-PRINTER THE NATURAL FREQUENCIES, PERIODS,
C EQUIVALENT DAMPING
C
C WRITE(LNP,21)
C 21 FORMAT(1H1,55X,19HNATURAL FREQUENCIES/56X,19(1H-)//
C 1 48X,10HPERCENTAGE/6X,4HMODE,9X,9HFREQUENCY,7X,6HPERIOD,8X,
C 2 7HDAMPING/6X,4H---/)
C
C NR=NREQ
C IF(IPNF.NE.0) NR=2
C DO 22 I=1,NR
C FREQ=W(I)/6.28318
C PER=6.28318/W(I)
C DAMP=100.0*0.5*(ALPHA/W(I)+BETA*W(I))
22 WRITE(LNP,24) I,FREQ,PER,DAMP
C 24 FORMAT(6X,I3,4X,1P8E15.4)
C
C IF(IPNF.NE.0) WRITE(LNP,25)
C 25 FORMAT(1H0,20X,59HFREQUENCIES HAVE BEEN INPUTTED - NOT CALCULATED
C 1 IN THIS RUN)
C IF(M.EQ.0.OR.IPNF.NE.0) RETURN
C
C MM=IABS(M)
C DO 26 I=1,NREQ
C 26 W(I)=1.0/SQRT(LUMAS(I))
C WN=W(NREQ)
C DO 31 I=1,MM,8
C NB=I
C NL=I+7
C IF(NL.GT.MM) NL=MM
C WRITE(LNP,27) (J,J=NB,NL)
C 27 FORMAT(1H1,52X,25HNORMAL MODES OF THE FRAME/53X,25(1H-)//
C 1 5X,6HD.O.F.,1X,8(8X,4HMODE,I3))
C WRITE(LNP,28)
C 28 FORMAT(5X,6(1H-)//)
C DO 29 K=NB,NL
C ENK=E(NREQ,K)*WN
C DO 29 J=1,NREQ
C 29 E(J,K)=E(J,K)*W(J)/ENK
C DO 31 J=1,NEQ
C DO 30 K=NB,NL
C W(K)=0.
C 30 IF(JUG(J).NE.0) W(K)=E(JUG(J),K)

```

```

31 WRITE(LNP,24) J,(W1(K),K=NB,NL)
C
RETURN
END

SUBROUTINE MOTION (COORD,DR,SD,PROPS,S,DYSTIF,ACC,VEL,D,TSD,SDE,
1 MASS,AXIAL,AMOM,C,CMAX,MEMNP,MTYPE,JUG,S12,
2 XAXIAL,XAMOM,XTSD,F,IS)
*****
SUBROUTINE TO CONTROL THE REPEATED ELASTIC, AND WHERE NECESSARY,
THE ELASTO-PLASTIC ANALYSES OF THE FRAME.
*****
COMMON / CONST/ NNP,NMEM,NE,NEQ,NREQ,NSEQ,NBW1,NBW2,NBW3,NTYPE
1 / DIGIT/ ISAVE(19),ISAFE(19)
2 / DIME/ ND1,ND2,ND3,ND4
3 / ECCO/ IPNODE,IPDATA,IPNF,IPANAL,IPLAS,IPVERT,IPHOTO,
4 / IPVM,IPHL,IPMASS,IPCONM
5 / EQUAKE/ DT,IPAD,ISTART,T,TR,GFACTR,GRAV,TOR,B,KP,KMF,KPA
6 / FREQ/ C1,C2,M,ALPHA,BETA
7 / INTEG/ A3,A4,A5,A6
8 / MEMBER/ TRANS,CL,BITA,XL,YL,AREA,GAREA,ERTIA,END1,END2,
9 EMOD,GMOD,SM,A,F1,F2,F3,SDM,N1,N2,MT,N,ITRIG
A / SYSTEM/ INP,LNP,IPCH,NDS1,NDS2,NDS3

DIMENSION SM(6,6),A(3,6),DRM(3),MNP(2),TRANS(3,6),SDM(6),XS(3),
1 COORD(ND1,1),
2 AMOM(ND2,1),C(ND2,1),CMAX(ND2,1),MEMNP(ND2,1),
3 MTYPE(1),AXIAL(1),DR(1),ACC(1),VEL(1),D(1),TSD(1),
4 SD(1),MASS(1),JUG(1),S(1),DYSTIF(1),S12(1),SDE(1),
5 PROPS(NB3,1),XAMOM(ND2,1),XAXIAL(1),XTSD(1),F(ND2,1)

REAL MASS

EQUIVALENCE (ISAVE(1),DACC),(ISAVE(2),TDT),
1 (MNP(1),N1),(MNP(2),N2)

DATA NPLUS,NMINUS /+1,-1/

REWIND NDS1
NS=(NBW2*(2*NE+1-NBW2))/2

ZERO VECTORS AND MATRICES REQUIRED FOR THE ANALYSIS.

DO 1 I=1,NE
VEL(I)=0.0
1 ACC(I)=0.0
DO 2 I=1,NEQ
DR(I)=0.0
SD(I)=0.0
SDE(I)=0.0
2 XTSD(I)=0.0
DO 4 I=1,NMEM
XAXIAL(I)=0.0
XAMOM(I,1)=0.0
XAMOM(I,2)=0.0
DO 4 J=1,6
C(I,J)=0.0
4 CMAX(I,J)=0.0

ZERO THOSE VARIABLES NORMALLY INITIALIZED IN THE STATIC ANALYSIS.
IF(IS.EQ.1) GO TO 7
DO 5 I=1,NEQ

```

```

5 TSD(I)=0.0
C
7 A1=(1.0/TOR+0.5*ALPHA)/(B*TOR)
A2=1.0+0.5*BETA/(B*TOR)
A3=-A1*TOR
A4=ALPHA*TOR*(1.0-0.25/B)-0.5/B
A5=-0.5*BETA/B
A6=TOR*BETA*(1.0-0.25/B)
A7=(DT/TOR)**3
A8=DT*(1.0-DT*DT/(TOR*TOR))
A9=DT*DT*0.5*(1.0-DT/TOR)
A10=0.5/(B*DT)
A11=1.0-0.5/B
A12=DT*(1.0-0.25/B)
A13=1.0/(B*DT*DT)
A14=-A13*DT
A15=(TOR-DT)/DT
C
K=0
IFLAG=0
KKMF=KMF-1
KKP=KP
KKPA=KPA
NIT=1
ISAVE(3)=INP
ISAFE(3)=NDS3
ISAVE(4)=LNP
ISAFE(4)=LNP
ISAVE(5)=0
ISAFE(5)=0
CALL PIKCHA (COORD,MEMNP,F,TIME,1)
GO TO 45

SOLVE THE EQUATIONS OF MOTION FOR THE INCREMENTAL DISPLACEMENT
VECTOR.

FORM THE DYNAMIC STIFFNESS MATRIX (DYSTIF) STORED IN VECTORIZED
(RECTANGULAR) UPPER TRIANGULAR BANDED FORM, DIAGONAL BY DIAGONAL.
'CHOLSKY-DECOMPOSE' THE APPROPRIATE PART.

8 READ(NDS1) (S(I),I=1,NS)
REWIND NDS1
CALL DSTIFF (S,SD,DYSTIF,S12,JUG,MASS,A1,A2)

FIND THE INITIAL ACCELERATION OF THE GROUND.

IFLAG=1
CALL DIGAC (&101)
DACC1=DACC
KT=0
TIME1=TDT
TIME=TDT
IF(IPVERT.EQ.0) GO TO 16

REWIND NDS3
CALL SWAP
CALL DIGAC (&102)
DACC1=DACC
CALL SWAP
GO TO 16
C
15 KT=KT+1
RKT=KT
TIME=TIME1+RKT*DT
16 TDT=TIME+DT
NIT=0
IDF=1
CALL DIGAC (&101)
DACC2=DACC

```



```

DACC =DACC1+A15*DACC2
DACC1=DACC2
DACC =DACC *GRAV*GFACTR
IF(IPVERT.EQ.0) GO TO 17
CALL SWAP
TDT=TIME+DT
CALL DIGAC (6102)
DACC2=DACC
DACCV =DACC1+A15*DACCV2
DACC1=DACCV2
DACCV =DACC2*GRAV*GFACTR*IPVERT
CALL SWAP

FORM THE INCREMENTAL DYNAMIC FORCING FUNCTION VECTOR (DR).
17 CALL DFORCE (DACC,DACCV,D,ACC,VEL,DR,S,S12,MASS,JUG,IDF)

NIT=NIT+1
IAGAIN=0
IF(NIT.NE.1) GO TO 25
DO 20 I=1,NE
20 D(I)=0.
25 DO 26 I=1,NE
26 SD(I)=DR(I)

SOLVE, BY BACK-SUBSTITUTION, THE EQUATION
(DYNAMIC STIFFNESS)*(DISPLACEMENT)=(FORCING FUNCTION)
I.E. (DYSTIF)*(SD)=(SD) FOR (SD).

CALL SYMS8L (NREQ,NBW3,DYSTIF,SD,NREQ,2)

RECOVER THE CONDENSED INCREMENTAL DISPLACEMENT VECTOR AS 'SD'
AND THE FULL VECTOR AS 'DR'.

CALL RECOV (SD,DR,JUG,S12)

'SD', OF LENGTH 'NE', COVERS A TIME PERIOD OF 'TOR'.
TRANSFORM 'SD' INTO THE DISPLACEMENT OVER A TIME PERIOD OF 'DT'.

DO 35 I=1,NE
35 SD(I)=A7*SD(I)+A8*VEL(I)+A9*ACC(I)
D(I)=D(I)+SD(I)

DO 36 I=1,NE
36 DR(I)=SD(I)
DO 37 I=1,NEQ
37 SD(I)=0.
J=JUG(I)
IF(J.NE.0) SD(I)=DR(J)
DO 38 I=1,NE
38 DR(I)=0.

'SD' IS NOW THE EXPANDED INCREMENTAL DISPLACEMENT VECTOR OF
LENGTH 'NEQ' OVER A TIME OF 'DT' SECONDS.

IF(KMF.EQ.1) GO TO 45
KKMF=KKMF+1
DO 41 I=1,NEQ
41 IF(KKMF.LT.KMF) GO TO 63
KKMF=0
DO 43 I=1,NEQ
43 SDE(I)=SDE(I)
SDE(I)=0.0

UPDATE THE MEMBER FORCES.

45 CONTINUE
ISTIF=0

```

```

DO 62 N=1,NMEM
N1=MEMNP(N,1)
N2=MEMNP(N,2)
MT=MTYPE(N)

CALL MFORCE (COORD,F,PROPS,SD,DRM)

ITRIG=0

CALL MCURV (AXIAL,AMOM,TSD,DRM,PROPS,F,C,CMAX,XS)

IF NECESSARY, MODIFY THE STIFFNESS OF THE FRAME.

IF(ITRIG.EQ.0) GO TO 61

FORM THE OLD STIFFNESS MATRIX.

DO 57 I=1,6
DO 57 J=1,6
SMIJ=0.
DO 56 L=1,3
56 SMIJ=SMIJ+TRANS(L,I)*A(L,J)
57 SM(I,J)=SMIJ

SUBTRACT THE OLD MEMBER STIFFNESS.

CALL ALTRMX (S,SM,JUG,MNP,NMINUS)

TRANSFORM EXCESSIVE MEMBER FORCES BACK ON TO THE SYSTEM.

DO 59 I=1,2
DO 59 J=1,3
IJ=(I-1)*3+J
JUGI=JUG(MNP(I)-1)*3+J
IF(JUGI.EQ.0) GO TO 59
DRI=0.
DO 58 L=1,3
58 DRI=DRI+TRANS(L,IJ)*XS(L)
DR(JUGI)=DR(JUGI)+DRI
IF(DRI.NE.0) IAGAIN=1
59 CONTINUE

CREATE THE NEW MEMBER STIFFNESS.

60 CALL MSTIFF (3)

ADD THE NEW MEMBER STIFFNESS.

CALL ALTRMX (S,SM,JUG,MNP,NPLUS)

ISTIF=1
61 IF(ABS(AXIAL(N)).GT.ABS(XAXIAL(N))) XAXIAL(N)=AXIAL(N)
IF(ABS(AMOM(N,1)).GT.ABS(XAMOM(N,1))) XAMOM(N,1)=AMOM(N,1)
62 IF(ABS(AMOM(N,2)).GT.ABS(XAMOM(N,2))) XAMOM(N,2)=AMOM(N,2)
CONTINUE

IF NECESSARY, RELAX RESIDUAL MOMENTS.
REMOVE CARD CONTAINING 'IAGAIN=0' IF THIS REQUIRED.

IAGAIN=0
IF(IPLAS.EQ.3) IAGAIN=0
IF(IAGAIN.EQ.0) GO TO 63
IDF=2
GO TO 17

UPDATE VELOCITY, ACCELERATION AND TOTAL DISPLACEMENT VECTORS.

63 DO 64 I=1,NREQ

```

```

      VELI=VEL(I)
      ACCI=ACC(I)
      VEL(I)=A10*D(I)+A11*VELI+A12*ACCI
64  ACC(I)=A13*D(I)+A14*VELI+A11*ACCI
      IDF=1
      DO 68 I=1,NEQ
      J=JUG(I)
      IF(J.EQ.0) GO TO 68
      TSD(I)=TSD(I)+D(J)
      IF(ABS(TSD(I)).GT.ABS(XTSD(I))) XTSD(I)=TSD(I)
68  CONTINUE

C      IF(ISTIF.NE.1.AND.NIT.EQ.1) GO TO 73
      IF(IPLAS.EQ.3) GO TO 72
      ISTIF=2
      CALL PRINTR (TIME,AXIAL,AMOM,C,TSD,ISTIF)
      CALL PIKCHA (COORD,MEMNP,F,TIME,2)
      IF(NIT.NE.1) WRITE(LNP,689) NIT
689  FORMAT(20H NO. OF ITERATIONS =,I3)
      WRITE(LNP,69)
69  FORMAT(1H0,132(1H-))

C      DO 71 I=1,NE
      IF(S(I).NE.0.0) GO TO 71
      S(I)=0.1E-06
      WRITE(LNP,70) I
70  FORMAT(1H,10(13H---WARNING---)/1H,34HSTIFFNESS MATRIX DIAGONAL T
      TERM NO.,I3,17H HAS BECOME ZERO.)
71  CONTINUE

C      72 WRITE(ND1) (S(I),I=1,NS)
      CALL DSTIFF (S,SD,DYSTIF,S12,JUG,MASS,A1,A2)

C      73 CONTINUE

C      IF(IFLAG.NE.0) GO TO 83
      WRITE(LNP,80)
80  FORMAT(1H1)
      GO TO 8

C      83 IF(KKP.NE.KP) GO TO 94
      KKP=0
      IF(ISTIF.EQ.2) GO TO 94

C      CALL PRINTR (TIME,AXIAL,AMOM,C,TSD,ISTIF)

C      94 KKP=KKP+1

C      IF(KKPA.NE.KPA.OR.KPA.EQ.0) GO TO 97
      KKPA=0
      CALL AUXOUT (TIME,AXIAL,AMOM,C,CMAX,TSD,K)

C      97 KKPA=KKPA+1

C      CHECK AS TO WHETHER THE E/Q HAS REACHED TIME TR YET.
      IF (TIME.LT.TR) GO TO 15

C      WRITE(LNP,100)
100  FORMAT(44HOREQUIRED LENGTH OF E/Q RECORD HAS BEEN RUN.)
      GO TO 113

C      101 WRITE(LNP,111)
      GO TO 113
102  WRITE(LNP,112)

C      GO TO 113
111  FORMAT(1H1,33HRAN OUT OF HORIZONTAL E/Q RECORD.)

```

```

112  FORMAT(1H1,31HRAN OUT OF VERTICAL E/Q RECORD.)
113  LOAD=2
      CALL OUTPUT (LOAD,XAXIAL,XAMOM,COORD,MEMNP,XTSD)
      IF(IPLAS.EQ.0) RETURN
      CALL-DUCTIL (MTYPE,MEMNP,COORD,CMAX,PROPS)

C      RETURN
      END

```

```

C      SUBROUTINE MSTIFF (II)
C      *****
C      MEMBER STIFFNESS FORMATION.
C      THIS SUBROUTINE IS FOR THREE DEGREES OF FREEDOM PER NODE
C      WITH THE POSSIBILITY OF A PIN AT EITHER OR BOTH ENDS.
C      SHEAR DEFORMATION, RIGID END BLOCKS AT EITHER END AND BRACED
C      MEMBERS CAN BE ALLOWED FOR.
C      SYSTEM USED IS RIGHT-HANDED CARTESIAN ONE.
C
C      II=1 GEOMETRICAL TRANSFORMATION MATRIX (TRANS) ONLY FORMED.
C      II=2 ASSUMES TRANSFORMATION MATRIX ALREADY KNOWN, CALCULATES
C            (A) AND (SM).
C      II=3 CALCULATES (TRANS),(A) AND (SM).
C      II=4 CALCULATES (TRANS) AND (A).
C      *****
C      COMMON/MEMBER/ TRANS,CL,BETA,XL,YL,AREA,GAREA,ERTIA,END1,END2,
C      1      EMOD,GMOD,SM,A,F1,F2,F3
      DIMENSION SM(6,6),TRANS(3,6),A(3,6)

C      IF(II.EQ.2) GO TO 7

C      ALPHA, WHICH IS THE ANGLE OF THE MEMBER TO THE SYSTEM X CO-ORD,
C      HAS THE SIGN OF THE DIRECTION OF THE RESULTANT TRANSFORMATION,
C      I.E. CLOCK-WISE IS NEGATIVE.

C      HL=SQRT(XL**2+YL**2)
      CL=HL-END1-END2
      SINE=-YL/HL
      COSINE=XL/HL

C      FORM TRANSFORMATION MATRIX TO BOTH TRANSFORM ELEMENT DISPLACEMENTS
C      TO MEMBER DEFORMATIONS AND SYSTEM CO-ORDINATES TO MEMBER
C      CO-ORDINATES

C      DL=END1/CL
      TRANS(1,1)=-COSINE
      TRANS(1,2)=SINE
      TRANS(1,3)=0.0
      TRANS(2,1)=-SINE/CL
      TRANS(2,2)=-COSINE/CL
      TRANS(2,3)=-1.0-DL
      TRANS(3,1)=TRANS(2,1)
      TRANS(3,2)=TRANS(2,2)
      TRANS(3,3)=-DL
      DO 1 I=1,3
      TRANS(1,I+3)=-TRANS(1,I)
      TRANS(2,I+3)=-TRANS(3,I)
      1 TRANS(3,I+3)=-TRANS(2,I)
      DL=END2/CL
      TRANS(2,6)=-DL
      TRANS(3,6)=-1-DL

C      BETA=0.0
      IF(GAREA.NE.0.0) BETA=6.0*EMOD*ERTIA/(CL**2*GAREA*GMOD)

```

```

C      IF(II.EQ.1) RETURN
C      DO 2 I=1,6
C      DO 2 J=1,6
2     SM(I,J)=0.0
C
C      SET UP THE MEMBER DEFORMATION STIFFNESS MATRIX
C      BASIC=2.0*EMOD*ERTIA/CL
C      SM(1,1)=F1*EMOD*AREA/CL
C      IF(F2.EQ.0..OR.F3.EQ.0.) GO TO 3
C      SM22=BASIC*(2.0+BETA)/(1.0+2.0*BETA)
C      SM23=BASIC*(1.0-BETA)/(1.0+2.0*BETA)
C      IF(F2.GT.1.E7) GO TO 4
C      IF(F3.GT.1.E7) GO TO 5
C      FJJ=.75+F2+F3+F2*F3
C      FII=F2*(.75+F3)/FJJ
C      FIJ=F2*F3/FJJ
C      FJJ=F3*(.75+F2)/FJJ
C      GO TO 6
C
C      3 FIJ=0.0
C      SM22=3.0*BASIC/(2.0+BETA)
C      SM23=0.0
C      FII=F2/(.75+F3)
C      FJJ=F3/(.75+F2)
C      GO TO 6
C
C      4 FII=(.75+F3)/(1.0+F3)
C      FIJ=F3/(1.0+F2)
C      FJJ=FII
C      GO TO 6
C
C      5 FII=F2/(1.0+F2)
C      FIJ=FII
C      FJJ=(.75+F2)/(1.0+F2)
C
C      6 SM(2,2)=FII*SM22
C      SM(2,3)=FIJ*SM23
C      SM(3,2)=SM(2,3)
C      SM(3,3)=FJJ*SM22
C
C      APPLY TRANSFORMATION TO MEMBER DEFORMATION STIFFNESS MATRIX
C
C      7 DO 9 I=1,3
C      DO 9 J=1,3
C      A(I,J)=0.0
C      DO 9 K=1,3
C      9 A(I,J)=A(I,J)+SM(I,K)*TRANS(K,J)
C      IF(II.EQ.4) RETURN
C
C      MATRIX(A) IS THAT WHICH WILL TRANSFORM NODAL DISPLACEMENTS
C      TO MEMBER REACTIONS.
C
C      DO 11 I=1,6
C      DO 11 J=1,6
C      SM(I,J)=0.0
C      DO 11 K=1,3
C      11 SM(I,J)=SM(I,J)+TRANS(K,I)*A(K,J)
C
C      MATRIX(SM) IS THE MEMBER STIFFNESS.
C
C      RETURN
C      END

```

```

C      SUBROUTINE OUTPUT (LOAD,AXIAL,AMOM,COORD,MEMNP,TSD)
C      *****
C      SUBROUTINE TO PRINT OUTPUT FROM MAIN PROGRAM.
C      *****
C      COMMON / CONST/ NNP,NMEM
C      1 / DIME/ ND1,ND2
C      2 / ECCO/ DUM(3),IPANAL,IPLAS
C      3 /SYSTEM/ INP,LNP,IPCH
C
C      DIMENSION AXIAL(1),AMOM(ND2,1),COORD(ND1,1),TSD(1),MEMNP(ND2,1)
C
C      IF(LOAD.EQ.1) WRITE(LNP,9)
C      9 FORMAT(1H1,51X,29HRESULTS OF THE STATIC LOADING/52X,29(1H-)/)
C      IF(LOAD.EQ.2) WRITE(LNP,10)
C      10 FORMAT(1H1,49X,35HMAXIMUM VALUES OBTAINED IN ANALYSIS/50X,35(1H-)/)
C      1)
C      WRITE(LNP,11)
C      11 FORMAT(63X,7HMEMBERS/63X,7(1H-)//5X,6HMEMBER,6X,11HAXIAL FORCE,
C      1 5X,8HMOMENT 1,7X,8HMOMENT 2,21X,12HAXIAL DISPL.,3X,
C      2 10HROTATION 1,3X,10HROTATION 2/5X,6(1H-)//)
C      DO 12 I=1,NMEM
C      NP1=MEMNP(I,1)
C      NP2=MEMNP(I,2)
C      XL=COORD(NP2,1)-COORD(NP1,1)
C      YL=COORD(NP2,2)-COORD(NP1,2)
C      HL=SQRT(XL**2+YL**2)
C      SINE=YL/HL
C      COSINE=XL/HL
C      EXTEN=TSD(3*NP2-2)*COSINE+TSD(3*NP2-1)*SINE
C      1 -TSD(3*NP1-2)*COSINE-TSD(3*NP1-1)*SINE
C      12 WRITE(LNP,13) I,AXIAL(I),AMOM(I,1),AMOM(I,2),EXTEN,TSD(3*NP1),
C      1 TSD(3*NP2)
C      13 FORMAT(6X,I3,4X,1P3E15.5,15X,3E15.5)
C
C      IF(LOAD.EQ.1) WRITE(LNP,9)
C      IF(LOAD.EQ.2) WRITE(LNP,10)
C      WRITE(LNP,14)
C      14 FORMAT(64X,5HNODES/64X,5(1H-)/31X,13HDISPLACEMENTS/
C      1 6X,4HNODE,12X,1HX,14X,1HY,13X,2HOZ/1H+,50X,1H-/6X,4(1H-)//)
C      DO 15 I=1,NNP
C      15 WRITE(LNP,13) I,(TSD((I-1)*3+J),J=1,3)
C
C      16 FORMAT(1H0,32X,68H(NOTE - MOMENTS AT POINTS OF PLASTICITY MAY EXHI
C      1BIT SOME OVERSHOOT.))
C
C      RETURN
C      END
C
C      SUBROUTINE PDATE (DATE)
C      *****
C      COMPUTER-DEPENDENT SUBROUTINE WHICH PROVIDES CURRENT DATE.
C      AVAILABLE AS AN INTRINSIC ON THE IBM 360/44 SYSTEM.
C      OUTPUT IS FOR WRITING IN 544 FORMAT.
C      *****
C      DIMENSION DATE(5),AM(12),AM1(12),AM2(12)
C
C      DATA AM/'01 02 03 04 05 06 07 08 09 10
C      1 11 12
C      2 AM1/'JANU FEBR MARC APRI MAY JUNE JULY AUGU SEPT OCT

```

```

30 NOVE, DECE //,
4 AM2//ARY UARY H 19 L //,R//R, //,BLANK// ST //,EMBE BER
5 MBER MBER //,D// 19 //,R//R, //,BLANK// ST //,EMBE BER
6 DONT//FUNN //,AKNOW//Y

C
B=TIME (15)
DATE(1)=CONCAT (BLANK,B,47,31,16)
DATE(5)=CONCAT (BLANK,B,47,15,16)
DATE(4)=0
AMONTH=CONCAT (BLANK,B,47,47,16)
DO 2 I=1,9
2 IF (DATE(1).EQ.AM(I)) DATE(1)=CONCAT (DATE(1),BLANK,47,7,8)
DO 3 I=1,12
M=I
3 IF (AMONTH.EQ.AM(I)) GO TO 5
DATE(2)=DONT
DATE(3)=AKNOW
RETURN

C
5 DATE(2)=AM1(M)
DATE(3)=AM2(M)
IF (M.EQ.9) DATE(4)=CONCAT (DATE(4),R,47,47,8)
RETURN
END

SUBROUTINE PHOTO (COORD, MEMNP)
*****
SUBROUTINE TO GIVE AN APPROXIMATE LAY-OUT OF FRAME ON LINE-PRINTER
*****
COMMON/SYSTEM/ INP, LNP, IPCH
1 / DIME/ ND1, ND2
2 / CONST/ NNP, NMEM
3 / ECCO/ IPNODE

C
DIMENSION COORD(ND1,1), MEMNP(ND2,1), NOD(3)
INTEGER GRID(72,131), PLUS/6H+ //, DASH/6H- //,
1 SLASH/6H/ //, ASTER/6H* //, BLANK/6H //,
2 NUMB(10)/60H0 1 2 3 4 5 6 7
3 8 9 /

C
IF IPNODE = 1 THEN NODES ARE NUMBERED ON THE PRINT-OUT.
DO 5 I=1,72
DO 5 J=1,131
5 GRID(I,J)=BLANK

C
DO 6 I=1,NNP
6 COORD(I,1)=COORD(I,1)*10.0/8.0
FIND MAXIMUM HEIGHT AND WIDTH OF FRAME.
HPOS=0.0
HNEG=0.0
WPOS=0.0
WNEG=0.0
DO 10 I=1,NNP
IF (COORD(I,1).GT.WPOS) WPOS=COORD(I,1)
IF (COORD(I,1).LT.WNEG) WNEG=COORD(I,1)
IF (COORD(I,2).GT.HPOS) HPOS=COORD(I,2)
10 IF (COORD(I,2).LT.HNEG) HNEG=COORD(I,2)
WIDTH=WPOS-WNEG
HEIGHT=HPOS-HNEG
SCALEW=WIDTH/131.0

```

```

SCALEH=HEIGHT/70.0
SCALE=SCALEW
IF (SCALEH.GT.SCALEW) SCALE=SCALEH

C
NL=0.5*(131.0-WIDTH/SCALE)+1
PUT GROUND FORMATION IN (HORIZONTAL).

C
DO 15 I=1,131
GRID(71,I)=DASH
15 GRID(72,I)=SLASH

C
PLOT MEMBERS.
DO 30 I=1,NNP
N1=MEMNP(I,1)
N2=MEMNP(I,2)
DO 30 J=1,150
AJ=J
NX=(COORD(N1,1)-WNEG+AJ/150.0*(COORD(N2,1)-COORD(N1,1)))/SCALE
NY=(COORD(N1,2)-HNEG+AJ/150.0*(COORD(N2,2)-COORD(N1,2)))/SCALE
30 GRID(71-NY,NX+NL)=ASTER

C
PLOT JOINTS.
DO 40 I=1,NNP
NX=(COORD(I,1)-WNEG)/SCALE
NY=(COORD(I,2)-HNEG)/SCALE
NX=NL+NX
NY=71-NY
GRID(NY,NX)=PLUS
IF (IPNODE.EQ.0) GO TO 40
DO 35 J=1,3
IDIG=I/10**J
M=I/10**J-1
IDIG=M-10*IDIG
35 NOD(4-J)=NUMB(IDIG+1)
JJ=1
IF (I.LT.100) JJ=2
IF (I.LT.10) JJ=3
36 IF (NX+3.GT.131) NX=NX-4
DO 37 J=JJ,3
37 GRID(NY+1,NX+J)=NOD(J)
40 CONTINUE
WRITE(LNP,48)
48 FORMAT(1H1)
DO 49 I=1,72
49 WRITE(LNP,50) (GRID(I,J),J=1,131)
50 FORMAT(1H,131A1)
WRITE(LNP,51)
51 FORMAT(/41X,51HAN APPROXIMATE PICTURE OF THE FRAME BEING ANALYSED.
1 /41X,51(1H-))

C
DO 52 I=1,NNP
52 COORD(I,1)=COORD(I,1)*8.0/10.0

C
RETURN
END

SUBROUTINE PIKCHA (COORD, MEMNP, FH, TIME, II)
*****
THIS IS A PICTURE PRODUCING SUBROUTINE FOR LOCATING PLASTIC HINGES
AND PLACES OF AXIAL YIELDING OR SLACKNESS.
II=1 CREATES THE BASIC PICTUREF.

```



```

C 60 IF(FH(I,3).LE.1.E7) GRID(L(NH-NY,NX+NL))=OH
CONTINUE
IF(IPANAL.EQ.0) WRITE(LNP,84) TIME
IF(IPANAL.GT.0) WRITE(LNP,85) TIME
IF(VW.EQ.1.) GO TO 81
DO 80 I=1,NH1
80 WRITE(LNP,83) (GRID(L(I,J)),J=1,NW)
RETURN
C 81 DO 82 I=1,NW
82 WRITE(LNP,83) (GRID(L(J,NW+1-I)),J=1,NH1)
83 FORMAT(1H,132A1)
84 FORMAT(1H,38HPLASTICITY CHANGED AT END OF LOAD STEP,15)
85 FORMAT(1H,45HPLASTICITY CHANGED AT END OF THIS TIME-STEP (,F9.5,
1 7H SECS.))
C RETURN
END

SUBROUTINE PRINTR (TIME,AXIAL,AMOM,C,TSD,ITRIP)
*****
SUBROUTINE TO PRINT OUT THE SPECIFIED ANSWERS AT EACH TIME STEP.
*****
COMMON /SYSTEM/ INP,LNP,IPCH
1 / DIME/ ND1,ND2
2 / CONST/ NNP,NMEM
3 / ECCO/ DUM,IPANAL
4 /ANSWER/ NXT,NYT,NZT,M1T,M2T,AXT,NX,NY,NZ,M1,M2,AX
DIMENSION AXIAL(1),AMOM(ND2,1),C(ND2,1),TSD(1),NX(30),NY(30),
1 NZ(30),M1(30),M2(30),AX(30),DUM(3)
C INTEGER AX,AXT
IF(IPANAL.EQ.0) WRITE(LNP,1) TIME
IF(IPANAL.GT.0) WRITE(LNP,2) TIME
1 FORMAT(10H LOAD STEP,15)
2 FORMAT(7H TIME =,F9.5,6H SECS.)
IF(NXT+NYT+NZT.NE.0) WRITE(LNP,4)
4 FORMAT(7H DISPL.)
IF(NXT.NE.0) WRITE(LNP,5) (TSD(NX(I)),I=1,NXT)
5 FORMAT(1H+,9X,3HX,1P8E15.5,3(/13X,8E15.5))
IF(NYT.NE.0) WRITE(LNP,6) (TSD(NY(I)),I=1,NYT)
6 FORMAT(10X,3HY,1P8E15.5,3(/13X,8E15.5))
IF(NZT.NE.0) WRITE(LNP,7) (TSD(NZ(I)),I=1,NZT)
7 FORMAT(10X,1H0/1H+,9X,3H-Z,1P8E15.5,3(/13X,8E15.5))
C M=M1T+M2T+AXT
IF(M.NE.0) WRITE(LNP,8)
8 FORMAT(8H REACTS.)
IF(M1T.NE.0) WRITE(LNP,9) (AMOM(M1(I),1),I=1,M1T)
9 FORMAT(1H+,9X,3HM1,1P8E15.5,3(/13X,8E15.5))
IF(M2T.NE.0) WRITE(LNP,10) (AMOM(M2(I),2),I=1,M2T)
10 FORMAT(10X,3HM2,1P8E15.5,3(/13X,8E15.5))
IF(AXT.NE.0) WRITE(LNP,11) (AXIAL(AX(I)),I=1,AXT)
11 FORMAT(10X,3HAX,1P8E15.5,3(/13X,8E15.5))
C IF(ITRIP.EQ.0) GO TO 21
C J=0
K=0
L=0
DO 12 I=1,M1T
IF(M1T.EQ.0) GO TO 13

```

```

12 IF(C(M1(I),2).NE.0.0) J=1
13 IF(M2T.EQ.0) GO TO 15
DO 14 I=1,M2T
14 IF(C(M2(I),3).NE.0.0) K=1
15 IF(AXT.EQ.0) GO TO 17
DO 16 I=1,AXT
16 IF(C(AX(I),1).NE.0.0) L=1
17 IF(M.EQ.0.OR.J+K+L.EQ.0) GO TO 21
WRITE(LNP,18)
18 FORMAT(8H PL.DISP)
IF(M1T.NE.0) WRITE(LNP,19) (C(M1(I),2),I=1,M1T)
19 FORMAT(1H+,9X,3HC1,1P8E15.5,3(/13X,8E15.5))
IF(M2T.NE.0) WRITE(LNP,20) (C(M2(I),3),I=1,M2T)
20 FORMAT(10X,3HC2,1P8E15.5,3(/13X,8E15.5))
IF(AXT.NE.0) WRITE(LNP,11) (C(AX(I),1),I=1,AXT)
C 21 WRITE(LNP,22)
C 22 FORMAT(1X,132(1H-))
RETURN
END

```

```

FUNCTION RAMOSG (T)
*****
FUNCTION TO SOLVE RAMBERG-OSGOOD EQUATION BY TRIAL AND ERROR.
*****
COMMON / CURVE/ AMT,AMO,AMY,TO,TY,R,CONV,CYC,DMDC,LNP
IF(CONV.EQ.0.0) CONV=.001
AM=AMT
AMY1=CYC*AMY
DO 1 I=1,100
BM=AM
AM1=ABS((AM-AMO)/AMY1)**(R-1.)
AM=AM-((AM-AMO)*(1.+AM1)-(T-TO)*AMY/TY)/(1.+R*AM1)
1 IF(ABS(AM-BM).LE.ABS(CONV*AM)) GO TO 3
WRITE(LNP,2)
2 FORMAT(* CONVERGENCE NOT ATTAINED AFTER 100 CYCLES*)
STOP 100
3 RAMOSG=AM
DMDC=AMY/((1.+R*(ABS((AM-AMO)/AMY1)**(R-1.))*TY)
RETURN
END

SUBROUTINE READR (NR,NI,IND,A,NA)
*****
FREE-FORMAT INPUT DECODER ROUTINE A.J.CARR 1971
COMPUTER-DEPENDENT, BUT CAN BE EASILY MODIFIED TO SUIT ALL MARQUES
*****
DIMENSION A(1),NA(1),N(10)
COMMON /CARD/NSTOP,NTRAP,INPUT(80)
INTEGER BLANK,DOT,BAR,E,DOLLAR,PLUS1,PLUS2
DATA N/60H0 1 2 3 4 5 6 7
1 9 /,BLANK/6H /,DOT/6H /,BAR/6H- /,E/6HE /
2 /,DOLLAR/6H$ /,PLUS1/6H+ /,PLUS2/6H& /

```

```

NSTOP=0
I1=0
I2=0
IFLAG=-1
IF(NR.EQ.0) GO TO 4
DO 1 I=1,NR
1 A(I)=0.0
4 IF(NI.EQ.0) GO TO 3
DO 5 I=1,NI
5 NA(I)=0
3 I=0
READ( 5,2,END=1010) INPUT
2 FORMAT(80A1)
IF(IND.EQ.-1) RETURN
C
10 I=I+1
IF(I.LE.80) GO TO 11
IF(IND.EQ.0) RETURN
GO TO 3
11 ID=INPUT(I)
IF(ID.IS.BLANK) GO TO 10
IOP=0
FOP=0.0
KP=0
ISIGN=1
IF(ID.EQ.PLUS1.OR.ID.EQ.PLUS2) GO TO 60
IF(ID.IS.BAR) GO TO 40
GO TO 41
40 ISIGN=-1
GO TO 60
41 IF(IFLAG.EQ.1.OR.ID.NE.DOT) GO TO 44
IFLAG=0
GO TO 60
44 IF(ID.EQ.E.AND.IFLAG.EQ.0) GO TO 70
45 IF(ID.IS.BLANK) GO TO 70
DO 46 M=1,10
46 IF(ID.EQ.N(M)) GO TO 47
GO TO 1020
47 ICHAR=M-1
IF(IFLAG.EQ.0) KP=KP+1
IOP=IOP*10+ICHAR
FOP=FOP*10.0+FLOAT(ICHAR)
60 I=I+1
IF(I.GT.80) GO TO 70
ID=INPUT(I)
IF(IFLAG) 41,44,45
70 IF(IFLAG) 71,75,85
71 IF(I2.EQ.NI) GO TO 90
I2=I2+1
NA(I2)=IOP*ISIGN
GO TO 90
75 IFLAG=-1
IF(I1.EQ.NR) GO TO 90
I1=I1+1
A(I1)=FOP*FLOAT(ISIGN)
IF(KP.EQ.0) GO TO 82
DO 81 IOP=1,KP
81 A(I1)=A(I1)/10.0
82 IF(ID.NE.E) GO TO 90
IFLAG=1
GO TO 10
85 IFLAG=-1
KP=IOP*ISIGN
A(I1)=A(I1)*(10.0**KP)
90 IF(I1.EQ.NR.AND.I2.EQ.NI) RETURN
GO TO 10
C
1010 I=1
1020 WRITE( 6,1021)

```

```

1021 FORMAT(18HOCARD FORMAT ERROR )
WRITE( 6,1022) INPUT
1022 FORMAT(4H ***,80A1,3H***)
DO 1023 KP=1,80
1023 INPUT(KP)=BLANK
INPUT(I)=DOLLAR
WRITE( 6,1022) INPUT
IF(INTRAP.EQ.0) STOP
NSTOP=1
RETURN
END

```

```

SUBROUTINE RECOV (SD,DR,JUG,S12)
*****
SUBROUTINE TO RECOVER THE DISPLACEMENT VECTOR IN TWO STAGES.
1ST STAGE RECOVERS THE REDUCED VECTOR FROM THE ACTUAL EQUATION
SOLVER. 2ND STAGE RECOVERS THE FULL VECTOR WHOSE POSITIONS AGREE
WITH THE ORIGINAL NODAL NUMBERING.
*****
COMMON/ CONST/ NNP,NMEM,NE,NEQ,NREQ,NSEQ,NBW1,NBW2
DIMENSION SD(1),DR(1),JUG(1),S12(1)

LOC(I,J)=(J-1)*NREQ+(J*(J-1))/2+I
IF(NSEQ.EQ.0) GO TO 4

N1=NREQ+1
DO 1 I=N1,NE
1 SD(I)=0.000

DO 3 I=1,NSEQ
L=I+NREQ
K=L-1
SDL=SD(L)
JR=L-NBW2+1
IF(JR.LT.1) JR=1
DO 2 J=JR,K
D1=S12(LOC(J,I))
2 SDL=SDL-D1*SD(J)
3 SD(L)=SDL

C
DO 5 I=1,NEQ
J=JUG(I)
DR(I)=0.0
5 IF(J.NE.0) DR(I)=SD(J)

C
*DR* IS THE FULL DISPLACEMENT VECTOR , *SD* THE CONDENSED ONE.

RETURN
END

```





```

      C=A(I,J)/AII
      DO 1 K=J,M1
      JK=LOC(J,K)
      1 A(JK)=A(JK)-C*A(LOC(I,K))
      2 A(I,J)=C
      3 CONTINUE
      IF(II.NE.3) RETURN

      REDUCE THE VECTOR B=L O Y WHERE Y IS STORED IN B.

101 DO 5 I=1,N
      AII=A(LOC(I,I))
      BI=B(I)
      IF(I.EQ.N) GO TO 5
      II=I+1
      M1=I+M-1
      IF(M1.GT.N) M1=N
      DO 4 J=II,M1
      4 B(J)=B(J)-A(LOC(I,J))*BI
      5 B(I)=BI/AII

      BACK-SUBSTITUTE Y=U X WHERE X IS STORED IN Y.

      I=N
      6 I=I-1
      IF(I.EQ.0) GO TO 8
      II=I+1
      M1=I+M-1
      IF(M1.GT.N) M1=N
      DO 7 J=II,M1
      7 B(I)=B(I)-A(LOC(I,J))*B(J)
      8 CONTINUE
      GO TO 6
      8 CONTINUE
      RETURN
      END

SUBROUTINE SYMSBL (N,M,A,B,NMAX,II)
*****
PROGRAM TO SOLVE THE MATRIX EQUATION A*X=B.
THIS IS A VERSION OF SYMSOL FOR USE WHEN THE SEMI-BAND ONLY IS
STORED AS A FULL RECTANGULAR MATRIX.

II = 1 REDUCES (A) TO ITS TRIANGULAR FORM.
II = 2 CARRIES OUT THE BACK-SUBSTITUTION METHOD TO OBTAIN (X).
II = 3 DOES BOTH.

*****
DIMENSION A(NMAX,1),B(1)
GO TO (100,101,100),II
M IS THE BAND-WIDTH OF MATRIX (A).
REDUCE MATRIX TO A=LDU.

100 DO 3 I=1,N
      DO 2 J=2,M
      C=A(I,J)/A(I,1)
      L=I+J-1
      IF(N.LT.L) GO TO 2
      JJ=0
      DO 1 K=J,M
      1 JJ=JJ+1

```

```

      1 A(L,JJ)=A(L,JJ)-C*A(I,K)
      2 A(I,J)=C
      3 CONTINUE
      IF(II.NE.3) RETURN

      REDUCE THE VECTOR B=LDY WHERE Y IS STORED IN B.

101 DO 5 I=1,N
      DO 4 J=2,M
      L=I+J-1
      IF(N.LT.L) GO TO 5
      4 B(L)=B(L)-A(I,J)*B(I)
      5 B(I)=B(I)/A(I,1)

      BACK-SUBSTITUTE Y=UX WHERE X IS STORED IN Y.

      I=N
      6 I=I-1
      IF(I.EQ.0) GO TO 8
      DO 7 J=2,M
      L=I+J-1
      IF(N.LT.L) GO TO 7
      7 B(L)=B(L)-A(I,J)*B(L)
      8 CONTINUE
      GO TO 6
      8 CONTINUE
      RETURN
      END

SUBROUTINE TMASS (MASS,LUMAS,JUG,MEMNP,MTYPE,F,COORD,PROPS,NPFI,
IM)
*****
SUBROUTINE TO SET UP LUMPED MASS AND/OR CONSISTENT MASS MATRICES.

IPMASS=0 IF DO NOT WANT MEMBER MASSES INCLUDED.
IPMASS=1 IF DO NOT WANT NODE LUMPED MASSES INCLUDED.
IPMASS=2 IF BOTH TYPES OF MASS TO BE INCLUDED.
IM =1 FOR FINDING EQUIVALENT LUMPED MASS VECTOR UNCONDENSED.
IM =2 FOR CONDENSED MASS MATRICES - BOTH LUMPED + CONSISTENT.
*****
COMMON/ CONST/ NNP,NMEM,NE,NEQ,NREQ,NSEQ,NBWL
1 / DIME/ ND1,ND2,ND3
2 / ECCO/ DUM1,IPDATA,DUM2(7),IPMASS,IPCONM
3 /EQUAKE/ DUM3(6),GRAV
4 /MEMBER/ TRANS,CL,BETA,XL,YL,AREA,GAREA,ERTIA,END1,END2,
5 EMOD,GMOD,SM,A,F1,F2,F3
6 /SYSTEM/ INP,LNP
7

DIMENSION JUG(1),MEMNP(ND2,1),MTYPE(1),MNP(2),COORD(ND1,1),
1 F(ND2,1),PROPS(ND3,1),MASS(1),LUMAS(1),NPFI(1),
2 MM(6,6),TRANS(3,6),P(8),SM(6,6),A(3,6),WT(3)

REAL MASS,LUMAS,MM
INTEGER BINARY

EQUIVALENCE (AREA,P(1)),(GAREA,P(2)),(ERTIA,P(3)),(END1,P(4)),
1 (END2,P(5)),(EMOD,P(6)),(GMOD,P(7)),(UNIMAS,P(8))

DATA NPLUS/+1/

IF(IM.EQ.1) GO TO 4

SET UP THE PRINCIPAL DIAGONALS OF BOTH THE CONSISTENT AND NON-

```

```

C      CONSISTENT CONDENSED LUMPED MASS MATRICES.
C
C      DO 1 I=1,NEQ
1     LUMAS(I)=0.0
C      DO 2 I=1,NEQ
C      J=JUG(I)
C      2 IF(J.NE.0) LUMAS(J)=LUMAS(J)+MASS(I)
C      IF(IPMASS.EQ.0) GO TO 4
C
C      NM=(NBW1*(2*NE+1-NBW1))/2
C      IF(NM.LT.NEQ) NM=NEQ
C      DO 3 I=1,NM
C      MASS(I)=0.0
C      3 IF(I.LE.NREQ) MASS(I)=LUMAS(I)
C      GO TO 6
C
C      SAVE UNCONDENSED INPUTTED LUMPED-MASS MATRIX IN (MASS).
C
C      4 DO 5 I=1,NEQ
C      IF(IPMASS.EQ.1) LUMAS(I)=0.0
C      5 MASS(I)=LUMAS(I)
C      IF(IPMASS.EQ.0) RETURN
C      6 DO 11 I=1,NMEM
C      N=MTYPE(I)
C      MNP(1)=MEMNP(I,1)
C      MNP(2)=MEMNP(I,2)
C      XL=COORD(MNP(2),1)-COORD(MNP(1),1)
C      YL=COORD(MNP(2),2)-COORD(MNP(1),2)
C      DO 7 J=1,8
C      P(J)=PROPS(N,J)
C      IF(UNIMAS.EQ.0.0) GO TO 11
C      F1=F(I,1)
C      F2=F(I,2)
C      F3=F(I,3)
C      CALL MMASS(MM,UNIMAS)
C      IF(IM.EQ.1) GO TO 8
C      IF(IPCONM.EQ.C) GO TO 8
C
C      CALL ALTRMX(MASS,MM,JUG,MNP,NPLUS)
C
C      8 DO 10 II=1,2
C      NOD1=(MNP(II)-1)*3
C      DO 10 JJ=1,3
C      NF1=NOD1+JJ
C      IF(IM.NE.1) NF1=JUG(NF1)
C      IF(NF1.EQ.0) GO TO 10
C      II=(II-1)*3+JJ
C      A1=1.0
C      A2=1.0
C      IF(IM.EQ.1) GO TO 9
C      IF(JUG((MNP(1)-1)*3+JJ).EQ.0) A1=0.0
C      IF(JUG((MNP(2)-1)*3+JJ).EQ.0) A2=0.0
C      9 LUMAS(NF1)=LUMAS(NF1)+A1*MM(II,JJ)+A2*MM(II,JJ+3)
C      IF(IPCONM.EQ.0) MASS(NF1)=LUMAS(NF1)
C      10 CONTINUE
C      11 CONTINUE
C
C      IF IM=1 LUMAS IS THE TOTAL EQUIVALENT NCN-CONSISTENT UNCONDENSED
C      LUMPED-MASS VECTOR.
C      MASS CONTAINS THE ORIGINAL INPUTTED UNCONDENSED LUMPED-
C      MASS VECTOR.
C
C      IF IM=2 LUMAS IS THE CONDENSED LUMPED-MASS VECTOR,
C      MASS IS THE CONDENSED CONSISTENT-MASS MATRIX.
C
C      IF(IM.NE.1) RETURN
C      IF(IPDATA.EQ.0) RETURN

```

```

C      WRITE(LNP,13)
C      13 FORMAT(1H1,41X,49HFINAL COMBINED LUMPED MASS (WEIGHT UNITS) AT NOD
C      1E/42X,49(1H-1//6X,4HNODE,9X,8HX D.O.F.,7X,8HY D.O.F.,6X,9HOZ C.O.F
C      2,1H+,47X,1H-/6X,4H----/)
C      DO 15 I=1,NNP
C      NFIX=NPFIX(I)
C      DO 14 J=1,3
C      II=3*(I-1)+J
C      14 WT(J)=(1-BINARY(NFIX,4-J))*LUMAS(II)*GRAV
C      15 WRITE(LNP,16) I,(WT(J),J=1,3)
C      16 FORMAT(6X,I3,4X,1P3E15.4)
C
C      RETURN
C      END

```

```

C      SUBROUTINE ISTIFF(S,JUG,MEMNP,MTYPE,COORD,PROPS,F)
C      *****
C      SUBROUTINE TO SET UP DIRECT STIFFNESS MATRIX IN A FORM,
C      PARTITIONED OR OTHERWISE, DICTATED BY THE JUGGLING VECTOR 'JUG'.
C      *****
C      COMMON/ CONST/ NNP,NMEM,NE,NEQ,NREQ,NSEQ,NBW1,NBW2
C      / DIME/ ND1,ND2,ND3
C      / MEMBER/ TRANS,CL,BETA,XL,YL,AREA,GAREA,ERTIA,END1,END2,
C      3      EMOD,GMOD,SM,A,F1,F2,F3
C
C      DIMENSION S(1),JUG(1),MEMNP(ND2,1),MTYPE(1),MNP(2),COORD(ND1,1),
C      1      PROPS(ND3,1),F(ND2,1),A(3,6),SM(6,6),TRANS(3,6),P(7)
C
C      EQUIVALENCE (AREA,P(1)),(GAREA,P(2)),(ERTIA,P(3)),(END1,P(4)),
C      1      (END2,P(5)),(EMOD,P(6)),(GMOD,P(7))
C
C      DATA      NPLUS/+1/
C
C      NS=(NBW2*(2*NE+1-NBW2))/2
C      DO 1 I=1,NS
C      1 S(I)=0.0
C
C      FORM THE BEAM-STIFFNESS MATRICES.
C
C      DO 10 I=1,NMEM
C      N=MTYPE(I)
C      MNP(1)=MEMNP(I,1)
C      MNP(2)=MEMNP(I,2)
C      XL = COORD(MNP(2),1)-COORD(MNP(1),1)
C      YL = COORD(MNP(2),2)-COORD(MNP(1),2)
C      DO 5 J=1,7
C      5 P(J)=PROPS(N,J)
C      F1=F(I,1)
C      F2=F(I,2)
C      F3=F(I,3)
C
C      CALL MSTIFF(3)
C
C      (SM) IS MEMBER STIFFNESS.
C      (TRANS) IS SYSTEM TO MEMBER CO-ORDINATE TRANSFORMATION.
C      (A) IS NODAL DISPLACEMENT TO MEMBER REACTION TRANSFORMATION.
C
C      SET UP THE TOTAL STIFFNESS MATRIX BY THE DIRECT STIFFNESS METHOD.
C      10 CALL ALTRMX(S,SM,JUG,MNP,NPLUS)
C
C      TOTAL STIFFNESS MATRIX (S) IS NOW FORMED.

```

RETURN  
END

SUBROUTINE YIELD

\*\*\*\*\*

SUBROUTINE TO SET YIELD MOMENTS - ACCORDING TO THE MEMBER'S AXIAL  
LOAD WHERE APPLICABLE.

IF P15 =0.0, MEMBER IS ASSUMED TO BE A COLUMN WITH ALL FOUR  
YIELD MOMENTS IDENTICAL.  
POSITIVE, MEMBER HAS Y-M OF +-P14 AT END 1, +-P15 AT END 2.  
NEGATIVE, MEMBER HAS Y-M OF +P14,+P15 AT END 1, +P14,+P15  
AT END 2.

\*\*\*\*\*

COMMON /YIELDS/ PAX,P14,P15,P16,P17,P18,P19,YMP(2),YMN(2)

IF(P15) 2,4,3

2 YMP(1)=P14  
YMN(1)=P15  
YMP(2)=-P15  
YMN(2)=-P14  
RETURN

3 YMP(1)=P14  
YMN(1)=-P14  
YMP(2)=P15  
YMN(2)=-P15  
RETURN

4 YM=0.0  
IF(PAX.LE.0.0) GO TO 7  
IF(PAX.LT.P19) YM=P14\*(P19-PAX)/P19  
GO TO 9  
7 IF(PAX.LE.P17) GO TO 8  
YM=PAX\*(P16-P14)/P17+P14  
GO TO 9  
8 IF(PAX.GT.P18) YM=(PAX-P18)\*P16/(P17-P18)  
9 YMP(1)=YM  
YMN(1)=-YM  
YMP(2)=YM  
YMN(2)=-YM  
RETURN  
END